

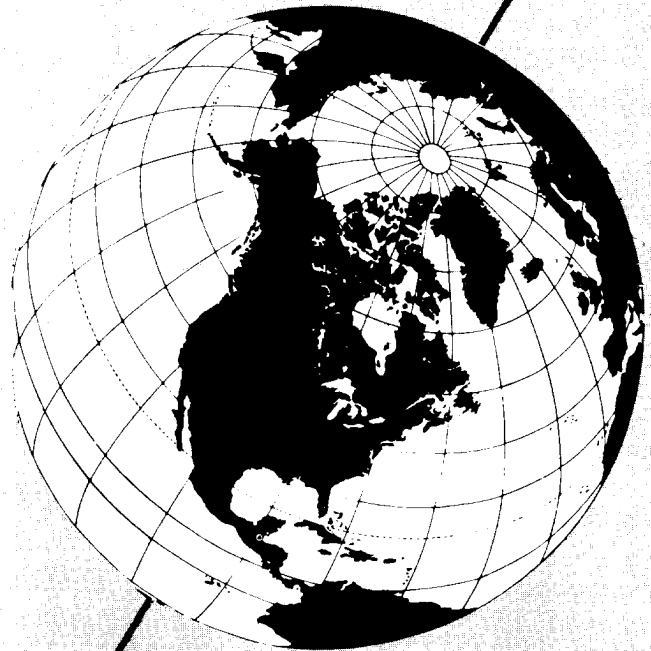
Research Report 70

JULY 1962
Reprinted AUGUST 1996

Stratigraphic Studies in the Snow and Firn of the Greenland Ice Sheet

DISTRIBUTION STATEMENT B
Approved for public release
Distribution Unlimited

DTIC QUALITY INSPECTED 4



19980217 529

SNOW, ICE AND PERMAFROST
RESEARCH ESTABLISHMENT
Corps of Engineers
U. S. ARMY

Research Report 70

JULY 1962
Reprinted AUGUST 1996

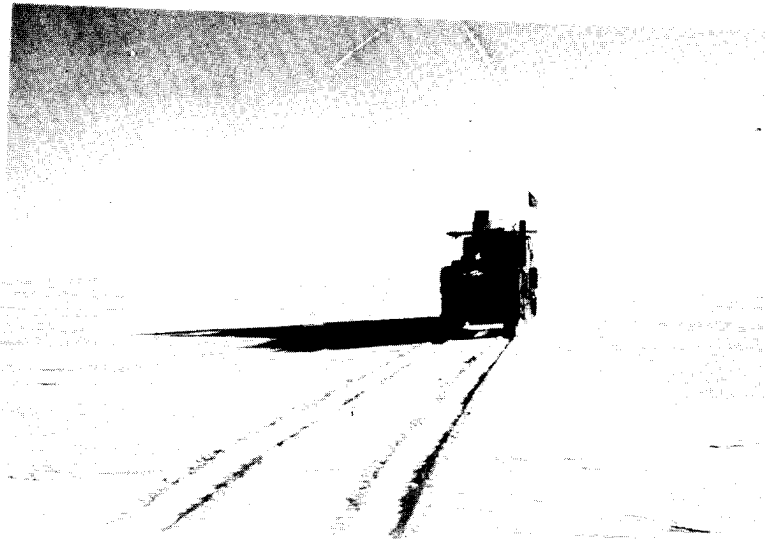
Stratigraphic Studies in the Snow and Firn of the Greenland Ice Sheet

by Carl S. Benson

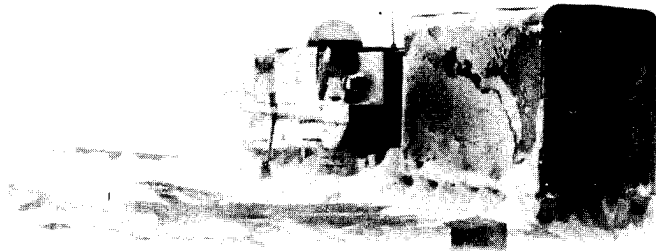
See pages F1–F8 immediately following for new
and corrected information added by the author,
August 1996.

**U.S. ARMY SNOW, ICE AND PERMAFROST
RESEARCH ESTABLISHMENT
Corps of Engineers**

Distribution of this document is unlimited



I



II

THE GREENLAND ICE SHEET

I. On the trail during a clear day with a smooth and firm snow surface.

II. Station 2-50, 4 August 1953, during a 3-day blizzard. The pit, lying to the left of the wannigan, is covered by a tarpaulin supported by a framework of timbers. Glaciological measurements were made in covered pits during storms with but minor interruption of schedule (Fig. 4g). The ability to navigate and work regardless of weather was essential, especially in planning and keeping up to the 1955 time table.

FOREWORD TO THE 1996 REPRINTING

SIPRE Research Report 70 has been reprinted because it is still in demand and being referred to, but is out of print and largely unavailable. Also, since 1962 several ice cores have been taken to the bottom of the Greenland Ice Sheet along the traverses covered in the report. Research Report 70 contains data which demonstrate lateral continuity of strata (at 10- and 25-mile intervals) extending several hundred miles both north and south from where these cores were taken.

(A) The most recent cores, done in 1990-1993, are the U.S. GISP2 (Greenland Ice Sheet Project Two) Core (72°34'N, 38°28'W) and the nearby European GRIP (Greenland Ice Core Project) Core (72°34'N, 37°37'W). These core sites are near Station 4-325 (72°28'N, 40°20'W) of Research Report 70.

(B) The 1966 Camp Century core site (77°10'N, 61°08'W) is near Station 2-20 (77°13'N, 61°01'W) of Research Report 70.

All the original data in this report are now on file at the World Data Center-A (WDC-A) for Glaciology, Boulder, Colorado.

The reprinting of Research Report 70 now also allows presentation of:

- (1) A summary of changes in the glacier facies concept (introduced as diagenetic facies, but herein referred to as The Assemblage of Glacier Facies).
- (2) A table summarizing the location of all the pit and core sites of Figures 28 and C1, and data sheets 1 through 10.
- (3) A list of errata; aside from these corrections, no revisions have been made to the report.

As originally published by SIPRE in July 1962 Research Report 70 applied the concepts of stratigraphy and sedimentation to the Greenland Ice Sheet. It dealt with the diagenetic environment where post-depositional changes transform snow into glacier ice. The stratigraphy of snow was shown to be preserved over four years by direct observation. It is interpretable to the extent that it could be followed over traverses extending inland from Thule, Greenland, at 77°N to the center of the ice sheet, south to 70°N, through the French Central Station (also Wegener's Eismitte) and out to the west coast. A stratigraphic "fence diagram" showing annual layers, in water equivalent, with a maximum extent from 1933 to 1955, along 1100 miles (1800 km) of traverse was presented in Figure 28.

The stratigraphic concepts were extended to introduce "diagenetic facies" within the Greenland ice sheet as a geologic formation. The concept of Glacier Facies introduced in Research Report 70 has proven useful. But in the last three decades it has undergone changes which makes it more useful, and this is an opportunity to summarize them.

1. THE ASSEMBLAGE OF GLACIER FACIES

Changes in the concept of Glacier Facies during the last three decades are minimal and are summarized here. Some changes in terminology make the concept more useful. The boundaries between the facies are still based on the same physical measurements. The significant conceptual improvements are at the complex lower end of the facies spectrum.

The new terminology (underlined) is as follows:

1. The Firn Line becomes the Snow Line,
2. The Saturation Line becomes the Wet Snow Line,
3. The Dry Snow Line remains unchanged,
4. The Ablation Facies becomes the Ice Facies,
5. The Soaked Facies becomes the Wet Snow Facies,
6. The Percolation Facies and the Dry Snow Facies remain unchanged.
7. The Equilibrium Line separates the glacier into two areas; the Ablation Area and the Accumulation Area.

The original term "soaked", for what is now the wet snow facies, was too strong. This was first pointed out by Müller (1962), who introduced the term "slush limit"; material below the slush limit is water saturated. After conversation with Müller, Benson (1967) introduced the term Wet Snow Line and discussed Müller's point. The prime condition of the wet snow facies is that the grains are raised to the melting point and are wet on their surfaces. There is a need to subdivide the wet snow facies to account for the part that is truly saturated with water and in which slush flows can occur. The boundary is Müller's Slush Limit, the Slush Zone extends down glacier, within the wet-snow facies, from the slush limit to the snow line which separates the wet-snow facies from the ice facies.

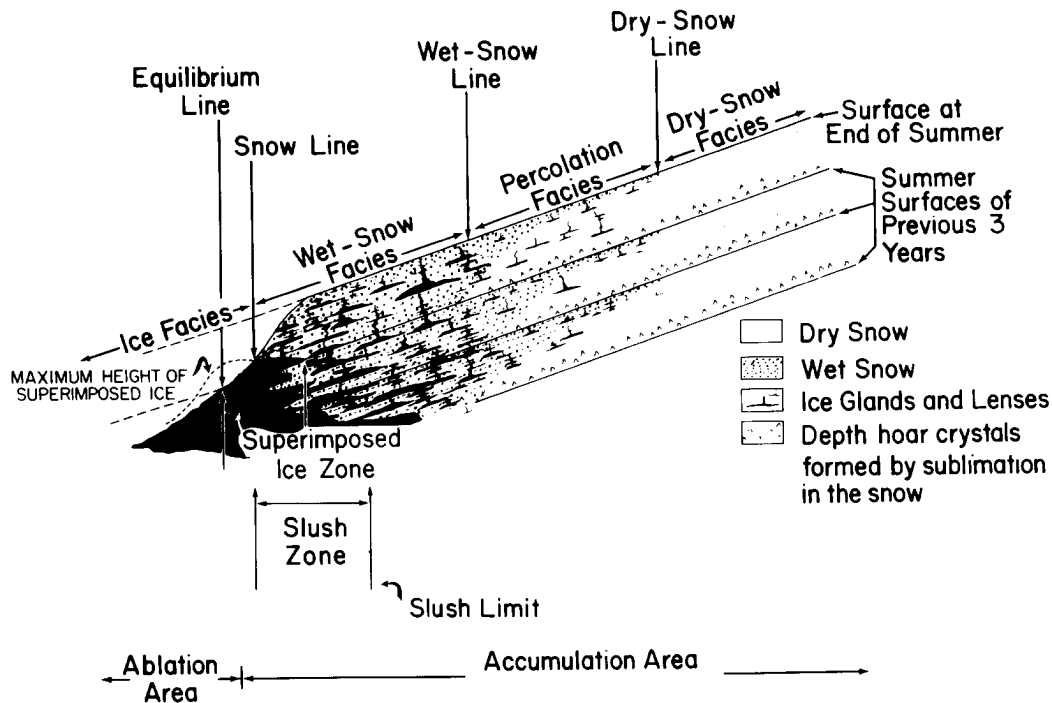
Some of the snow which is raised to the melting point and saturated with water refreezes to form superimposed ice. Superimposed ice straddles the boundary between the ice facies and the wet-snow facies; for this reason it is defined as the Superimposed Ice Zone.

The complexity of the wet snow facies causes it to be the only one which has zones within it.

The lines separating facies are: snow line, wet-snow line, and dry-snow line.

The facies refer to physical characteristics of the material: ice, wet-snow and dry-snow; the term "percolation" defines the facies in which the annual unit is not wetted completely and the outstanding characteristic is the presence of ice glands and lenses within the snow formed by freezing of melt water percolating from the surface. The wet snow line and the dry snow line are not visible from the surface by aircraft or LANDSAT satellite imagery (Williams, and others, 1991); but SAR imagery penetrates the surface and can locate these lines. This is because the dry snow facies has no internal reflectors, absorbs the signal, and appears dark on the image, but the percolation facies contains ice lenses and glands which make excellent reflectors, so it appears light on the image (Fahnestock and others, 1993).

The glacier facies of the accompanying diagram, from Benson (1994), should replace Figure 15.



REFERENCES

Benson, C.S. 1967. Polar Regions Snow Cover, in: Physics of Snow and Ice, Part 2, Edited by J. Oura, Institute of Low Temperature Science, Hokkaido University, Sapporo, Japan, p.1039-1063.

Benson, C.S. 1994. Glacier Facies: With Special Reference to Greenland, Report on the 4th Workshop on Mass Balance and Related Topics of the Greenland Ice Sheet. Open File Series 94/13, Greenland Geological Survey. Øster Volgade 10, DK-1350 Copenhagen K, DENMARK.

Fahnestock, M. A., R.A. Bindshadler, R. Kwok, and K. Jezek. 1993. Greenland Ice Sheet Surface Properties and Ice Dynamics from ERS-1 SAR Imagery, SCIENCE, Vol. 262, p. 1530-1534. (see also: Melt-Related Hydrologic Zones on the Greenland Ice Sheet Imaged with ERS-1 Synthetic Aperture Radar, EOS, Vol. 73, No. 43 Oct. 27, 1992/ supplement, p.175.

Müller, F. 1962. Zonation in the Accumulation Area of the Glaciers of Axel Heiberg Island, NWT, Canada, J. Glaciol., Vol. 4, p. 302-313.

Williams, R. S., Jr., D. K. Hall, and C. S. Benson. 1991. Analysis of Glacier Facies using Satellite Techniques, J. Glaciol., Vol. 37, p.120-128.

2. TABLE SUMMARIZING STATIONS

STATION LOCATION, TEMPERATURE, AND ACCUMULATION

See Appendix C, Figure C1, the Data Sheets #1-10, and Figure 28

Station	Latitude	Longitude	Altitude	Temp.	Accum.
	N	W	meters	(°C)*	cm w.e.**
Data Sheet 1 (1954)					
0-6	76° 22.0'	67° 59.5'	736	—	50
0-13	76 24.1	67 37.9	823	—	65
0-18	76 24.1	67 18.5	799	—	60
0-24	76 26.6	67 00.5	830	—	60
0-27	76 27.6	66 50.9	765	—	50
0-31	76 27.9	66 31.3	699	—	55
0-35	76 31.1	66 23.2	874	-10.0	67
0-40	76 33.5	66 07.8	889	—	65
0-45	76 34.6	65 50.0	1055	—	60
0-50	76 36.5	65 35.3	1212	—	65
0-55	76 40.5	65 27.1	1263	—	65
Data Sheet 2 (1954)					
00-10	76° 46.8'	66° 21.6'	1146	—	30
00-15	76 45.6	66 10.8	1195	—	—
00-20	76 44.4	66 00.0	1295	—	25
00-25	76 43.2	65 49.2	1300	—	—
1-0	76 43.3	65 23.4	1310	-17.0	65
Data Sheet 3 (1954)					
1-0	76° 43.3'	65° 23.4'	1310	-17.0	65
1-10	76 48.2	64 53.4	1419	-19.7	40
1-20	76 53.4	64 23.8	1486	-20.3	33
1-30	76 57.8	63 54.0	1519	-20.9	25
1-40	77 02.9	63 23.3	1571	-21.5	23
1-50	77 09.0	62 54.0	1630	-23.1	23
2-0	77 14.3	62 19.7	1704	-23.0	21

Station	Latitude	Longitude	Altitude	Temp.	Accum.
	N	W	meters	(°C)*	cm w.e.**
Data Sheet 4 (1953,1954, 1955)					
1-50	77° 09.0'	62° 54.0'	1630	-23.1	23
1A-10	77 01.3	62 22.0	1720	-24.0	36
1A-20	76 55.2	62 00.0	1660	-22.5	45
Data Sheet 5 (1954)					
2-0	77° 14.3'	62° 19.7'	1704	-23.0	21
2-10	77 14.0	61 40.0	1788	-23.6	25
2-20	77 13.0	61 01.3	1864	-23.9	30
2-30	77 11.0	60 23.6	1887	-24.2	38
2-40	77 10.6	59 44.5	1885	-23.7	40
2-50	77 09.1	59 05.5	1877	-23.5	40.7
2-60	77 07.7	58 26.7	1905	-24.0	39
2-70	77 05.6	57 49.1	1919	-23.8	40
2-80	77 03.5	57 11.8	1944	-24.0	39.5
2-90	77 02.0	56 33.0	1959	-24.6	41
2-100	76 59.9	56 00.8	1992	-24.0	40
Data Sheet 6 (1955)					
2-125	77° 02.5'	54° 31.0'	2152	-26.60	32
2-150	77 02.8	52 55.0	2273	-27.40	27
2-175	77 03.4	51 20.0	2392	-28.40	24
2-200	77 03.5	49 36.0	2475	-29.60	22
2-225	77 04.0	48 01.0	2536	-31.10	18.5
2-250 (4.0)	76 57.9	46 59.0	2616	-30.70	16.5

Station	Latitude	Longitude	Altitude	Temp.	Accum.
	N	W	meters	(°C)*	cm w.e.**
Data Sheet 6A (1953)					
2-100	77° 00.0'	56° 04.0'	1992	-24.0	40
2-120	77 11.3	55 45.1	2140	-24.7	31
2-140	77 13.5	53 46.7	2228	—	29
2-160	77 15.4	52 30.7	2313	—	27
2-180	77 16.8	51 13.4	2387	—	23.5
2-200	77 18.0	49 56.4	2441	-28.7	22
Data Sheet 7 (1955)					
4-0 (2-250)	76° 57.9'	46° 59.0'	2616	-30.7	16.5
4-25	76 38.2	45 42.0	2674	-31.0	17.5
4-50	76 19.0	45 06.0	2720	-30.7	17.5
4-75	75 59.1	44 35.0	2749	-31.0	18.5
4-100	75 38.2	43 57.0	2778	-30.6	18.8
4-125	75 17.8	43 25.0	2821	-30.9	20.5
4-150	74 56.0	42 58.0	2851	-30.6	21
4-175	74 35.4	42 33.0	2873	-30.2	22
4-200	74 13.3	42 10.0	2918	-30.3	23
Data Sheet 8 (1955)					
4-225	73° 52.4'	41° 48.0'	2941	-29.8	23
4-250	73 31.0	41 25.0	2972	-30.0	23
4-275	73 10.0	41 06.0	3003	-29.4	25
4-300	72 48.9	40 45.0	3046	-29.7	27
4-325	72 28.0	40 20.0	3104	-29.5	28.5
4-350	72 07.0	39 56.0	3128	-29.5	29
4-375	71 46.2	39 36.0	3131	-29.0	29.5
4-400	71 25.5	39 20.0	3126	-29.2	30.5
4-425 (5.0)	71 05.0	38 58.0	3123	-29.8	30.5

Station	Latitude	Longitude	Altitude	Temp.	Accum.
	N	W	meters	(°C)*	cm w.e.**
Data Sheet 9 (1955)					
5-0 (4-425)	71° 05.0'	38° 58.0'	3123	-29.80	30.5
5-20	71 00.0	39 40.0	3071	-27.70	33.5
5-40 (FCS)	70 53.8	40 42.1	3005	-27.20	35.5
5-65	70 46.5	41 38.0	2882	-25.80	40
5-90	70 37.8	42 37.0	2763	-24.30	45
5-115	70 27.0	43 35.0	2646	-24.30	47
5-140	70 18.0	44 33.0	2466	-21.60	51
Data Sheet 10 (1955)					
5-150	70° 15.0'	44° 58.0'	2407	-21.80	54
5-160	70 10.5	45 22.0	2342	-21.10	53
5-170	70 06.3	45 44.0	2283	-21.30	55
5-180	70 02.4	46 08.0	2206	-20.80	55
5-190	69 58.6	46 30.0	2146	-19.90	55
5-200	69 55.0	46 56.0	2012	-19.60	60
5-210	69 52.2	47 18.0	1963	-18.60	58
5-220	69 48.1	47 40.0	1861	-17.50	56
5-230	69 43.9	48 03.0	1746	-15.10	53.5
<p>* The mean annual temperature refers to the temperature measured 10m below the snow surface where melting is negligible. The effects of melt are discussed on p. 55. Corrections to the 10m depth at places where measurements were from shallower depths are given in Appendix B.</p> <p>** w.e. = water equivalent, rounded to the nearest cm in most cases.</p> <p>FCS = French Central Station (1948-1951), and Eismitte (1930-931).</p>					

3. ERRATA LIST FOR SIPRE (CRREL) RESEARCH REPORT 70

- Page 28: Figure 18 was incorrect. The figure is now corrected to match the text.
- Page 39: Fifth line up from the bottom: (see Fig. 26) should be (see Fig. 27).
- Page 41: Second line up from the bottom: (Epstein and Benson 1951) should be (Epstein and Benson 1961).
- Page 43: Caption for Figure 32, second line below the equation should read: Thus $d = -10$ means that O18/O16 ratio of the sample is 1% or 10% lower than that of mean ocean water.
- Page 44: Equation (1) the lower case q_n and q_2 should be upper case, i.e., Q_n and Q_2 .
- Page 46. The lower case q 's should be replaced by upper case Q 's. In the second line, the subscripts should all be 2.
- Page 76. Below Equation 8 the line describing v_p is incomplete. It should read as follows: $v_p = (v - v_i) =$ volume of pore space per unit mass of snow.
- Page 78. Table IX -- column 2, line 3: change "5 to 46" to 5 to 6.
- Page 81. This page was redone to eliminate the non-symmetric form of integration in equation 13.
- Page 92. Third reference from top: Warniek should be Warnick.

PREFACE

This paper is one of a series of reports on USA SIPRE* Project 022.01.029, Structure of ice cap névé in Greenland (formerly Project 22.2.3). This paper is a comprehensive report on Mr. Benson's work on this project during 1952 through 1955. Work on the project was performed for the Snow and Ice Basic Research Branch, James A. Bender, chief.

During the course of 4 years' field work in northwest and central Greenland many individuals and several organizations have contributed to the work. Without the aid of men of the North Atlantic Constructors (NAC) it would have been very difficult to outfit the expeditions. Especially in 1955, Mr. William E. Perkins contributed generously of his time and opened NAC shops to the expedition. The Transportation Arctic Group, Northeast Air Command, and First Engineer Arctic Task Force provided the bulk of logistic support from Thule, Greenland. The 6614th Air Transport Group carried out four perfect free airdrops to the 1955 expedition.

Special acknowledgement is due to Mr. J. Peter Johnson (now at St. Lawrence University, Canton, N. Y.), the writer's co-worker throughout the 140-day field season of 1953.

Invaluable assistance, under extreme environmental conditions, was given by Mr. George R. Toney (U. S. Weather Bureau) and Mr. Stephen W. Miller (Stanford Research Institute) in 1953, and by Mr. Dale Beranek (Trans Arctic Group) in 1954.

Mr. James A. Bender and Mr. Richard H. Ragle (both of SIPRE) were assistant party leaders during the first and second halves, respectively, of the 1954 field season. Mr. Ragle also provided valuable assistance in preparation of glaciological and altimetry data from the 1954 season and was assistant party leader in 1955.

Mr. B. W. Gardner, Jr., Associate chief, Animal Products Division of the Quartermaster Food and Container Institute, provided the 1955 expedition with 1500 lb of light-weight test items of frozen and dehydrated foods. This contribution made it possible to operate at 4.7 lb food-cargo per man day as opposed to 10 lb per man day which is standard for Army sled trains; thus, it increased the range of travel and permitted greater independence from time-consuming airdrops.

Mr. A. N. Brunson of Brunson Instrument Company provided a newly designed Sun Compass to test and use in 1955.


The other personnel of the 1955 expedition also contributed greatly to the success of the expedition: Robert W. Christie, M. D. (expedition physician), James B. Holston, B. A. (expedition radioman), Alan C. Skinrod, M. S. (mechanical engineer - expedition mechanic), and George Wallerstein, Ph. D. (astrophysicist - expedition navigator).

* Redesignated U. S. Army Cold Regions Research and Engineering Laboratory, 1 February 1961.

PREFACE (cont'd)

The author wishes to express his thanks to Dr. Henri Bader, then Chief Scientist, for granting complete freedom in planning and complete support in carrying out this study. Thanks are due also to Don L. Anderson and Drs. W. Barclay Kamb and Robert P. Sharp of the California Institute of Technology for helpful discussions, and to Dr. Sharp for reading and criticizing the manuscript in its several stages.

This report has been reviewed and approved for publication by the Office of the Chief of Engineers, United States Army.



W. L. NUNGESSER
Colonel, Corps of Engineers
Director

Manuscript received 26 April 1960

Department of the Army Project 8-66-02-400

CONTENTS

	Page
Preface -----	ii
Summary -----	vi
Chapter I. Introduction -----	1
Operations and logistics -----	3
Chapter II. Methods of investigation -----	4
Region of investigation -----	4
Pit studies -----	4
Elevation measurements -----	8
Chapter III. Stratigraphy and accumulation -----	13
Introduction -----	13
Diagenesis without melt -----	13
Diagenesis with melt -----	19
Diagenetic facies defined on glaciers -----	24
Grain size -----	25
Description of three stratigraphic features -----	26
Principles of stratigraphic interpretation -----	30
Selection of a reference datum in the annual stratigraphic sequence -----	30
Stratigraphic correlation -----	33
Distribution of annual accumulation -----	34
Independent checks on the stratigraphic interpretations -----	41
Chapter IV. Temperature distribution -----	44
Seasonal temperature variation on the snow surface -----	44
Seasonal temperature variation below the snow surface -----	46
Distribution of mean annual temperature on the ice sheet -----	53
Chapter V. Diagenetic facies - a classification of glaciers -----	61
Temperature -----	61
Hardness -----	61
Density -----	67
Glacier facies - a classification of glaciers -----	73
Chapter VI. Densification of snow and firn -----	76
Load - volume relationship -----	76
Depth-density relationship -----	81
Chapter VII. Climatological implications -----	84
Introduction -----	84
Katabatic winds and accumulation -----	84
Annual heat exchange -----	85
The balance of the Greenland Ice Sheet -----	85
References -----	89
Appendix A: Stratigraphy, meteorology and glaciology -----	A1
Appendix B: Mean annual temperature -----	B1
Appendix C: The data sheets -----	C1

ILLUSTRATIONS

Figure	2
1. Location of traverses -----	2
2. Test stations in northwest Greenland ----- facing p.	5
3. Sketch of a typical test pit -----	5
4. Stratigraphic observations and density sampling -----	6, 7
5. Stratigraphic photo sections ("thin sections") -----	9, 10
6. Pit wall photography -----	11, 12
7. Snow surface features -----	14-17
8. Stratigraphic data combined with photo section -----	18
9. Iced firn layers at station 2-100, 1953 -----	19
10. Ice masses in snow strata -----	20

CONTENTS (cont'd)

Figure		
11.	Percolation of gasoline through snow at -30C -----	21
12.	Air temperature records, July and August 1954 -----	22
13.	Active percolation channels-----	23
14.	Frozen melt crust at station 2-70, 1954-----	24
15.	Generalized cross-section of glacier facies -----	25
16.	Grain size classification -----	26
17.	Histograms of snow grain size analyses -----	27
18.	Cumulative curves of snow grain size analyses -----	28
19.	Photomicrographs of snow grains -----	29
20.	Rammsonde profile through wind slab -----	30
21.	Wind slabs in pit wall and on snow surface -----	31
22.	Four years' data at station 1-0 -----	
23.	Three years' data at station 0-35-----	
24.	Four years' data at station 2-30-----	facing p. 34
25.	Four years' data at station 2-70-----	
26.	Displacement of snow surface relative to markers on poles -----	35
27.	Computed depth-time curves compared with data points---	36
28.	Summary of accumulation data from traverse of Figure 1 -----	facing p. 36
29.	Accumulation-altitude relationship -----	38
30.	Contours of gross annual accumulation-----	40
31.	Degree days above freezing at Thule, Greenland -----	41
32.	Stratigraphic data compared with O^{18}/O^{16} ratios -----	42, 43
33.	Temperature profiles at stations 1-0, 2-0, 2-50, 2-100, and 2-120 -----	47
34.	Temperature profiles measured in late summer on the west slope of the Greenland ice sheet -----	49
35.	Isotherms in upper 5 m on west slope of the Greenland ice sheet during peak of melt season -----	51
36.	Annual temperature variations at and below the snow surface -----	52
37.	Mean annual temperature plotted against altitude on the west slope of the Greenland ice sheet -----	54
38.	Computed isotherms compared with data in top 5 m -----	57
39.	Mean annual temperature plotted against time and latitude for stations along the west coast of Greenland ----	59
40.	Distribution of mean annual temperature on the Greenland ice sheet -----	60
41.	Integrated ram hardness plotted against depth -----	64
42.	Integrated ram hardness plotted against position for the years 1953, 1954, and 1955 -----	65
43.	Temperature dependence of ram hardness-----	66
44.	Depth-density curves -----	68
45.	Depth-load curves -----	70
46.	Load in cm H_2O at depth 5 m below snow surface along traverse in Figure 1 -----	72
47.	Variation of facies boundaries with altitude and latitude in west Greenland -----	74
48.	Distribution of facies on the Greenland ice sheet -----	75
49.	Specific volume plotted against load -----	78
50.	Critical temperature vs critical density-----	79
51.	Relation between $dv/d\rho$ and v at station 2-100 -----	80
52.	Depth-density relationship at station 2-100 -----	83
53.	"Cold content" in the upper 5 m during melt season -----	86

CONTENTS (cont'd)

	Page
Figure	
54. Distribution of gross accumulation on the Greenland ice sheet -----	88
C1. Location of data sheets -----	C2
C2. Stratigraphic symbols -----	C3

TABLES

Table	
I. Monthly mean temperatures at Eismitte (1930-31)-----	45
II. Air temperature data for station 2-100, Greenland -----	45
III. Values of constants in eq 2 -----	46
IV. Isotherms during peak of the melt season -----	50
V. Maximum deviation from mean annual temperature in the top 16 m of snow -----	53
VI. Temperature-altitude relation measured 3 m below the snow surface during summer at 77°N latitude-----	55
VII. Mean annual air temperature data from coastal meteorological stations -----	58
VIII. Reproducibility of depth-load curves-----	71
IX. Critical values observed on Seward Glacier and in Greenland -----	78
X. Distribution of gross accumulation on the Greenland ice sheet -----	88
XI. Balance of the Greenland ice sheet -----	89

SUMMARY

The Greenland ice sheet is treated as a monomineralic rock formation, primarily metamorphic, but with a sedimentary veneer of snow and firn. The sedimentary part is perennial above the firn line, and the classical methods of stratigraphy and sedimentation can be profitably applied to it.

During a 4-yr period 146 pit studies and 288 supplementary Rammsonde profiles were made along 1100 miles of over-snow traverse (Fig. 1). Temperature, density, ram hardness, and grain size were measured in the strata exposed in each pit.

Stratification of snow results from variations in the conditions of deposition and is emphasized by subsequent diagenesis. Summer layers are coarser-grained and have generally lower density and hardness values than winter layers; they may also show evidence of surface melt. The onset of fall is usually identified by an abrupt increase in density and hardness accompanied by a decrease in grain size. This stratigraphic discontinuity is used as the annual reference plane.

Strata in the upper 10 to 20 m compose a succession of annual sequences which are preserved in recognizable form for at least several decades. Correlation of annual layers between pits, spaced 10 to 25 miles apart along the traverse of Figure 1, gives a picture of annual accumulation during the past 5 to 20 yr for western Greenland between 69 and 77°N. The control established by these data, together with information from earlier expeditions (primarily those of Koch-Wegener and deQuervain) and from permanent coastal meteorological stations, have been used to make a map showing the distribution of gross annual accumulation, essentially the equivalent of annual precipitation, for the entire ice sheet (Fig. 30). In general, the accumulation contours follow the north-south trend of the coast lines, with extremes of less than 10 cm H₂O in the northeast and more than 90 cm H₂O per year in the south; the average for the ice sheet is 34 cm H₂O per year. The zone of maximum precipitation lies close to the coast in two regions, one on the east coast between Angmagssalik and Scoresbysund, the other on the west coast between Upernavik and Thule.

In addition to the existence of a useful stratigraphic record four diagenetic facies are recognized on the ice sheet.

- 1) The ablation facies extends from the outer edge, or terminus, of the glacier to the firn line. The firn line is the highest elevation to which the annual snow cover recedes during the melt season.
- 2) The soaked facies becomes wet throughout during the melting season and extends from the firn line to the saturation line, i. e., the uppermost limit of complete wetting. The saturation line is the highest altitude at which the 0C isothermal surface penetrates to the melt surface of the previous summer.
- 3) The percolation facies is subjected to localized percolation of melt water from the surface without becoming wet throughout. Percolation can occur in snow and firn of subfreezing temperatures with only the pipe-like percolation channels being at the melting point. A network of ice glands, lenses, and layers forms when refreezing occurs. This facies extends from the saturation line to the upper limit of surface melting, the dry-snow line. Negligible soaking and percolation occur above the dry-snow line.

4) The dry-snow facies includes all of the glacier lying above the dry-snow line, and negligible melting occurs in it.

The saturation line can be identified by discontinuities in temperature, density, and ram hardness data, and it may also be located by examination of melt evidence in strata exposed on pit walls. It is as sharply defined as the firn line; but the dry-snow line, although determined by the same methods, is an ill-defined transition zone 10- to 20-miles wide.

The facies represent a response to climate, therefore changes in the location of facies boundaries may be used as indicators of secular climatic change. Since facies are not restricted to the Greenland ice sheet, they provide the basis for a general areal classification of glaciers which gives a greater resolution of characteristics than Ahlmann's "geophysical classification." In particular, the facies classification permits subdivision of large glaciers which span the entire range of environments from temperate to polar. Ahlmann's useful distinction between temperate and polar glaciers takes on new meaning in the light of glacier facies. Thus, a temperate glacier exhibits only the two facies below the saturation line whereas one or both of the facies above the saturation line are present on polar glaciers. An attempt has been made to map the distribution of facies on the Greenland ice sheet (Fig. 48).

The gradients of mean annual temperature on the ice sheet may be approximated as 1C/100 m (altitude) and 1C per degree latitude. The altitude gradient is controlled by strong outgoing radiation, producing deep inversions and katabatic winds. The katabatic winds are warmed adiabatically as they descend along the surface of the ice sheet, and this is the primary control determining the temperature gradient along the snow surface. The latitude gradient is based on temperature measurements made above 2000 m on the ice sheet, and on average values from meteorological stations spanning 20° of latitude on the west coast. A contour map of isotherms based on these gradients compares well with temperature values obtained from pits on the ice sheet (Fig. 40).

The densification of snow and firn is discussed for the case where melting is negligible. The assumption is that accumulation remains constant at a given location and, under this assumption, the depth-density curve is invariant with time as stated by Sorge's law. As a layer is buried it moves through a pressure gradient under steady-state conditions, and it is assumed that the decrease in pore space with increasing load is simply proportional to the pore space, i. e.,

$$\frac{dv}{d\sigma} = -m(v - v_i) \quad (8)$$

where

$$v = \frac{1}{\rho} = \text{specific volume of firn } (\rho = \text{firn density}),$$

$$v_i = \text{specific volume of ice} = 1.09 \text{ cm}^3/\text{g},$$

$$\sigma = \int_0^z \rho dz = \text{load at depth } \underline{z} \text{ below the snow surface}$$

and

m = a parameter which depends on the mechanism of densification. For mathematical simplicity it is treated as a constant at a given location.

SUMMARY (cont'd)

The depth-density equation obtained from eq 8 is

$$z = \frac{1}{m\rho_i} [K - (\epsilon + \ln \epsilon)] \quad (14)$$

where

$$K = \epsilon_0 + \ln \epsilon_0,$$

$$\epsilon = \frac{\rho_i - \rho}{\rho} = \text{void ratio for snow of density } \rho, \text{ and}$$

$$\epsilon_0 = \frac{\rho_i - \rho_0}{\rho_0} = \text{void ratio for snow of density } \rho_0,$$

$$\rho_0 = \text{density of snow when } \sigma = 0.$$

The consequences of the assumption in eq 8 compare favorably with observation. A fundamental change in the mechanism of densification is recognized within 10 m of the snow surface. The concept of a "critical density" is introduced. Before the density of snow attains the critical value it is compacted primarily by packing of the grains. The critical density represents the maximum value obtainable by packing and further compaction must proceed by other mechanisms. The rate of change of volume with increasing load decreases by a factor of 4 when the critical density is exceeded. The same equations hold in the case where melt is not negligible but the rates of densification are higher.

Bauer's (1955) estimate for the balance of the ice sheet is revised. Two corrections are applied: (1) the average annual accumulation value of 31 cm H₂O originally estimated by Loewe (1936) is revised to 34 cm H₂O as a result of this study; (2) the relative areas of ablation and accumulation zones in Greenland north of 76°N are more accurately defined. The net result is a slightly positive balance which is interpreted to mean that the Greenland ice sheet is essentially in equilibrium with present-day climate.

STRATIGRAPHIC STUDIES IN THE SNOW AND FIRN
OF THE GREENLAND ICE SHEET

by
Carl S. Benson

CHAPTER I. INTRODUCTION

A primary question about ice masses of the world today concerns their material balance; i. e., are they in balance with present-day climate or not? In order to answer this question it is necessary to know current rates of accumulation and ablation. A major part of this study is the determination of the amount and distribution of accumulation on the Greenland ice sheet. But the basic purpose has been to extend our knowledge of the overall physical environment of the ice sheet — the accumulation picture is only a part of this. Improvement in our knowledge of the Greenland ice sheet contributes to understanding the nature of ice sheets in general, including extinct ones of the Pleistocene.

The primary objective of this study is to demonstrate that the methods of stratigraphy and sedimentation can be successfully applied to the study of snow and firn. Such stratigraphic investigations differ from studies of other rock formations primarily in technique. Parameters used in interpretation are measured variations in density, hardness, grain size, and observations of melt and wind evidence (when present). This approach has proved fruitful in determining the prevailing climatological conditions on the Greenland ice sheet.

The term "ice sheet" is defined in Ahlmann's (1948) classification of glaciers, which is summarized with special reference to the Greenland ice sheet in Appendix A. Emphasis on the stratigraphic nature of the ice sheet in this study has led to a more quantitative classification of glaciers than has been possible before.

Determination of annual accumulation, one of the most important results obtained from snow stratigraphy on the ice sheet, depends on the ability to identify annual units in the strata. Sorge (1933, 1935) found that annual units could be identified at Eismitte (Fig. 1) by measuring firn density, since winter layers are slightly denser than summer layers. Fortunately, Eismitte was located where annual units are thick (about 1 m) and where density differences between summer and winter strata are pronounced. Sorge's research program, done at a single station, did not include correlation of several year's strata on a regional scale.

Koch and Wegener (1930) correlated the Jungschneedecke across Greenland during the summer of 1913 (Fig. 1). Their Jungschneedecke consisted of a layer of fine-grained snow and firn which was underlain by a coarse-grained low-density layer. They assumed that the Jungschneedecke represented the accumulation since fall of 1912. Theirs is the best recorded example of stratigraphic correlation in snow of the Greenland ice sheet.

In our study the Greenland ice sheet* has been treated as a monomineralic rock formation, primarily metamorphic but with a sedimentary veneer. In terms of areal exposure, this is the most extensive formation in Greenland, covering 1,726,400 km² (675,000 square miles) or about 80% of the total surface area (including islands). The metamorphic part consists of glacier ice which has been metamorphosed through flowage caused by unbalanced stresses. Herein, attention is confined to the sedimentary veneer, which is perennial above the firn line, has a maximum thickness of about 90 m, and consists of snow and firn.

The sedimentary veneer of the Greenland ice sheet is especially important because of its intimate relationship with climate. The annual climatic cycle produces recognizable annual sequences of strata, and the interpretation and correlation of these units form an important part of this study. Measurement of the water equivalent of annual layers on the ice sheet is the only satisfactory method of determining the amount of precipitation

* The term "Greenland ice sheet" is a suitable formation name without the addition of "formation." This is convenient because it does not entail new terminology. The Greenland ice sheet is often referred to as the "Greenland Ice Cap" or "inland ice."

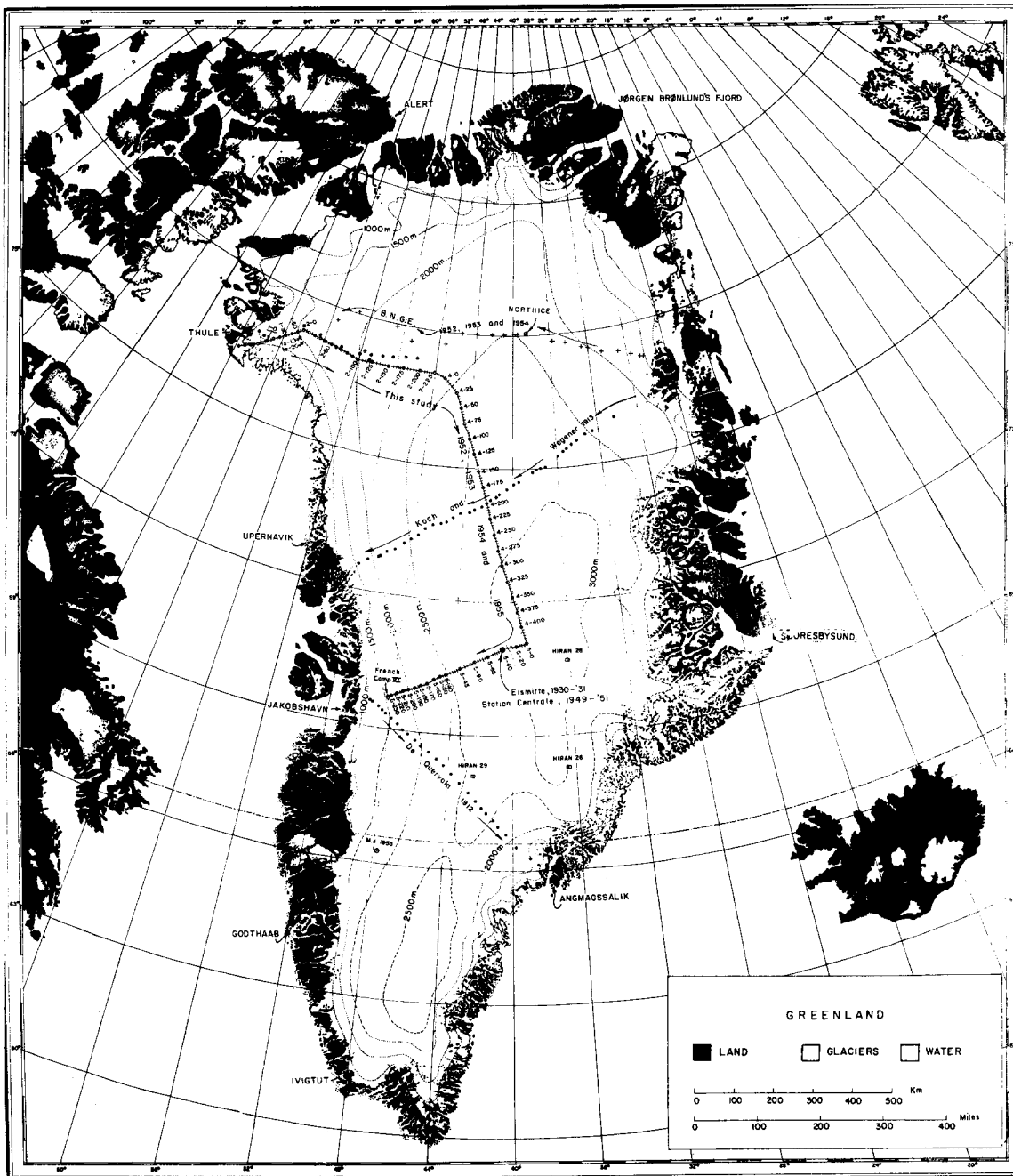
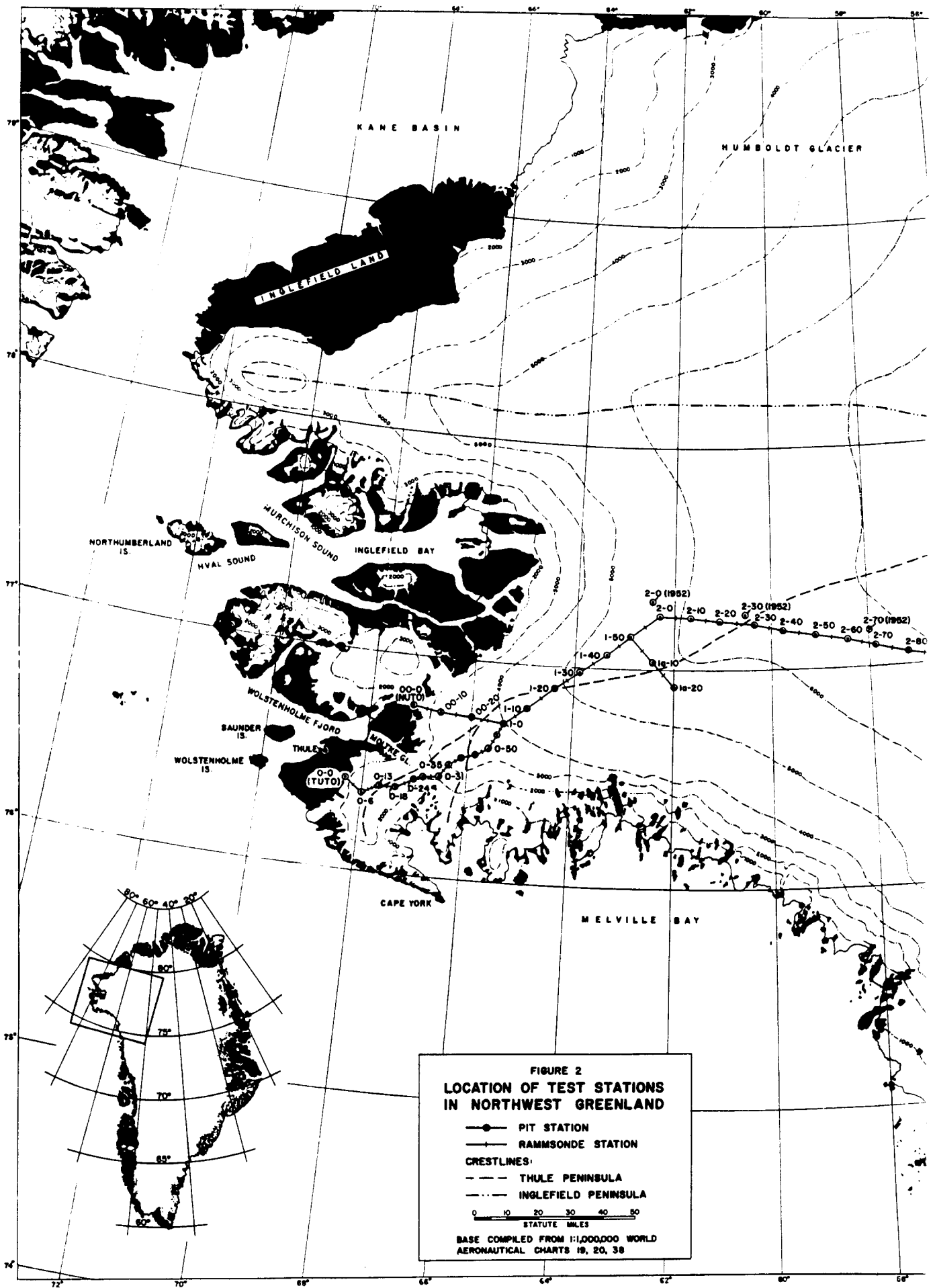


Figure 1. Location of traverses. Circled points along the traverse of this study represent pit stations, the tick marks represent Rammsonde stations. See Figure 2 for a detailed map of the stations in northwest Greenland. The other traverses shown are referred to in the bibliography as: DeQuervain and Mercanton (1925), Koch and Wegener (1930), and Bull (1958; British North Greenland Expedition, B.N.G.E.). The HIRAN Stations were part of a U. S. Air Force project in 1956. The location of Project Mint Julep (Schuster, 1954) is indicated by the point labeled M. J. 1953.



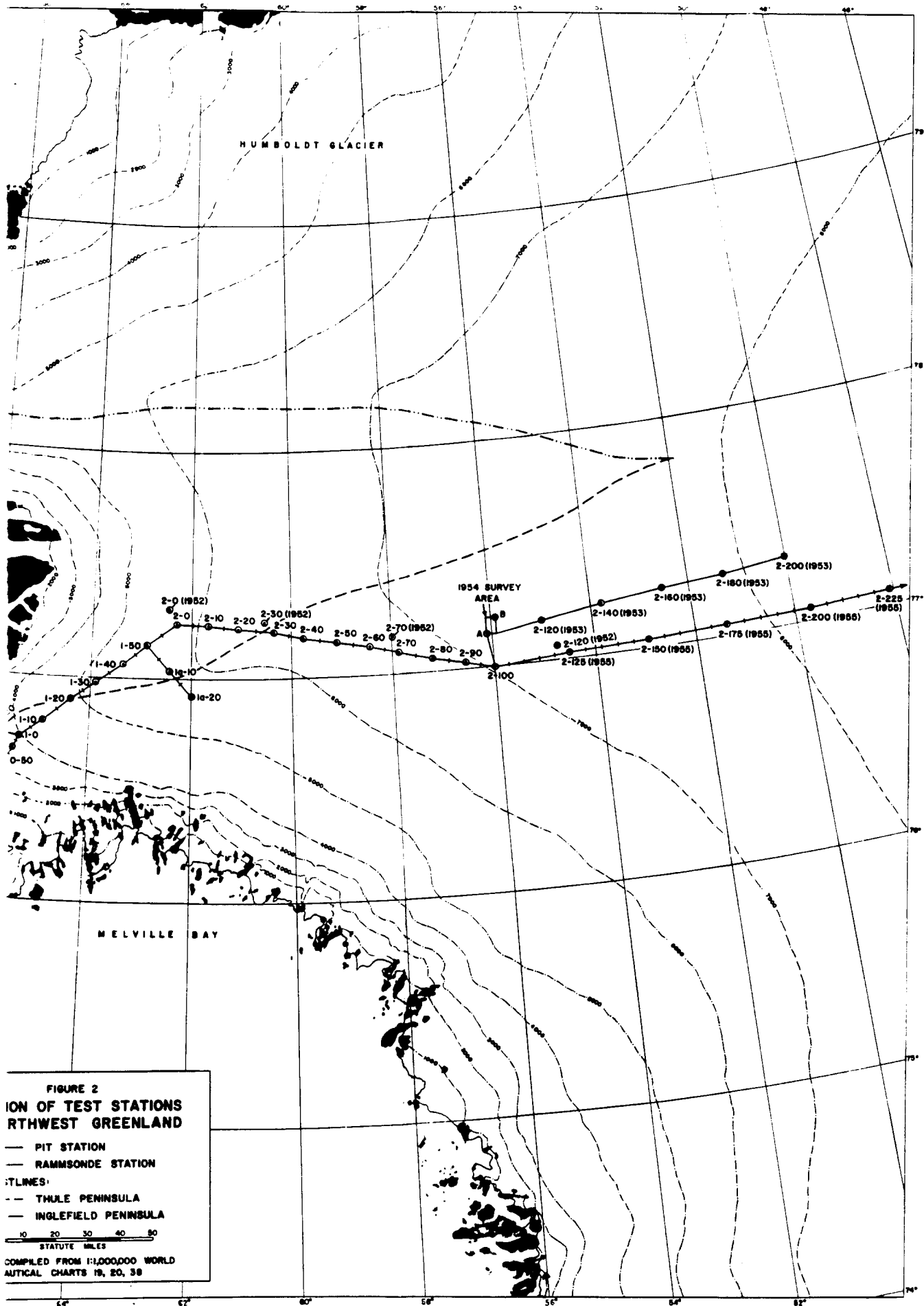


FIGURE 2
LOCATION OF TEST STATIONS
IN NORTHWEST GREENLAND

— PIT STATION
 — RAMMSONDE STATION

(---) CONTOUR LINES
 - - THULE PENINSULA
 — INGLEFIELD PENINSULA

0 10 20 30 40 50
 STATUTE MILES

COMPILED FROM 1:1,000,000 WORLD
 NAUTICAL CHARTS 19, 20, 38

2

in Greenland. Precipitation gages at meteorological stations along the coast are strongly influenced by local conditions of exposure, and give readings which are invariably too low and only for a single point location. In contrast, the ice sheet is an infinite set of automatically recording precipitation gages. It is only necessary to learn how to read the records.

Correlation of annual stratigraphic units from the edge of the ice sheet to the high-altitude interior regions led to the development of the concept of diagenetic facies on glaciers. In 1952, regional differences clearly related to the temperature decrease with altitude, were recognized in physical properties of the upper snow layers. However, the 1952 data were not sufficient to permit recognition of the facies (nor could detailed correlation be done between all seven pits, which were spaced about 50 miles apart). Subsequent field work has clarified the picture and the combined results from 1952, 1953, and 1954 (Benson, 1959) permitted interpretation and correlation of 17 yr of snow and firn strata and established the concept of diagenetic facies on the ice sheet.

Essentially the research has taken on two main aspects: first, the recognition of annual stratigraphic units, involving detailed analysis at each station, and, second, the comparison of gross variations in properties between facies. Both aspects combine in defining a quantitative classification of glaciers based on the existence of facies on the ice sheet.

Sedimentation on the ice sheet may be compared with underwater transportation and deposition in a basin. On the ice sheet there is a dome or highland of deposition rather than a basin. Masses of air transport a load of water vapor which condenses, crystallizes, and is precipitated as the air cools on ascending the slope of the ice sheet. After or during a snowfall, winds transport snow grains by saltation and in suspension along the surface. To some extent this smooths local irregularities in the original distribution of the snow. At this point, the blowing and drifting snow is an aeolian sediment and surface features of wind erosion and deposition, such as sastrugi, barchans, and ripple marks, are observed (Fig. 7).

Post-depositional, i. e., diagenetic,* changes transform the snow into firn. The diagenetic environment extends downward for an unspecified depth, but includes most of the sedimentary veneer. The firn layers record specific meteorological conditions or events, such as warm spells which produce various degrees of melting, and windstorms or blizzards which produce hard wind slabs. In general, meteorology, sedimentation, and diagenesis are so closely interrelated on the ice sheet that the stratigraphy provides a climatic record.

Presentation of the data, gathered over a 4-yr period from 434 test sites along 1100 miles of traverse, posed a problem which has been partly solved by assembling the data from 79 representative pit stations on 10 data sheets (following p. C3). Special points have been abstracted into figures throughout the text.

Operations and Logistics

Operational and logistical problems were both cumbersome and complex. A full treatment of this part of the program is in preparation and some aspects of it have been described (Benson, 1955b, 1955c; Benson and Ragle, 1956).

The total one-way length of traverse was 1100 miles (Fig. 1), but the total vehicle mileage recorded during the four field seasons was 12,860. Weasels (M29C Cargo Carriers), modified for arctic use, together with cargo sleds and wannigans (built by the members of the expeditions) provided transportation and living quarters (see p. ii). Resupply in the field was provided by aircraft based at Thule and Sondrestrom Air Bases. The major logistic burdens of fuel, food, trail markers, and technical equipment exceeded 100,000 lb of cargo. Most of this was free-dropped (i. e., without parachutes) from low-flying aircraft (about 20 ft above the snow surface).

* The term "metamorphism" was used by Bader et al. (1939) to describe the phenomena called "diagenesis" in the present paper. According to accepted usage, it is preferable to refer to post-depositional changes in sedimentary layers as "diagenetic changes." Metamorphic processes occur in glacier ice of the metamorphic part of the Greenland ice sheet and will not be considered in this paper.

CHAPTER II: METHODS OF INVESTIGATION

Region of Investigation

The overall region of investigation is shown in Figure 1. During 1952, 1953, and 1954 the work was confined to northwestern Greenland between Thule and station 4-0 (Fig. 2). The density of stations is greatest in this area and one or more pit studies were made at many of the stations during each year of the project. The major objective during the first 3 yr was a detailed study of the strata deposited between 1937 and 1954 (Benson, 1959). During 1955, stratigraphic control was extended along the traverse shown in Figure 1, and the combined results of the four field seasons are presented here.

The peninsular region on the west coast of Greenland between 76 and 79°N enters the discussion several times and it is convenient to introduce the following terminology:

a) Thule peninsula lies between Melville and Inglefield Bays, and produces a ridge on the ice sheet which is well defined for over 150 miles.

b) Inglefield peninsula lies between Inglefield Bay and the Kane Basin. It also produces a well defined ridge on the ice sheet. The ridge crests of Thule and Inglefield peninsulas meet at about 52°W (Fig. 1, 2).

The entire traverse (Fig. 1, 2) is subdivided into seven trail segments, labeled 00, 0, 1, 1a, 2, 4, and 5. The points on the traverse are identified by two numbers: the first refers to the trail-segment, the second to the number of miles along the trail-segment from its origin. A total of 434 test sites were occupied (146 pit studies and 288 Rammsonde profiles measured at points between pit stations).

Two points of access to the ice sheet were used, Camp Nuto on Nunatarssuaq, and Camp Tuto 12 miles from Thule Air Base. The trails from these origin points converge at station 1-0. Station 1-0 is known as "Station Morris" and was called "point Alpha" prior to May 1955. Stations along the trail from Tuto to Morris are numbered "0-n" where n is the distance in miles from Tuto (from 0 to 60). Stations between Nuto and Morris are numbered "00-n" where n is the distance from Nuto (from 0 to 30).

The trail between 1-0 and 2-0 (segment 1) is 60 miles long and remained constant during the four years. The 20-mile trail originating at station 1-50, labeled 1a, was covered in 1955 only.

The trail between 2-0 and 4-0 (segment 2) is 250 miles long and varied slightly in detail as shown in Figure 2. Work extended to 2-125 in 1952, to 2-200 in 1953, to 2-100 in 1954 and to 2-250 (i. e., 4-0) in 1955.

The north-south segment is labeled 4 and the southern east-west segment is number 5. There is no trail segment number 3.

Pit Studies

Pits 3 to 6 m deep were dug in areas undisturbed by foot or vehicle traffic (Fig. 3). Extreme care was taken to avoid disturbance of the section exposed on the test wall (Fig. 4). Pits were always covered at night and during stormy or windy days (see Fig. 4d and p. ii). Without cover, 4 m pits have been completely filled with drift snow in less than 10 hr. Work can proceed satisfactorily in a covered pit during storms.

Stratigraphic control was extended below the pit floors by core drilling at most stations. The 3-in. diam hand auger, developed by the Arctic Construction and Frost Effects Laboratory* and modified by U. S. Army SIPRE,* was used. The maximum length of core obtained, 11 m, was at station 2-0 (1954) giving a total depth penetration of 17 m (56 ft) at that station. The depth of drilling was determined solely by the amount of time available to obtain, describe, cut, measure, and weigh the core samples. A reasonable estimate is 1 hr for each meter of core. The following measurements were made at test stations.

* Redesignated U. S. Army Cold Regions Research and Engineering Laboratory, 1 February 1961.

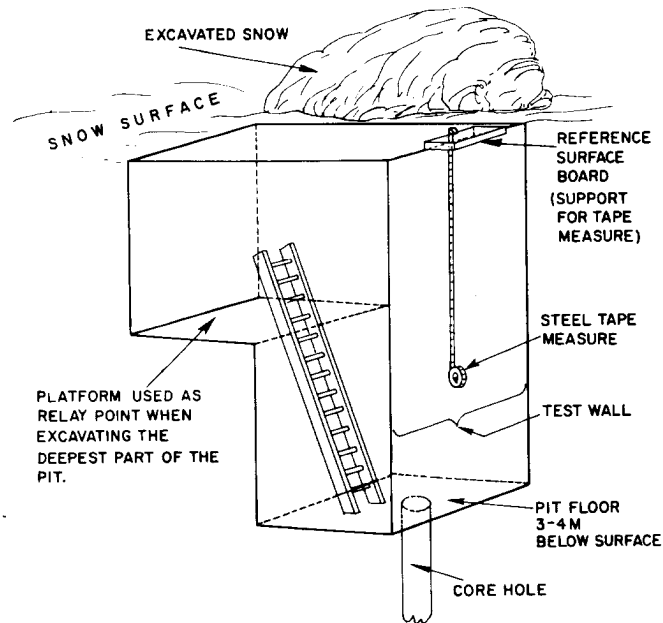


Figure 3. Sketch of a typical test pit. Pits were dug in places undisturbed by foot or vehicle traffic. Waste snow was not thrown over the test wall and no one walked within several feet of its edge. Test walls, located on the south side to avoid direct sunshine, were made clean and vertical. A board on the snow surface served as a mount for the steel tape measure and also as a radiation shield for thermometers in the snow (see Fig. 4a, f).

Temperature

A temperature profile was measured at 10 cm intervals on the pit wall with Weston bimetallic thermometers. This was done concurrently with the excavation to avoid significant disturbance of natural thermal conditions. Additional temperature measurements were obtained from the bottom of the core holes. The thermal effect of an open pit on the surrounding snow is indicated in Figure 33 by curves 4 and 4a from station 2-50. The test pit of 4 August was left open and revisited on 21 August; it had been completely filled by drifting snow. The snow that filled the pit was at the temperature of the snow surface, and since August is one of the warmer months, heat was added to the surrounding firn.

Hardness

The Rammsonde penetrometer measures the resistance of snow to the penetration of a cone. It was developed by Haefeli (Bader et al., 1939, p. 128-132) and was slightly modified at USA SIPRE after the 1952 field season. It is used as the standard for hardness measurement in this work. The Rammsonde has a distinct advantage over other hardness measuring instruments because reliable profiles can be obtained from the surface to a depth of 4 m without digging a pit. Such profiles, obtained at points between pit stations, proved useful in making stratigraphic correlations from pit to pit.

The Canadian hardness gage was also used in 1952. It did not add to the general stratigraphic picture in proportion to the time required for its proper use, since five measurements for each layer were required to obtain an average value. It is also more subject to operator variation than the Rammsonde. Comparison of several hardness measuring instruments in south Greenland (Schuster, 1954) supports this conclusion.



Figure 4a. Brushing test wall of pit to make strata stand out clearly in the upper 6 m, where resistance to this "erosion" varies markedly. Note undisturbed surface at edge of test wall.

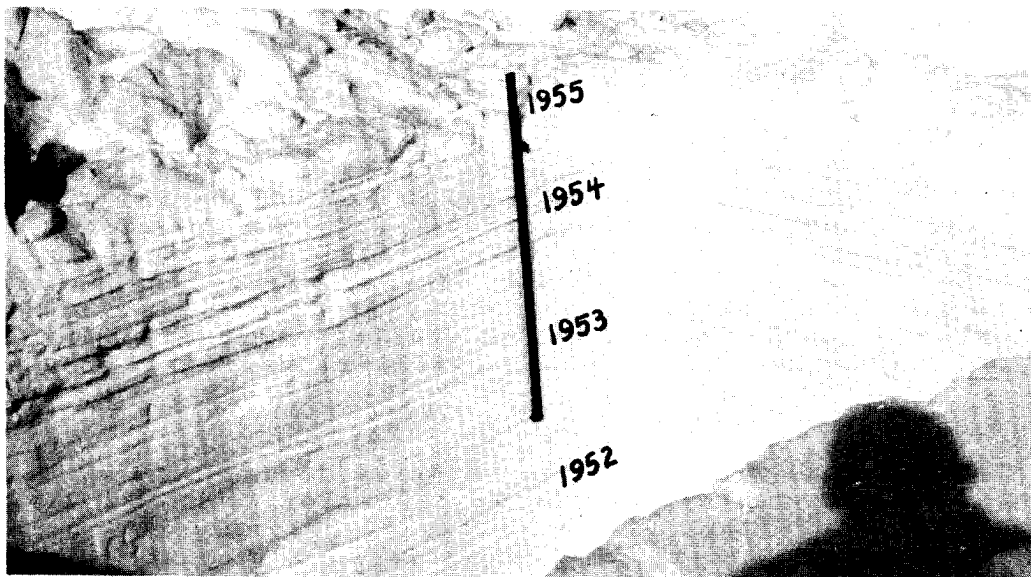
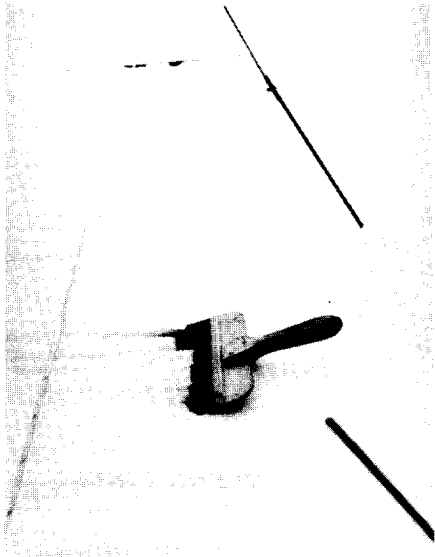


Figure 4b. Rear walls of a test pit showing strata which can be traced around the four walls of the pit. Summer layers of 1952, 1953, 1954 and 1955 (labeled) are slightly softer than the winter layers.



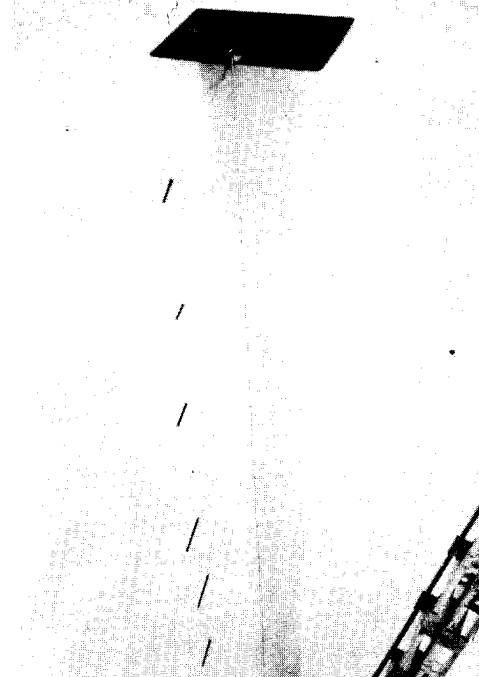
4c.



4d.



4e.



4f.

Figure 4c. Test wall of pit at station 2-60 (1954) prepared for sampling.

Figure 4d. Inserting density sample tubes. A thin metal plate used to push sample tubes beyond the face of the test wall makes the lines cutting across the circles. Samples were placed in an attempt to get representative measurements for individual layers, but sometimes it was impossible to avoid sampling across layer boundaries. Placement of tubes with respect to a hard layer is shown.

Figure 4e. Pit at station 2-30 (1954) covered because of wind. Right edge of "slot," left when density tubes are sawed out, is nearly vertical so that a thin slice can be cut from it to prepare photo sections (e.g., Figs. 5, 8).

Figure 4f. Test wall at station 4-0 (1955) with thin section cut from left edge of slot. Dowels placed in prominent low-density summer layers. 1951 summer is not marked; it was abnormally cool and produced a minimum discontinuity (see data sheets).

Density, stratigraphy, and grain size

The standard USA SIPRE 500 cm³ snow-sampling tubes were used for density measurements.

Stratification in firn, as in other sediments, reflects differences in the environment of deposition and diagenesis. Snow is unlike other sediments in that it does not record variations in the source of supply. Discontinuities between firn layers are often abrupt and stand out clearly when the test-wall is brushed (Fig. 4b). Brushing was done before the tubes were placed, so that sampling across layer boundaries could be avoided as much as possible (Fig. 4a, d). The brushing technique is not useful below 6 m because of increased hardness. When all tubes were placed (70-80) and their locations recorded, a detailed stratigraphic description was made with special attention to evidence of melt and wind action. Noteworthy relations between tubes and layer boundaries, especially when boundaries were cut by tubes, were shown by brief sketches.

The characteristics of individual snow and firn layers affect the accuracy attainable in density measurements. The reproducible accuracy in homogeneous ice-free firn layers varied from ± 0.003 to ± 0.005 g/cm³. Layers affected by melt are more difficult to sample, iced firn being the worst. Accuracy is possibly ± 0.01 g/cm³ in such material. The overall accuracy throughout was of the order of ± 0.005 g/cm³. Significant density variations between firn layers are greater. Changes of 0.02 to 0.03 g/cm³ are common and abrupt changes of 0.10 g/cm³ are not rare.

Grain-size differences were determined by sieve analyses on selected layers (Fig. 17, 18). The sieving was done in the pit bottoms where air temperature was below -15C. Photomicrographs of grains (magnifications of 9, 18 and 28 diam) were taken as a record (Fig. 19).

Photography

Taking samples of firn to the office or laboratory for subsequent study is prohibitively expensive and inconvenient. Since photographs of properly brushed pit walls do not always reveal sufficient detail, as is apparent in Figures 4a-f, two techniques were developed to obtain photographic records of stratigraphic features.

Stratigraphic photo sections ("thin sections"). When the density tubes are completely removed from the test wall, a slot remains (Fig. 4e). The walls of this slot were made as smooth and vertical as possible; horizontal cuts through them were avoided. A slice 8 to 10 cm thick was sawed from one side of the slot extending from the snow surface to the test wall base. Such sections have considerable strength and could be carried out of the pits and assembled in proper order on the snow surface even though some layers were loosely bonded. They were trimmed with a saw to a thickness of 1 to 2 cm (Fig. 5a, b) assembled with top at left (observer facing sun), and finally cleaned with a trowel and whiskbroom until nearly uniform in thickness. Dowels were set at 1 m intervals along the final assembly. An overall photograph was made of each "stratigraphic section" (Fig. 5c) followed by a close-up photo of each meter (Fig. 5d).

Strata of high and low density correlate well with dark and light layers respectively on the photos (Fig. 8). However, slight differences in the transmission of light through firn layers cannot be correlated directly with density because factors such as icing, grain size variations, and thickness of the section are involved.

Pit wall photography. The above technique is effective on clear days when direct sunlight is available, but it does not work on cloudy days or during "whiteouts." On such days, the technique shown in Figure 6a was used. When bright sunlight is available, the upper meter of the test wall may be photographed after brushing, taking full advantage of shadows (Fig. 6b). Details of deformed strata can be made more photogenic by exposing a cleanly-brushed section to the flame and smoke of a blowtorch, because capillary absorption of the moisture so produced differs within the strata (Fig. 6c).

Elevation Measurements

In 1953 two separate records of elevation measurements were kept: one by George Toney of the U. S. Weather Bureau, and one by Robert Zavadil in connection with his gravity studies (Barnes and Zavadil, 1954). Corrections for atmospheric pressure changes were applied from records at Thule and at several stations maintained on the ice sheet during the field season.



Figure 5a. Slices about 10 cm wide sawed from slots in the test walls (Fig. 4e) were carried to the snow surface where thin sections were sawed from them.

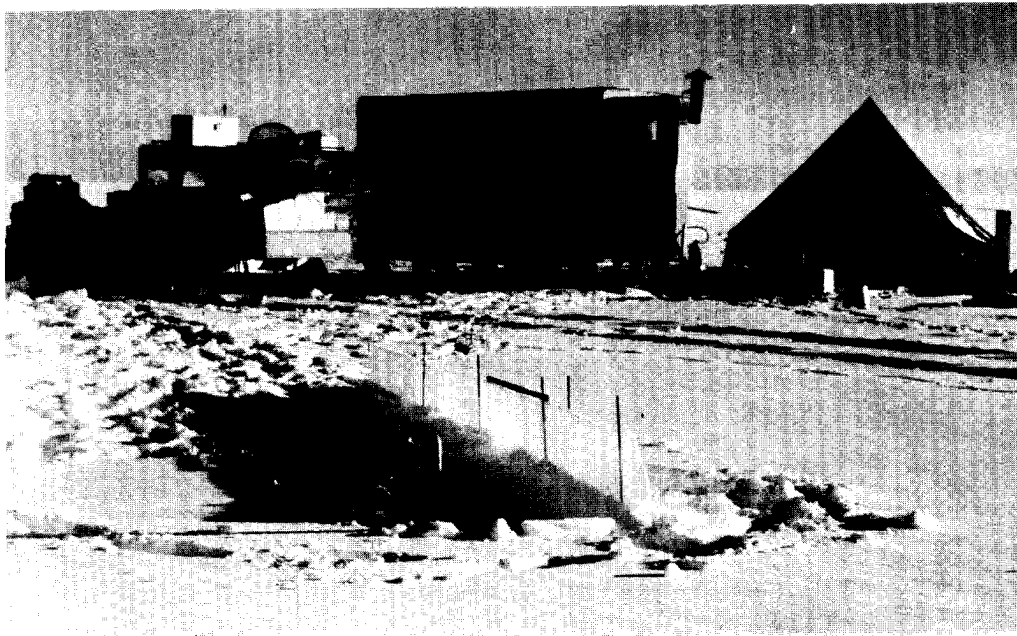


Figure 5b. Thin sections, trimmed with trowel and broom to a final thickness of 1 to 2 cm, are assembled with top at left ready to be photographed.

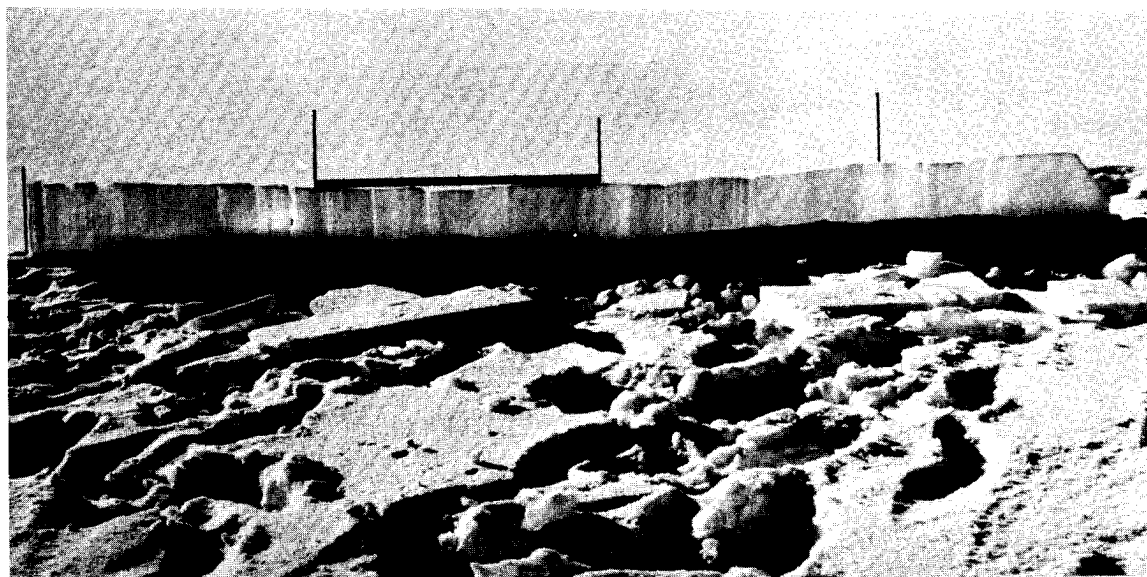


Figure 5c. Stratigraphic section from top 4 m at station 2-90 (1954). Dowels indicate 1 m intervals, top of section is at the left.

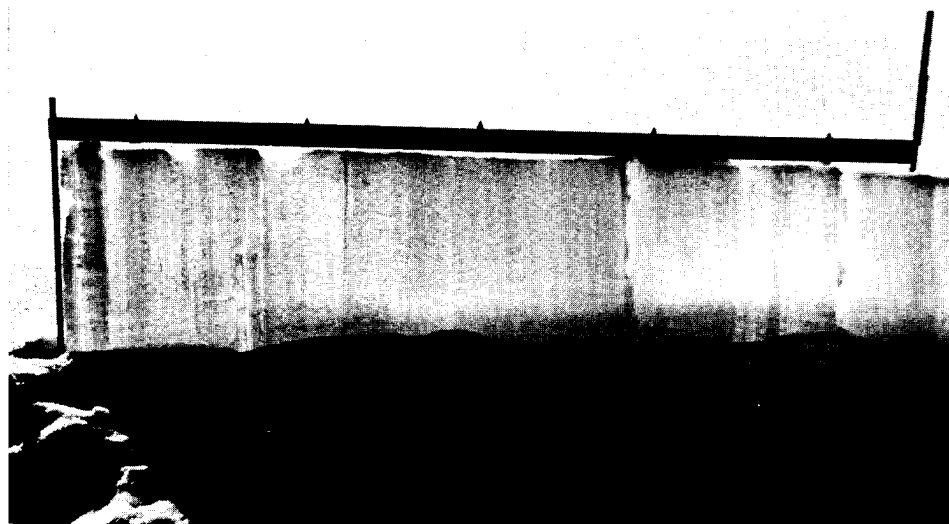


Figure 5d. Top meter of the section shown in Figure 5c. Close-up photos such as this, taken of each meter at most stations in 1954 and 1955 serve as detailed supplements to the stratigraphic field notes. Brass clips fastened to the meter stick facilitate measurements. In these photos the clips are at 10, 30, 50, 70, and 90 cm.

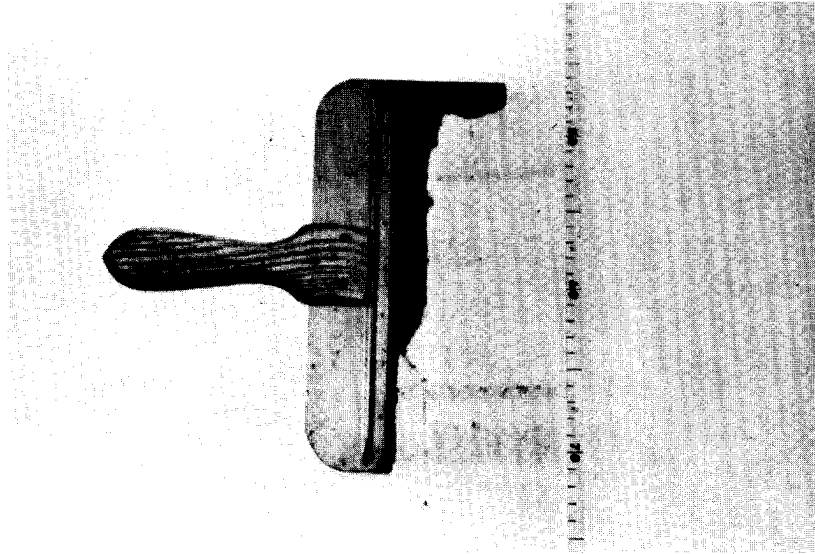


Figure 6a. Station 2-100 (1953) depth range 140 to 177 cm. Stratigraphic detail photographed by inserting a dark trowel behind the pit wall. The trowel must be inserted very carefully to avoid breaking the brittle snow.

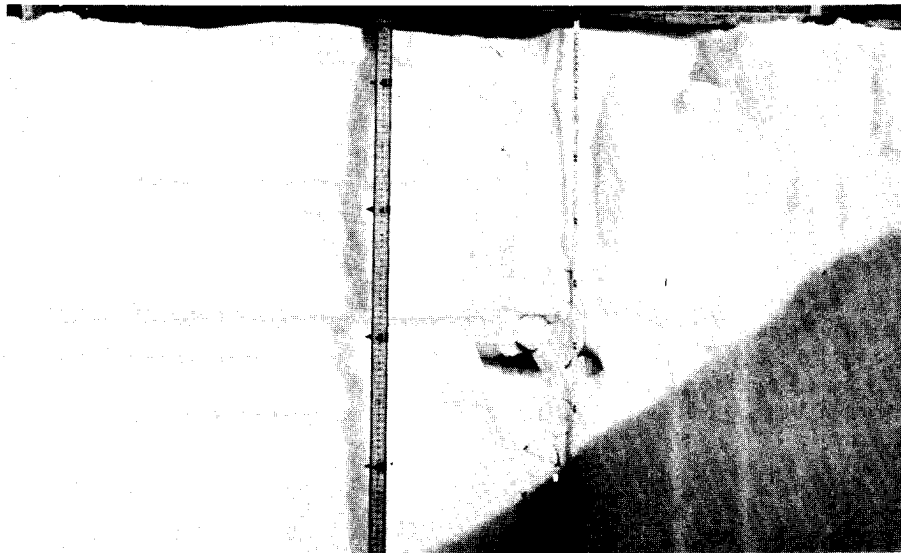


Figure 6b. The top 90 cm at station 1-50 (1954) was photographed using shadows. The 5 cm soft layer overlain by three closely spaced wind crusts at 45 cm was identified at stations 1-50, 2-0, 2-10, and 2-20, i. e., for 30 miles (see 1954 data sheets).

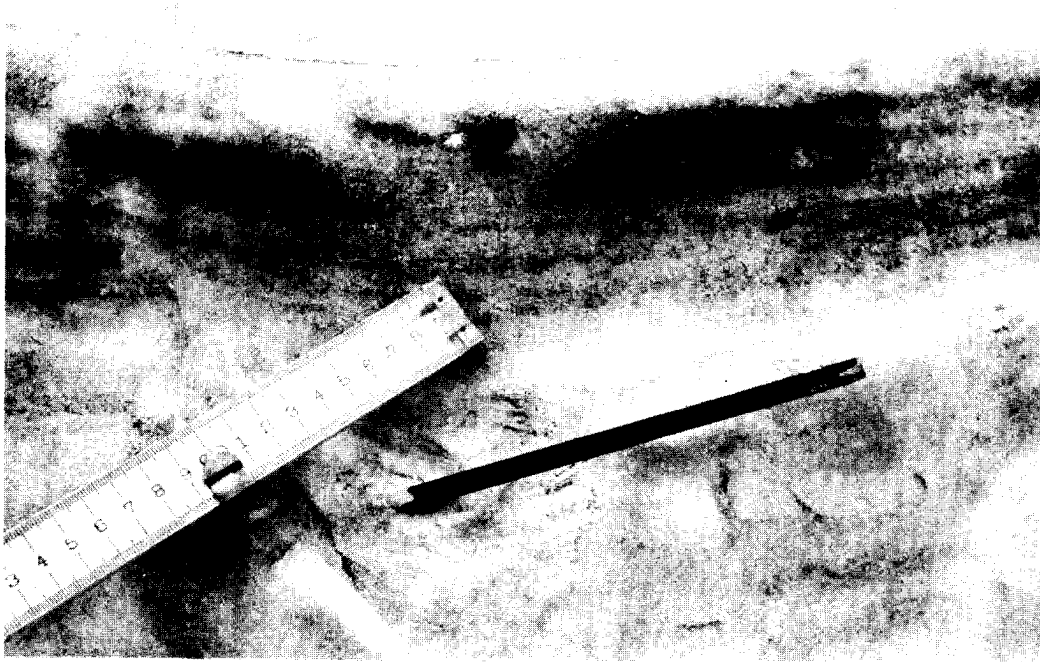


Figure 6c. Close-up of strata exposed at station 2-30 (1954). The pit wall was exposed to the flame and smoke of a blowtorch to make details more photogenic. The buried surface of 2 August 1953 has been broken by a footprint at the point marked by the arrow. Unbroken layers have drifted into the footprint.

In 1954 elevation differences between stations were recorded by a Paulin-system surveying altimeter with readings made at 1 mile intervals. The time scheduled was 1 mile in 10 min; thus, the 10 mile moves between stations were completed in 1 hr and 40 min, reducing the number of barometric changes important to the elevation program. Parts of the trail were covered four times; the entire trail was covered twice. The records from 1953 and 1954 agree well with each other (Benson, 1959).

In 1955 the altimetry program was carried on as in 1954 with the added improvement of using two altimeters. The expedition vehicles were split into two groups of two weasels each. One group recorded barometric variations at a pit station while the other group made altimeter readings for every mile enroute to the next station. The time schedule required motion of both groups for about 2 of the 5 hr required for the 25-mile move between stations.

CHAPTER III: STRATIGRAPHY AND ACCUMULATION

Introduction

Stratigraphic work in firn consists of identifying variations in a layered sequence and extending recognizable features laterally by correlation with other measured sections. The objectives are similar to those of stratigraphic studies of other rock formations, but there are obvious differences in technique. Although differences between firn layers are often easy to see or feel, measurements of density, hardness and grain size are necessary in order to express these differences quantitatively. The walls of hand-excavated pits constitute the "exposed sections." The primary objective is to determine the prevailing environmental conditions on the ice sheet, and the identification of annual units of accumulation is one of the more significant results.

Stratigraphic relations were initially studied by excavating pits at selected sites each year. It was found that individual firn layers maintain their identity as they are buried under the snowfall of succeeding years and that strata could be correlated between adjacent pits across traverses several hundred miles long. This knowledge made it possible to identify annual firn layers in pits dug in regions not previously visited.

Stratigraphic interpretations were checked using certain artificially established surfaces. The simplest method is the location of buried surfaces disturbed by foot and vehicle traffic (Fig. 6c). Such surfaces are observed by digging special pits at places known to have been previously disturbed by traffic. The 1953 summer surface was marked by spreading soot at certain locations. This works well where melting is slight. Also, dated aluminum tags were fastened 2 m above the snow surface on bamboo poles. In 1954 squares of plywood, about 30 cm (1 ft) on a side, were placed on the snow surface and located between two poles near each pit station. These boards identify precisely dated snow surfaces.

Markers placed on a pole do not, in themselves, provide valid measurements of accumulation because of snow settling around the pole. Therefore, pole-marker measurements were used only as a supplement and accumulation measurements are not based on them alone.

Since planes between strata exposed in pit walls represent buried snow surfaces, examination of the snow surface and the processes which operate on it is useful. The area under consideration is primarily a wind-blown desert of dry snow throughout the year. Typical snow surfaces are illustrated in Figure 7a-h.

Data from all stations are assembled on data sheets* and included at the end of this thesis. The location of each data sheet is indicated in Figure C1. In the text the data sheets are referred to by the numbers assigned in Figure C1.

An example of the correlation between pit data and the mosaic of thin-section photos is illustrated in Figure 8. The reason for drawing sharp boundaries between firn layers in the stratigraphic column and in the density profile is clear from the photomosaic in this figure.

Diagenesis without melt

Diagenetic changes in snow and firn are accelerated at higher temperatures. This behavior is related to poorly known details of atomic structure in the surface layers of ice and to the influence of temperature on this structure. Two related phenomena easily observed within 15 deg of the melting point are: (1) an increase in vapor pressure with temperature, especially above -10C, † and (2) the presence of a liquidlike film on ice surfaces; evidence of this is greatest within 5C of the melting point and nearly absent below -15C (Weyl, 1951; Nakaya and Matsumoto, 1953).

* The format of the data sheets is explained in Appendix C.

† Bader, *et al.* (1939), p. 9, gives a useful P-T diagram of the ice-water-vapor system. The following values are listed for convenient reference:

Temperature (C)	Vapor pressure of ice (mm Hg)
0	4.58
-5	3.30
-10	1.97
-15	1.26
-20	0.79
-25	0.48



7a.

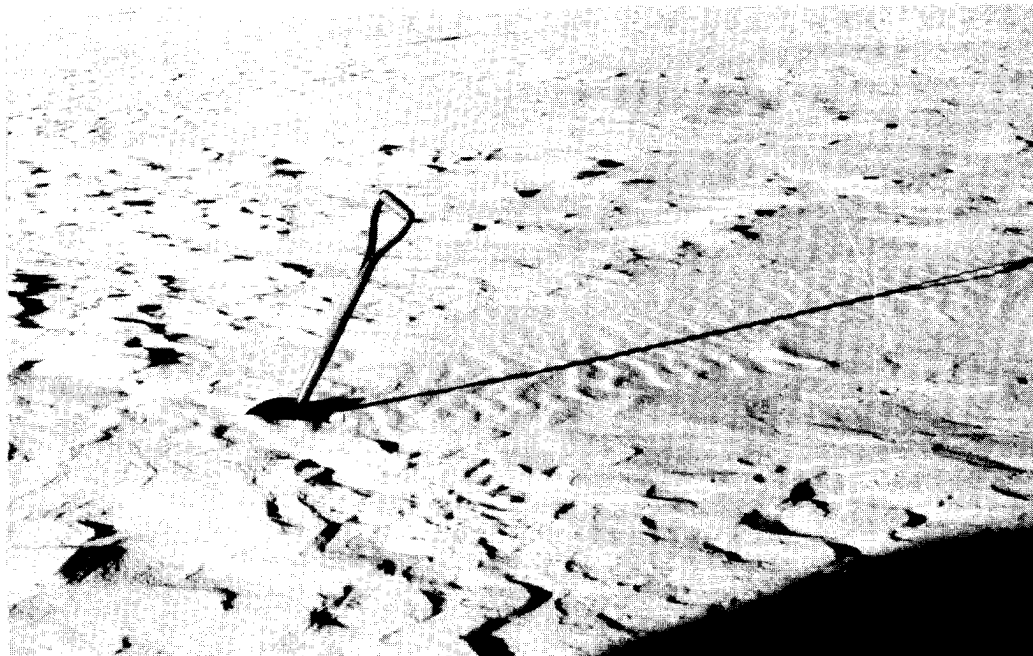


7b.

Figures 7a,b. Snow barchans near station 2-90, July 1954. The snow surface is being subjected to wind erosion and deposition. Material picked up from the surface is deposited on the crescent shaped dunes, "barchans." These snow barchans migrate at a rate of about 1 m/hr; they are moving toward the camera in Figure 7a and away from it in Figure 7b. The foreground of each is a typical eroded snow surface.



7c.



7d.

Figures 7c,d. Ripple marks on lee side of smooth areas. Wind movement from left to right in Figure 7c and from right to left in Figure 7d. Note erosional features in center of Figure 7d. Snow surface was so hard in 7d that it was not broken by men on foot (note absence of footprints to and from shovel).

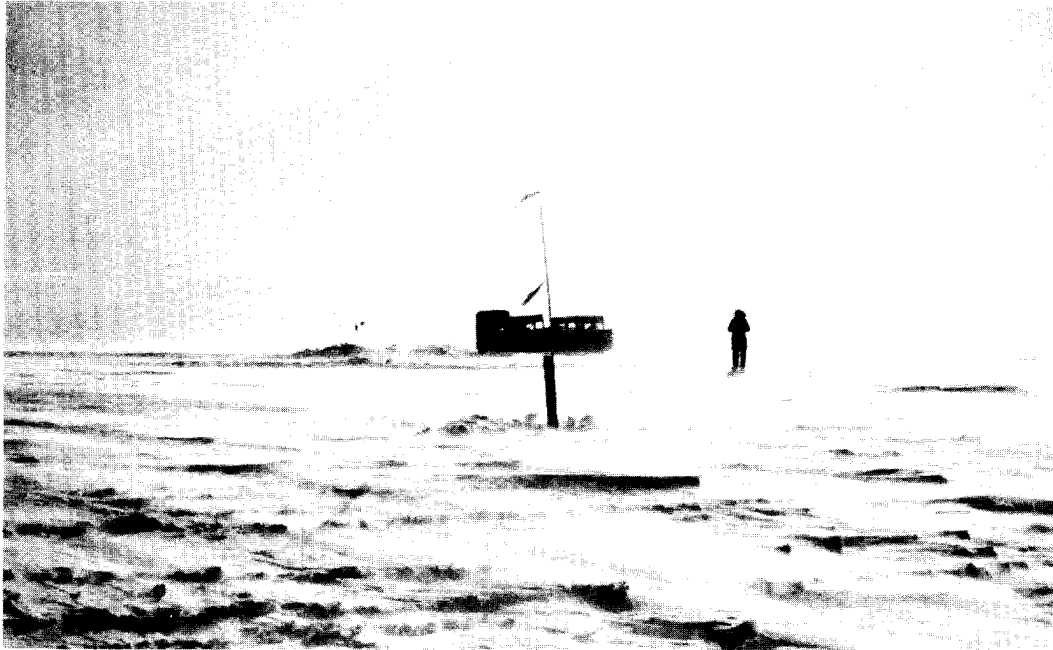


Figure 7e. Drifting snow moving from right to left. Surface erosion is taking place and barchans are beginning to form.



Figure 7f. Blowing snow at the tail end of a severe blizzard (gusts over 70 mph). The camp of four weasels is shown after 12 hr at station 00-20, 12 June 1954.



Figure 7g. Snow drift formed between 0200 and 1400 at station 00-20 on 12 June 1954. The tracks which go under the drift were made 12 hr before this photo was taken.



Figure 7h. Sastrugi at station 2-0, 4 Sept 1952. Sastrugi are erosion-deposition features formed by wind. They are often very hard (Fig. 20) and have caused serious damage to vehicles and sleds. The surface shown here is typical of that present between stations 1-30 and 2-30 after the blizzard of 2 Sept 1952 (see pages 32-33 and Figure 20).

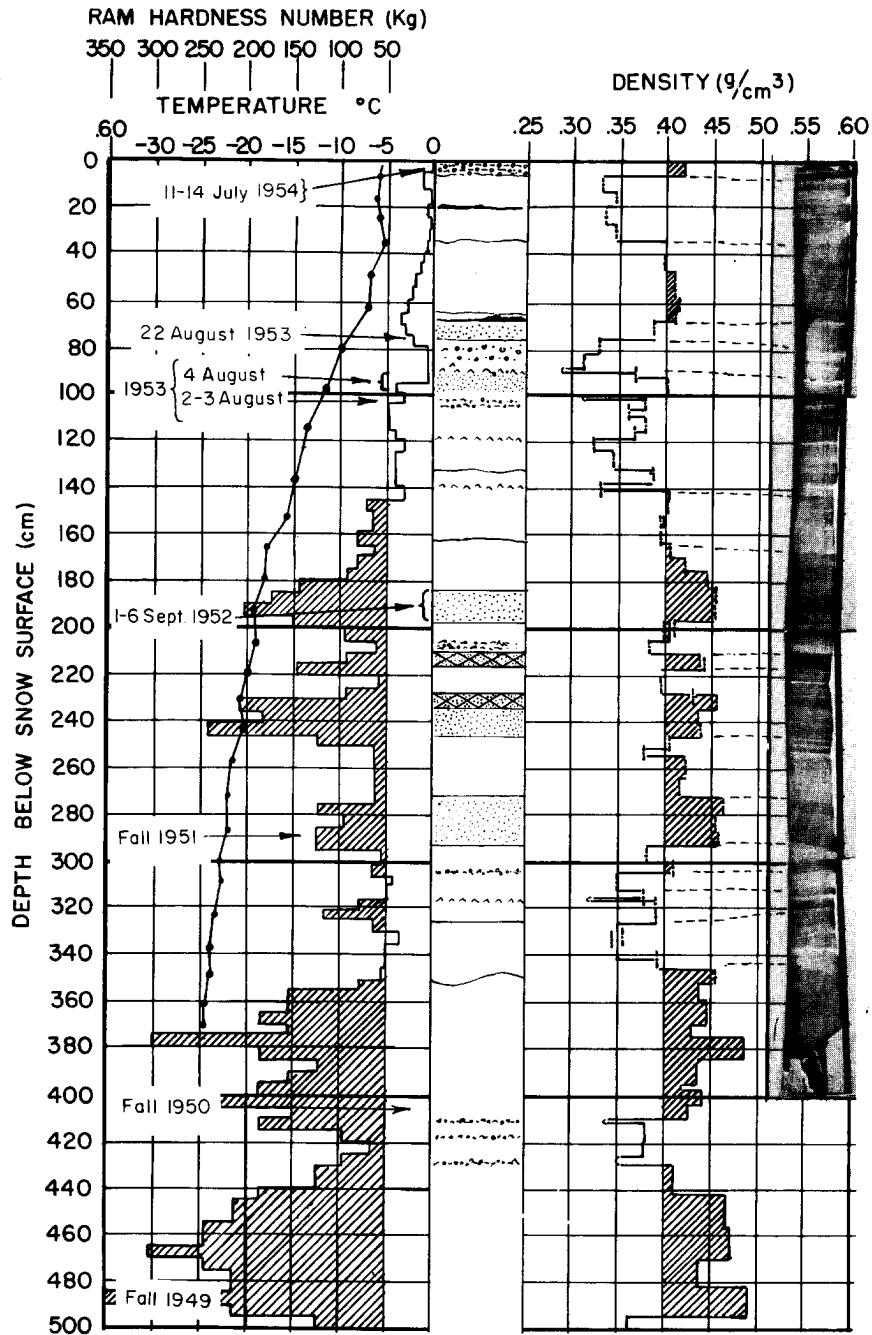
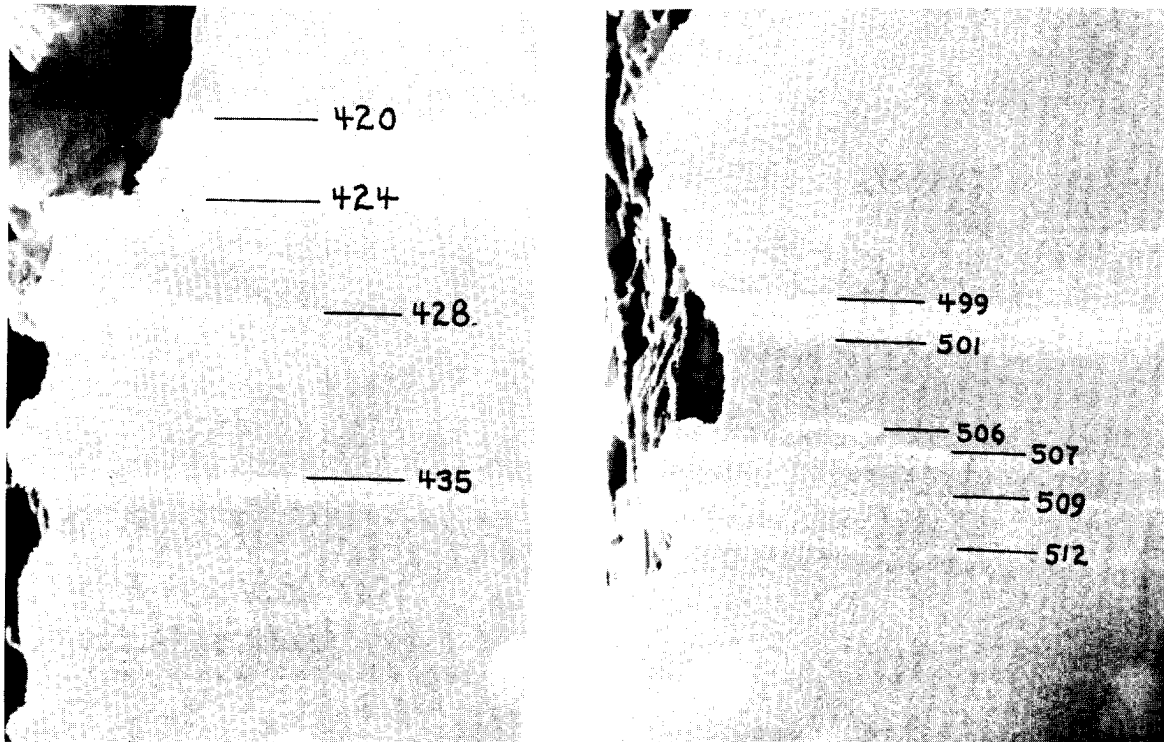


Figure 8. Stratigraphic data and photo section for station 2-90, 20 July 1954. Strata of high and low density generally correlate with dark and light strata respectively on the photos. Layer boundaries are usually well defined although not always horizontal. The wavy layers near 350 cm depth probably represent a buried snow surface similar to the ones shown in Figure 7a, b, and h.



a. Detail of the iced-firn layer of 1949 at 420 to 424 cm. The small ice lens at 428 cm was formed by percolation (Fig. 10). The thin layer of coarse, bonded grains at 435 cm resulted from an earlier period of surface soaking during the same year.

b. Detail of the 1948 summer melt layers. The iced firn between 499 and 501 cm resulted from the warmest period of the 1948 summer. The small ice lens at 506 cm resulted from percolation. Other melt crusts are shown at depths 507, 509, and 512 cm. All depths measured from the snow surface of August 1953.

Figure 9. Layers of iced firn at station 2-100, 1953.

In firn strata these phenomena give rise to vapor transfer and sublimation, together with migration of near-surface molecules. The net results are changes in grain size and shape and in the bonds between grains. Such changes are most pronounced in newly fallen snow and in layers of very fine-grained firn, because they have maximum surface area per unit mass (Bader, *et al.*, 1939; deQuervain, 1945).

Diagenesis with melt

The extent of summer melting varies greatly over the traverse, and the following concepts are useful:

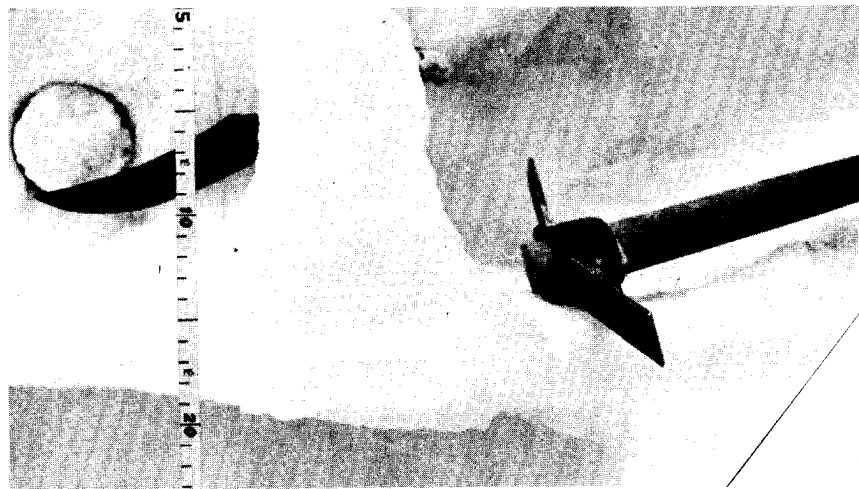
Soaking

When a given mass of snow is at 0°C and wet throughout, it is said to be "water-saturated" or "soaked." When soaked firn refreezes it becomes "iced firn." Iced firn layers in the stratigraphic section indicate melt which occurred on the snow surface (Fig. 9).

If the snow at a particular location becomes soaked down to the level which had been soaked during the previous summer, then that location is subject to complete soaking.

Localized percolation

Melt water can percolate downward along restricted "channels," and move laterally along favorable layers. This can occur in snow with negative temperatures, only the percolation channels being at the melting point. While active, the percolation channels



a. Ice gland formed during the summer of 1950 at station 1-0 and observed 5 m below the snow surface of July 1953 (see Data sheet 3).



b. This ice gland, with layers and lenses formed at station 2-70 during the heat wave of 11 to 15 July 1954 (Fig. 12). The zero point on the meter stick is at the left and marks the 1 m depth in the pit. The ice layer at 110 cm, and the lens at 130 cm formed on depth hoar layers (see station 2-70, Data sheet 5). Percolating melt-water, originating at the snow surface during the four warm days, penetrated nearly 2 m below the snow surface which at this station includes 2-yr accumulation. The ordinary effect of a summer here is to produce only a crust of iced firn as in Fig. 9.

Figure 10. Ice masses in snow strata.

Figure 11. Percolation of gasoline in snow at -30C at station 0-5, 27 March 1953. Two minutes after pouring gasoline on the snow surface a vertical cut exposed the network of glands and lenses shown here. The temperature profile measured in the snow during this test was:

Depth (cm)	Temp (C) (to the nearest half deg)
0	-30.0
8	-29.5
19	-29.0
25	-28.0
32	-26.5
40	-25.0
47	-25.0
52	-23.5
61	-23.0
68	-23.0



appear slightly slushy (Fig. 13); they refreeze to form ice glands, lenses, and layers (Fig. 10a, b).

Ice layers, lenses, and glands are described as follows:

- a) Ice layers extend over large areas parallel to the strata with only minor interruptions.
- b) Ice lenses are lens-shaped layers which pinch out laterally. They are parallel to the firn strata.
- c) Ice glands are pipe-like vertically extending masses which occasionally spread laterally to form lenses and layers. They are the frozen percolation channels which feed lenses and layers.

Lenses and layers are "concordant structures" whereas glands are "discordant."

Percolation of moisture through snow and firn is primarily a wetting process, and subsurface melting is not an essential part of the mechanism (see Fig. 11). When the percolating liquid is water, the temperature of the percolation "channels" is raised to the melting point. However, temperatures several degrees below the melting point have been measured between channels within the percolation network.

Melt phenomena observed at station 2-70, 11 - 15 July 1954

The process of surface melt, percolation, and refreezing to form iced firn on the surface, and ice glands, lenses, and layers at depth, was observed at station 2-70 during the exceptional "heat wave" of 11 - 15 July 1954. The heat wave was accompanied by a slight drizzle (apparently produced by the occlusion of a front over the area centered at 2-0) up to altitudes of about 7000 ft. Summer rains are common at sea level in polar regions but very rare at altitudes above 6000 ft at 77° N latitude. Air temperature records during this heat wave and the one of 10 - 15 August 1954 are summarized in Figure 12. Negligible melt occurred above 7500 ft, but the effects of the heat wave and its precipitation were recorded by the formation of a wind slab (see Fig. 32c). The melt process observed at 2-70 during the 11 - 15 July "heat wave" will be described in some detail because it illustrates the general mechanism.

A pit was dug on 13 July solely for the purpose of observing melt action in the firn. The snow surface was at 0C and damp. Slightly damp slushy lenses, layers, and glands were observed on the pit walls (Fig. 13). They were best developed near a large ice gland at one corner of the pit. The snow and firn near the active percolation channels remained at subfreezing temperature.

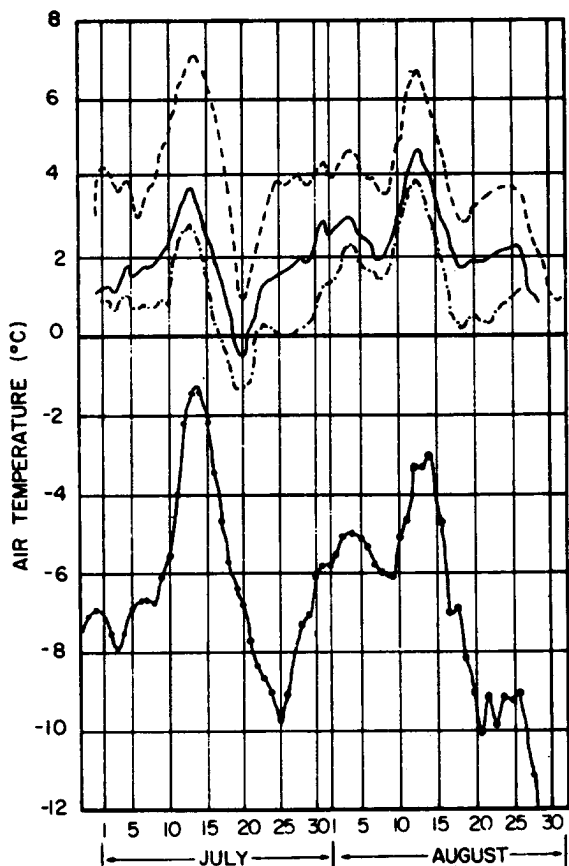


Figure 12. Daily mean air temperature (5-day running means) at:

Station	Elevation (m)
0-0 (Camp Tuto)*	480
0-1 (Thule ramp)*	569
0-6 (Hardtop)*	736
2-100 (Site 2)†	1990

* Schytt (1955, p. 5)

† Site 2 Meteorological data, (USAF Air Weather Service).

Surface melt features. Surface melt usually results in layers of iced firn consisting of clusters of grains bonded together by frozen melt water. They form continuous, concordant strata which may be traced around the four walls of a test pit and are excellent stratigraphic horizons. Small ice glands and lenses are often found directly beneath layers of iced firn (Fig. 9).

Subsurface melt features. Subsurface melt features are produced by surface melting, percolation, and subsequent refreezing of the melt water. They are relatively clear ice masses with variable dimensions and, during an exceptionally warm period, may penetrate the firn of several previous years (Fig. 10b). The ice masses are usually so irregular that they cannot be traced around the four walls of a test pit. Individual ice lenses or layers are not good stratigraphic marker beds; however, a zone of abundant icing beneath a crust of iced firn constitutes a good stratigraphic unit. In lenses of variable thickness, the lower contacts are more nearly parallel to the strata. The latter observation has also been made in Spitsbergen (Ahlmann, 1948, p. 17).

On 15 July the percolation network had refrozen and ice masses were exposed on the walls of a new pit dug on that date for stratigraphic studies. The main ice lenses and layers spread out from the large ice gland shown in Figure 10b. Three temperature profiles measured in the top 2 m of the 15 July pit are shown on Data sheet 5 and in Figure 25. Profile 1, from the test wall, was not near a major ice gland and shows the normal mid-July decrease in temperature with depth. Profiles 2 and 3 show the warming effect of the percolation network surrounding the ice gland of Figure 10b.

The snow surface showed two interesting features after the heat wave:

(1) The top 3 to 5 cm consisted of a crust of iced firn with a pockmarked surface (Fig. 14).

(2) Slight depressions, spaced several meters apart, were everywhere (Fig. 14). Such surface depressions are probably located directly over major ice glands as hypothesized by Sharp (1951). Ice glands represent extreme local densification and the snow surface is the most likely place to expect an expression of this reduction in volume. This hypothesis was not checked by digging beneath the depressions in search of ice glands, but the spacing and arrangement of major glands is similar to that of major surface depressions. Also, depressions and glands formed simultaneously at station 2-70 during the only time that the formation of either was actually observed. Furthermore, surface depressions, like those of Figure 14, were seen only on this occasion in the percolation facies and were never seen in the dry snow facies.

Summary

The two basic types of melt may be generally classed as "surface" and "subsurface."

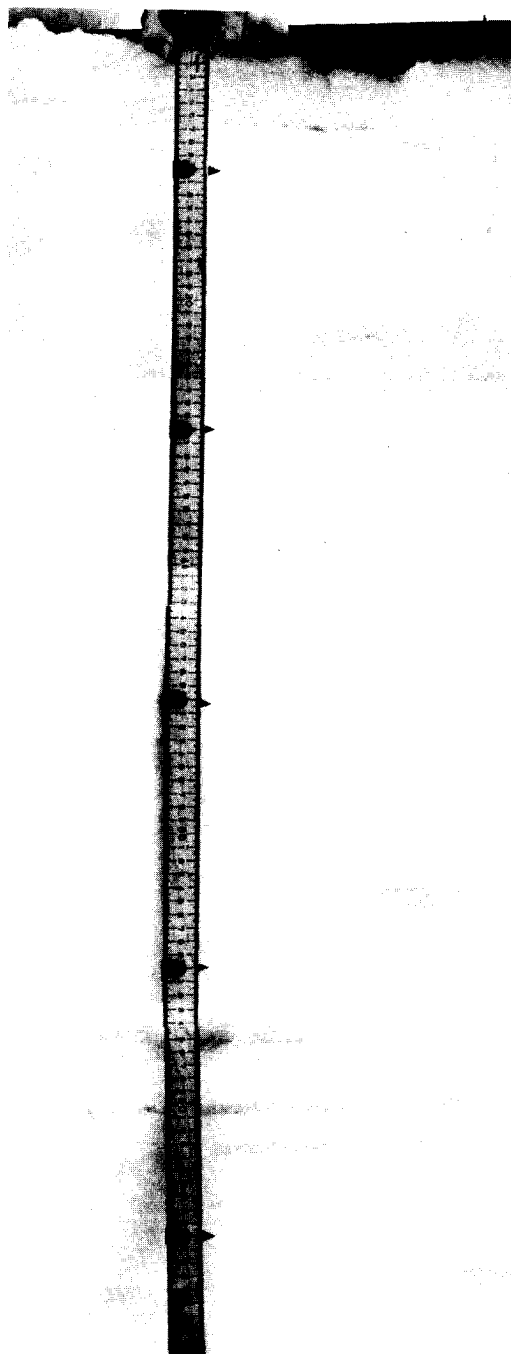


Figure 13. Active percolation channels. The pit wall shown was exposed on 13 July 1954 at station 2-70. The ambient snow temperature was -6 to -10°C (see Data sheet 5 and Fig. 25), yet percolation channels caused the slushy lenses shown here. Temperatures as low as -6°C were recorded between the wet slush-lenses at 70 and 91 cm.

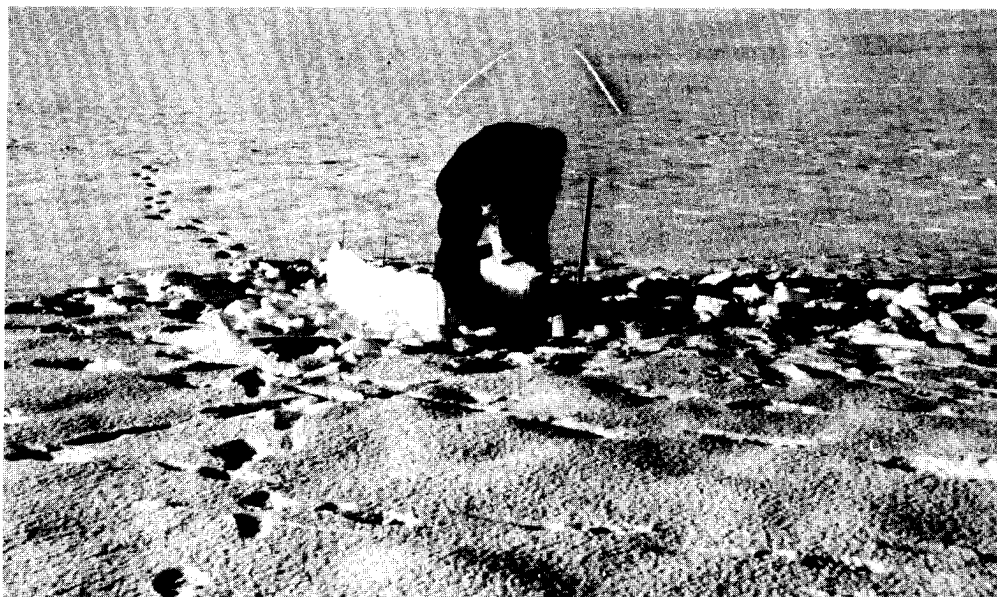


Figure 14. Frozen melt crust at station 2-70, 15 July 1954. The melt crust was 3 to 4 cm thick and resulted from the mid-July heat wave (Fig. 12). The depressions spaced about 1 to 2 m apart probably form over large ice glands such as illustrated in Figure 10b. The spacing of the large ice glands is about the same as the spacing between depressions. The glands and depressions both formed during 11 - 15 July 1954 (see p. 22).

Diagenetic facies defined on glaciers

A cursory glance at the data sheets reveals regional differences in the physical properties of the upper firn layers (compare Data sheets 1, 6, 7, and 10). The differences are caused primarily by variations in the effect of summer melt. A spectrum of melt action exists on the ice sheet. It varies from the extreme of melting the entire annual accumulation at some locations, to the complete absence of melt at others. This spectrum may be subdivided into four distinctive regions. Stratigraphically, these regions are facies. The ice sheet is thin in relation to its areal extent, and the facies actually represent lateral variations in the properties of a single stratigraphic unit, even though altitude, rather than distance, is used as a parameter in defining them.

Regional differences apparent on the data sheets are partly time-dependent as the observations span nearly 7 of the 12 months in a year. The concept of facies includes the element of time because the boundaries are established with respect to that time when maximum melt conditions prevail. During winter at 77° N the environment of deposition and diagenesis varies little from the edge of the ice sheet to the center. During summer, this region shows wide variation in its diagenetic environment, and these variations produce the facies.

Consider the diagenetic environment of a single annual layer of snow accumulation, spanning a range of elevations from sea level to the crest of the ice sheet, during the peak of the melt season. Below the firn line, the snow cover is stripped away revealing bare glacier ice. Complete soaking occurs between the firn line and the upper limit of complete soaking, the saturation line. Localized melt water percolation occurs between the saturation line and the upper limit of surface melting, the dry snow line. The firn line, saturation line, and dry snow line are facies boundaries separating the ablation, soaked, percolation, and dry snow facies. Figure 15 is a diagrammatic sketch of these relations.

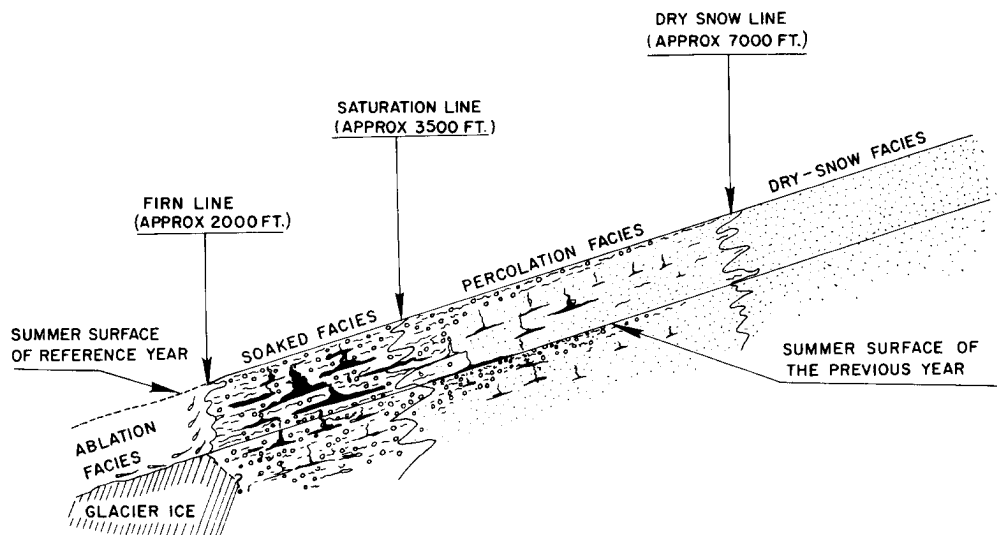


Figure 15. Generalized cross-section of glacier facies. The snow cover is completely stripped away in the ablation facies. The entire year's accumulation is raised to the melting point and wetted in the soaked facies. In the percolation facies the annual increment of new snow is not completely wetted nor raised to the melting point, and the amount of percolation decreases with altitude, becoming negligible at the dry snow line. Negligible melt occurs in the dry snow facies.

A quantitative classification of glaciers can be established on the basis of diagenetic facies. This will be presented at the end of Chapter V after demonstrating how facies boundaries are defined by measurements of firn temperature, ram hardness, and firn density.

Grain size

The international classification of snow grain size proposed by Schaefer, Klein, and deQuervain (1951) was used in this study with a subdivision of the medium-grain range (Fig. 16). Fine dust-like snow which drifts along the surface (Fig. 7f, g) has grains less than 0.1 mm in diam, while grains in soaked layers often exceed 4 mm. By far the majority of measured grains in non-soaked strata lie within the two Wentworth grades bounded by $\frac{1}{2}$ and 2 mm, or between +1 and -1 on the phi-scale of Krumbein (1934); the median diameter is between 0.5 and 1.0 mm. Grain size distribution histograms using the subdivisions of Figure 16 are shown in Figure 17.

Most samples are well sorted, although not to the extreme found in some beach deposits. They are comparable to St. Peter sandstone. Cumulative curves from several sediments are compared in Figure 18. Detailed analyses as shown in Figures 17 and 18 are not necessary for routine stratigraphic observations.

Grains in firn strata which have not been exposed to melt action are often slightly angular and predominantly less than 1 mm (Fig. 19a). When surface melt and soaking occur, grains become larger, more rounded, and are often bonded into clusters. The dimensions of clusters may exceed 5 mm, while individual grains are primarily larger than 2 mm with only about 10% less than 1 mm (Fig. 19b, c). Grains exposed to temperatures within about 5 deg of melting, but not soaked, fall in the medium-size range, between 1 and 2 mm. Their appearance differs from that of soaked grains only in degree; they are rounded and sometimes bonded together, but both the individual grains and the clusters are smaller than those of soaked layers (Fig. 19d, e).

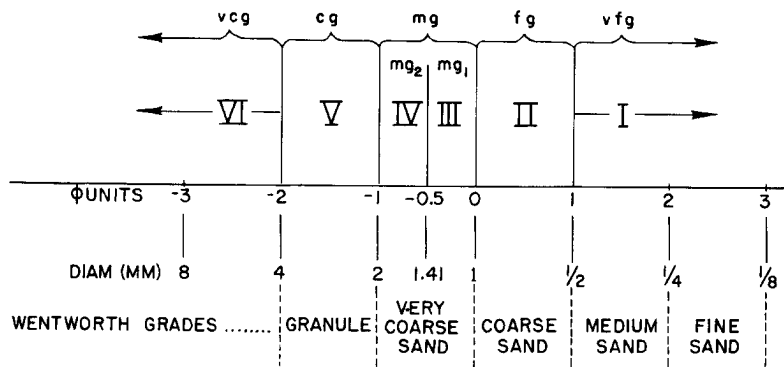


Figure 16. Grain size classification.

Classification of Schaefer, Klein, and deQuervain (1951).

vfg	very fine	< 0.5 (mm)	a
fg	fine	0.5 - 1.0	b
mg	medium	1.0 - 2.0	c
cg	coarse	2.0 - 4.0	d
vcg	very coarse	> 4.0	e

The numbers I through VI were used in this work with the medium grain range subdivided as shown.

The ϕ scale is defined as follows:

$$\phi = -\log_2 \xi, \quad \text{or} \quad \xi = 2^{-\phi}$$

where ξ = diameter in mm (Krumbein, 1934).

Crystal growth by sublimation produces hexagonal cup-shaped crystals (Fig. 19c) and irregular growth of depth hoar on individual grains or grain clusters (Fig. 19b, c). Grains rounded by melt and refrozen, but not subjected to significant crystal growth by sublimation, retain smooth surfaces (Fig. 19d, e).

Description of three stratigraphic features

In addition to the melt products described above, other stratigraphic features, useful in correlation, are: depth-hoar layers, wind slabs, and wind crusts.

Depth-hoar layers

"Depth hoar . . . is the most coarse-grained type of snow that can form without the presence of the liquid phase. It has a porosity of 67 to 78% and consists mostly of well-developed, clearly hemimorphic crystals with a base, a prism, and pyramids. . . Complete cup formations are often in evidence" (Bader, et al., 1939, p. 16).

Some depth-hoar layers have vugs with dimensions of several centimeters.

There is very little bonding between grains in a depth-hoar layer. It consists of a loose skeleton structure of ice crystals which will often collapse if disturbed. Depth-hoar layers, especially thick ones, are excellent stratigraphic horizons which can be correlated for hundreds of miles.

In addition to layers clearly recognized as depth hoar, other soft, loosely bonded layers consisting mostly of rounded grains exist. These are classified as depth-hoar layers in description of the stratigraphic section, or simply as coarse loosely-bonded layers. They most likely represent depth-hoar layers in which the grains have become rounded by sublimation over a period of several years.

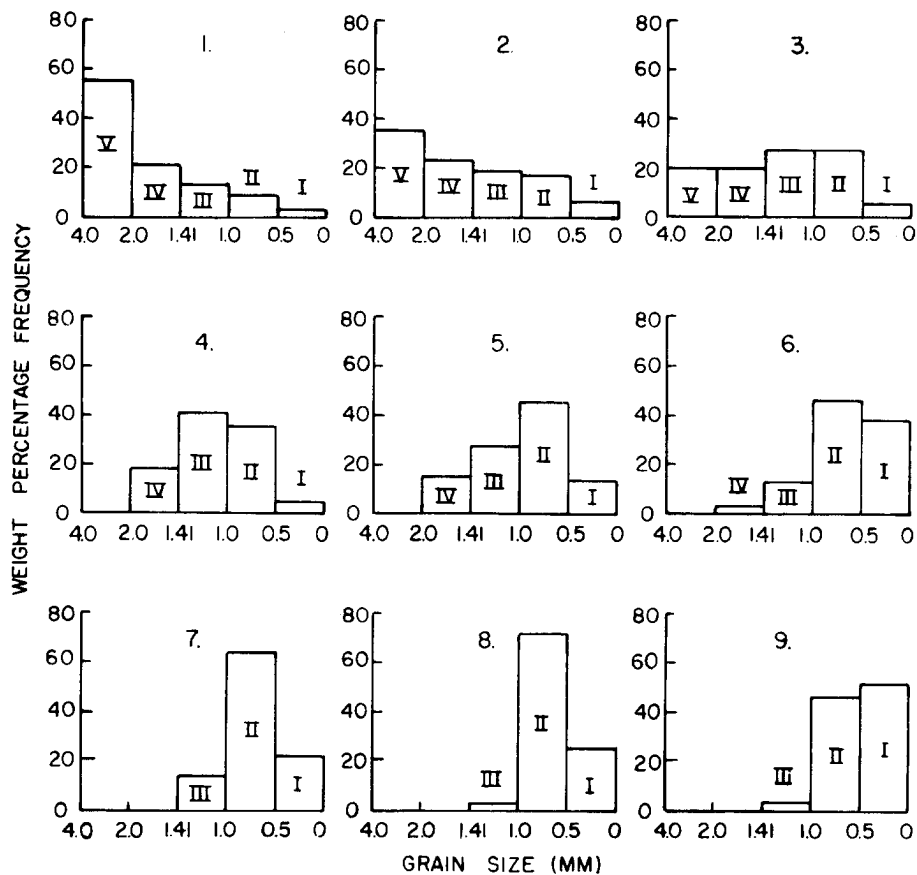


Figure 17. Histograms of snow grain size in non-soaked facies.

Sample	Station	Depth (cm)
1	4-0	275-276
2	2-0	378
3	2-0	162
4	2-225	78-83
5	1-0	110
6	1-0	240
7	2-30	60
8	2-30	160
9	1-0	30

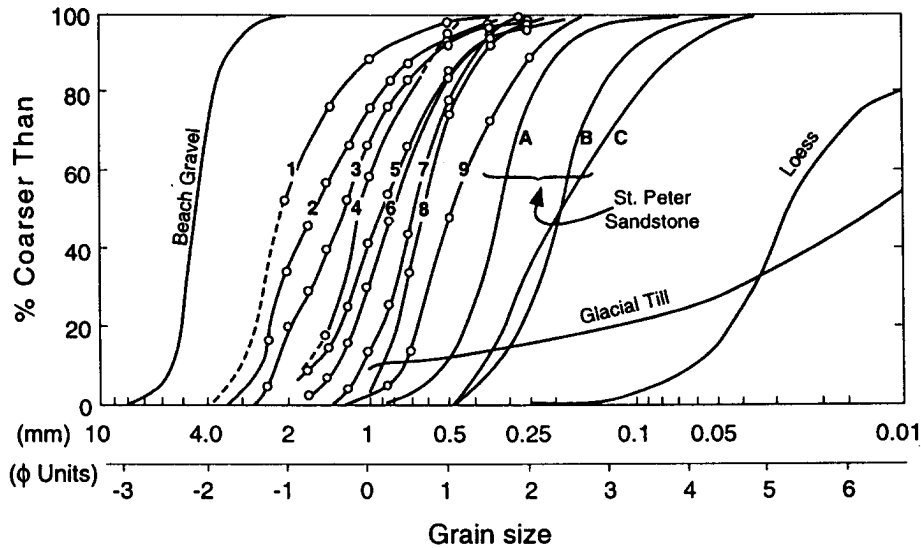


Figure 18. Cumulative curves. Curves 1 through 9 from the Greenland ice sheet were plotted from the data of Figure 17. Curves from St. Peter Sandstone were obtained by Thiel (1935) in the upper Mississippi Valley as follows:

Curve	Identification
A	0-10 ft from top
B	30-40 ft from top
C	Avg of 72 samples

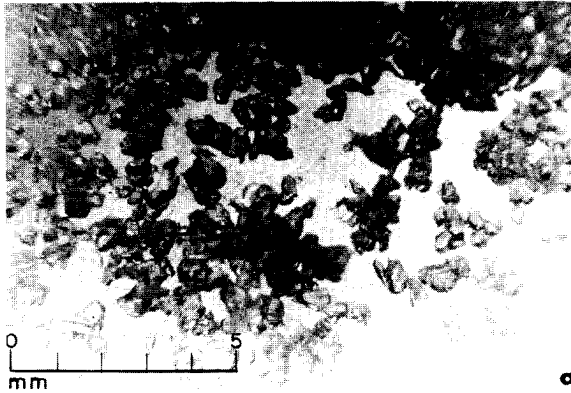
The other curves were obtained from the following sources:

- Beach gravel curve, Krumbein (1936)
- Glacial till curve, Krumbein (1933)
- Loess curve, Krumbein and Sloss (1951)

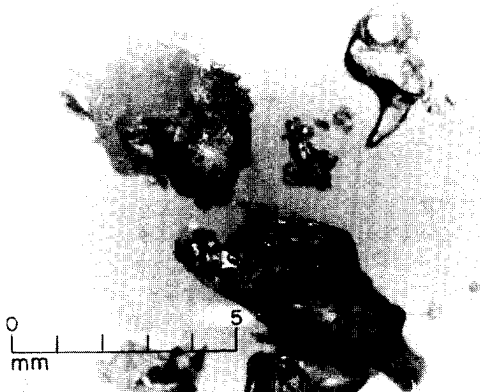
Wind slabs

Wind slabs consist of rounded, firmly bonded, fine or very fine grains. Viewed from a little distance they appear dull, lusterless, and chalky. Maximum values on the hardness profiles are associated with wind slabs and layers of ice or iced firn. The density of wind slabs (even very hard ones) is not exceptionally high. For example, the ram profile exceeding 300 kg in Figure 20 was made through a wind slab of density 0.37 g/cm³.

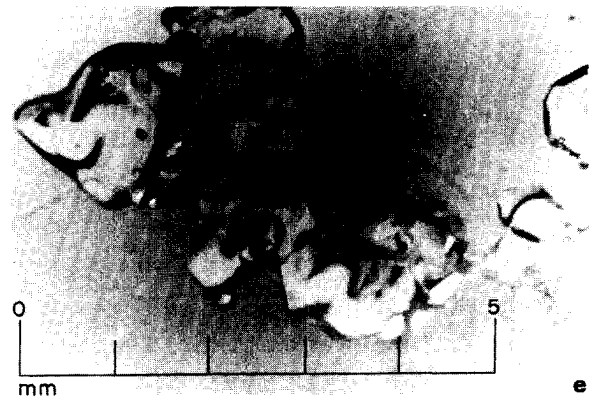
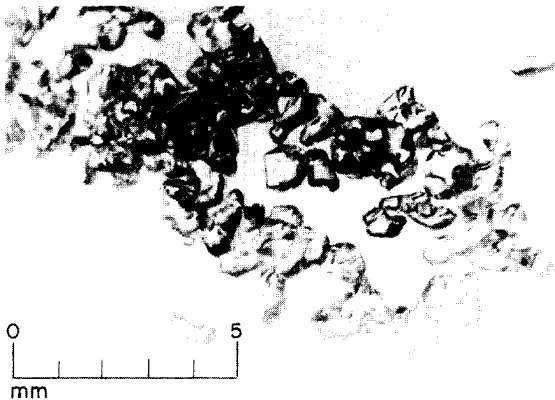
As stratigraphic units, wind slabs are usually variable in thickness and may lens out within the walls of a test pit (Fig. 21). However, the lenticularity may, in itself, provide a basis for correlation if a zone of wind slabs can be recognized in the stratigraphic sequence over a traverse. Lenticular wind slabs observed in pit walls result from burial of surfaces of erosion (Fig. 7a, b, e, h). Stratigraphically these buried erosion surfaces are unconformities. They are good stratigraphic horizons, because conditions leading to erosion with sastrugi and dune formation on the snow surface, with or without new deposition, are widespread. Sometimes the degree of induration of a hard layer, which can be correlated for 100 miles or more, varies laterally with bona fide wind slabs representing local extremes. Individual wind slabs at a given location are preserved for several years (see Data sheet 4).



a. From 120 cm (typical of the material from 57 to 126 cm). From strata deposited during the 1952-53 winter and unaffected by the 1953 summer; grains are predominantly less than 1 mm and slightly angular.



b, c. From 185 cm. Layers between 157 and 190 cm were subjected to surface melt and some soaking in 1952; as a result the grains became large, well-rounded, and bonded into clusters. Grains shown are from a 1-cm layer of very loosely bonded grains with depth hoar crystals. They indicate melt-water soaking, re-freezing, and subsequent sublimation. Sharp irregular growth of depth hoar is apparent on the rounded grains; several hexagonal cup-shaped hoar crystals may be seen in c.



d, e. From 203 cm (Fig. 22, Data sheet 3). From 196 to 240 cm, percolation took place in 1952 and the upper layers were close to 0°C without being soaked. Grains are rounded and bonded into clusters, but their surfaces are smooth. This is interpreted to mean that sublimation was not as important here as in b, c. (Note: scale in e is twice that of the other photos.)

Figure 19. Photomicrographs of firn grains. Samples scraped from the pit wall at station 1-0, 1953.

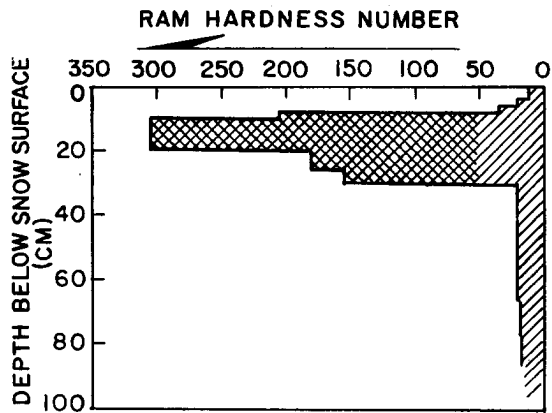


Figure 20. Rammsonde profile through wind slab at station 1-23, 4 Sept 1952.

Wind crusts

Wind crusts are thin (1 or 2 mm) layers of firmly-bonded, rounded, fine or very fine grains. When the pit wall is brushed with a whiskbroom they stand out like layers of stiff paper (Fig. 4b, 6b). They are abundant, and to some extent this reduces their usefulness as units for stratigraphic correlation. However, prominent individual wind crusts or characteristic groups have been useful in correlation. The three wind crusts shown in Figure 6b, with the loosely bonded layer immediately below, were traced for 40 miles in 1954 (stations 1-50, 2-0, 2-10, 2-20, and 2-30, Data sheets 3, 5).

Principles of stratigraphic interpretation

Interpretation of firn strata is based more on similar layered sequences than on positive identification of a specific layer, such as a particular wind crust or ice stratum. The stratigraphic sequence represents a response to change in environment. Since these changes occur over an annual cycle, similar sequences are produced each year. Summer strata are generally coarser-grained and have lower density and hardness values than winter layers; they may also show evidence of surface melt. Also, there is usually more variability in summer layers, with coarse-grained, loose layers alternating with finer-grained, higher density layers or even wind slabs of variable thickness. Winter layers are generally more homogeneous, with higher density and finer grain size than summer layers. Typical summer layers are seen in Figure 21b. The differences between summer and winter strata are most clearly seen in Figure 8. To measure annual accumulation by integrating depth-density profiles, a specific reference datum in this annual sequence is needed. It should form within a short time interval and must be recognizable in all facies.

Selection of a reference datum in the annual stratigraphic sequence

The short "fall season" produces a unique record in the firn. It is represented by a stratigraphic discontinuity in the form of a coarse-grained, low-density layer — often containing depth-hoar crystals — overlain by a finer-grained, harder layer of higher density. In regions where surface melt occurs, the discontinuity lies slightly above the topmost evidence of surface melt. The discontinuity at the base of the first year's snow is apparently the base of the Jungschneedecke of Koch and Wegener (1930, pp. 371-372).

Time of formation and stratigraphic nature of the discontinuity. The time of formation of the sequence containing the discontinuity was determined by the exact dating of specific layers, such as the one shown in Figure 6c. In 1953 the low density layer formed during middle and late August; and the discontinuity between it and the overlying higher density layer was fully developed by early September. Specifically, at 77°N latitude the discontinuity forms between 20 August and 10 September.

The discontinuity is easily recognized and may be traced continuously over long traverses. In 1953, 1954, and 1955, it was recorded at each of the 36, 68, and 27 stations, respectively, between 0-0 (Tuto) and 2-100. Sometimes the upper layer is a wind slab (see Fig. 20, and stations 1-50, 2-0, -30, -40, -50, -60, -70, -80, -90, and 2-100 on Data sheets 3, 5); sometimes it contains a series of thin, closely-spaced wind crusts (Fig. 6b; and Data sheets 3, 5 for stations 1-50, 2-0, 2-10, and 2-20); but always it is harder and of higher density than the layer below.

At some stations ice masses in the firn make it difficult to obtain accurate firn density measurements (stations 1-0 and 1-20 for 1948 to 1950, Data sheet 3). In these cases the ram hardness profiles are helpful in locating the discontinuity. Below the saturation line the discontinuity may be largely obscured by early July by melt water soaking and percolation.

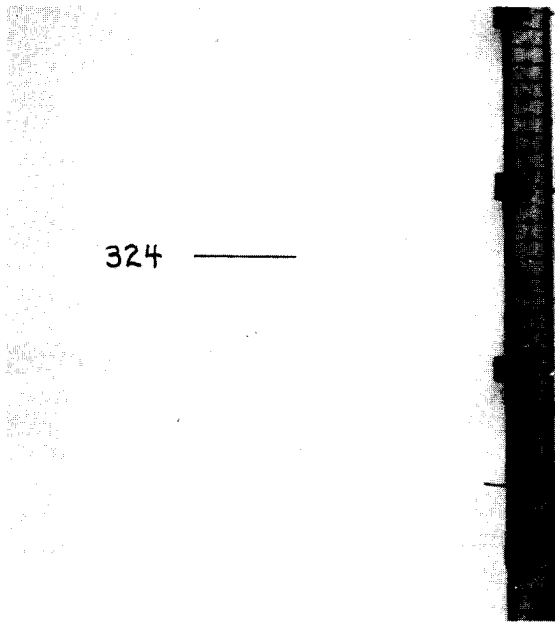


Figure 21a. Wind slab lensing out in pit wall at station 4-250, 1955.

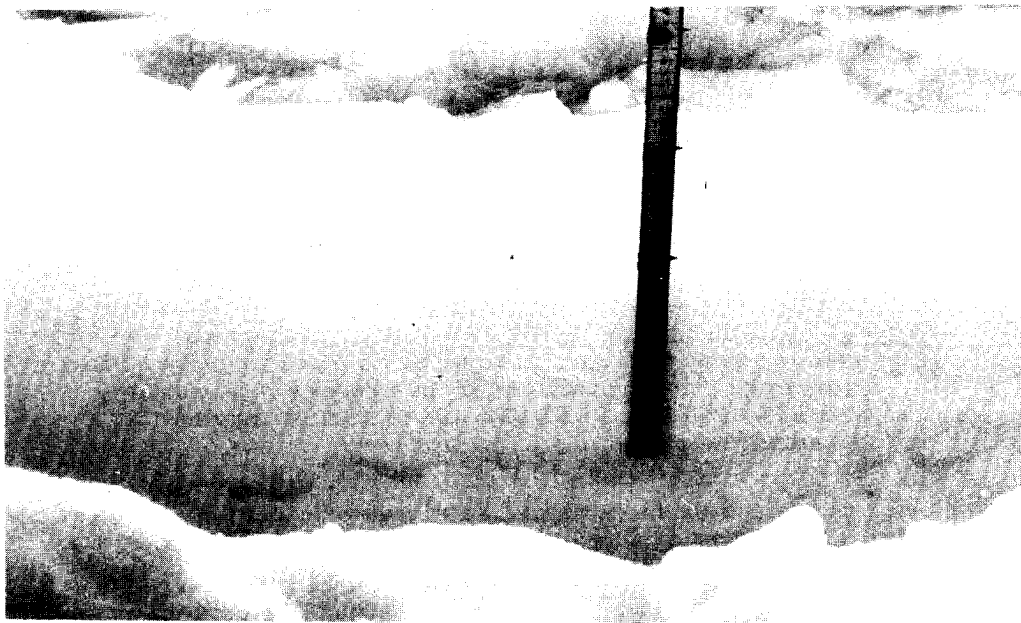


Figure 21b. Wind slab formed on snow surface at station 4-250, 2 July 1955. Several loose, low-density layers alternate with finer grained harder layers. This is typical of summer strata. The wind slab on the surface varies from 2 cm at the right to a thin wind crust at the left; it was more than 5 cm thick to the right of this photo.

Mechanism of formation of the discontinuity. At the end of August and during early September the temperature gradient in the upper firn layers is steep; i. e., 0.3C/cm or more (Fig. 33; station 1-0, curves 6, 7, 9; station 2-0, curves 4, 5; station 2-50, curves 4, 5; station 2-120, curve C). These temperature gradients produce vapor pressure gradients which cause upward diffusion of water vapor and possible loss of mass to the atmosphere.

By assuming an idealized situation with no movement of air through the firn, Bader (1939) computed the amount of moisture transferred by diffusion alone. His result was of the order of milligrams per centimeter square per day for the temperature range 0 to -10C. Because this is so small, he concluded that movement of air through the snow is essential to significant transport of moisture within or between layers.

Winds, especially very gusty ones, produce rapid fluctuations of air pressure within the upper snow layers, and increase the rate of vapor transfer. As a result, material is redistributed within the upper layers, and some material is removed. Actual removal of some water vapor from the snow by wind was observed by Seligman (1936, p. 107). It is also apparent from the low density of depth-hoar layers in pits (between 0.20 and 0.30 g/cm³) that moisture was extracted during their formation.

A combination of strong wind and steep temperature gradient in the fall would account for the formation of the low density layer. It would also account for the observation that this layer is thickest in the soaked and lower part of the percolation facies. (See Data sheets 1 through 6 especially.) Temperatures in the near-surface layers are highest in these facies. This results in maximum losses of mass by sublimation and evaporation, because the difference in vapor pressure between two firn levels depends on the range of temperature involved as well as on the temperature gradient. For example, the temperature range 0 to -10C produces more than twice the difference in vapor pressure produced by the range -10 to -20C (2.61 as compared with 1.18 mm Hg).

Part of the upward migrating water vapor escapes to the atmosphere, but the remainder is redeposited within the upper layers. According to Bader's computation for the case with no wind, these amounts are nearly equivalent. If new or drift snow is being deposited on the surface, this material will be indurated by the vapor deposited in it. The condensing (by sublimation) vapor will first fill in the cracks between grains, because vapor pressure is lowest there. This strengthens grain bonds and in the extreme case forms a wind slab. This process was described as wind packing by Seligman who concluded:

"... that wind-packing consists of the compacting of snow grains by the condensation of water vapour among them when subjected to the action of a moisture bearing wind. It is practically certain that at any rate some of this moisture is derived from the grains themselves. We can therefore define wind-packing as a special form of firnification accelerated by a wet wind. The mechanism of the processes is probably one of wind-accelerated diffusion which may or may not be influenced by the pulsations or pressure variations of the wind." (Seligman, 1936, p. 200).

It is suggested here that much of the moisture referred to as coming "from the grains themselves," is indeed from the low density layer below the wind slab.

The best example of wind-slab formation observed during the course of this work occurred on the first and second of September, 1952. On 3 September this wind slab covered the region 1-0 to 2-100, being most pronounced between 1-20 and 2-20 (Fig. 20)*; at 1-50 its formation involved the alteration of much of the 1952 layer (this is the only example of what might be called "wind erosion" of a significant portion of the annual accumulation; see Data sheet 4). The prevailing meteorological conditions satisfied Seligman's requirements as seen in the following summary:

* The observed maximum wind effects in the vicinity of 2-0 are attributed to the location of this region near the crest of the ridge forming Thule peninsula. In May 1955 the wind-blown surface between 1-30 and 2-10 (Fig. 7h) caused broken runners on sleds.

1) Observations in the vicinity of 2-120: Low clouds and light snowfall on 1 Sept turned into a blizzard during the night which lasted throughout the next day. Winds exceeded 40 mph, new snow was combined with blowing and drifting snow, and the air temperature remained near or above -5°C during the storm. On the morning of 3 Sept the sky was clear and the air temperature was below -25°C (see Fig. 33, station 2-120, curve C).

2) Observations on the trail between 2-100 and 1-0: The weather remained cool and clear until 5 Sept.

3) Observations between 1-0 and 0-35: Wet snow fell during the night of 5 Sept followed by warm weather (near 0°C). Rainfall on 6 Sept occurred up to elevations of 4000 ft.

Evidence of surface melt from 5 - 6 Sept exists above the wind slab of 1 - 2 Sept in the 1952 strata at some stations. Wind slabs formed during summer are especially prominent because they are overlain and underlain by coarser-grained, lower-density snow (Fig. 22, 32c).

Another example of wind-slab formation is associated with the 15 July 1954 heat wave. The cooling period which followed the heat wave (Fig. 12) produced a strong temperature gradient in the freshly deposited snow. Thermal conditions were similar to those which contribute to the fall discontinuity. At station 4-75, the heat wave resulted in a wind slab (Fig. 32c, Data sheet 7). The $\text{O}^{18}/\text{O}^{16}$ data support the inference that snow comprising this wind slab actually was deposited during the heat wave, because it has the highest δ value in the 1954 summer layer (Fig. 32c).

Examples of stratigraphic interpretation

Application of the above principles is illustrated in the following examples:

Four years' data at station 1-0. The four pits presented in Figure 22 were made within 100 m of each other. In 1954 two pit studies were made, one before and one after the melt season. The 19 August 1954 profile extended only to 160 cm, at which time the density and hardness profiles exceeded those of 3 June as indicated by the stippled areas.

The sequence of strata recorded in the 1952 pit is preserved and easily identified in the pits of 1953 and 1954. The 1951 summer sequence, together with the nearly homogeneous interval down to the 1950 summer surface, was recognized with special ease in each of three years of observation. The 1954 profile shows more evidence of percolation from the 1953 summer than does the 1953 profile. Although this could be partly due to local variations in percolation, it is primarily because warm weather continued for several weeks after the 1953 pit was completed.

Three years' data at station 0-35. The pit studies of 1953, 1954, and 1955 at 0-35 are assembled in Figure 23. The amount of melting at this station differs significantly from that at 1-0. Station 0-35 is below the saturation line, thus its entire annual accumulation increment is completely soaked each year. Stratigraphic correlation is difficult on the soaked facies because soaking of the firn produces rapid diagenetic changes. Features are not preserved for several years as shown in Figure 22.

Three years' data at station 1-50. The pit studies made in 1953, 1954, and 1955 at 1-50 are shown on Data sheet 4 together with the two 1955 pit studies from the trail segment 1a (1a-10 and 1a-20) at a 90° angle to the segment 1-0 to 2-0.

Four years' data at stations 2-30 and 2-70. Pit studies made in 1952, 1953, 1954, and 1955 at stations 2-30 and 2-70 are assembled in Figures 24 and 25 respectively. Except for the 1952 pits, (see Fig. 2) the pit studies at each station were made within 50 m of each other. Individual strata are correlated and the fall datum of each year is indicated. (Note: Year labels in Figs. 22-25 indicate the fall layers of each year.)

Stratigraphic correlation

Data sheets

Stratigraphic interpretations made independently at each of the 79 stations shown on the 10 data sheets have been correlated with each other. The correlation lines are intended to pass through the fall layers of each year. Locations of specifically dated strata are indicated where known. The data sheets are discussed in Appendix C.

Measurement of accumulation

The only reliable method of measuring snow accumulation, in terms of an equivalent amount of water, is to integrate the depth-density profile between dated depth intervals. For example, the two pit studies at station 1-0 in 1954 were stratigraphically correlated by matching identifiable layers at depths below 100 cm (Fig. 22). Integration of the depth-density profiles indicates a minimum increase of 10 cm H₂O in the upper 160 cm between 2 June and 19 August. This agrees well with the minimum of 12 cm H₂O obtained by direct measurement of snow added on surface marker boards at 1-0 during the same period of time. These are minimum values because the snow overlying the board on 19 August had been soaked and, as seen in Figure 22, some melt-water percolated downward; therefore, a larger accumulation between June and August might have been observed if the August pit had been deeper. It must also be pointed out that several large ice masses were omitted from the integration of the August density profile. It is difficult to estimate the water equivalent of such masses because of their irregular shape and distribution, but in this case their contribution is about 3 to 5 cm H₂O.

The above results differ from those obtained by measuring the displacement of the snow surface relative to markers on poles. Such measurements are subject to error because the poles are set in firn which is undergoing compaction (Hubley, 1954) as illustrated in the following summary:

<u>Height of marker above snow surface (cm) at station 1-0</u>	<u>Date</u>
200.0	21 Sept 1953
121.5	2 June 1954
98.5	14 June 1954
112.0	19 Aug 1954

It is clear that: 1) The 9.5-cm rise of the snow surface, amounting to 4.3 cm H₂O, between 2 June and 19 August does not measure accumulation accurately because, as indicated above, an accumulation of at least 10 cm H₂O occurred during this time. 2) The 13.5-cm descent of the snow surface between 14 June and 19 August does not represent ablation because net accumulation of at least 5 cm H₂O is indicated by the surface marker board during this period. Densification apparently was sufficient to cause the snow surface to move downward relative to the pole, in spite of net accumulation.

Pole-marker measurements also give inconsistent results at other stations as indicated in Figure 26.

Examples of water-content analyses

The depth-density profile from each station has been integrated to obtain a depth-load curve.* At a given station the load, in centimeters of water equivalent, at any depth may be read directly from the depth-load curve of that station. This makes it possible to determine the water equivalent of each identified annual layer, together with the average annual accumulation, at any station where the stratigraphy can be interpreted. By assuming constant annual accumulation at a given station one may use the observed depth-load curve to construct an idealized depth-time curve. The idealized depth-time curves for several stations are compared with data points in Figure 27.

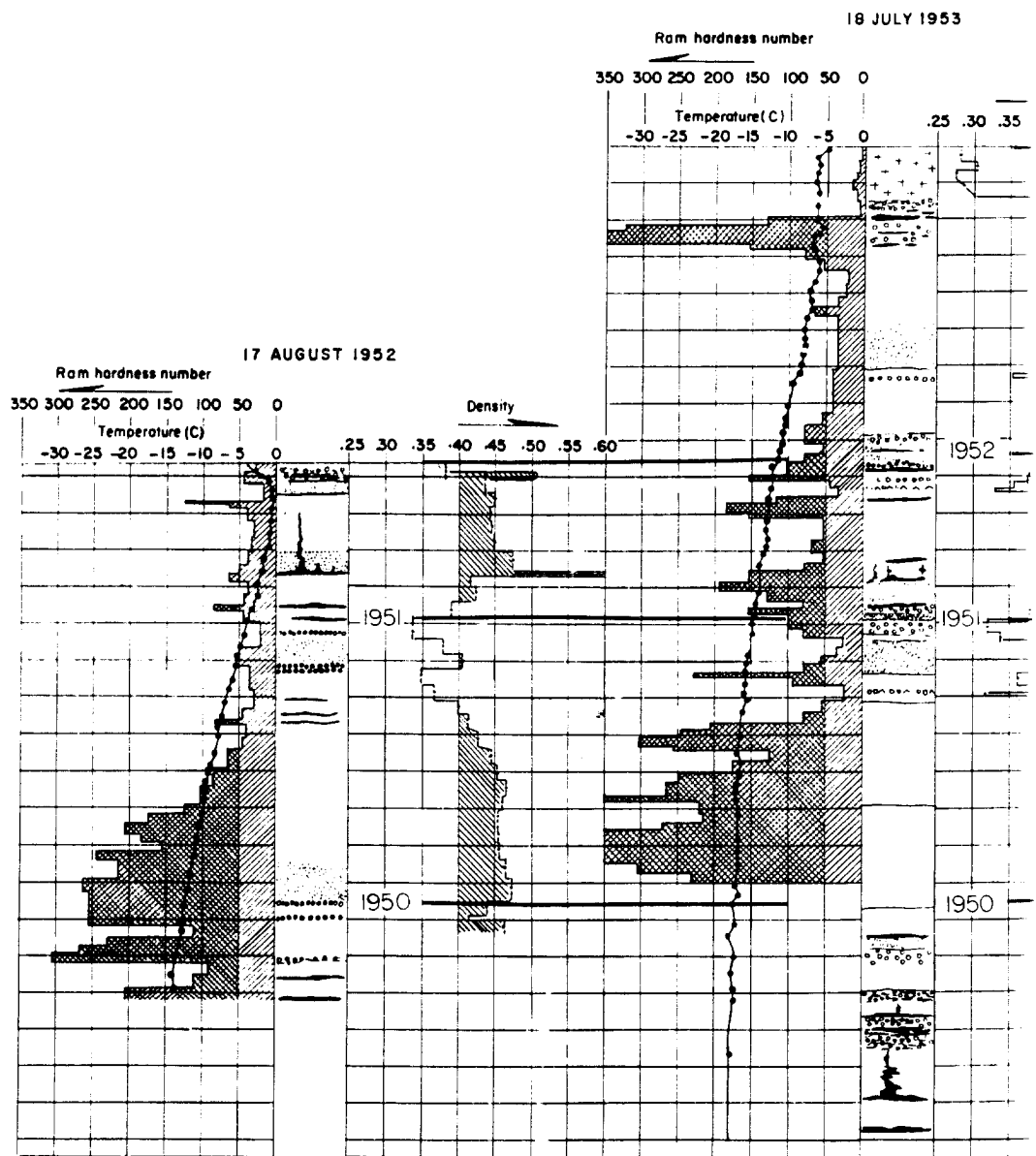
Distribution of annual accumulation

Annual accumulation on the ice sheet provides a reasonable measurement of total snowfall. In fact, the results presented below, aside from uncorrected evaporative losses,† are essentially precipitation measurements.

* Typical depth-load curves are shown in Figure 45.

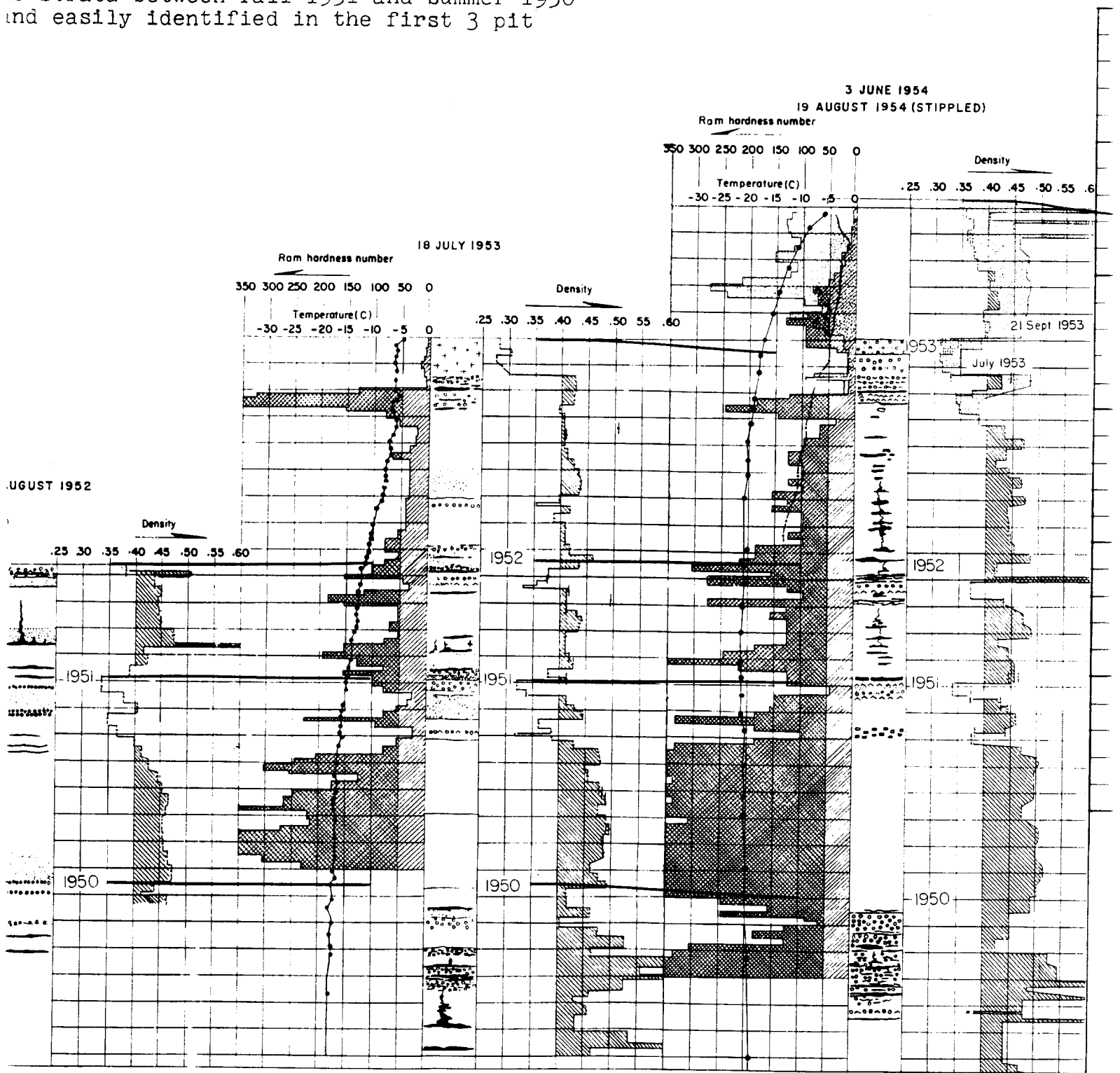
† Because of low temperatures, evaporation is slight except in marginal parts of the ice sheet where temperatures above 0C are encountered. However, stratigraphic measurements of accumulation, even though reduced by evaporation, exceed the precipitation measurements made at nearby meteorological stations with standard rain gages (see pp. 83, 84).

Figure 22.--Four years data at Station 1-0. The four pits were made within 100 m of each other on successive year each in an area undisturbed by the previous years study. In 1954 two studies were made, one before and one after the melt season. The density and hardness values of the 19 August, 1954 pit exceed those of 3 June as indicated by the stippled areas. Note that the strata between fall 1951 and summer 1954 are well preserved and easily identified in the first 3 pit studies.



our years data at Station 1-0. The four
 in 100 m of each other on successive years;
 disturbed by the previous years study. In
 re made, one before and one after the melt
 r and hardness values of the 19 August,
 se of 3 June as indicated by the stippled
 e strata between fall 1951 and summer 1950
 and easily identified in the first 3 pit

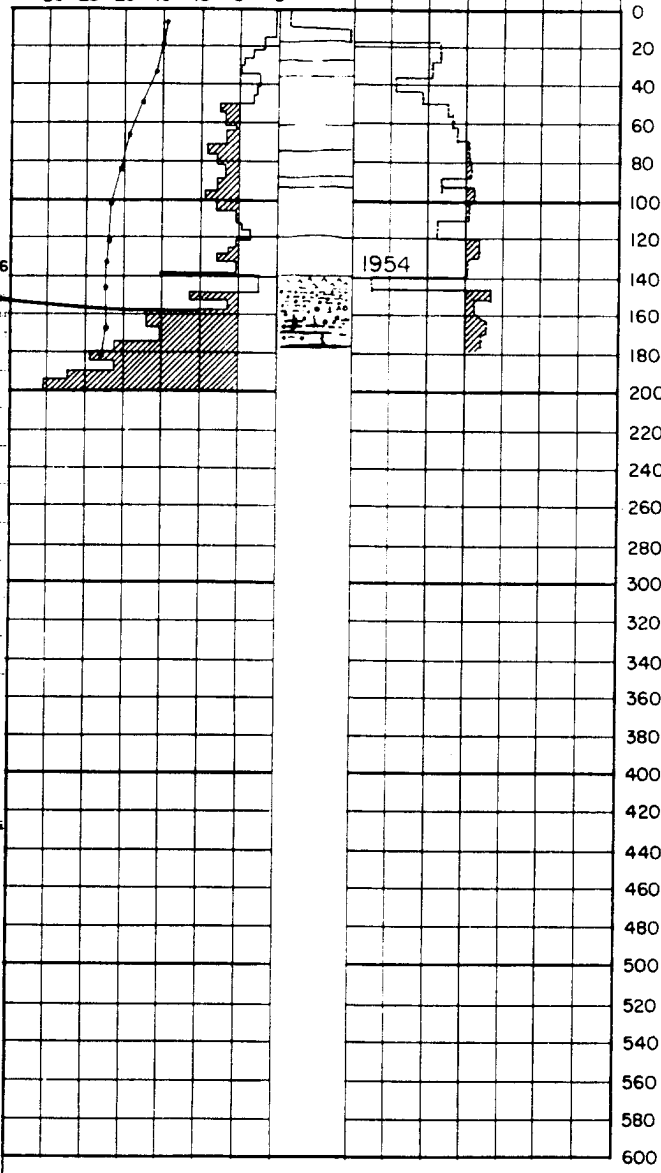
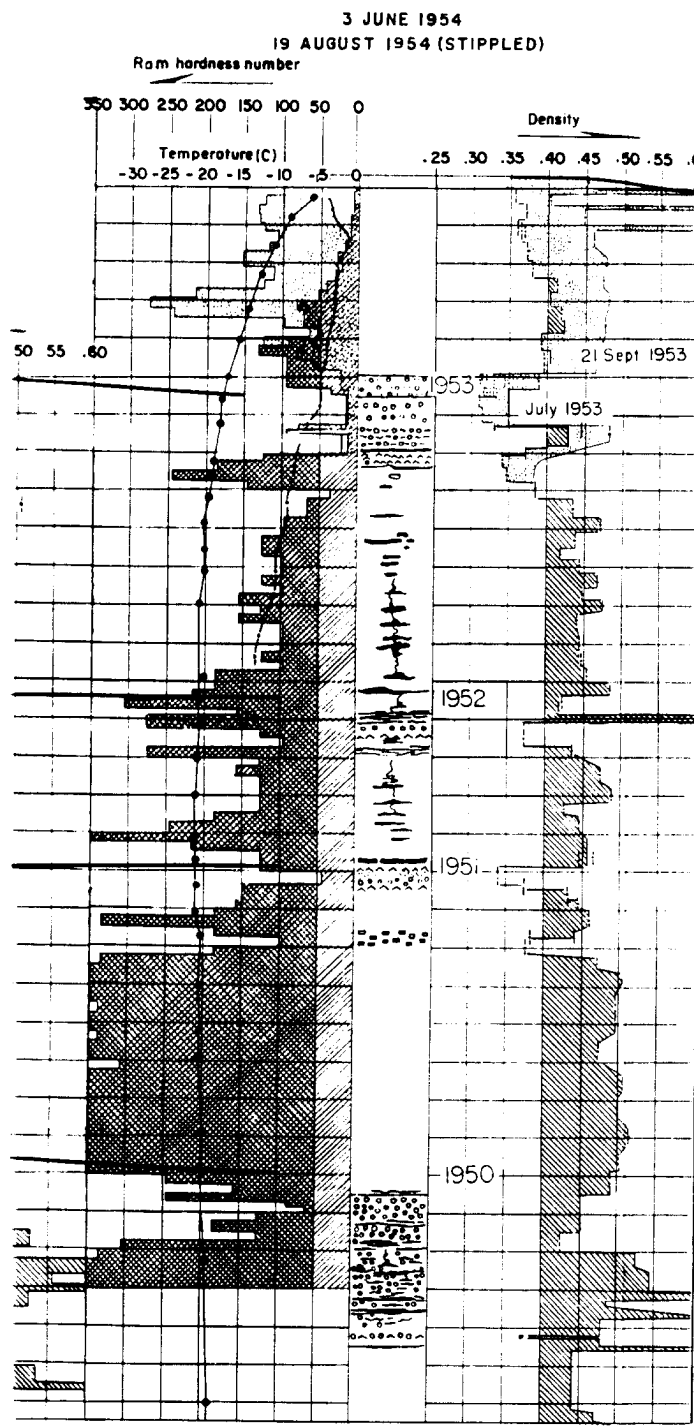
RAM
350



17 MAY 1955

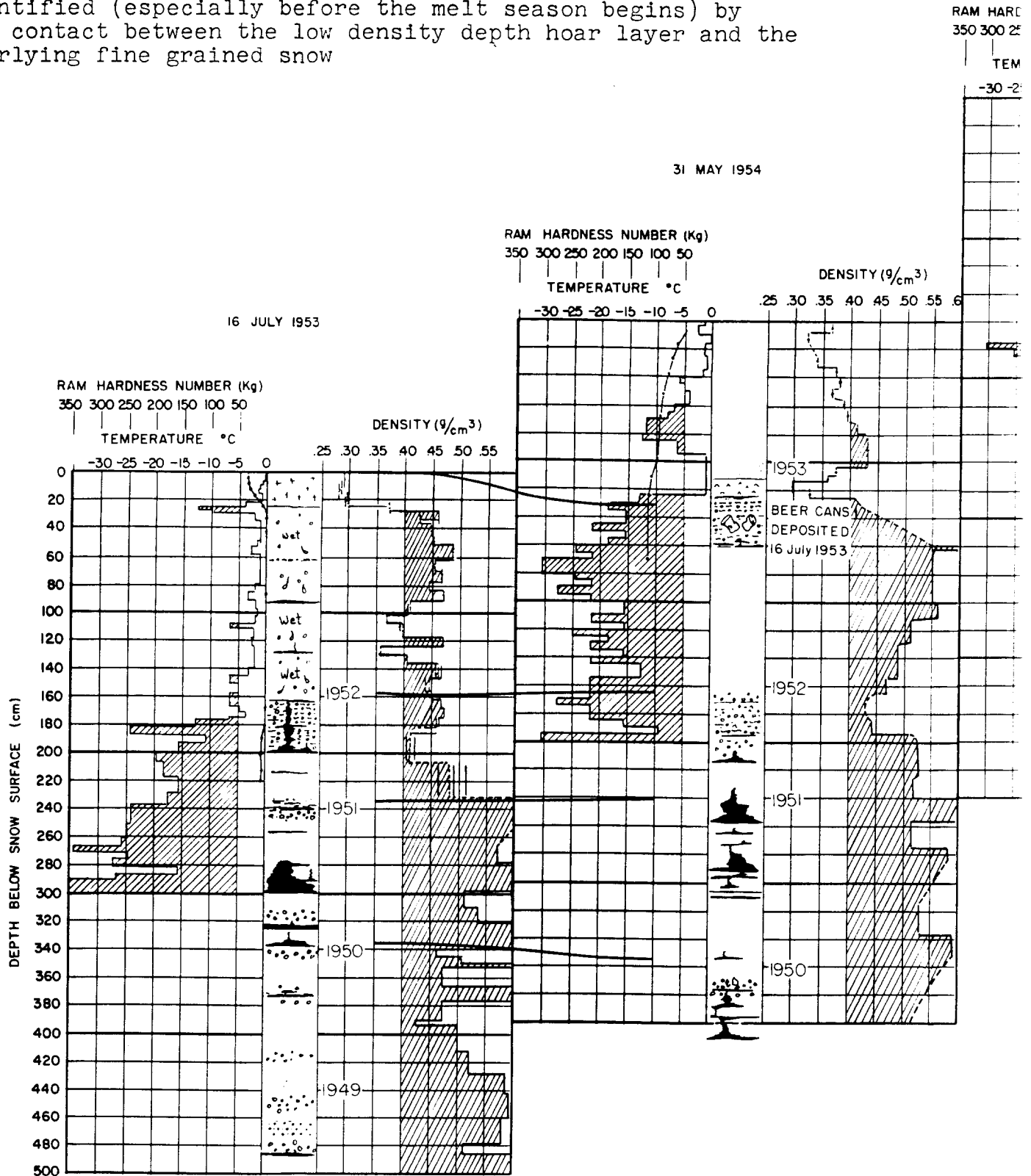
RAM HARDNESS NUMBER (Kg)
350 300 250 200 150 100 50
TEMPERATURE °C
-30 -25 -20 -15 -10 -5 0
DENSITY (g/cm³)
.25 .30 .35 .40 .45 .50 .55 .60

DEPTH BELOW SNOW SURFACE (cm)



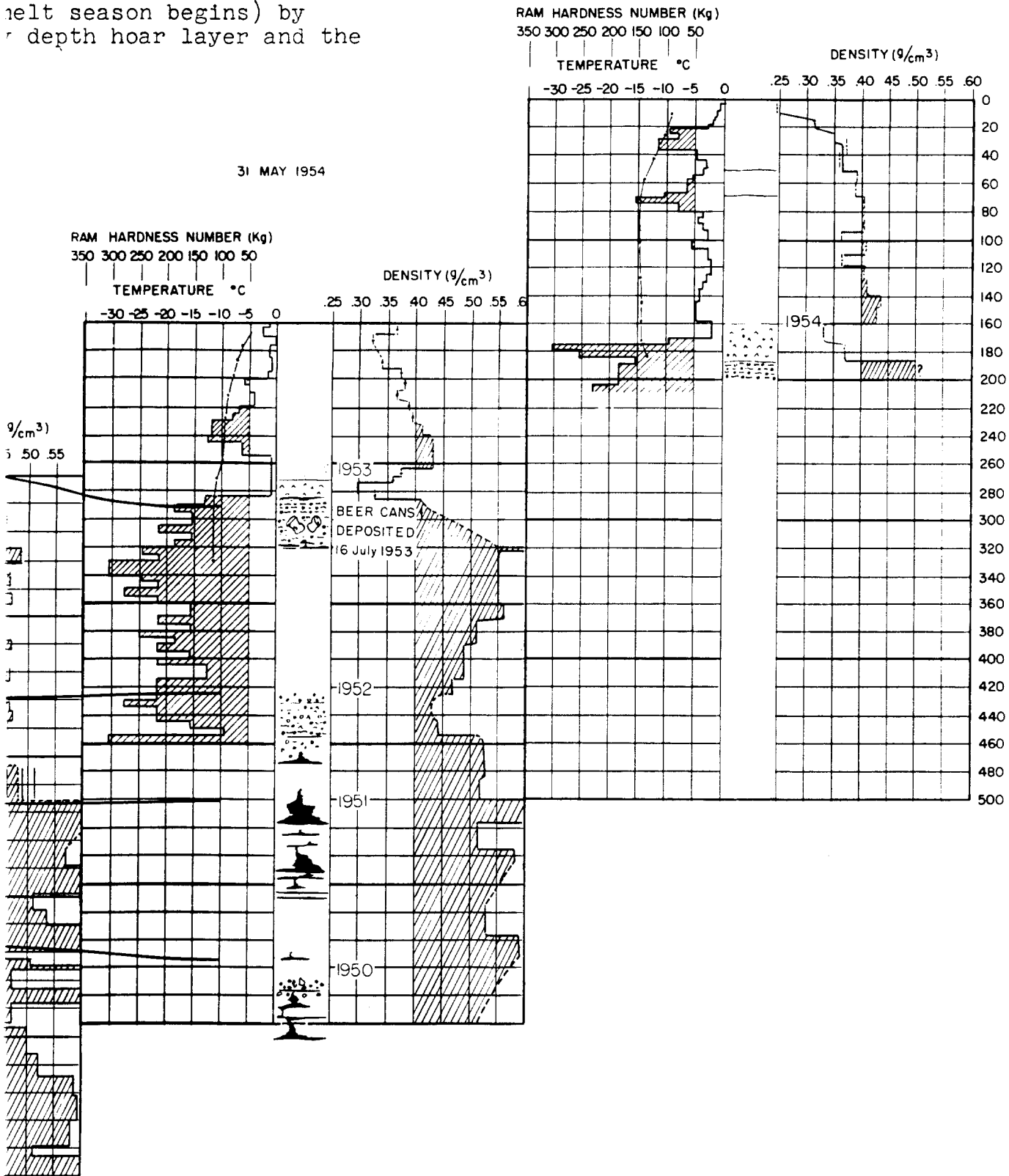
3

Figure 23.--Three years data at Station 0-35. This station lies in the soaked facies and stratigraphic details are not well preserved because of the amount of melt. However, the base of the first years accumulation is easily identified (especially before the melt season begins) by the contact between the low density depth hoar layer and the overlying fine grained snow



at Station O-35. This
 and stratigraphic details
 the amount of melt. How-
 accumulation is easily
 melt season begins) by
 depth hoar layer and the

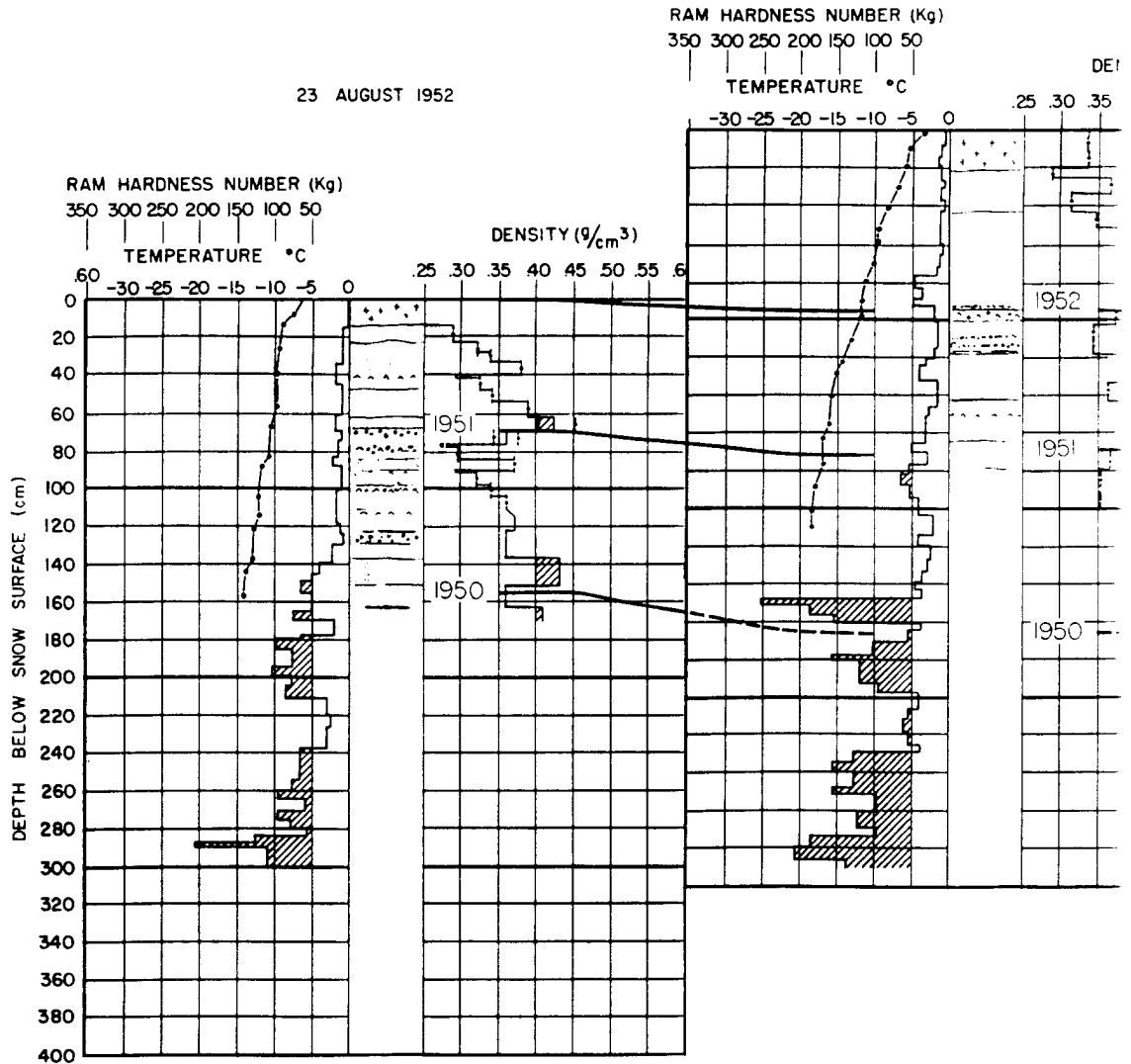
16 MAY 1955



2

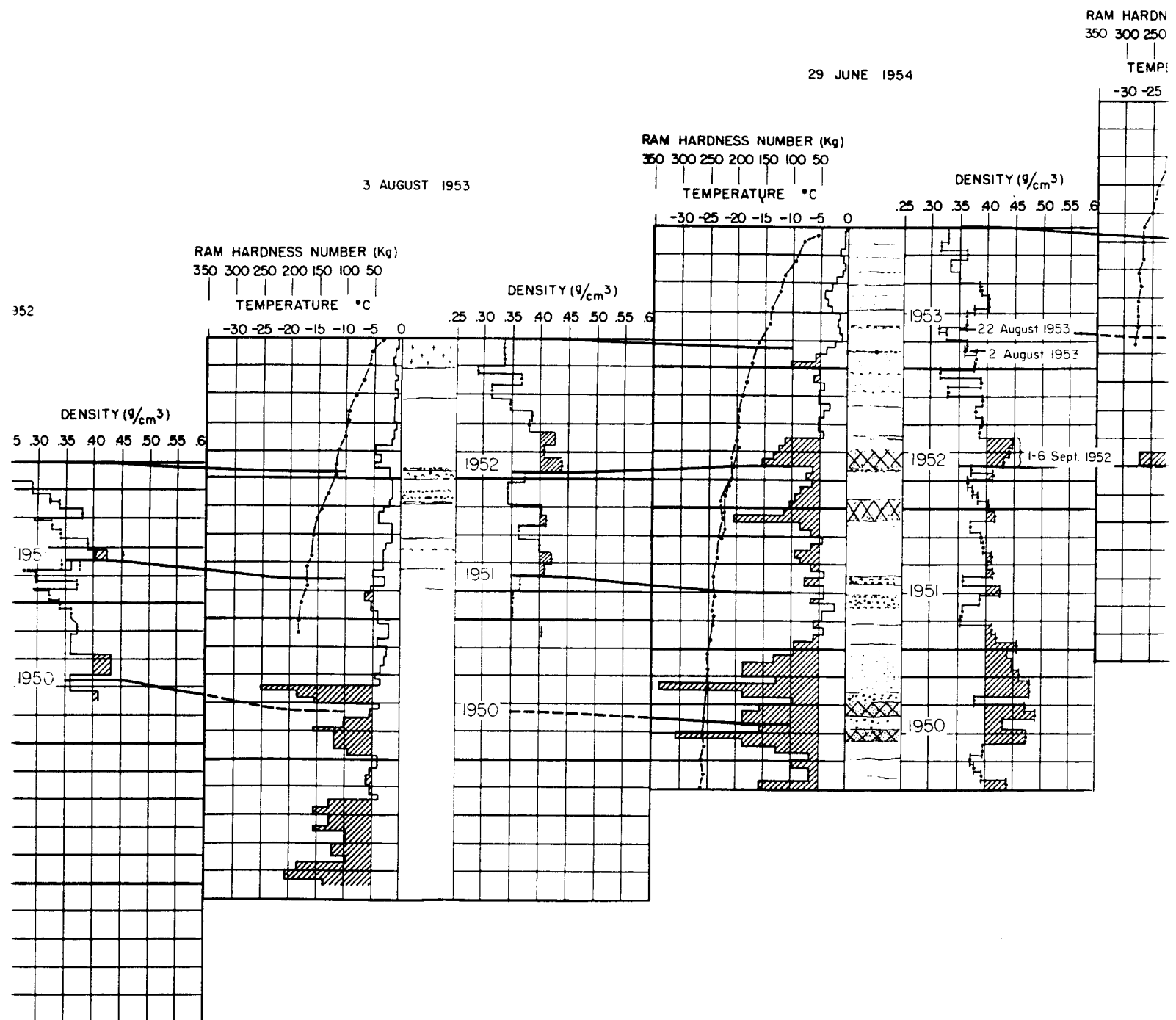
Figure 24.--Four years data at Station 2-30. The four pits were made within 100 m of each other on successive years except for the 1952 study which was about 3 miles northwest of the others (see Fig. 2).

3 AUGUST 1953

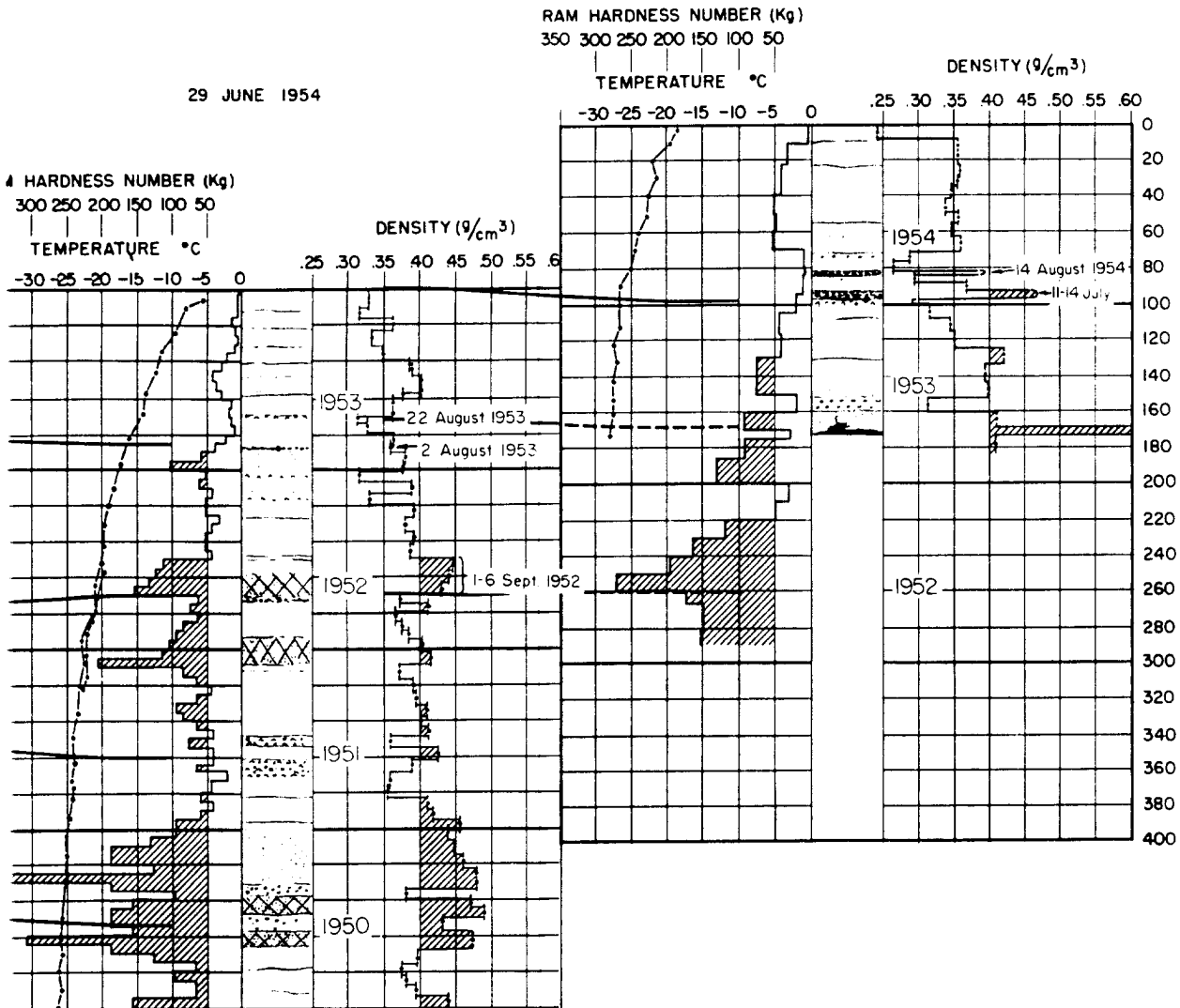


①

years data at Station 2-30. The
within 100 m of each other on successive
1952 study which was about 3 miles
as (see Fig. 2).



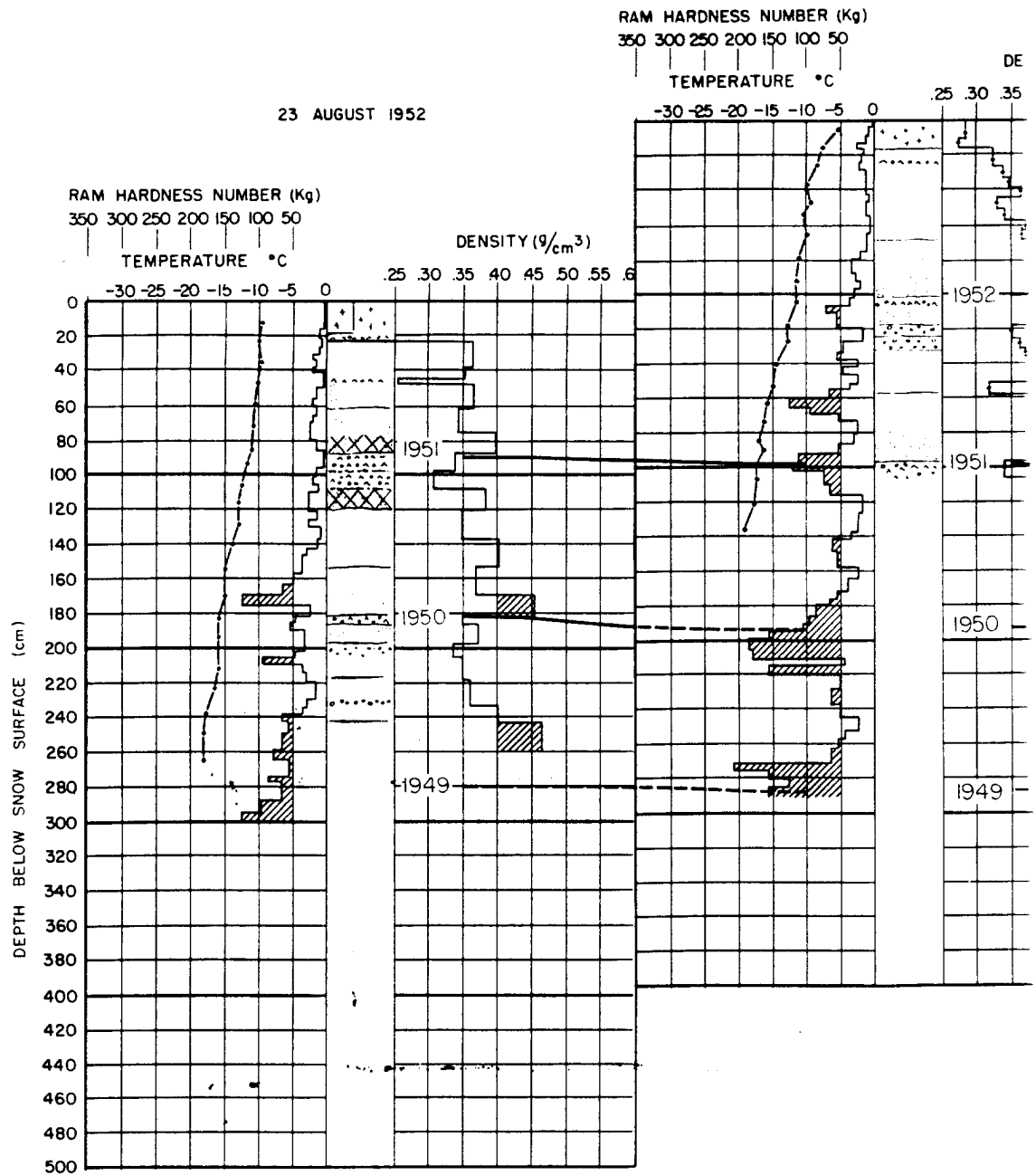
23 MAY 1955



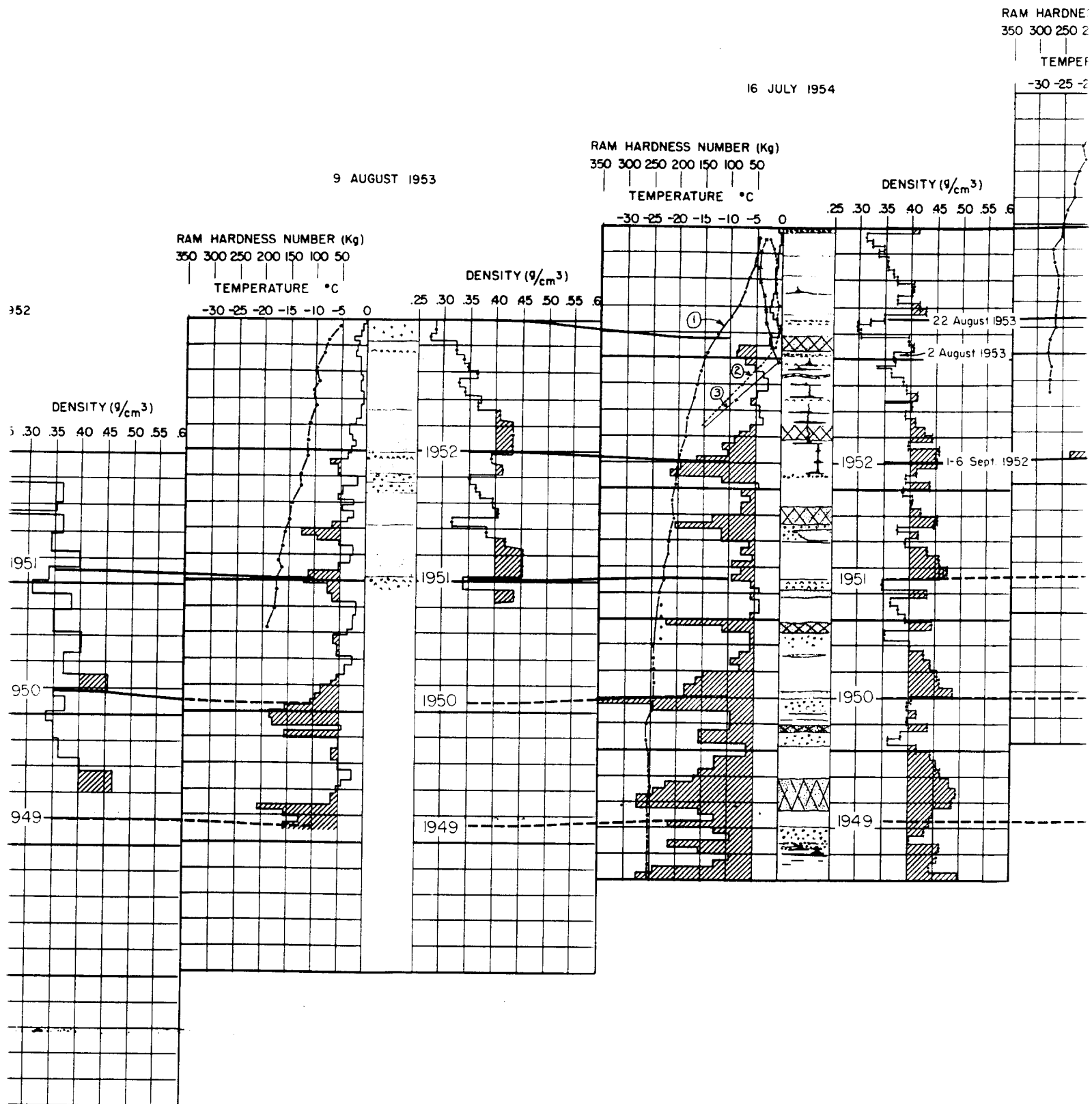
3

Figure 25.--Four years data at Station 2-70. The four pits were made within 100 m of each other on successive years except for the 1952 pit which was about 3 miles north west of the others (see Fig. 2).

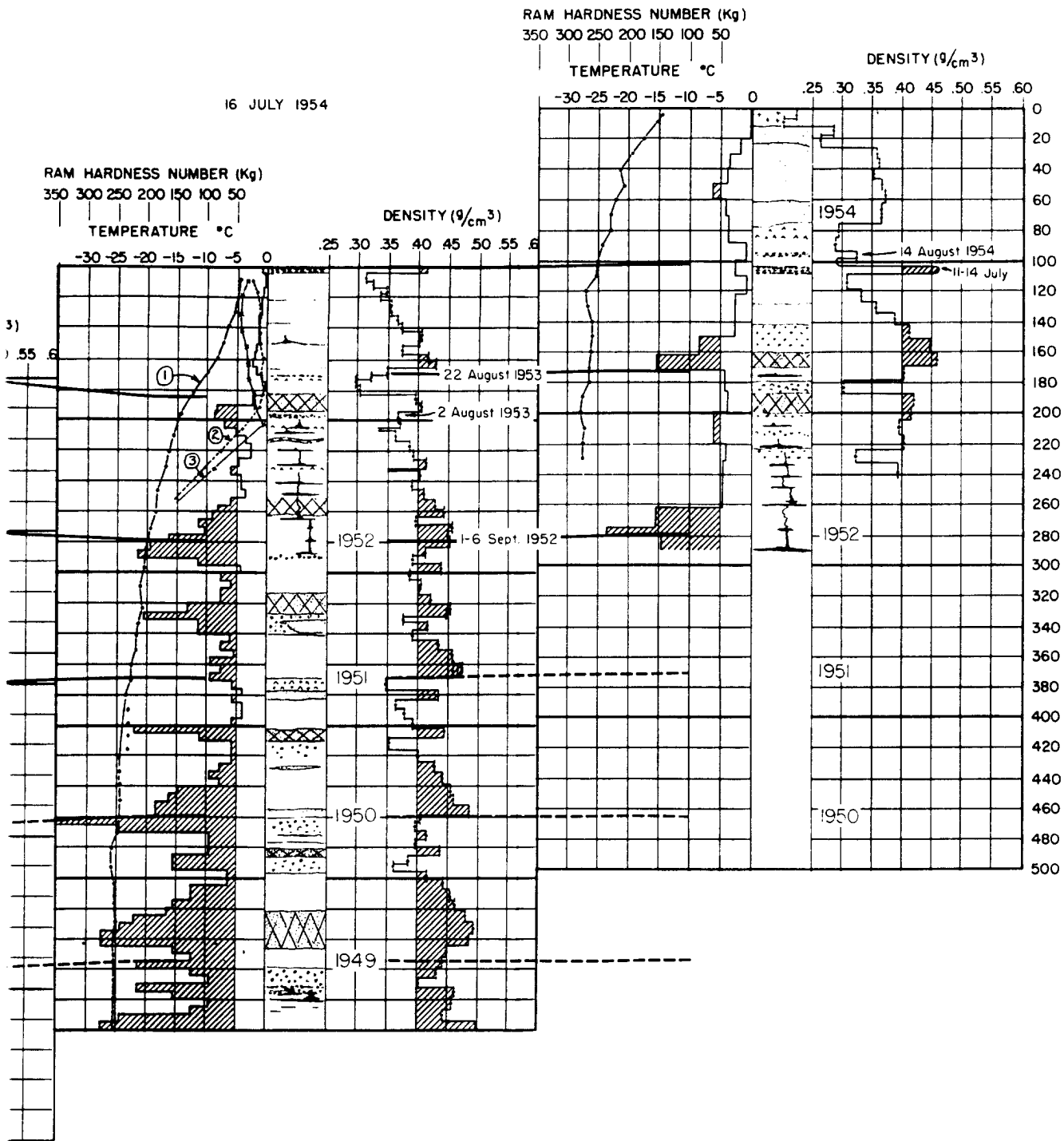
9 AUGUST 1953



years data at Station 2-70. The four
 100 m of each other on successive
 952 pit which was about 3 miles north-
 e Fig. 2).



25 MAY 1955



3

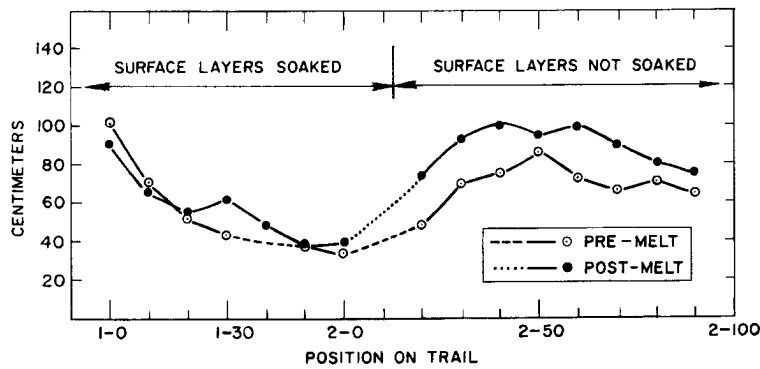


Figure 26. Displacement of the 1954 summer snow surface relative to markers placed on poles in 1953. "Pre-melt" measurements were made between 14 June and 5 July, and the "post-melt" series between 15 and 18 August. Net accumulation occurred over the entire traverse between measurements, but below 1830 m (6000 ft, station 2-20) summer melt produced sufficient densification and settling to nullify or exceed this upward displacement (relative to poles in the snow) of the surface.

Two qualifying statements are in order: 1) No marker was placed at 2-10 in 1953. 2) Errors were possibly introduced at 2-50 and 1-30 by the formation of large snow drifts around parked vehicles. The drifts probably influenced the accumulation registered on the poles even though the poles were not actually in the drifts. These errors were not compensated for in preparing this figure.

Combined data from the four years of observation reduced to water equivalent are shown in Figure 28. The snow surface of fall 1955 is the reference datum. Data between 0-0 (Tuto) and 1-0 are from pits which penetrate a maximum of 2 to 4 yr of firn; the variation in accumulation is greatest over this part of the trail because of irregular topography. Positions 0-27 and 0-31 lie near the lee side of large nunataks. All values between 0-0 and 1-0 lie within the range of 50 to 70 cm H_2O per year.

The minimum accumulation between 1-30 and 2-20 is attributed to topography. The trail between about 1-25 and 2-25 lies on the lee side of the Thule peninsula (Fig. 2). The ridge is a topographic barrier to cyclonic storms which move onto the ice sheet from Melville Bay and points south. The area south and east of the crest serves as a catchment basin, while that to the northwest (the lee slope) lies in a precipitation shadow. Saturated air masses are cooled as they ascend the windward side of the ridge, producing precipitation. As they pass over the gentle crest of the ridge and begin to descend they are no longer being cooled, hence precipitation decreases. Further release of large amounts of precipitation does not take place until the air mass moves upward again on the north side of Inglefield Bay. As a consequence of this, the coast of Melville Bay is characterized by glaciers which flow into the sea, while the north side of Thule peninsula is comparatively free of glaciers. The Inglefield Land peninsula also has glaciers on its south side but not on its north coast.

In 1955 the above interpretation of a precipitation shadow caused by the ridge between 1-0 and 2-0 was checked in the field by running traverse "1a" to the windward from 1-50. The values of accumulation at 1a-10 and 1a-20 are 36% and 49% higher than that recorded at 1-50 on the lee side of the ridge. Station 1a-10 is near the ridge crest while 1a-20 is definitely on the windward side (see Data sheet 4, Fig. 2, 28). A similar accumulation decrease occurs on the lee side of the ridge between 00-0 and 1-0 (see Data sheet 2, Fig. 28).

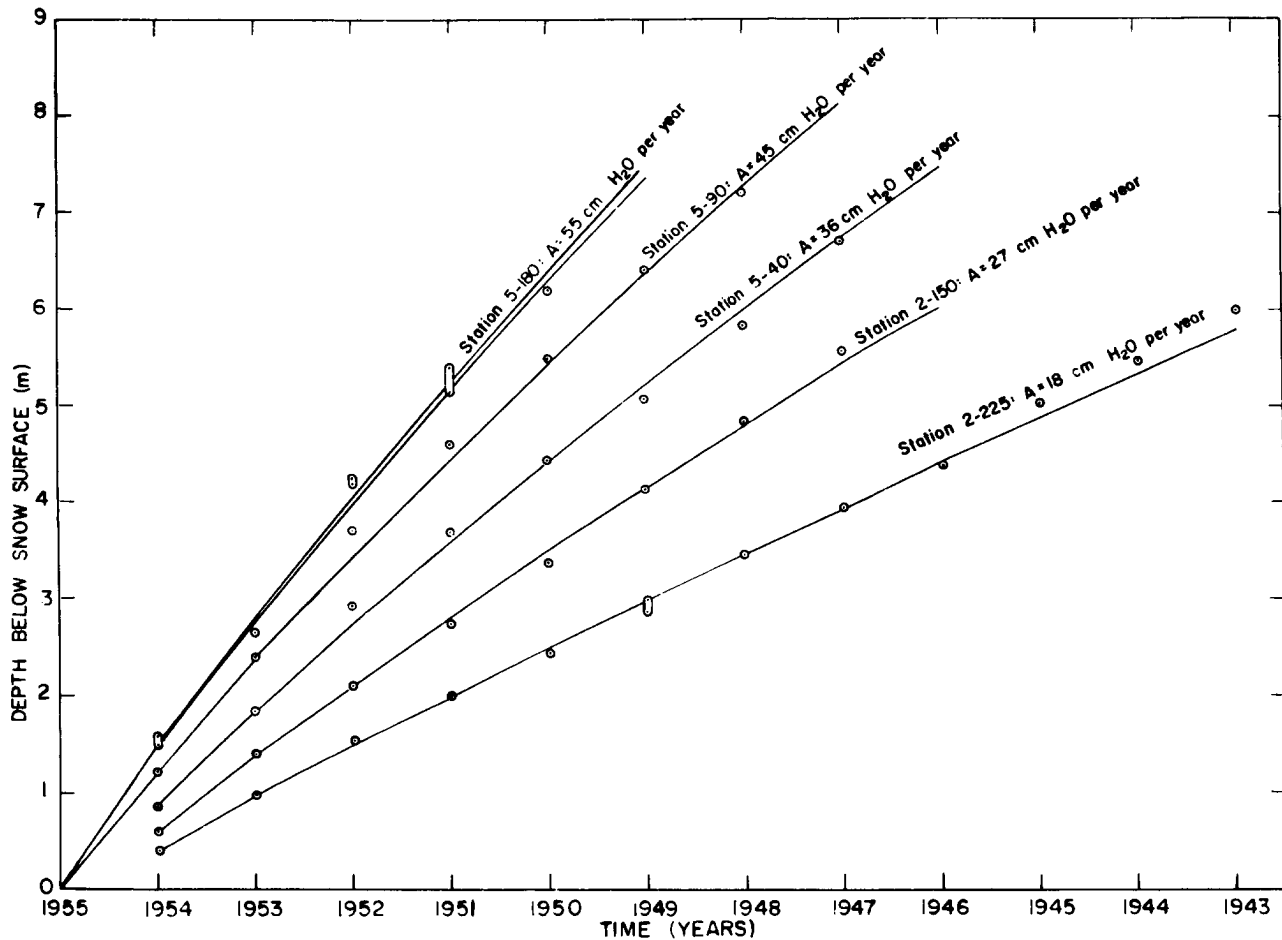


Figure 27. Computed depth-time curves with data points for several 1955 stations. The curves were computed by assuming a constant rate of accumulation, A cm H_2O per year.

The upper curve for station 5-180 was computed by neglecting ice masses, the lower one includes estimates for the contribution of ice. The difference between depth-load curves with and without estimates for ice is less than 1% at the other stations shown (see p. 69).

At stations 2-225 and 5-180 the depth to some yearly layers was not unequivocal and possible ranges are indicated. At stations 2-150, 2-225 and 5-40, 8, 5, and 6 cm H_2O respectively was subtracted from the computed load values to adjust for the incomplete first year; the annual reference datum is the beginning of fall and these stations were made on 31 May, 7 June, and 23 July respectively.

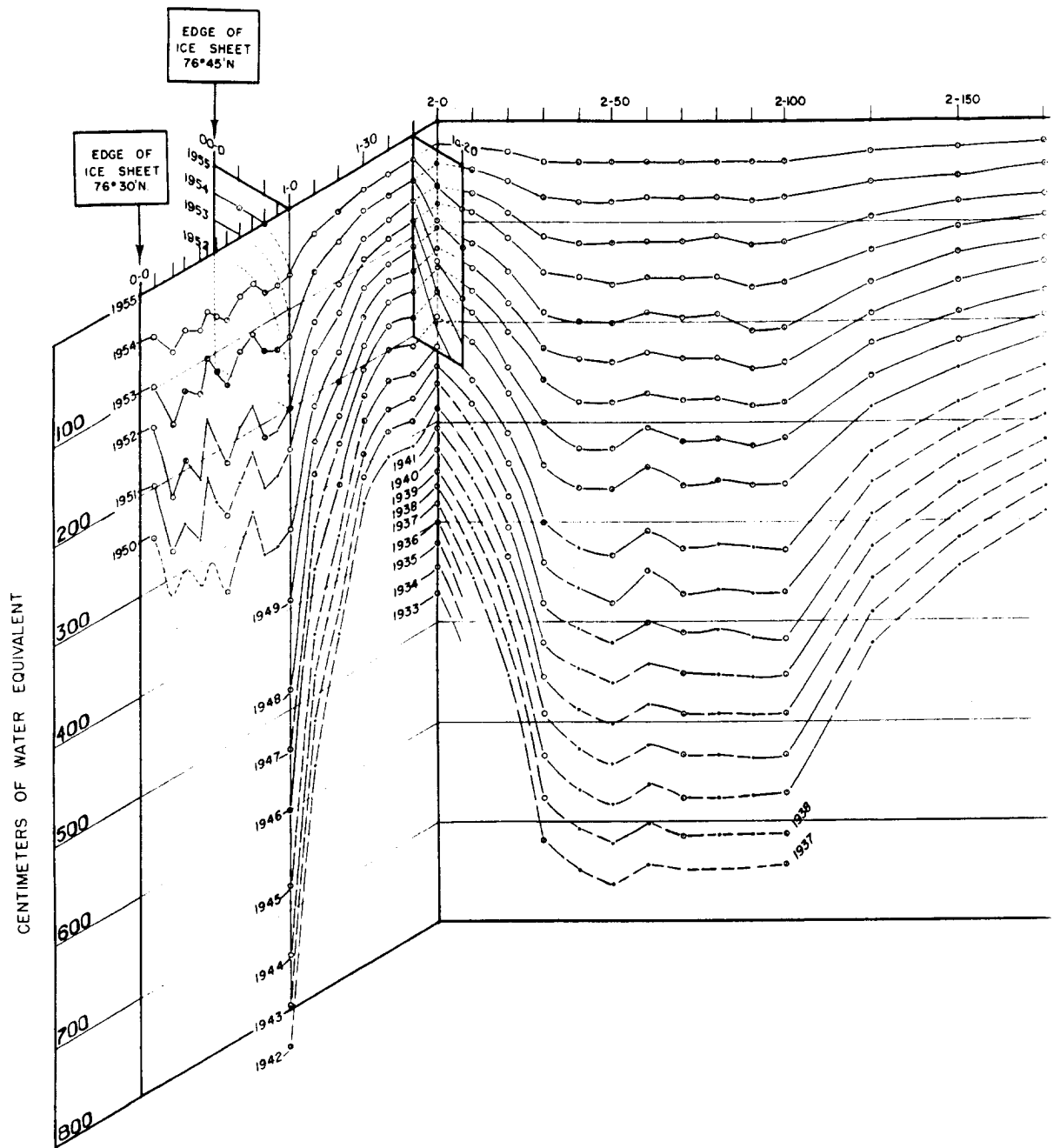
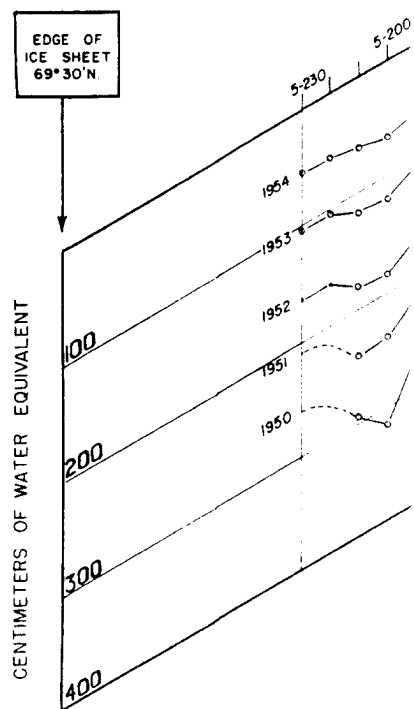
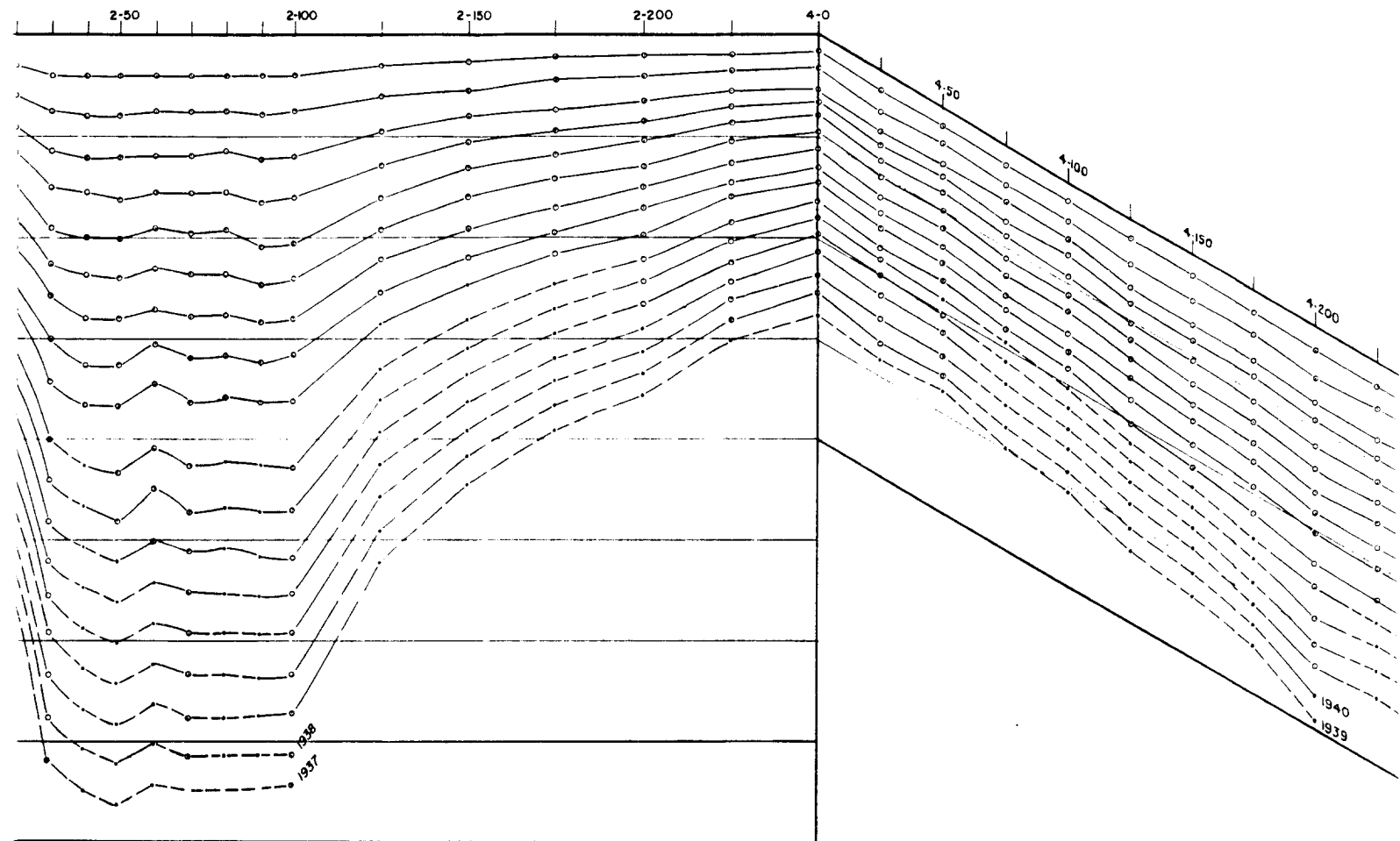
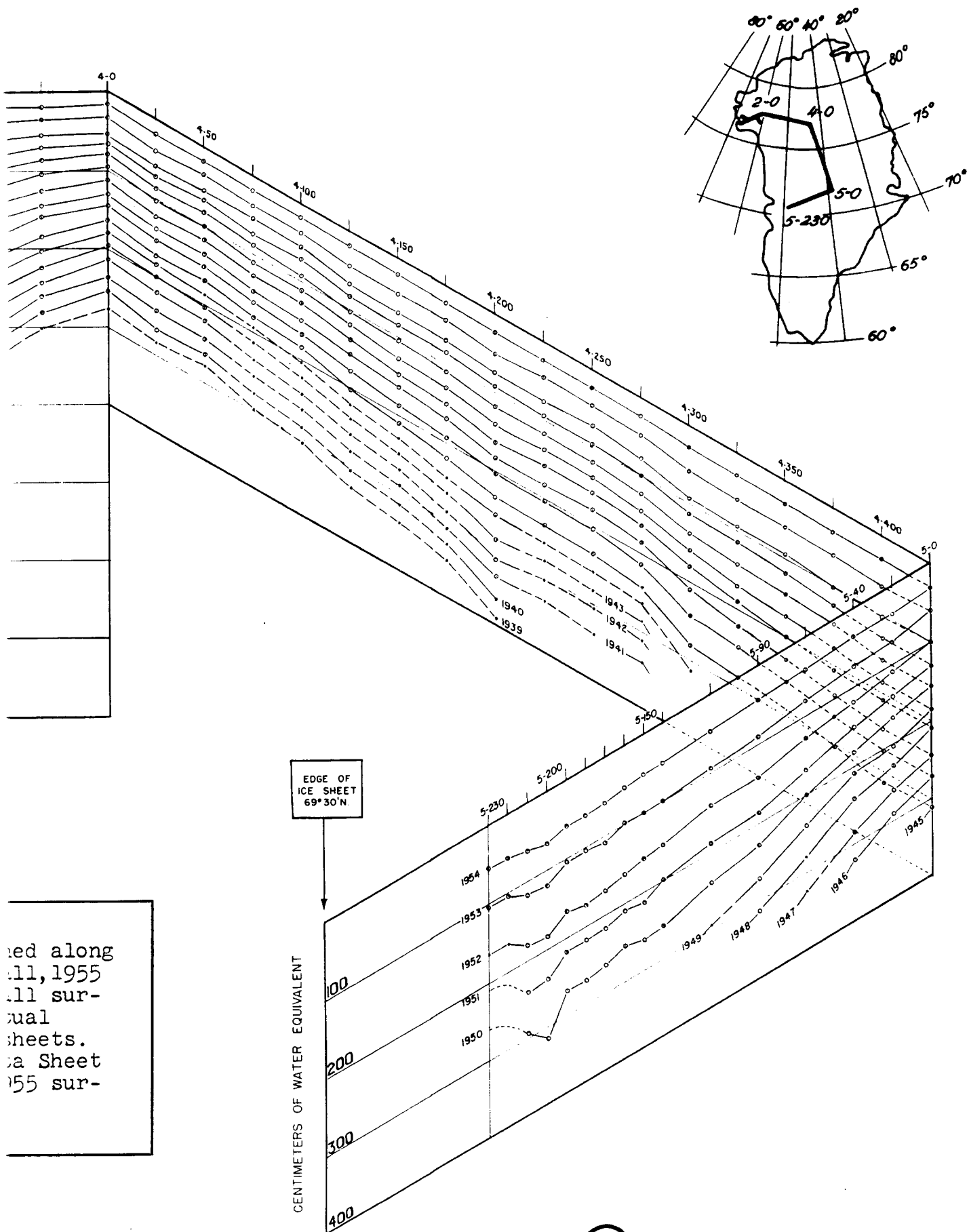


Figure 28.--Summary of accumulation data from the traverses of this study. The snow surface is the reference datum and the "depth" to a face is measured in cm of water equivalent. The snow depths, measured in the snow are given on the data sheets. Data from the two stations between 00-0 and 2) were obtained in 1954 only and adjusted to the snow surface (see Appendix 3 and the data sheets).



28.--Summary of accumulation data obtained along
 s of this study. The snow surface of fall, 1955
 ence datum and the "depth" to a given fall sur-
 ured in cm of water equivalent. The actual
 ured in the snow are given on the data sheets.
 e two stations between 00-0 and 1-0 (Data Sheet
 ined in 1954 only and adjusted to the 1955 sur-
 pendix 3 and the data sheets).



ed along
 11, 1955
 11 sur-
 val
 sheets.
 a Sheet
 55 sur-

Accumulation-altitude relationship

The variation of precipitation with altitude, as a moisture-bearing air mass ascends a slope, cannot be reduced to a fixed level as can be done with air temperature and pressure. Therefore, the usual precipitation map is the representation of actual isohyets (Conrad, 1944, pp. 182-183). In general,* it appears that precipitation increases with altitude on the windward slope up to a certain level. Above this it decreases as the air mass loses its water content. Precipitation continues to decrease up to the crest of the slope, and on the lee side it decreases even more rapidly downhill into a precipitation shadow. Many factors influence the precipitation-altitude relation such as the temperature and humidity of the air as it begins its ascent, the duration and intensity of the storm, and the inclination of the slope. The latter factor is especially important because steeper slopes increase the amount of precipitation in addition to providing steeper precipitation gradients. The altitude of the zone of maximum precipitation varies seasonally, being highest in summer and lowest in winter. According to Henry (1919) it also varies slightly with latitude, being less than 1000 m in the tropics and about 1500 m in temperate latitudes.

Average annual accumulation values for stations on south- or west-facing slopes, † windward to the storm winds, are plotted against altitude in Figure 29. There is far less scatter among the points in this figure than in precipitation - altitude diagrams for mountainous areas (Lee, 1941, p. 58). This is because of the uniformity of exposure on the smooth, gently sloping surface of the ice sheet. Most meteorological stations in mountain regions are located at population centers, and their exposure to the moisture-bearing winds varies from station to station. This variability in exposure produces such irregularities in the data that Meyer (1941) doubted that an accurate precipitation-altitude relation could be obtained. On the ice sheet, in addition to uniform conditions of exposure, some uniformity also results from winds moving new snow along the surface, which tends to smooth local irregularities in deposition from a single storm.

Figure 29 indicates maximum zones of accumulation at 2000 m at 70°N, and slightly above 1000 m at 77°N. Accumulation decreases with altitude above these altitudes at the rate of 3 cm H₂O per 100 m at 77°N and slightly less than this (about 2.7 cm H₂O per 100 m) at 70°N. This is close to the value (1.7 to 3.3 cm H₂O per 100 m) reported by Lee (1941) above the zone of maximum precipitation in the Sierra-Nevada Mountains.

Fewer data are available from windward slopes below the zones of maximum accumulation in Greenland than from above. Schytt's (1955) measurements of the 1953-54 accumulation between 0-0 and 0-20 are compatible with the results of this study and his average of 55 cm H₂O is indicated in Figure 29. His minimum accumulation of 28 cm H₂O was definitely influenced by local topography on Thule ramp (Schytt, 1955, p. 18). An estimate for the minimum annual accumulation in the Tuto area based on Data sheet 1 and Schytt's work, is 45 ± 5 cm H₂O per year.

Average annual precipitation values from meteorological stations at Thule and Jakobs-havn, located near sea level at the north and south extremes of the traverse, respectively, and Upernavik, midway between the extremes, are also indicated in Figure 29. However, it is necessary to qualify the use of these data on two points: 1) Measurements made at a meteorological station relate to a single point and the exact location and exposure of the precipitation gage is very important. For example, the Thule station is definitely in the precipitation shadow of Thule peninsula. Measurement of the water equivalent of yearly snow deposition over extended traverses or snow-survey courses (Church, 1933, 1942) enables one to recognize such local irregularities. 2) The percent of precipitation caught

* Based on records from: California coastal mountains (Hamlin, 1904); India, Java, Hawaii, and mainland U.S.A. (Henry, 1919); and Sierra-Nevada and southern California mountains (Varney, 1925; Lee, 1941).

† Stations omitted are 0-27 and 0-31 because they lie on the lee side of large nunataks and stations 1a-10 and 1-10 through 2-20 inclusive, because of their location on the crest or lee side of the Thule peninsula ridge.

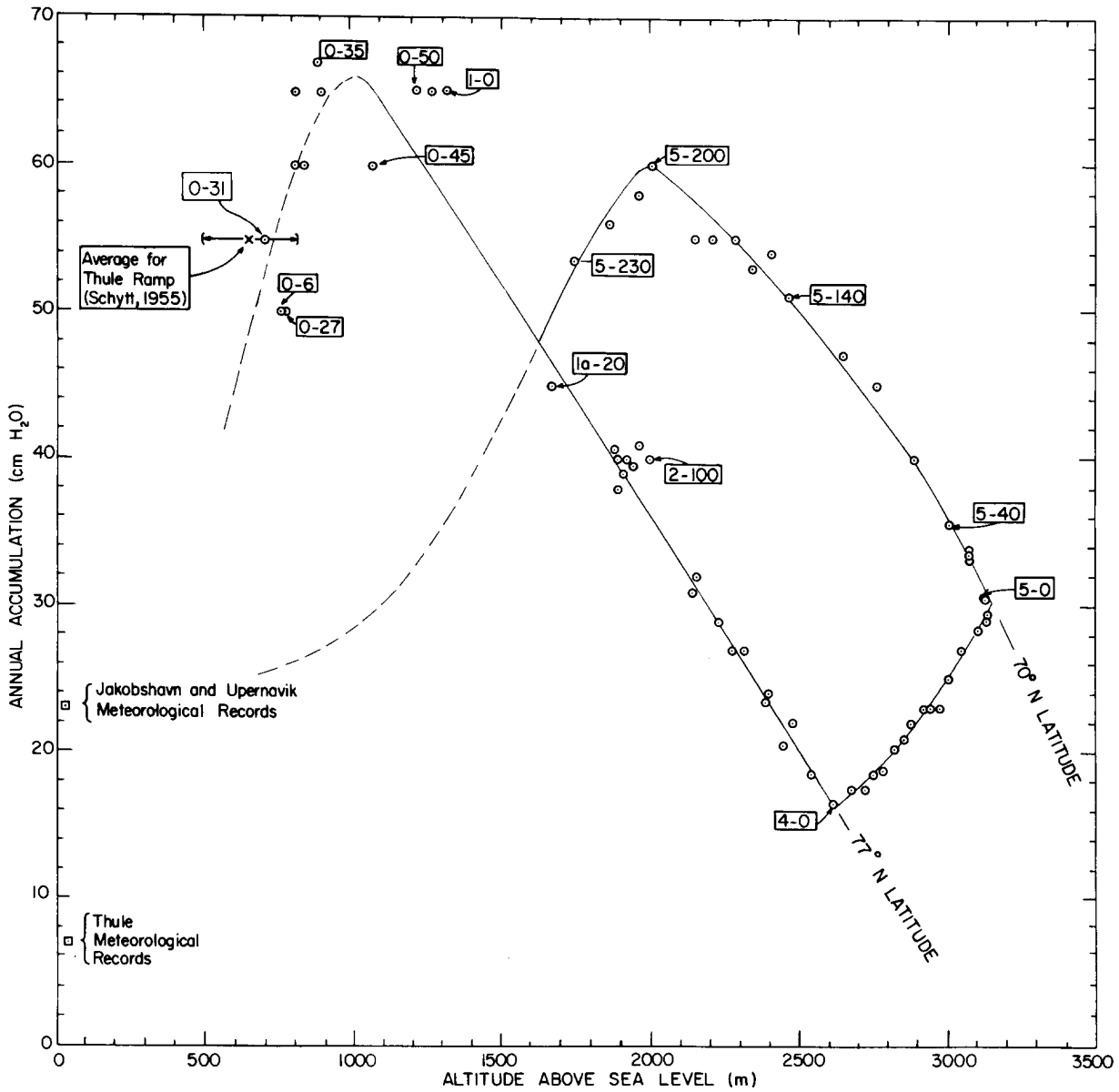


Figure 29. Accumulation - altitude relationship on the west slope of the Greenland ice sheet. Points are from south- or west-facing slopes, i.e., windward to storm winds. Each point represents an average of several years' accumulation (see Fig. 28). Data from meteorological records are anomalously low because of incomplete gage-catch. The Thule data are not representative for the coast of Melville Bay at 76°N because Thule lies in a precipitation shadow. The sea level accumulation value for south-facing slopes at 76-77°N is estimated to be at least 30 cm H₂O per year.

by standard, unshielded* precipitation gages decreases with increased wind speed (Brooks, 1938; Wilson, 1954). This is true regardless of whether the precipitation is in the form of rain or snow, but the lowest catch percentages, about 25%, occur in the case of snow storms. Black (1954) found that precipitation values recorded by the standard 8-in. precipitation gage at Barrow, Alaska were two to four times lower than those obtained by measuring the water equivalent of snow on the tundra. In general, precipitation in at least some, and perhaps many, arctic regions is greater than recorded values indicate. In Greenland, the two shortcomings of standard precipitation gages (location at a single point, and incomplete catch) can be eliminated by using the ice sheet as an infinite set of automatically recording precipitation gages.

Accumulation contour map

A contour map† of gross annual accumulation based on all available data,** is shown in Figure 30. In general, the accumulation contours follow the north-south trend of the coast lines. The zone of maximum precipitation lies close to the coast in two locations, one on the east coast between Angmagssalik and Scoresbysund, the other on the west coast between Upernavik and Thule.

The west coast swings from north-south to east-west to form the north shore of Melville Bay at 76°N. Cyclonic storms moving northward along the coast either ascend Thule peninsula here, or are deflected westward to Devon and Ellesmere islands. Accordingly the ice sheet near the coast between 74°30' and 76°30'N, and the east facing shores of the Canadian Islands between 75 and 81°N receive relatively heavy precipitation.

Storms from the Icelandic low pressure region meet Greenland's highest mountain barrier, over 3000 m altitude, on the east coast between Angmagssalik and Scoresbysund. This results in heavy precipitation on the windward (south- and east-facing) slopes and a precipitation shadow to the north. Few data are available for this region and the contours are based on: 1) the 90 cm H₂O per year precipitation recorded at Angmagssalik compared with 23 cm measured 300 km north of Angmagssalik at 3000 m altitude on the ice sheet, 2) numerous glaciers flowing into the sea south of Scoresbysund compared to the dry, unglaciated regions to the north, 3) the assumption that the zone of maximum precipitation lies below 2000 m here as on the west side of the ice sheet (Fig. 29), and 4) the analogous effect on precipitation exerted by Thule peninsula in northwest Greenland.

Few data points are available on the ice sheet south of 66°N. Accumulation contours are extrapolated through this region, based on precipitation records at Godthaab, Ivigtut, and Angmagssalik and on the accumulation - altitude relations observed (Fig. 29) farther north.

Because of insufficient data in north Greenland the 10 cm line is generalized without regard for topography. However, the southwest- and west-facing slopes of the peninsular

* Warnick (1953) discusses recent experimental work aimed at improving the efficiency of precipitation gages by various types of shielding.

† An accumulation contour map published by Diamond (1958) needs revision because the published value (Benson, 1955a) of 60 cm H₂O per year at 1-0 was quoted as 20. Also the values quoted for the 1955 "JELLO" traverse were preliminary uncorrected estimates.

** Mr. James A. Bender of USA SIPRE, using the methods described herein, measured the accumulation at each of the three HIRAN stations. Data from the British North Greenland Expedition are based on 5 pits and 30 Rammsonde profiles (Bull, 1958). The data of Koch - Wegener were obtained by using the same stratigraphic unit employed in this work, i. e., the discontinuity between the high density snow and the underlying softer snow. They also adjusted their data so that a full year's accumulation, from one fall level to the next was measured. This was necessary because they were in the area during June and July and therefore did not directly observe a full year's accumulation. The correction was of the same sort made in this work (see Fig. 26). DeQuervain's data were not adjusted and as annual values are at least 5 cm too low, 5 cm H₂O were added to his values before entering them in Figure 30. Recorded precipitation from coastal stations are listed; more than 50 yr of records were averaged at all stations except Thule, Alert, and Brønlund Fjord which cover 8, 3, and 2 yr respectively.

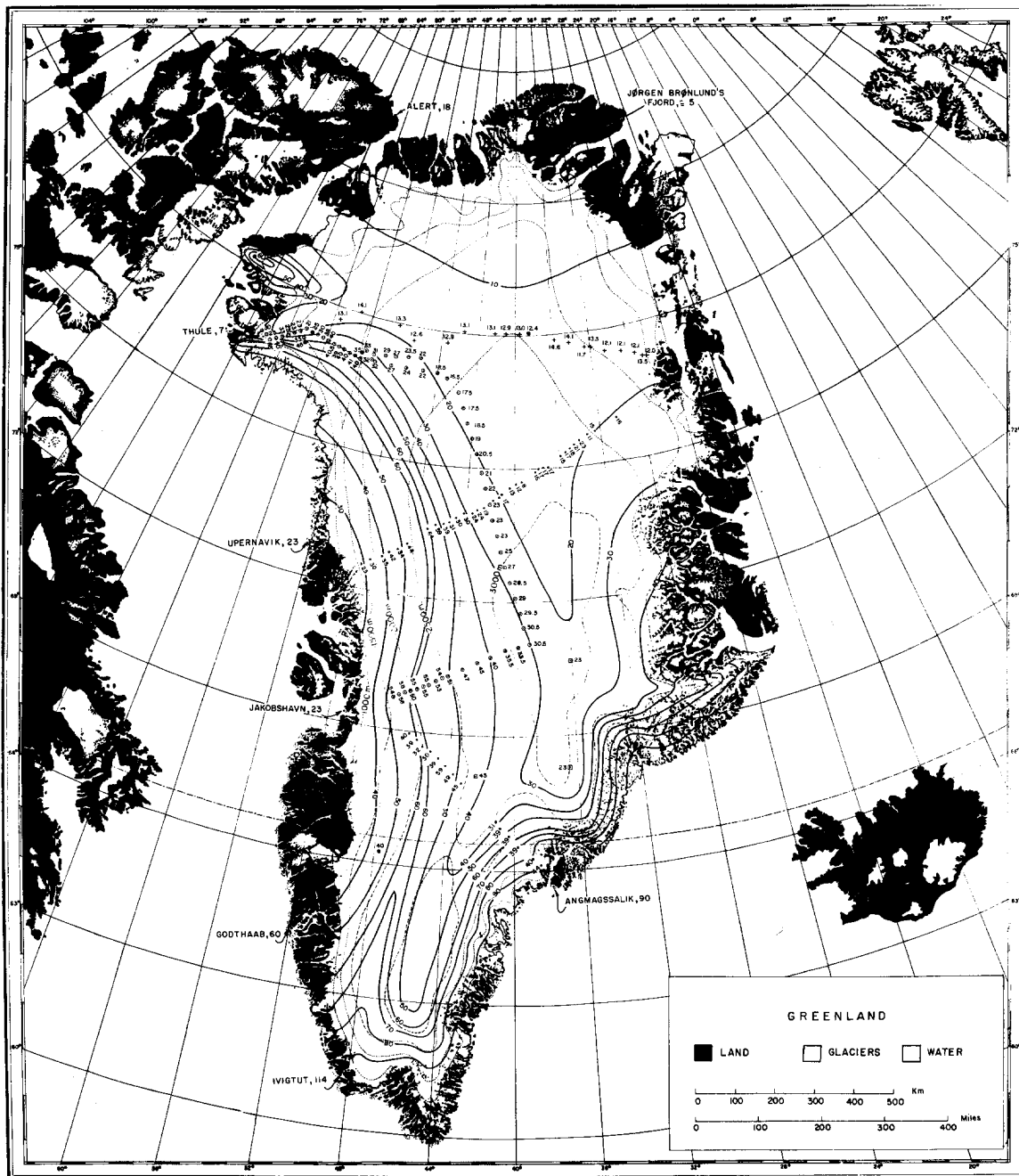


Figure 30. Contours of gross annual accumulation. See Figure 1 for identity of data points. Data from this study are based on averages of several years' accumulation (see Fig. 28). Data from Koch and Wegener (1930) were based on the same stratigraphic unit used in this study. Data from deQuervain and Mercanton (1925) have been adjusted by adding 5 cm H₂O to each value before entering it on the map. Data from the British North Greenland Expedition (Bull, 1958) are primarily based on Rammsonde profiles. Average precipitation values at coastal stations are indicated. Brøn-lund Fjord value is from Fristrup (1952).

ridges extending inland from Hall Land and Nares Land may be expected to have higher values of accumulation, just as do the Thule and Inglefield Land peninsulas, and for the same reason. These expectations seem to be supported by observations of local increases in accumulation in north Greenland made by Chester Langway (personal communication), which will be published by CRREL in the near future.

Independent checks on the stratigraphic Interpretations

Stratigraphic correlation in northwest Greenland was well established in 1954 (see Fig. 22-25 and Benson, 1959). However, the work included only 100 miles of traverse in the dry-snow

facies. Stratigraphy in the dry-snow facies must be interpreted in the absence of melt evidence, whereas, in the percolation facies, traces of melt evidence are useful in correlation. During the 1955 expedition, strata were successfully correlated from the percolation facies at 77°N through about 500 miles of the dry-snow facies and back into the percolation facies at 71°N (see data sheets). This, in itself, is considered a test of the method, but two independent checks exist and are described below.

Correlation between stratigraphic and meteorological records

Data at 1-0 extended 14.4 m below the snow surface in 1954. This represents a period of 11 yr (1943 to 1954). The stratigraphic record shows that the degree of melt action varied considerably from year to year during this period. If the amount of summer melt can be related to summer warmth, then meteorological records from coastal stations may provide a useful check on stratigraphic interpretations at stations near enough to be subject to the same general weather pattern. Thule is 70 miles from 1-0 and its meteorological records are continuous from 1947 to date. A single parameter, indicative of relative summer warmth may be obtained by totalling the degree days above freezing for each year. The calculations are based on average daily temperatures, i. e., if the average temperature on a particular day is 8C, it is counted as 8 deg days above freezing. The results are plotted in Figure 31.

The years 1947 and 1951, which produced the least melt at 1-0, are the coldest recorded at Thule. The heaviest melt recorded between Thule and 2-150 occurred in July 1954, and this is the warmest year on the Thule record. The moderately heavy melt during 1949, 1950, 1952, and 1953 correspond to years which are colder than 1954 but warmer than 1947 or 1951.

A word of caution may be appropriate regarding the correlation of warm years with abundance of melt evidence. A few very warm days may produce heavy melt action in firn, and such a brief "heat wave" may occur during an otherwise cool summer. However, the general agreement between Figure 31 and the record at 1-0 on Data sheet 3 is satisfying; it agrees with the interpretations shown in Figures 22 to 25 and provides an independent check on the stratigraphic methods.

O^{18}/O^{16} ratios in snow and firn layers

Variations in the O^{18} content of waters from natural sources are discussed by Epstein and Mayeda (1953). The variation is temperature-dependent and it was expected that differences between summer and winter precipitation on the ice sheet would be recorded in the O^{18}/O^{16} ratios of firn strata. During 1954 and 1955 a total of 300 samples were taken for study of the general relationship between O^{18}/O^{16} ratios and firn stratigraphy on the Greenland ice sheet (Epstein and Benson, 1951). For the present it is sufficient to state two major results:

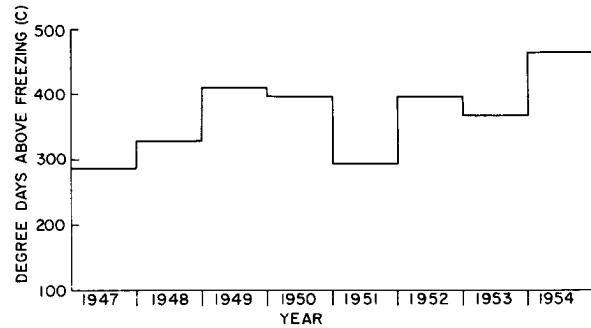
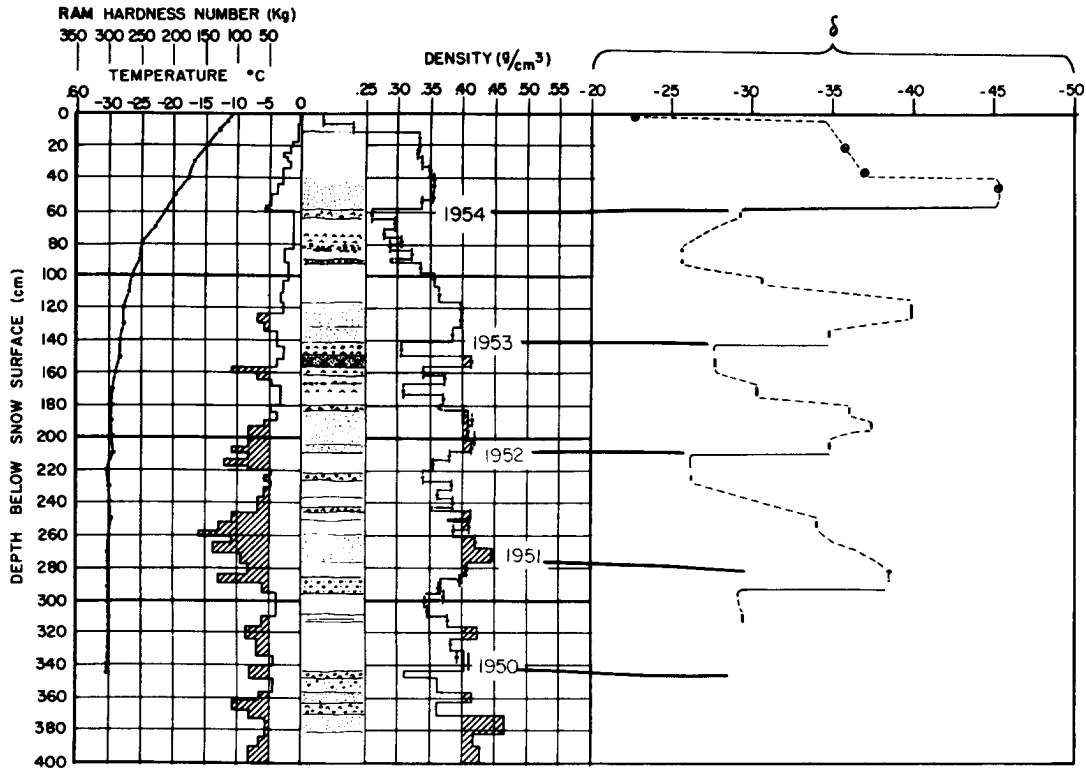
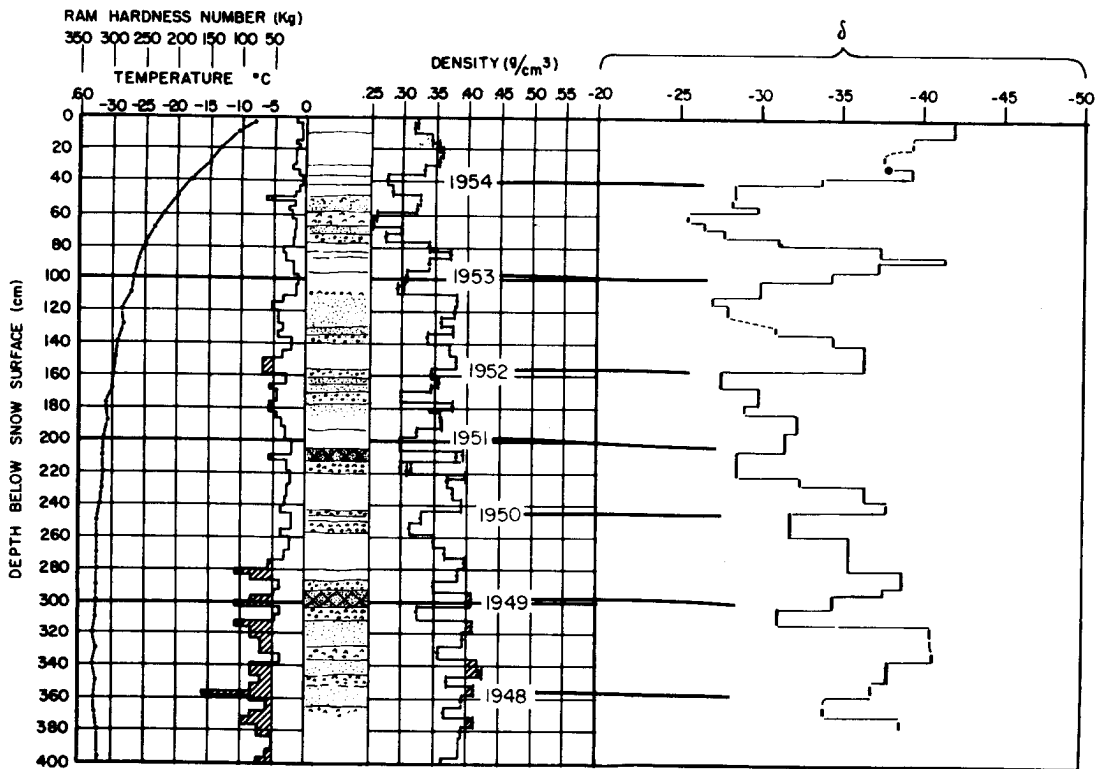


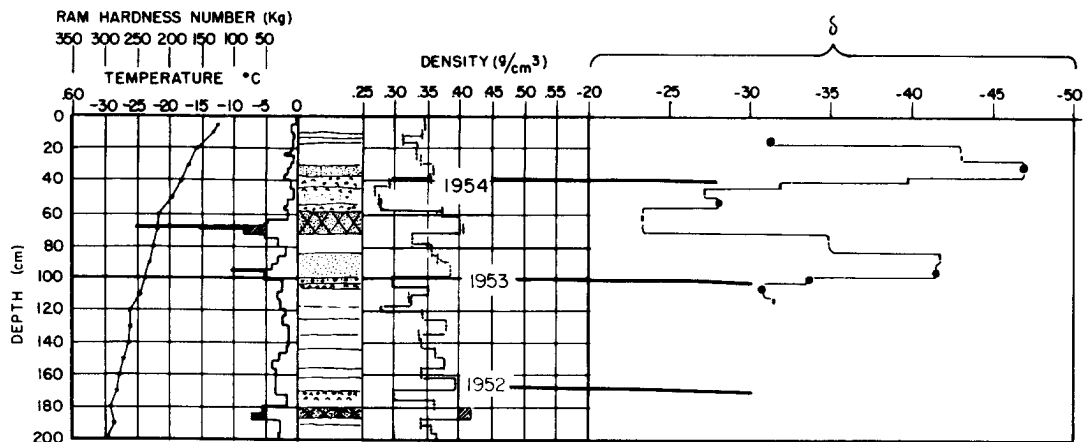
Figure 31. Degree days above freezing at Thule, Greenland 1947-1954. Data from U. S. Weather Bureau and USAF Air Weather Service.



a. Station 2-150, 31 May 1955. Elevation 2273 m (7060 ft).



b. Station 2-225, 6 June 1955. Elevation 2536 m (8320 ft).



c. Station 4-75, 17 June 1955. Elevation 2749 m (9019 ft).

Figure 32. Standard stratigraphic data compared with δ , the O^{18}/O^{16} ratio relative to mean ocean water.

$$\delta = \left[\frac{R_{\text{(sample)}} - R_{\text{(standard)}}}{R_{\text{(standard)}}} \right] \times 1000 = 1000 \left[\frac{R_{\text{sample}}}{R_{\text{standard}}} - 1 \right]$$

where R is the ratio H_2O^{18}/H_2O^{16} .

$\delta = 0.00$ for mean ocean water by definition (Epstein and Mayeda, 1953). Thus $\delta = -10$ means that O^{18}/O^{16} ratio of the sample is 1% or 10% lower than that of mean ocean water. The fall discontinuity as seen in the stratigraphic record correlates well with an abrupt change in the O^{18}/O^{16} ratios. The wind slab formed during the 1954 summer (Fig. 32c) has the highest O^{18}/O^{16} ratio. This suggests that it was formed during the 11-15 July 1954 heat wave which left melt evidence at altitudes below 7000 ft at this latitude.

1) The altitudinal effect: Snow deposited from a single storm shows lower O^{18}/O^{16} ratios at higher altitudes.

"In terms of per mil variation per 1000 ft of altitude, it is approximately 1.8 in northern Greenland, 1.7 on the west slope of the Sierra Nevada in California, 1.6 in the Pasadena area, California, and 0.6 on the Saskatchewan Glacier. The last value may not be reliable because of incomplete sampling." (Epstein and Sharp, 1959, p. 91).

2) The seasonal effect: Snow deposited in winter has less O^{18} than that deposited in summer. This produces an annual variation in O^{18}/O^{16} ratios which was observed by sampling every stratigraphic unit in the upper 4 m at stations 2-225 (47 samples) and 4-200 (59 samples). Samples through at least two yearly cycles were taken at stations 1-0 (1954), 2-70 (1954), 2-100 (1954), 1a-20 (1955), 2-150 (1955), 4-75 (1955), and 5-40 (1955); and samples across the fall discontinuity were taken at 12 of the stations between 4-275 and 5-230.

Comparison between O^{18}/O^{16} ratios and standard stratigraphic measurements are shown in Figure 32 and at station 1a-20 on Data sheet 4. Confidence in the interpretation of firn stratigraphy is gained by the agreement between the three independent methods of approaching the problem presented above.

CHAPTER IV. TEMPERATURE DISTRIBUTION

Temperature and density are the most important things to measure in snow and firn. This chapter summarizes the information obtained from temperature measurements at the snow surface and within the first 10 m below the snow surface. The altitudinal gradient of the mean annual temperature is based on meteorological processes which are expected to prevail in Antarctica as well as in Greenland. Therefore, the same altitudinal gradient should be expected in Antarctica as in Greenland.

Seasonal temperature variation on the snow surfaceData

Air temperature measurements, made in a standard meteorological instrument shelter for periods of at least one year, are available from two locations on the ice sheet (2-100 and 5-40)

<u>Station</u>	<u>Time interval</u>	<u>Observer</u>
2-100 (Site 2)	7 July 1953 - 31 May 1956	USAF Air Weather Service
5-40* (French Station Centrale)	5 Sept 1949 - 15 Aug 1951	Expedition Polaires Francaise
5-40 (Eismitte)	1 Aug 1930 - 6 Aug 1931	Johannes Georgi

* Not completely published as of June 1959.

Air temperatures measured in weather shelters are not obtained at constant height above the snow surface because of accumulation of new snow and snow drifting. For example, Georgi's thermometer varied in height from 1.20 to 2.21 m above the snow surface. To obtain uniformity, he devised and built an instrument to measure the air temperature 10 cm above the prevailing snow surface. These measurements began in February. He estimated the temperature difference between the shelter and a point 10 cm above the snow surface for the months preceding February. The snow surface temperature itself was estimated from the 10 cm values. The corrections are small compared to the marked variation in air temperature during a year but Georgi points out that the estimates of snow-surface temperatures are improved by applying them.* Georgi's estimated monthly averages of snow-surface temperature at Eismitte are listed with observed air temperature data in Table I.

No data are available to adjust the USAF data to obtain snow-surface temperatures. However, it is assumed that negligible error is made if Georgi's corrections are applied. The monthly averages for 2-100 are listed in Table II.

Analysis

Sorge (1935, p. 232-236) showed that the snow-surface temperatures of Table I can be represented by the first two terms of a Fourier series, i. e.:

$$f(t) = \sum_{n=0}^2 (P_n \cos nt + q_n \sin nt),$$

$$= P_0 + P_1 \cos t + Q_1 \sin t + P_2 \cos 2t + q_2 \sin 2t. \quad (1)$$

Equation 1 may be rewritten as a series involving cosine terms only,

$$f(t) = P_0 + a_1 \cos (t - A_1) + a_2 \cos (2t - A_2) \quad (2)$$

* Measurements by Nyberg (1938) indicate that the increase of temperature with height in the first 10 cm above the snow surface is an order of magnitude greater than estimated by Georgi.

Table I. Monthly mean temperatures at Eismitte* (C), 1930-1931.

Month	Air temp in the instrument shelter	Correction according to Georgi	Air temp 10 cm over the snow surface (rounded off)	Correction (est.)	Temp of the snow surface
Aug	-17.7	0	-17.7	0	-17.7
Sept	-22.1	-0.5	-22.6	0	-22.6
Oct	-35.6	-1	-36.6	-0.1	-36.7
Nov	-43.1	-1.5	-44.6	-0.2	-44.8
Dec	-38.8	-1.5	-40.3	-0.2	-40.5
Jan	-41.7	-2	-43.7	-0.3	-44.0
Feb	-47.5	-1.75	-49.0	-0.2	-49.2
Mar	-39.4	-1.00	-40.4	-0.1	-40.5
Apr	-31.0	+0.12	-50.9	0	-50.9
May	-20.1	+0.85	-19.5	+0.1	-19.2
June	-15.3	+0.86	-14.4	+0.1	-14.5
July	-10.8	-0.12	-10.9	0	-10.9
Avg	-30.2		-30.85		-30.94

* Eismitte of 1930-31 was the French Station Centrale of 1949-51 and Station 5-40 of this study.

Table II. Air temperature data (C) for station 2-100, Greenland.

Month	Air temperature				Avg	Georgi's correction	Temp at snow surface
	1953	1954	1955	1956			
1 Jan	-	31.67	36.11	36.83	34.8	-2.3	-37.1
2 Feb	-	30.56	31.11	35.67	32.4	-1.95	-34.4
3 Mar	-	33.89	34.44	35.22	34.5	-1.10	-35.6
4 Apr	-	23.89	30.67	26.72	27.1	+0.12	-27.0
5 May	-	16.11	16.44	19.50	17.3	+0.93	-16.4
6 June	-	8.89	8.33	-	8.61*	+0.96	-7.6
7 July	-	6.11	8.22	-	7.16*	-0.12	-7.3
8 Aug	8.33	7.22	12.00	-	9.17	0.0	-9.2
9 Sept	20.00	†	18.94	-	19.44*	-0.5	-19.9
10 Oct	28.89	25.56	18.22	-	24.20	-1.1	-25.3
11 Nov	35.00	27.78	31.72	-	31.50	-1.7	-33.2
12 Dec	41.67	38.33	36.78	-	38.90	-1.7	-40.6
Avg		-22.5	-23.6		-23.8		-24.4

* Based on data from 2 yr only.

† Avg of 1953 and 1955 data was used for Sept 1954.

where

$$a_1 = \sqrt{P_1^2 + q_1^2}, \quad A_1 = \tan^{-1} \frac{q_1}{P_1}$$

$$a_2 = \sqrt{P_2^2 + q_2^2}, \quad A_2 = \tan^{-1} \frac{q_2}{P_2}.$$

The data from station 2-100 (Table II) can also be represented by eq 1 and 2.

Values of the constants in eq 2 for the data of Tables I and II are summarized in Table III.

Table III. Values of constants in eq 2.

	5-40 Sorge's values	5-40* Sorge's values corrected	2-100 Avg of 3 yr' data	2-100 1954 values only
P_0 (C)	-31.0	-31.0	-24.4	-23.2
P_1 (C)	17.46	17.46	16.1	15.40
q_1 (C)	-1.63	-1.63	-0.552	-0.948
P_2 (C)	2.6	2.6	2.47	2.68
q_2 (C)	-1.6	-1.6	-0.197	-0.317
a_1 (C)	17.54	17.54	16.11	15.41
a_2 (C)	3.03	3.05	2.48	2.70
A_1	-6°15'	-5°20'	-1°58'	-3.52°
A_2	-27°50'	-31°35'	-4°34'	-6.75°

* Numerical errors are present in Sorge's values a_2 , A_1 , and A_2 . These are slight and do not affect his results.

The phase angles are expressed in terms of angular degrees with 30 deg set equal to 1 month and $t = 0$ on 15 July, so the phase angles in Table III give maximum values for the year and half-year waves as follows:

Station	Date of maximum value	
	Year wave	Half-year wave
5-40	10 July	1 July
2-100 (3 yr avg)	13 July	13 July
2-100, 1954 data	12 July	12 July

In general the annual temperature variation on the snow surface has the same phase throughout the north-south extent of the region considered in this paper, i. e., 70°N to 77°N. It reaches its maximum within ± 2 days of 12 July. Existing data suggest that the maximum occurs slightly earlier in the south than in the north. The maximum deviation from mean annual temperature is nearly the same over the region but, according to the available data, it is about 10% greater at 70°N than at 77°N latitude.

Seasonal Temperature Variation below the Snow Surface

Data

The temperature profiles of Figure 33 show the seasonal temperature variation below the snow surface at stations 1-0, 2-0, 2-50, 2-100, 2-120, and 2-200 in north Greenland. Similar curves for station 5-40 (Eismitte of 1930-1931) were presented by Sorge (1935).

It may be seen that profiles measured at the same station in different years, but at about the same time of year are remarkably similar. For example, the curves

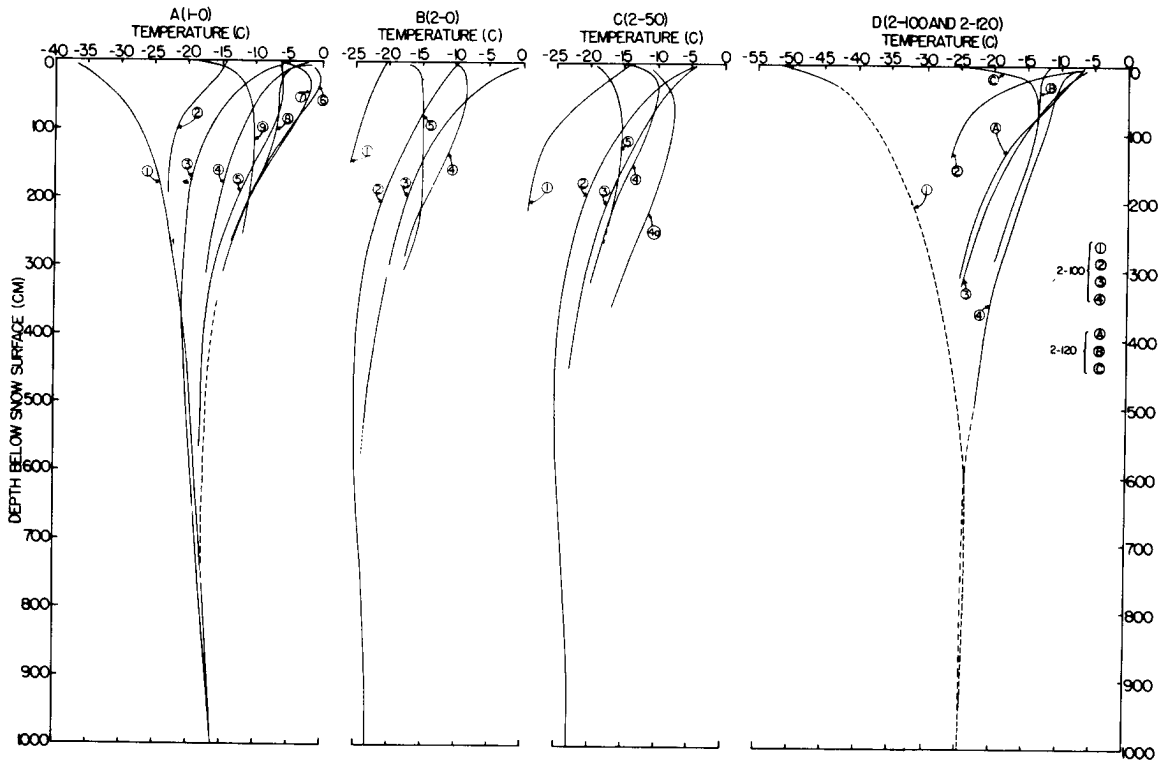


Figure 33. Temperature profiles at stations 1-0, 2-0, 2-50, 2-100, and 2-120.

Station			Station		
1-0	1	3 Mar 1954*	2-50	1	24 May 1955
	2	19 May 1955		2	9 July 1954
	3	3 June 1954		3	4 Aug 1953
	4	6 July 1953*		4	21 Aug 1953†
	5	18 July 1953		4a	21 Aug 1953†
	6	17 Aug 1952	5	18 Sept 1953	
	7	18 Aug 1954	2-100	1	? Mar 1954**
	8	19 Aug 1953*		2	28 May 1955
	9	21 Sept 1953		3	7 July 1954
		4		26 Aug 1953	
2-0	1	22 May 1955	2-120††	A	1 July 1952
	2	21 June 1954		B	30 Aug 1952
	3	27 July 1953		C	3 Sept 1952
	4	21 Aug 1952			
	5	19 Sept 1953			

* From measurements by L. H. Nobles.

† Curve 4 was measured in undisturbed snow 50 m from the pit of 4 August; 4a was measured 1 m from the test wall of the 4 August pit.

** Curve 2 based on observations in the winter by G. E. Frankenstein and the mean annual value at the deep pit.

†† Curve A measured by H. Bader within 1 mile of the 1954 survey area pit B. Curves B and C were obtained at 2-120, 1952. The elevations are nearly equal at these locations (see Fig. 1, 2).

measured on 17 August 1952, 19 August 1953, and 18 August 1954, at station 1-0 are practically indistinguishable below 160 cm. It is assumed that this annual reproducibility of temperature profiles implies that the ice sheet climate is sufficiently constant to permit comparison between temperature profiles measured in four different years as if they were all from the same year. Thus, at station 2-0 (Fig. 33) the measurements made at nearly the same time of month in May 1955, June 1954, July 1953, August 1952, and September 1953 illustrate a part of the annual cycle.

To evaluate temperature as a variable on the ice sheet its distribution at a given time must be known. As a parameter in defining facies, temperatures should be measured in the upper 3 to 5 m during the peak of the melt season. It has not been possible to obtain simultaneous measurements over a large area of the ice sheet, but temperature profiles obtained in August are available for most of the north (77°N) and south (70°N) legs of the traverse, i. e., 0-0 to 4-0 and 5-0 to 5-230 (Fig. 34a, b). These curves illustrate the altitudinal variation in firn temperature vs depth, during late summer, but to locate facies boundaries it is useful to represent the data as isotherms in the top 4 to 5 m of firn with altitude as the abscissa (Table IV, Fig. 35a, b). This shows the maximum penetration of isotherms during the melt season (see Ch. V). Clearly, the top 1-2 m of some temperature profiles are measurably influenced by the fall cooling wave. In such cases a reasonable estimate of temperatures during the peak of the melt season may be obtained by extrapolation as shown in Figure 34b. The amount of melt evidence in the upper layers, together with the shape of July profiles, is used to guide the extrapolation. All extrapolations are indicated in Table IV.

Analysis

Sorge (1935, p. 236-263) carried out a detailed mathematical analysis of the annual temperature variation with depth at Eismitte (station 5-40). He assumed that heat is transferred in the snow and firn purely by conduction and used the function:

$$f(z, t) = R_0 e^{-z \sqrt{\frac{\pi}{T\alpha}}} \cos\left(\frac{2\pi t}{T} - z \sqrt{\frac{\pi}{T\alpha}}\right), \quad (3)$$

where

R_0 is the amplitude* of temperature on the snow surface.

T is period (in our problem the period is 1 yr for the year wave and $\frac{1}{2}$ yr for the half-year wave).

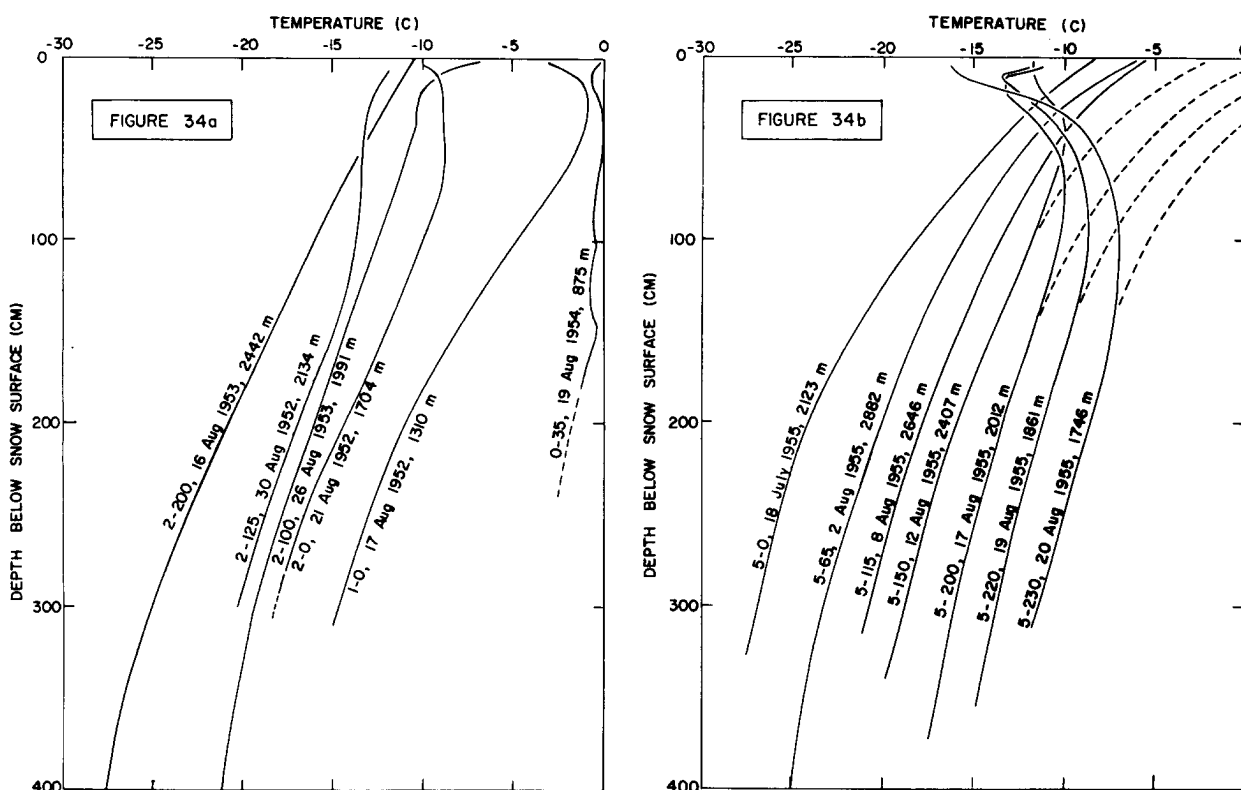
α is the thermal diffusivity of firn.

$R_z = R_0 e^{-z \sqrt{\frac{\pi}{T\alpha}}}$ gives the amplitude of the temperature variation at the depth z .

The term " $z \sqrt{\frac{\pi}{T\alpha}}$ " gives the phase angle at the depth z .

The temperature variation on the snow surface is expressed as the sum of two cosine terms. Therefore the temperature function at any depth may be obtained by substituting each of these surface functions separately into eq 3 and adding the results. This can be done as soon as values for α , the thermal diffusivity, are known. Sorge (1935, p. 237-239) points out that it is not correct to compute α by a least squares analysis of the observed temperature variations because the snow surface is not constant, as it always receives new accumulation, and the value of α itself is not constant over the depth range considered. A functional relationship between α and firn-density was experimentally determined, and values of α obtained from it were used to compute the temperature variations with depth. The computed and observed temperatures agreed closely; this fact was

* Sorge uses the term "halbamplitude" for R_0 but from the equation he means "amplitude" which is the half range. The use of "halbamplitude" for amplitude and "amplitude" for range is inconsistent in his paper. The term "amplitude" means half range except on pages 237, 240, 246, 257, and 259.



a. Measurements over a 1560 m (5120 ft) range of altitude at $77.0 \pm 0.3^\circ\text{N}$ latitude.

b. Measurements over a 1380 m (4530 ft) range of altitude at $70.4 \pm 0.7^\circ\text{N}$ latitude.

Figure 34. Temperature profiles measured in late summer on the west slope of the Greenland ice sheet.

interpreted as additional proof of the relation between α and ρ . The density profiles from stations 2-100 and 5-40 are so close that negligible error is made if Sorge's values of α are used in analyzing* the annual temperature-depth relations at 2-100.

Computed annual temperature variations at the snow surface and at several depths below the snow surface are plotted in Figure 36.

Maximum computed deviations from the mean annual value in the top 16 m of firn at stations 5-40 and 2-100 (Table V) show two features immediately:

a) The firn temperature 10 m below snow surface is never more than 0.3C from the mean annual value.

b) If the mean annual temperature is -20C or greater, the snow surface will be occasionally exposed to melting temperatures for a period of at least one month.

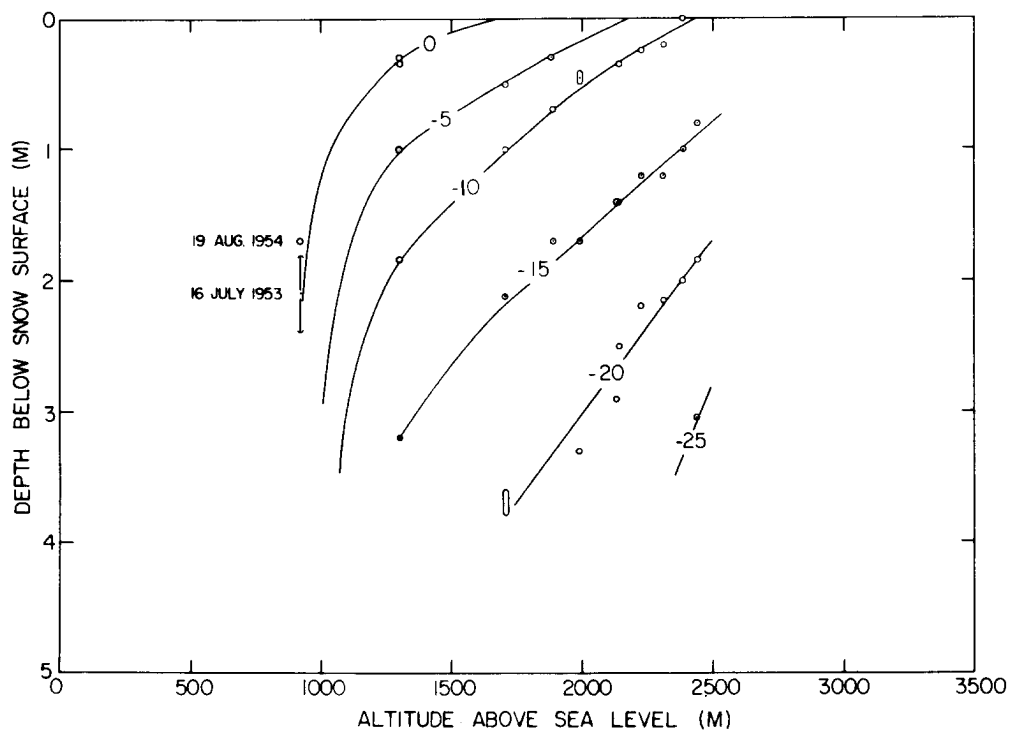
The occurrence of melting on the snow surface has been neglected in the analysis. Therefore, the analysis may give positive temperatures for the snow surface at some locations. All positive values must be considered to be 0C . They cause the actual mean annual temperature to be higher than computed.

* This type of analysis does not give the complete picture because heat is also transferred in the upper layers by convection. The effects of this are discussed later.

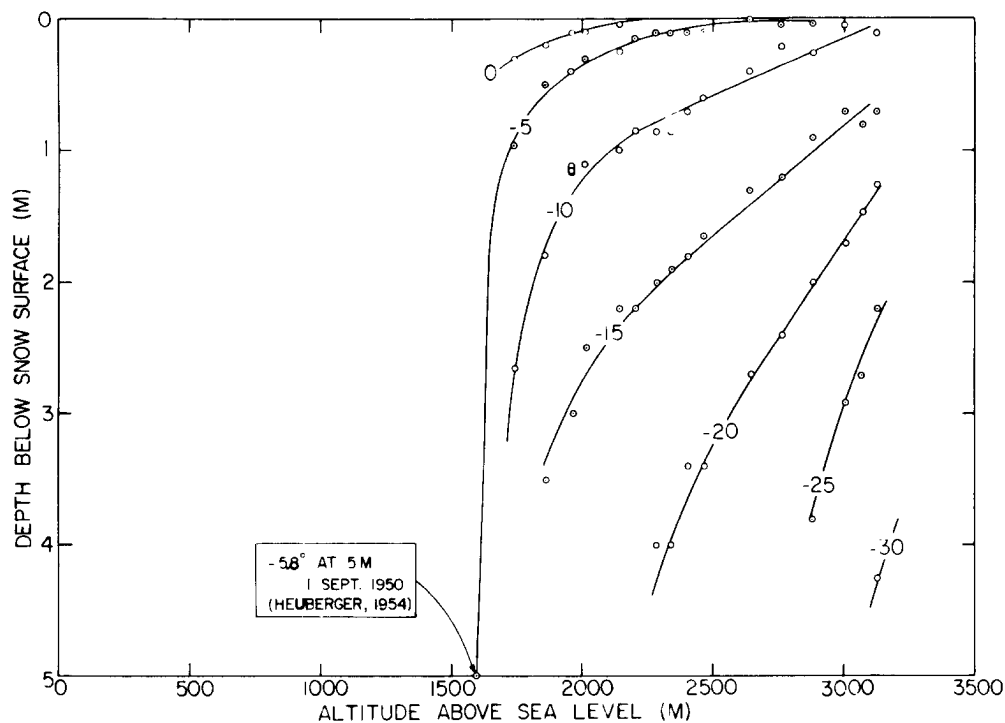
Table IV. Location of isotherms during peak of the melt season at: (A) $77.0 \pm 0.3^\circ\text{N}$ and (B) $70.4 \pm 0.7^\circ\text{N}$.

Elevation		Depth below snow surface (cm)									
Station	(m)	Date	0C	-5C	-10C	-15C	-20C	-25C	-30C		
A											
2-200	2442	15-8-53	-	-	-	80	184	304	-	-	-
2-180	2387	15-8-53	-	-	0	100	200	-	-	-	-
2-160	2313	14-8-53	-	-	20	120	215	-	-	-	-
2-140	2228	14-8-53	-	-	24	120	219	-	-	-	-
2-120	2140	11-8-53	-	-	35	140	250	-	-	-	-
2-120	2134	30-8-52	-	-	-	140	290	-	-	-	-
2-100	1990	26-8-53	(0)*	(10)	25	170	330	-	-	-	-
2-30	1887	23-8-52	(0)	(30)	60	170	-	-	-	-	-
2-0	1704	21-8-52	(5)	50	100	212	370	-	-	-	-
1-0	1302	17-8-52	(30)	100	184	320	-	-	-	-	-
1-0	1302	18-8-54	(35)	100	184	-	-	-	-	-	-
0-35	914	16-7-53	180	-	-	-	-	-	-	-	-
0-35	914	19-8-54	170	-	-	-	-	-	-	-	-
B											
5-0	3123	18-7-55	-	-	13	70	130	230	420	-	-
5-20	3072	20-7-55	-	-	-	85	150	270	-	-	-
5-40	3005	23-7-55	-	-	6	75	165	290	-	-	-
5-65	2882	2-8-55	-	4	30	100	205	380	-	-	-
5-90	2763	6-8-55	-	4	18	125	250	-	-	-	-
5-115	2646	8-8-55	-	-	40	135	270	-	-	-	-
5-140	2466	10-8-55	-	-	60	165	340	-	-	-	-
5-150	2407	12-8-55	(0)	(10)	50	180	340	-	-	-	-
5-160	2342	13-8-55	(0)	(10)	10-80	190	(400)	-	-	-	-
5-170	2283	14-8-55	(0)	(10)	50	15/205	(400)	-	-	-	-
5-180	2206	15-8-55	(0)	(15)	60	220	-	-	-	-	-
5-190	2146	16-8-55	(5)	(25)	65	230	-	-	-	-	-
5-200	2012	17-8-55	(10)	(30)	80	255	-	-	-	-	-
5-210	1963	18-8-55	(10)	(40)	50/105	0/300	-	-	-	-	-
5-220	1861	19-8-55	(20)	(50)	40/160	355	-	-	-	-	-
5-230	1746	20-8-55	(30)	(90)	30/155	13	-	-	-	-	-
French Camp VI	1598	28-8-50	-	(-5.8C)	800	4000	-	-	-	-	-
				500							

* Extrapolated values (in parentheses) indicate depths at peak of melt season (see p. 48). Extrapolated values are plotted in Figure 35; unadjusted values are plotted in Figure 38.



a. $77.0 \pm 0.3^\circ \text{N}$ latitude.



b. $70.4 \pm 0.7^\circ \text{N}$ latitude

Figure 35. Isotherms in the upper 5 m on the west slope of the Greenland ice sheet during the peak of the melt season. Data points are from Table IV.

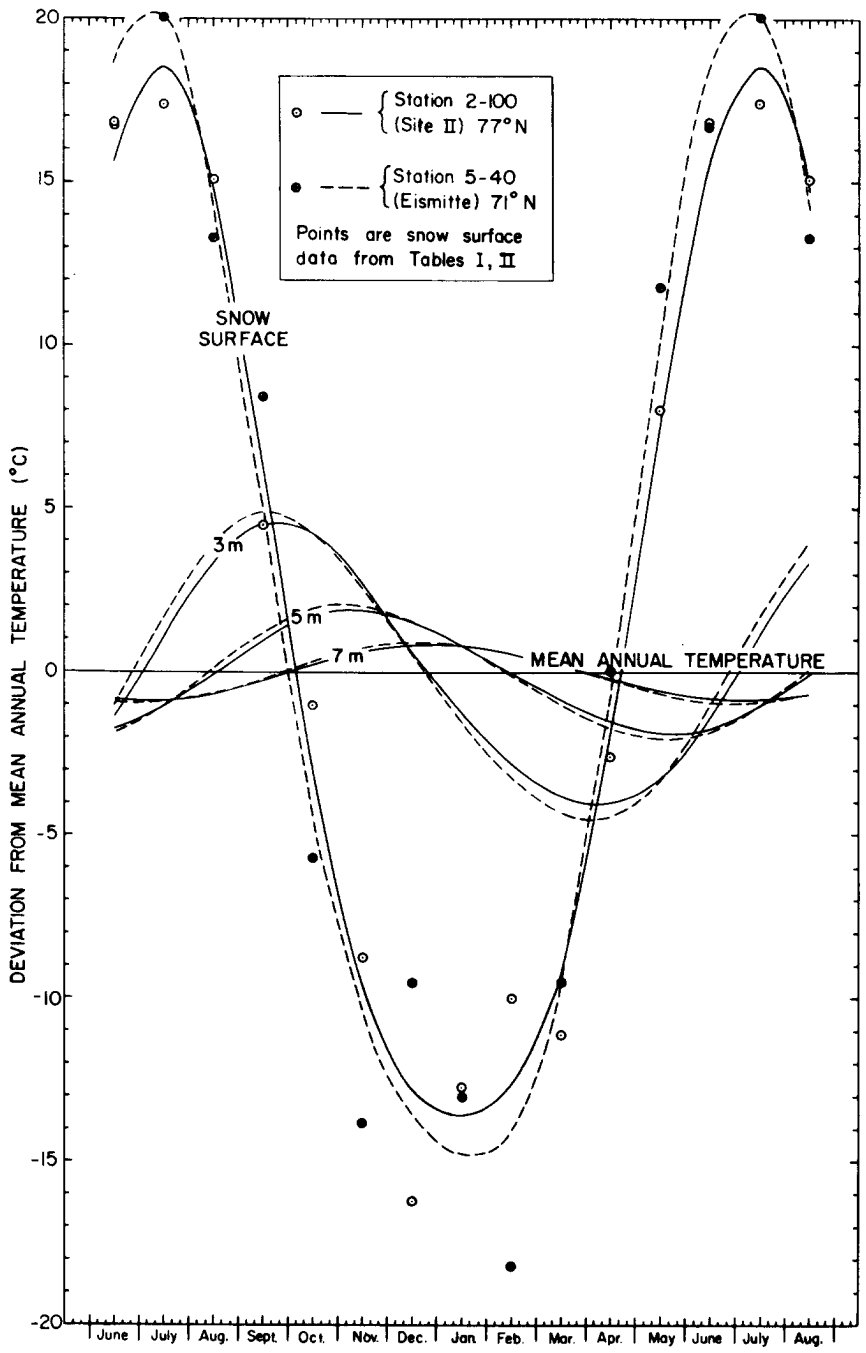


Figure 36. Annual temperature variations at the snow surface and at depths 3, 5, and 7 m below the surface. Curves for the snow surface were computed from eq 2 with values of constants from Table III. Curves for depths below the surface were computed from eq 3. Data points are from the snow surface at station 5-40 (Eismitte, Table I); and station 2-100 (Table II).

Table V. Maximum theoretical deviation (C) from mean annual temperature.

Depth below snow surface (m)	71°N Station 5-40	77°N Station 2-100
0	20.59	18.59
1	12.73	11.51
2	8.00	7.28
3	5.13	4.66
4	3.33	3.03
5	2.20	2.00
6	1.46	1.34
7	0.983	0.899
8	0.667	0.609
9	0.464	0.414
10	0.310	0.284
11	0.216	0.198
12	0.143	0.132
13	0.102	0.094
14	0.071	0.065
15	0.048	0.044
16	0.034	0.031

Temperature values obtained at depths shallower than 10 m deviate from the mean annual value by more than 0.3C. However, a correction for the deviation from mean value at a given date and depth can be computed from eq 3. This is done in Appendix B; to minimize the effects of convection, no depths less than 3 m were used (see p. 56).

Distribution of Mean Annual Temperature on the Ice Sheet

The data of Appendix B plotted against altitude in Figure 37 suggest the possibility of mapping the distribution of mean annual temperature on the ice sheet, because they indicate the rate of change of temperature with altitude and latitude.

Altitude gradient

The altitude gradients in Figure 37 can be related to processes in the atmosphere* by assuming that the air in contact with the snow surface has the same temperature as the snow. The altitude gradient is nearly 1C/100 m at 70° and 77°N; this is essentially the magnitude of the dry-adiabatic rate of temperature change for vertically moving air. It is important to note that these gradients refer to the rate of change of temperature measured along the surface of the ice sheet (or a parallel surface 10 m below the snow surface) and are not to be confused with the meteorological "lapse-rate" which refers only to the vertical temperature gradient (dT/dz) in the free atmosphere. The lapse rate is not generally applicable to air temperature at different elevations along the surface of the earth, because horizontal variations in air masses may occur. This is especially true in Greenland because the lapse rate over the entire ice sheet is usually positive as a result of strong inversions, whereas the rate of change of temperature along the surface (Fig. 37) is close to or even greater than the dry adiabatic rate.

* A summary of the meteorological concepts and terms involved in this discussion is given in Appendix A.

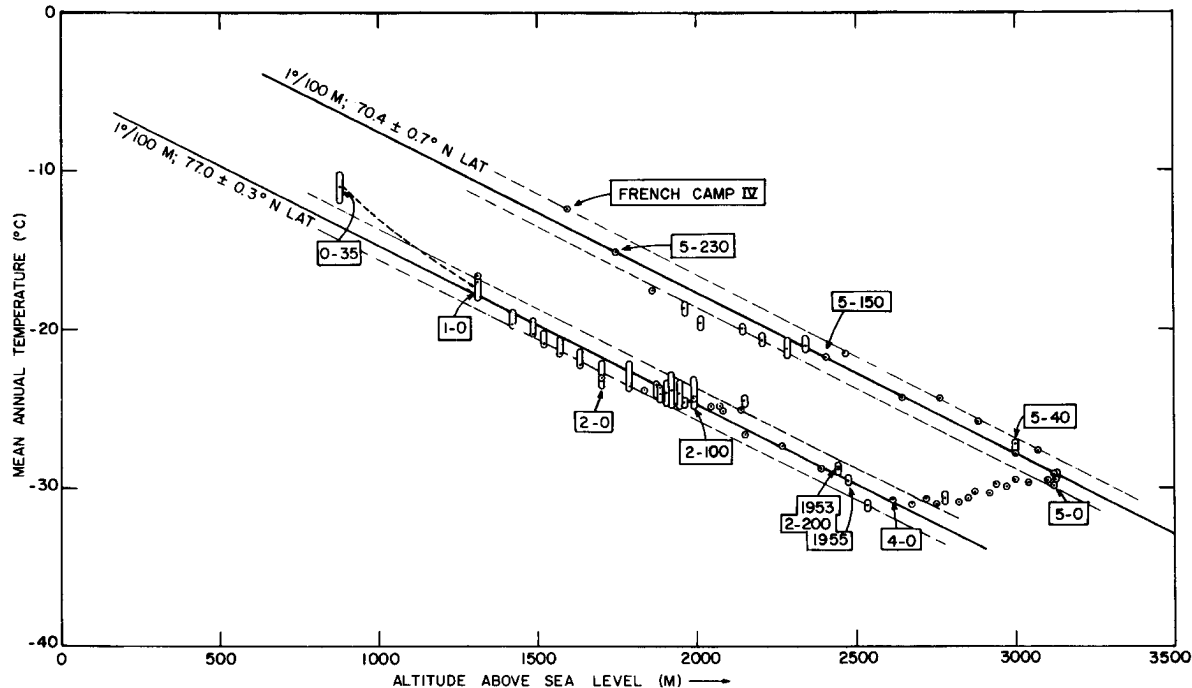


Figure 37. Mean annual temperature plotted against altitude on the west slope of the Greenland ice sheet. Error in temperature values varies from ± 0.5 to 1.0C (App. B). Absolute altitude values are known to within about ± 30 m, but the relative error between stations is less than this. The altitude gradient at 77 and 70°N is approximately $1\text{C}/100$ m; altitude and latitude effects nearly cancel each other on the north-south leg between stations 4-0 and 5-0. Dashed lines indicate a $\pm 1\text{C}$ range around the gradient at 77 and 70°N .

In continental arctic regions and especially over snow surfaces, strong inversions are commonly formed as the ground is cooled by net outgoing radiation (Wexler, 1936). Typical inversions in polar continental air often extend 1 or 2 km above the earth's surface and are in turn overlain by a nearly isothermal layer; the normal negative lapse rate is generally not found below 2 km in winter. The result of this temperature distribution is an extremely stable stratification of air. A high density layer (with negligible vertical motion within it) about 500 m thick, covers the ice sheet and flows under the influence of gravity. This is the origin of the commonly observed katabatic winds.

The west slope of the ice sheet between 70° and 77°N is subject to winds from all directions, but two predominate: 1) katabatic winds from the southeast, and 2) cyclonic storm winds from the southwest. The katabatic winds are warmed according to the dry adiabatic rate as they descend along the surface of the ice sheet. The storm winds, composed of saturated air masses, cool at a rate considerably less than dry adiabatic as they rise along the surface of the ice sheet. If the gradients in Figure 37 are caused primarily by the movement of air over the snow surface, the implication is that the prevailing winds are katabatic. This agrees with observation, but does not lend support to the concept of a glacial anticyclone.* It merely states that cyclonic storm winds, which nourish the ice

* Hobbs' theory of the "glacial anticyclone" was based largely on the observed drainage of cold air radiating outward from the highest elevations. This is not adequate basis for his anticyclone theory. An excellent review of the meteorological data on Greenland and a critical appraisal of the glacial anticyclone theory may be found in Dorsey (1945), Matthes (1946), and Matthes and Belmont (1950).

sheet, do not significantly upset the thermal regimen of the upper firn layers. Instead, they produce minor perturbations in the thermal equilibrium controlled by the nearly constant drainage of cold air from the interior, the katabatic winds.

The above discussion is based on the assumption that temperature gradients along the snow surface are controlled entirely by adiabatic processes in the air moving over the surface. The effects of radiation are assumed constant over the region considered, and the analysis is not applicable in the soaked facies because of abundant melt.

Three factors in addition to the ascent of moisture-laden storm winds on the ice sheet will cause the vertical temperature gradient recorded at a constant depth below the snow surface to deviate from the dry-adiabatic rate: 1) Cooling of the snow surface by radiation is more efficient at higher elevations because the water vapor content of the air is lowest there. This tends to make the gradient along the snow surface larger than adiabatic. 2) More melt occurs at the lower of any two positions considered. This also makes the gradient along the snow surface larger than adiabatic. 3) The air of katabatic winds can absorb more moisture from the snow at the lower of any two elevations because its temperature is higher. This produces more cooling by latent heat transfer at the lower elevation and tends to make the gradient less than adiabatic. However, the rate at which moisture is removed depends on wind speed; of two positions at the same elevation, the one with most wind action will have the lower snow temperature.

Deviations from the dry-adiabatic gradient observed during late summer at 77°N (Fig. 34a) may be evaluated in the light of the meteorological processes outlined above. The data at 3 m depth are least dependent on local, short-duration meteorological perturbations; if only these values are used, the vertical temperature gradient between stations 1-0 and 2-200 is 0.91C/100 m. The gradient varies from one trail segment to the next (Table VI).

Table VI. Rate of temperature decrease with elevation along the surface, from measurements 3 m below snow surface during summer at 77°N.

Location	Elevation difference (m)	ΔT (C)	Gradient C/100 m
1-0 to 2-200	1139	10.4	0.91
1-0 to 2-0	402	3.3	0.82
2-0 to 2-100	286	1.5	0.52
2-100 to 2-200	451	5.6	1.24

The maximum deviations from the adiabatic gradient occur in the trail segments which terminate at 2-0; and they are attributed mainly to the wind action on the ridge crest (p. 32). Between positions 1-0 and 2-0 there is a significant difference in the amount of summer melting, and the maximum gradient is observed in this segment of the trail. This may be accounted for if the firn temperatures at 1-0 are higher than their "adiabatic value" because of melt action, while those at 2-0 are lower because of dessication. Between 2-0 and 2-100, the difference in melt evidence is not great and the minimum gradient observed over this interval may be entirely due to dessication at 2-0.

The overall gradient, from 1-0 to 2-200, is slightly less than adiabatic in late summer (0.91C/100 m), but slightly greater when mean annual values are considered (1.05C/100 m). Although these departures from the adiabatic gradient are not large, they are in the right direction because: 1) thermal control exercised by katabatic wind is weakest in summer, 2) heat loss by radiation is maximum during the winter, and 3) penetration onto the ice sheet by moisture-laden storm winds, with gradients only half as great as the dry adiabatic, is most frequent in summer. This probably occurs because the high pressure area over the interior moves farther south in winter, tending to let only the very large storms penetrate deeply.

Vertical air temperature gradients measured during June and July, 1912 in south (66 to 77°N latitude) Greenland (deQuervain and Mercanton, 1925, p. 153-156) were greater than dry-adiabatic during times of strong outgoing radiation, approaching the

dry-adiabatic while föhn (katabatic) winds prevailed, and less than half of the dry-adiabatic gradient during stormy or overcast days. These observations, combined with the observed gradient of mean annual temperature in the firn which is greater than the dry-adiabatic gradient, indicate that strong cooling by radiation is a prevailing mean annual condition which is accompanied by deep inversions and produces the katabatic winds.

Some uncertainty exists in the mean annual temperature values obtained by applying eq 3 to measurements, because convection was not considered. Air moves through the upper layers of the snow pack, and the associated convection is several times more effective in transporting heat than is conduction (Bey, 1951). The effects of convection decrease with depth and were minimized in preparing Appendix B by using no data from less than 3 m below the snow surface. All temperatures computed in Appendix B are probably within a degree of the value at 10 m, according to checkpoints existing at stations where 10 m data are available.

Figure 38 compares observed isotherms (uncorrected data of Table IV) with those computed from eq 3 using an assumed altitude gradient of 1C/100 m. The difference between measured and computed values is attributed to convection and decreases with depth as expected.

Sorge (1935, p. 246) observed that maximum temperatures occurred earlier than computed down to 7 m below the snow surface, being 10 - 14 days early at 6 - 7 m. He attributed this deviation to convection caused by air circulation in the tunnel connecting the Eismitte living quarters with the glaciology pit. The presence of the tunnel undoubtedly influenced his measurements, but air circulation through the porous snow alone causes noticeable convection (Fig. 38).

Latitude gradient.

The latitude gradient may be obtained from two independent sets of data. First, from measurements on the ice sheet itself (Fig. 37) and, second, from sea-level meteorological stations on the west coast of Greenland. Mean annual temperatures on the ice sheet are known with greatest accuracy at stations 2-100 and 5-40. They indicate the following values:

71°N latitude: -28.0C at 3000 m

77°N latitude: -24.5C at 2000 m.

If the altitude gradient of 1C/100 m is used, the resulting latitude gradient is 1.08C per degree latitude.

Meteorological records from Ivigtut, Godthaab, Jakobshavn, and Upernavik are nearly continuous from about 1875 to the present. These stations, together with those recently established at Thule (1946) and on Ellesmere Island (Alert, 1950) provide information over a range of 21.5 deg of latitude. They are all less than 32 m above sea level and may be regarded as equal in altitude for the present discussion. Records from these stations are summarized in Table VII and Figures 39a and b. The average air temperature has increased, especially since about 1920. Therefore, values shown for Thule and Alert (since 1946) correlate with the upper limit of data points obtained farther south (Fig. 39b).

The latitude gradient, expressed in degree C per degree latitude, is 0.8 from Ivigtut to Upernavik, 1.4 from Upernavik to Thule, and 1.0 from Thule to Alert. The gradient measured north of Upernavik is closest to that observed on the ice sheet. This is probably because the sea north of Upernavik is covered by ice and snow during the major portion of the year, thus making the environment more continental than it is farther south.

Summary

A simplified model of the distribution of mean annual temperature (i. e., the temperature measured 10 m below snow surface at any time of year) may be summarized as follows:

1) The altitude gradient is based on the assumption that the prevailing meteorological environment of the ice sheet is a strong cooling by radiation, producing a temperature inversion and nearly steady drainage of dense air by katabatic winds. The air is warmed

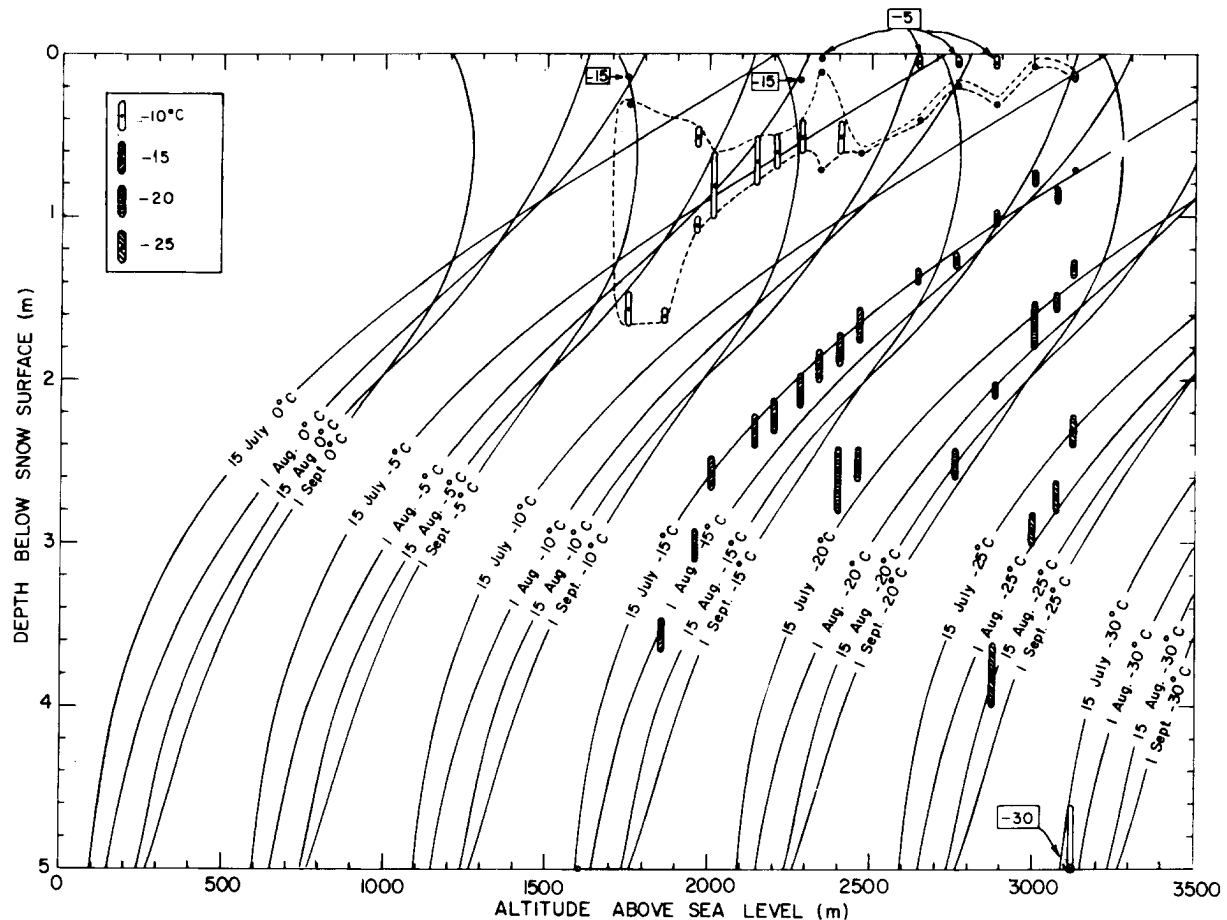


Figure 38. Isotherms computed from eq 3 for 15 July, 1 Aug, 15 Aug, and 1 Sept using an assumed altitude gradient of 1C/100 m. Data points are observed values from Table IV. Eq 3 is based on the assumption that all heat is transferred through the snow by conduction. However, it is clear that the fall cooling cycle has progressed more rapidly than predicted by the conduction model. The 0 and -5C isotherms have been completely removed from the snow by mid-August and the -10C isotherm is well ahead of its computed position. The difference between measured and computed values is attributed to convection and decreases with depth as expected. The depth range (see data sheets) of each temperature value is indicated by the vertical extent of the line enclosing the data point.

as it descends along the ice sheet at the dry-adiabatic rate of about 1C per 100 m. This process in the air controls the altitude gradient of temperature, measured 10 m below the snow surface, above the saturation line.

2) The latitude gradient of temperature is based on the measurements at stations 2-100 and 5-40; this gives a latitude gradient of 1.08C per degree latitude. An isotherm map of mean annual temperatures, constructed with these gradients, is presented in Figure 40, with data points indicated.

Where mean annual temperature is higher than about -15C, deviations from the altitude gradient are to be expected because of downward percolating melt water. Such areas include the entire soaked facies and possibly the lowest extreme of the percolation facies. Data are not available to show the variation in the altitude gradient of temperature across the saturation line, and no attempt was made to correct for this in constructing Figure 40.

Table VII. Mean annual air temperature.*

Decade	Ivigtut 61.2°N		Godthaab 64.2°N		Jakobshavn 69.2°N		Upernavik 72.8°N		Thule 76.5°N		Alert 82.5°N	
	A	B	A	B	A	B	A	B	A	B	A	B
1871-1880	1	1.2	5	-1.4	8	-4.6	6	-8.2	-	-	-	-
1881-1890	10	0.2	8	-2.5	7	-6.0	10	-9.3	-	-	-	-
1891-1900	10	0.6	3	-1.6	10	-6.3	7	-8.5	-	-	-	-
1901-1910	10	0.6	8	-2.0	10	-5.3	10	-8.3	-	-	-	-
1911-1920	8	1.4	10	-1.6	7	-5.7	10	-8.4	-	-	-	-
1921-1930	8	1.4	10	-0.7	7	-3.7	10	-6.8	-	-	-	-
1931-1940	10	1.7	10	-0.5	10	-3.3	6	-6.4	-	-	-	-
1941-1950	10	2.0	10	-0.6	7	-4.0	7	-6.1	4	-11.3	-	-
1951-1960	-	-	-	-	-	-	-	-	4	-11.7	7	-17.9

A: Number of years for which data are available in the stated decade.

B: Average annual air temperature (C) in the stated decade.

* Data from: Danish Meteorological Institute, U. S. Weather Bureau, U. S. Air Force Air Weather Service, and Canadian Department of Transport, Meteorological Branch.

The data in Table VII are summarized in Figures 39a, b. The increase in temperature since early in this century (Ahlmann, 1953) is readily apparent.

The latitude gradient may be 0.1 to 0.2 units too high south of 69°N latitude because the proximity of open water on either side of the ice sheet tends to make the climate more maritime in this region than it is farther north. Sea-level stations indicate that the latitude gradient is lower in south than in north Greenland (Fig. 39b) but in the absence of data from the ice sheet itself no attempt was made to correct for this in Figure 40.

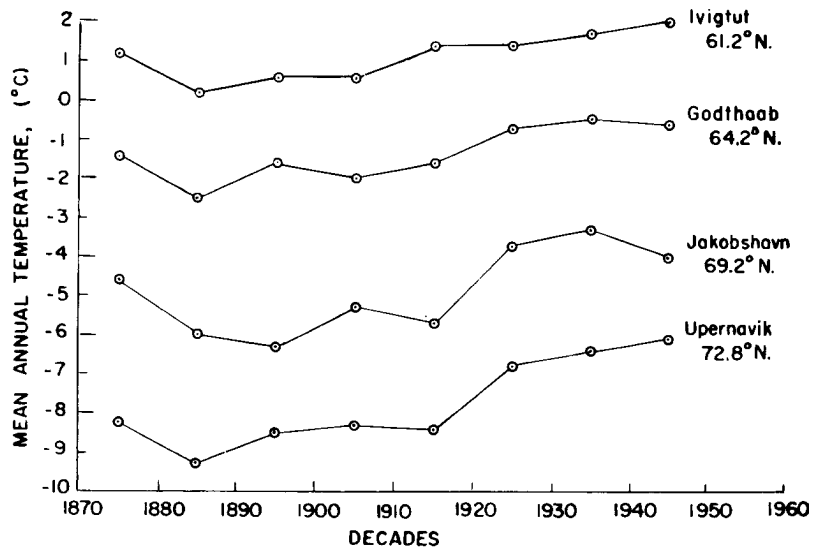


Figure 39a. Mean annual temperature vs time on the west coast of Greenland (data from Table VII).

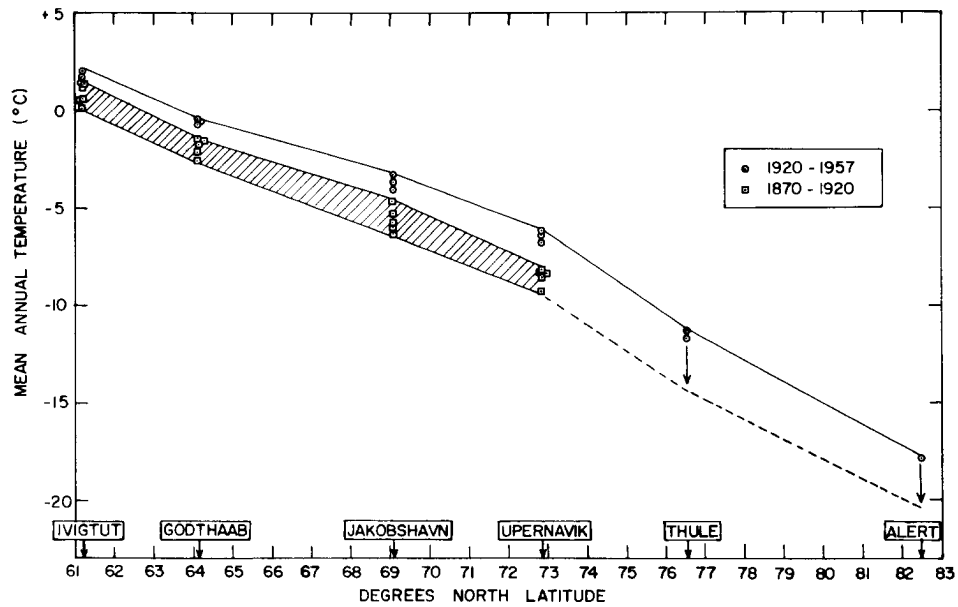


Figure 39b. Mean annual temperature vs latitude along the west coast of Greenland (data from Table VII).

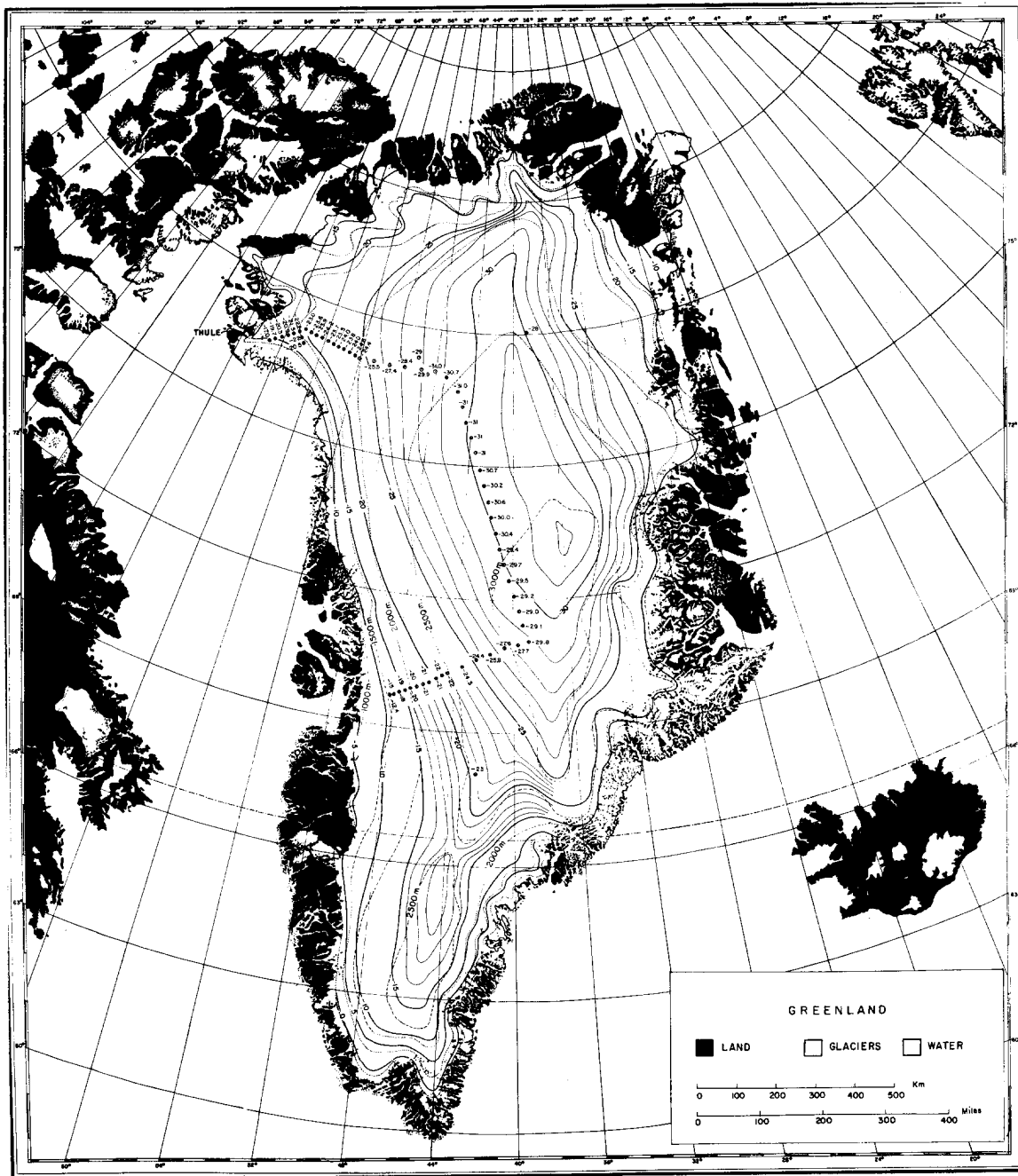


Figure 40. Isotherms of mean annual temperature computed from the altitude gradient of 1C/100 m and the latitude gradient of 1C per deg latitude. Data points are from Appendix B, except for the value at Northice (Bull, 1956) and the one for HIRAN Station 29 (Bader, 1956).

CHAPTER V. DIAGENETIC FACIES - A CLASSIFICATION OF GLACIERS.

Diagenetic facies on glaciers are defined on page 24. This chapter demonstrates the differences between these facies and shows that their boundaries can be located by physical measurements.

Temperature

All of the temperature data has been presented in Chapter IV. In defining facies boundaries it is necessary to know the temperature distribution during the peak of the melt season. This is most easily seen by mapping isotherms in the top 5 m of snow from sea level to the crest of the ice sheet (Fig. 35).

Facies in terms of temperature data.

Snow and firn are soaked to the depth of the 0C isotherm. This soaked layer includes the entire annual increment of accumulation at altitudes below $1070 \pm m$ (about 3500 ft) at $77^\circ N$, and below $1550 \pm m$ (about 5100 ft) at $70^\circ N$ (Fig. 35a, b). By definition, these positions locate the saturation line.

In terms of temperature the dry-snow line is not as sharply defined as the saturation line or the firn line. It is the uppermost limit of observable melt, yet traces of melt are found at least once in about 20 yr high in the dry-snow facies. For sake of definition, the dry-snow line is placed at the highest altitude where the average $-5C$ isotherm, measured in the melt season, intersects the snow surface; therefore, it is always above the $-25C$ mean annual isotherm of Figure 40. It lies at about $2150 \pm m$ (7050 ft) at $77^\circ N$ latitude and about 3000 m (9850) ft) at $70^\circ N$ latitude.

HardnessRam hardness number

The ram hardness number R (see data sheets) represents the resistance to penetration which a given snow layer offers to the cone of the penetrometer as it moves through that layer. The mechanism of this penetration is complex, and involves both compressional and shearing stresses. These details are ignored and R is regarded simply as a resisting force; for convenience, it is presented as kg-force on the data sheets. The correlation between density and Rammsonde (or "ram hardness") profiles is generally good.

A discussion of equations used to evaluate R is given by Haefeli (Bader, et al., 1939, p. 128-132). He outlines "three different ways" of computing R . These "three different ways" actually involve a single approach to the problem, and the effects produced by bouncing of the hammer are ignored. Haefeli's eq 30 and 31 are eq 6 and 7 below.

Ram hardness number R is computed by equating the work done on the snow, as the cone moves through it, to the energy given up by the falling hammer and the descending penetrometer. If we ignore all impacts after the first one, i. e., neglect the effects of bouncing, we have:

$$R \Delta z = Mgh + (M+m)g \Delta z \quad (4)$$

where Δz = amount of penetration produced by one fall of the hammer,

M = mass of hammer,

m = mass of penetrometer,

h = height of fall of hammer,

g = acceleration of gravity, and,

α = fraction of energy still in the system after the first impact.

$$\alpha = \frac{(M - \epsilon m)^2 + Mm(1 + \epsilon)^2}{(M + m)^2}$$

where ϵ = the coefficient of restitution, $0 \leq \epsilon \leq 1$.

For convenience we set:

$$\begin{aligned} Mg &= P = \text{the weight of the hammer, and} \\ mg &= Q = \text{the weight of the penetrometer.} \end{aligned}$$

Then

$$a = \frac{(P - \epsilon Q)^2 + PQ(1 + \epsilon)^2}{(P + Q)^2}$$

and

$$R = \frac{Ph}{\Delta z} a + P + Q. \quad (5)$$

The value of R is dependent upon the value of ϵ . If $\epsilon = 1$, the collision between hammer and penetrometer is completely elastic; if $\epsilon = 0$ it is completely inelastic. These extremes are:

(a) if $\epsilon = 1$, then $a = 1$ and

$$R_{\max} = \frac{Ph}{\Delta z} + (P + Q) \quad (6)$$

(b) if $\epsilon = 0$, then $a = \frac{P}{P + Q}$ and

$$R_{\min} = \frac{P^2 h}{\Delta z (P + Q)} + (P + Q). \quad (7)$$

To simplify and standardize the application of the Rammsonde it is assumed that $\epsilon \cong 1$ and eq 6 is used exclusively.

Continuity of strata

The reproducibility of ram hardness profiles where strata are continuous has been observed repeatedly in Greenland (Benson, 1959) and was clearly demonstrated by Haefeli (Bader et al., 1939). Thus, once the physical properties of firn layers are recorded in pits, the Rammsonde may be used to determine lateral continuity of strata in a particular region.

Integrated ram hardness profiles

The direct comparison of profiles is useful in correlating individual strata between pit stations. However, one may observe significant differences in the range of hardness values between the different regions (see data sheets). It is desirable to examine the nature of the variation in hardness between the facies, but the direct comparison of many profiles from a large area would clearly be cumbersome for this purpose. It is necessary to reduce the data on each profile to a few significant values which can be more easily compared. One such reduction is effected by integrating the profiles.

The ram hardness number is expressed in units of force. When it is integrated over a depth interval the resulting quantity is the work done on the snow as the penetrometer moves through the stated interval.* In practice, this integration is performed by multiplying each depth increment Δz by its hardness number R and adding these values from $z = 0$, at the snow surface, to any desired depth. The intervals Δz do not approach zero, nor does the number of intervals increase indefinitely; yet, it is convenient to regard the

the summation as an "integral" and to examine $\int_0^z R dz$ as a function of z . The total

* The ram hardness number is expressed in units of kg-force. Thus, the integrated Rammsonde profile has units of kg-f cm. These are converted into joules by the following relations:

$$\begin{aligned} 1 \text{ joule} &= 10.2 \text{ kg-f cm} \\ 1 \text{ kg-f cm} &= 0.098 \text{ joule.} \end{aligned}$$

work done by the penetrometer in moving from the snow surface to a stated depth \underline{z}_i may be written as

$$R_i = \int_0^{\underline{z}_i} R dz.$$

For convenience the values \underline{z}_i are taken at 1-m intervals. The maximum depth of ram profiles from the snow surface is 4 m. Therefore, a maximum of four values (R_1 , R_2 , R_3 , and R_4) may be obtained from each profile and they are cumulative values by definition.

The use of overlapping profiles at pit stations is justified to eliminate discontinuities at a single deep pit (Benson, 1959). However, such composite profiles cannot be used to compute the four R values because, by definition, these values measure the work required to penetrate from the snow surface to a given depth. Furthermore, one often desires to use ram profiles made at locations where there is no pit. If these are to be compared with pit-station ram profiles it is essential that all of the measurements be made in the same way.

Integrated ram data for six 1953 stations are presented in Figure 41. The measurements were made during the melt season. At station 0-20, the very low values in the upper 2 m and the rapid increase below 3 m are typical features of the soaked facies. The low initial values are due to the weakness of water-soaked firn. The rapid increase below 3 m results from the abundance of ice layers, lenses, and glands at depth. Ram profiles in the soaked facies often cannot be carried as deep as 4 m, because R_4 generally exceeds 5000 joules. The spread in R values between station 1-0 and the other stations in the percolation facies (2-0, 2-50, and 2-100) is caused by the relatively greater amount of iced firn and icy layers at 1-0. Station 1-0 is near the lower end of the percolation facies. The R values decrease rapidly with increased elevation inland from 1-0. As an example, it may be noted that R_4 does not exceed 3000 joules after position 1-15 has been passed (Fig. 42a). Station 2-200 is the only example shown of the dry-snow facies, but it is representative.

Temperature dependency of ram hardness

The R values of each station in 1953, 1954, and 1955 are plotted in Figure 42. The R values are progressively greater from 1953 to 1955. This is a temperature effect. Expedition SOLO crossed the saturation line in mid-July 1953, CRYSTAL crossed it in late May 1954, and JELLO crossed it in mid-May 1955. The strength of ice is dependent upon temperature (Butkovitch, 1954), and this may be expected to affect the ram resistance of a snow pack.

The temperature variation of R_1 in the percolation and dry-snow facies is shown in Figure 43. The percolation facies is subdivided into an upper and lower part. The greater variation at lower altitudes in the percolation facies reflects the increase in melt action. At temperatures near the melting point the ram resistance is low, but at temperatures below the melting point the increase in ram resistance is roughly proportional to the amount of melt bonding between grains. The variation as well as the range of R is low in the dry-snow facies because the snow and firn rarely attain temperatures as high as -5°C , and melt bonding between grains is minimal. The values of R_{2-1} and R_{3-2} , i. e. the work required to penetrate the second and third meters respectively, when plotted against their minimum temperatures show results similar to those of Figure 43 but with more scatter of the data points.

Where significant soaking occurs, the variation of R_1 values with temperature must be considered separately. For example, at 0-35 the top meter of firn has three very different physical manifestations:

- 1) New snow prior to the melt season (at this time the top meter of snow may be nearly identical from the edge of the ice sheet to the dry-snow line);
- 2) Completely wetted snow during the height of the melt season (at this time R_1 has its minimum value and the difference between soaked and non-soaked facies is readily apparent);
- 3) Iced firn in the fall and early winter (at this time the value of R_1 is extremely high).

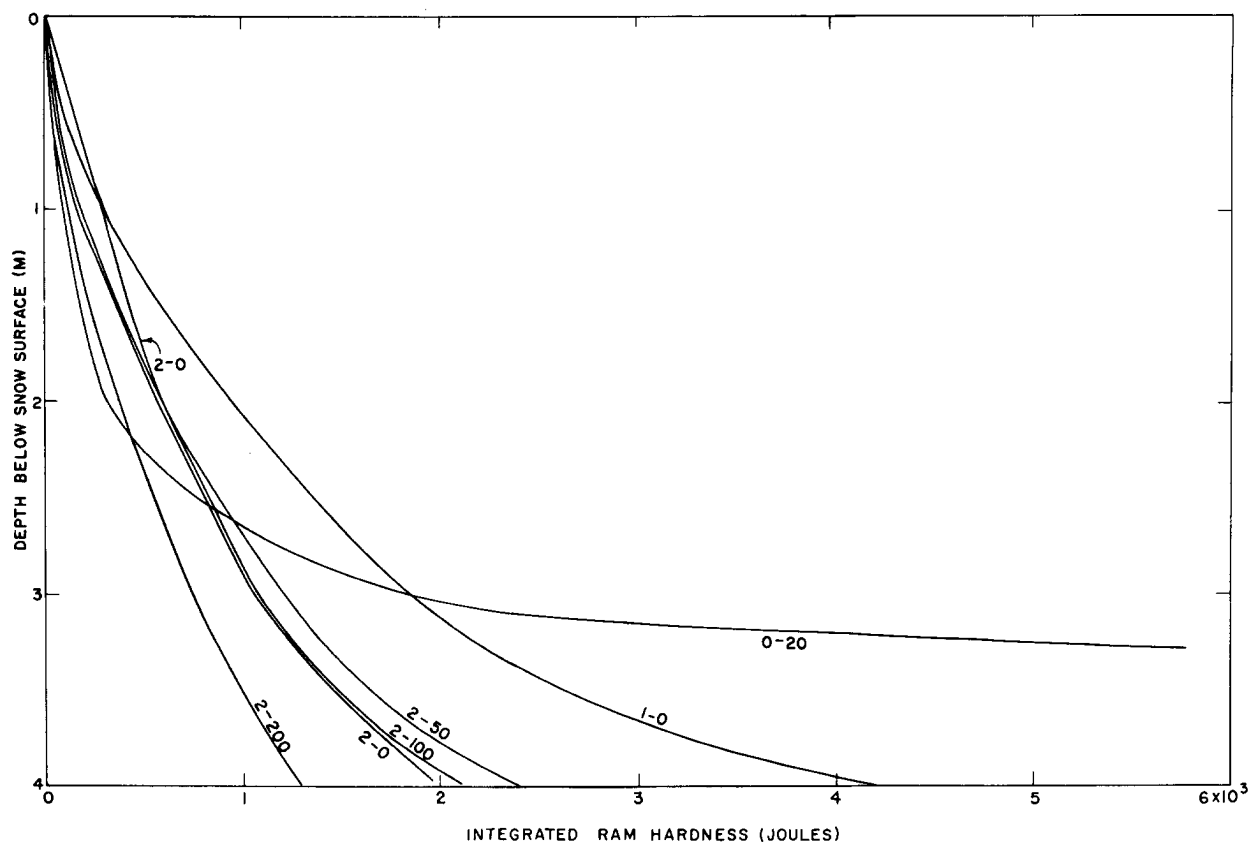
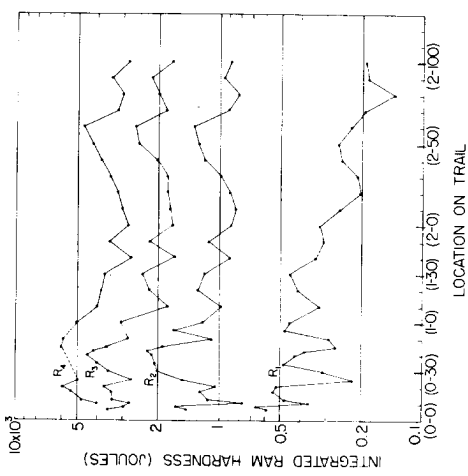


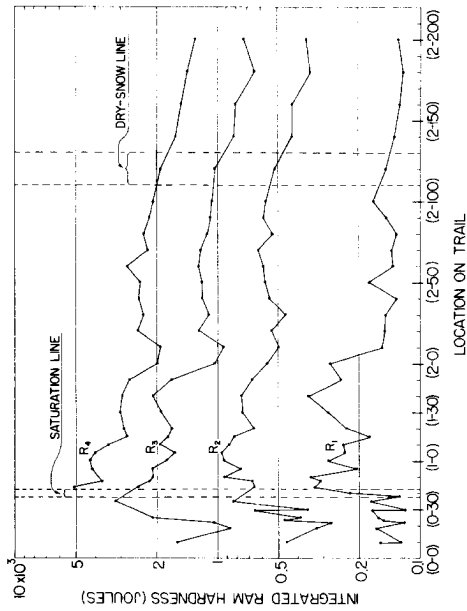
Figure 41. Integrated ram hardness plotted against depth for six of the 1953 stations. The measurements were made at the peak of the melt season.

Figure 42 (p. 65). Integrated ram hardness values, 1953, 1954, 1955. R_1 represents work done in penetrating from the snow surface to a depth of 1 m; R_2 represents work to penetrate from the snow surface to a depth of 2 m, etc. 1953 measurements were made during the peak of the melt season and the saturation line stands out clearly because soaked snow is easier to penetrate than non-soaked snow. In 1954 and 1955 the saturation line was traversed prior to the melt season so no discontinuity was observed. The increase in R_1 values from 1953 through 1955 is a temperature effect (see Fig. 43).

Integrated Ram Profiles 1954



Integrated Ram Profiles 1953



Integrated Ram Profiles 1955

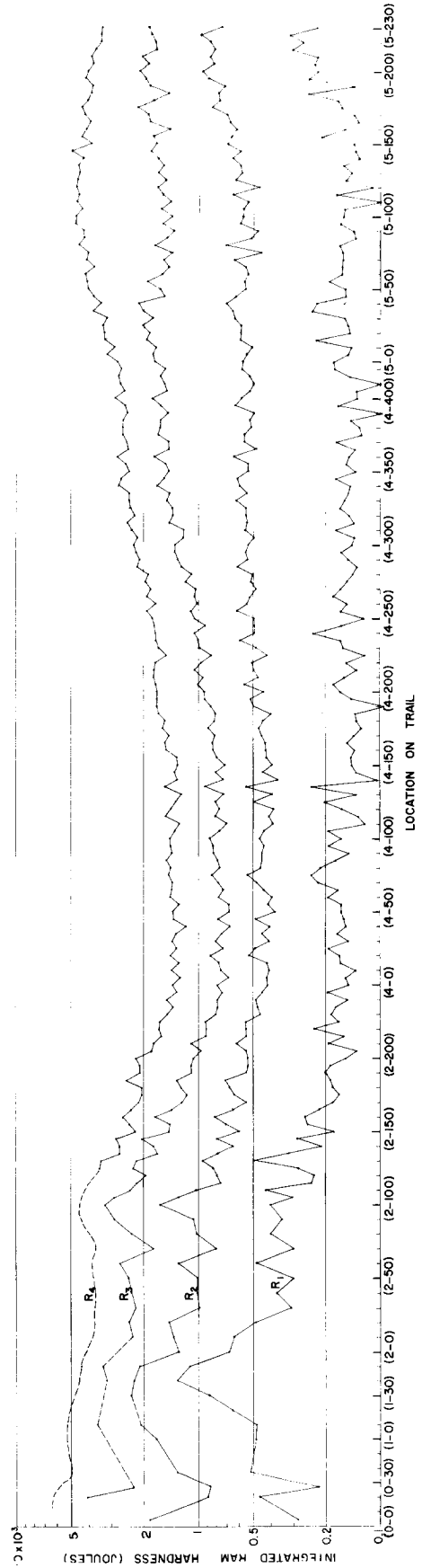


Figure 42.

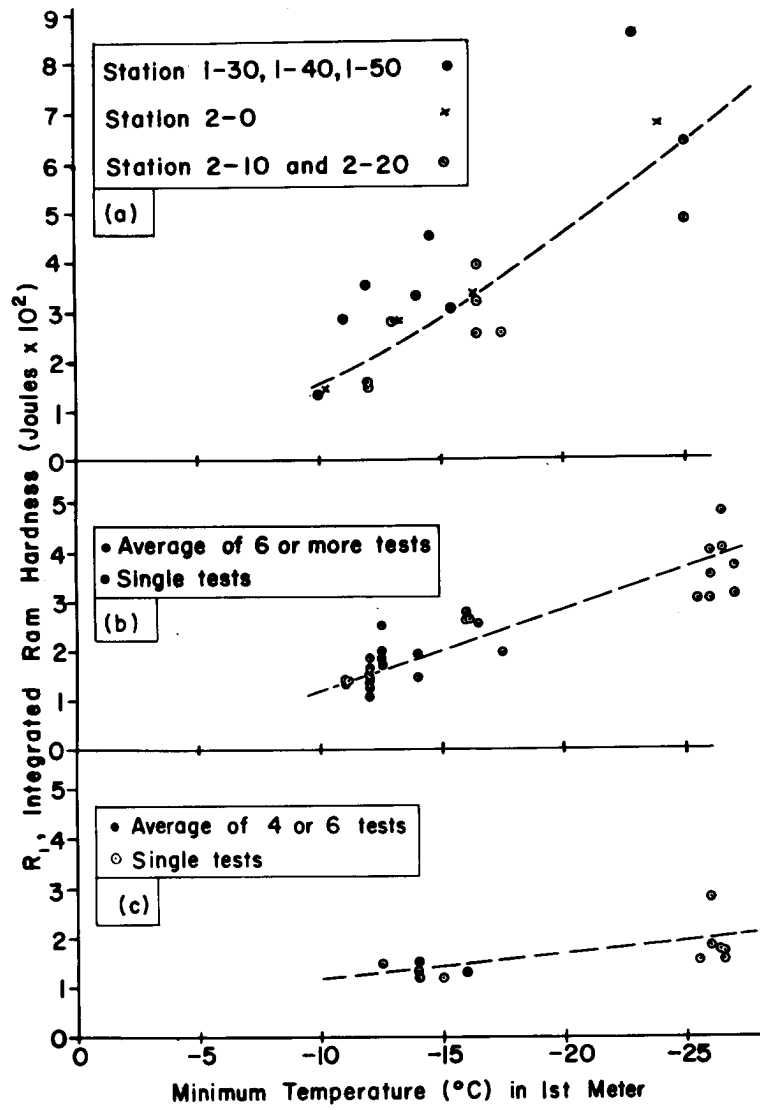


Figure 43. R_1 plotted against minimum temperature in the 1st meter:
 a. Percolation facies below 1850 m at 77°N.
 b. Percolation facies above 1850 m at 77°N.
 c. Dry-snow facies.

Temperature coefficients for \bar{R} within a given facies are easiest to recognize in the first meter. The rate of increase in the value of \bar{R}_1 with the minimum temperature in the top meter may be summarized as follows:

	Temperature coefficient for \bar{R}_1	
	kg-f cm/C	joule/C
Dry-snow facies	30	3
Upper* percolation facies	170	17
Lower* percolation facies	320	31

* Above or below 6000 ft (1830 m) at 77°N latitude.

Facies in terms of hardness data

In 1953 measurements were made during the melt season and the discontinuity in \bar{R}_1 near 0-40 locates the saturation line (Fig. 42a). The low values on the left were obtained in the soaked facies while the upper meter was wet. The higher values on the right are from the percolation facies. Therefore, between 0-0 and 1-0, the saturation line may be placed at an altitude of about 1050 m (3500 ft) in agreement with the analysis of the isotherms in Figure 35a. From ram data, the saturation line may be located without digging pits. In 1954 and 1955 the measurements were made before melting had occurred, and, accordingly, there is no discontinuity between the soaked and percolation facies.

The dry-snow line is not uniquely determined by Rammsonde data. In general, the values \bar{R}_i are lowest in the dry-snow facies, but the limiting values at the facies margin are temperature dependent. For example, in August 1953 the \bar{R}_4 value was less than 2000 joules above the dry-snow line. In May 1955 the \bar{R}_4 value was less than 3000 joules above the dry-snow line (Fig. 42).

Density

Variation in density as a stratigraphic parameter was discussed in Chapter III. Here attention is focused on the gross changes in density with depth and especially with differences between the depth-density curves of different facies.

Depth-density data

Average density values for each meter are plotted against depth in Figure 44. Data are from Greenland, with the exception of those from the Upper Seward Glacier, Yukon Territory, Canada (Sharp, 1951), and from the Snow Dome of Mt. Olympus.* The latter glaciers are temperate and the data are from the soaked facies of each.

The data from 2-100 (Fig. 44, Curve 4) and from Eismitte (Sorge, 1935, p. 134) show that the slope of the depth-density curve decreases below a depth of 8 to 10 m. These stations lie in the upper extreme of the percolation facies. In the soaked facies the change in rate of densification occurs at shallower depths (at about 4-5 m in the Seward Glacier). It is also clear from Figure 44 that the range of firn density decreases as we move upward from the soaked through the dry-snow facies; and that the rate of increase of density with depth is greater in soaked facies than in non-soaked facies.

Summer melting of firn increases the rate of densification, and the difference in amount of melt above and below the saturation line is expressed by a grouping of the depth-density curves. Data from a 1000-mile traverse in the percolation and dry-snow facies all lie within the range defined by the 1-0 and 4-0 curves. Station 0-35, only 23 miles from 1-0, has significantly higher density values and a greater rate of densification with depth; it lies in the soaked facies.

The decrease in density with elevation observed in the non-soaked facies results in part from the corresponding decrease in temperature. Melt is negligible at high elevations and the primary cause of densification is the load of snow which is added annually. But, because the strength of ice increases as temperature decreases, the colder firn is more able to resist the compressive stresses of the overburden. This reduces the rate of densification.

* Measured by Benson in 1957.

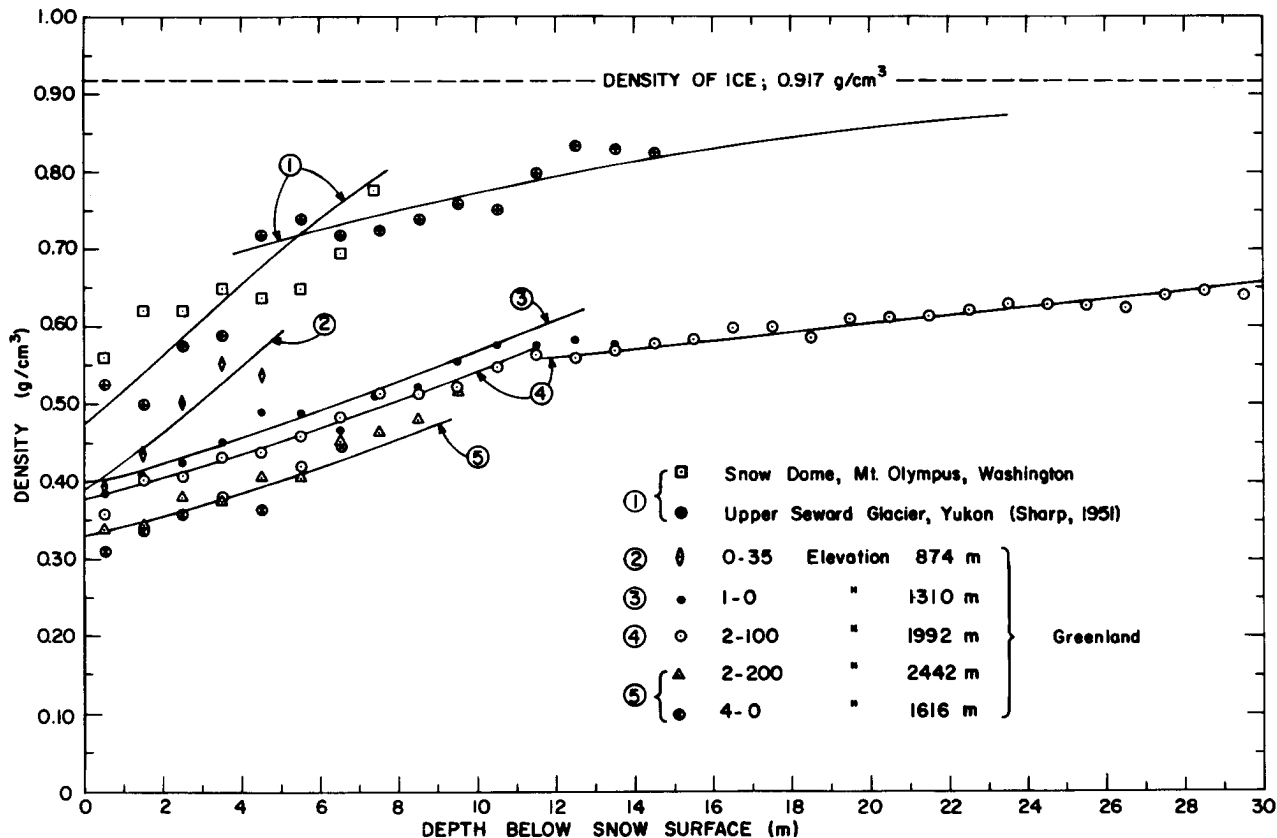


Figure 44. Depth-density curves. Each point represents the average density over a depth interval of 1 m. Data are averages of 2 yr measurements from snow surface to 4 m at 0-35, to 6 m at 1-0, and to 10 m at 2-100; all other points are based on single observations. Curves in this figure were computed from eq 14. The values of constants (see also eq 9 and Fig. 49) are as follows:

Station	Depth range*	ρ_0	ν_0	K	m
Seward Glacier and Mt. Olympus	$0 < z < z_c$	0.475	2.12	0.859	37.5×10^{-4}
	$z_c < z < \infty$	0.640	1.56	-0.405	12.0×10^{-4}
Greenland:					
0-35	$0 < z < z_c$	0.390	2.56	1.651	37.5×10^{-4}
1-0	$0 < z < z_c$	0.395	2.53	1.599	16.0×10^{-4}
	$z_c < z < \infty$	0.695	1.44	-0.820	4.3×10^{-4}
2-100	$0 < z < z_c$	0.378	2.65	1.779	16.0×10^{-4}
	$z_c < z < \infty$	0.500	2.00	0.652	4.3×10^{-4}
2-200 (1953)	$0 < z < z_c$	0.330	3.03	2.357	18.0×10^{-4}
4-0 (1955)	$0 < z < z_c$				

* z_c = depth of discontinuity (change in rate of densification).

Depth-load data

If firn density could be expressed as a function of depth, i. e., $\rho = \rho(z)$, one could obtain the load at any depth z by integrating $\rho(z)$ from snow surface; $\sigma = \int_0^z \rho dz$.

Without knowing $\rho(z)$ the integration may be approximated by a summation. This has been done for all stations and the results are summarized in Figure 45.

A tentative grouping of curves according to facies is indicated but more data are obviously desirable in the soaked facies. Except for the data from Seward Glacier and Mt. Olympus, the contribution of ice masses in the firn was neglected in computing the depth-load curves of Figure 45. This was done because the irregular and discontinuous shapes of the ice masses make it difficult to get an exact measure of their water equivalent. Depth-load curves which include estimates of the water equivalent of ice masses have been computed; they differ from the curves of Figure 45 as follows:

Station	Depth range (m)	Avg increase of load values if water equivalent of ice masses is estimated
0-35	0-6	7%
1-0	0-14	4%
2-0	0-14	2%
Stations above 6000 ft elev at 77° N lat 2-20 to 2-200	0-14 (max)	less than 1%

The inclusion of estimates for the water equivalent of ice masses increases the differences between facies shown in Figure 45. It also removes the 2-0 curve from its apparently anomalous position* on the lower boundary of the percolation facies and places it between the curves for 2-50 and 2-100. The differences between curves bounding the facies are:

Facies	Difference between load curves bounding the facies at depth of 5 m below snow surface	
	Without estimates for water equivalent of ice masses (Fig. 45)	With estimates for water equivalent of ice masses
Soaked and percolation	11%	16%
Percolation and dry-snow	2.5%	4%

The gaps between groups of curves are significant because curves measured in pits dug within 100 m of each other in consecutive years are reproducible to within an error of about 1%. Table VIII summarizes the reproducibility of depth-load curves from the four stations which had pits deeper than 4 m in both 1953 and 1954. The average difference is 0.63%.

* The dessicating effect of wind in summer and fall may account for the fact that firn density and hardness values (neglecting ice layers) at 2-0 are lower than those measured at higher and lower altitudes in the percolation facies; in fact they are the lowest recorded in any deep pit of the percolation facies (see Fig. 42a, 45). This could be due to the extraction of sufficient moisture from the snow to offset some of the densification produced by summer melting. The minimum accumulation in the 2-0 region allows the fall cooling process to affect a greater part of the annual layer here (perhaps the entire layer) than at positions with more accumulation.

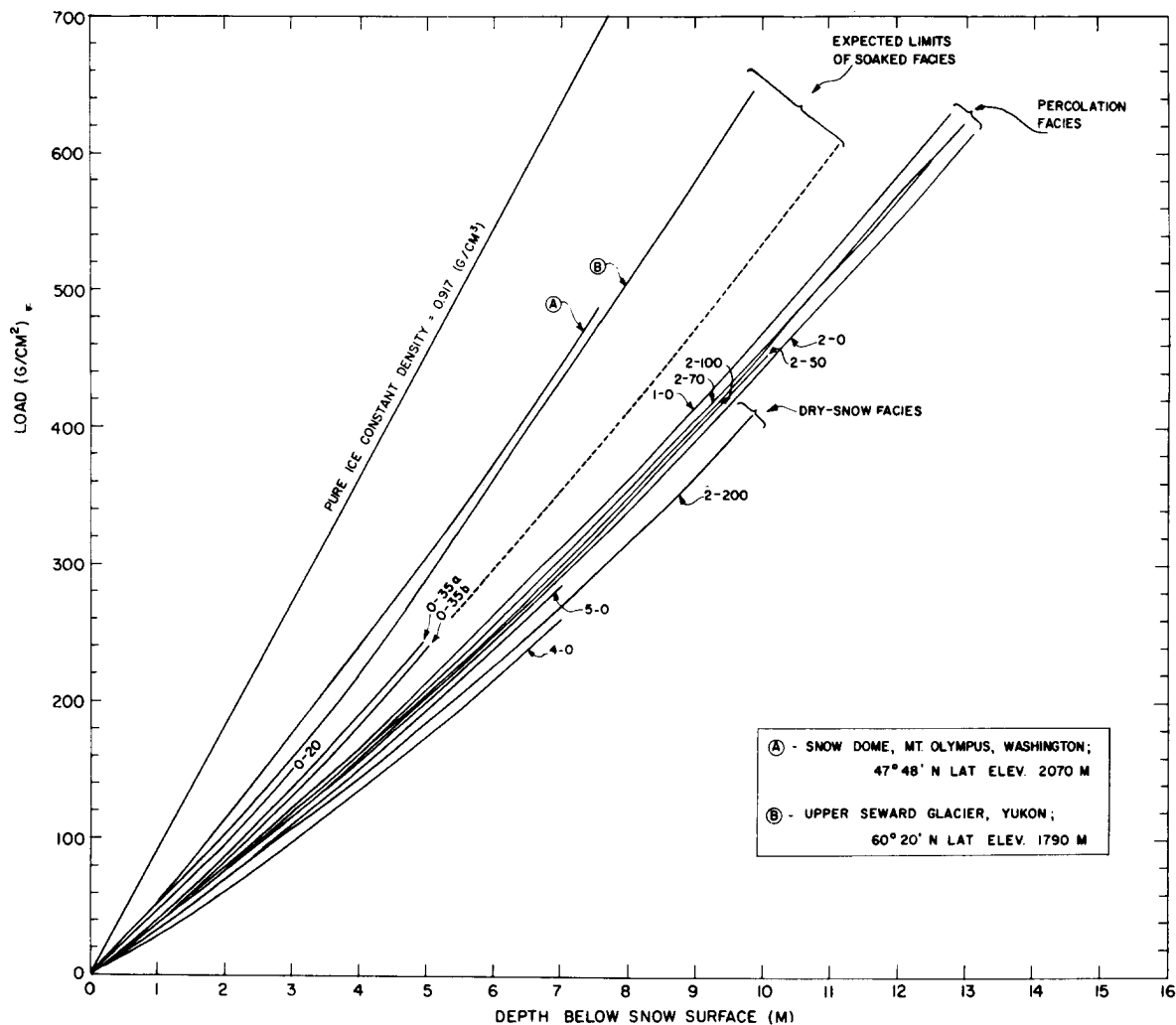


Figure 45. Depth-load curves. Curves from the soaked facies lie between those shown for Snow Dome, Mt. Olympus, Washington and station 0-35, of this study.

Curves 0-20 and 0-35a are based on measurements of July 1953 when the firn was completely soaked. Curve 0-35b is from data obtained before melting occurred in the spring of 1954.

All curves from the percolation facies lie within the region bounded by the curves 1-0 and 2-0.

All curves from the dry-snow facies lie within the region bounded by the curves 4-0 and 5-0.

The curve for pure ice represents the limiting case.

Table VIII. Reproducibility of depth-load curves. 1954 pits were dug within 100 m of the 1953 pits at each station.

Station	Depth (m)	Load (g/cm ²)		% Difference	
		1953	1954		
1-0	4	166.88	166.15	0.43	
2-0	4	155.06	155.76	0.45	
2-50	4	159.15	160.24	0.68	
2-100	4	159.86*	161.73	0.16*	
1-0	6	264.06	264.97	0.34	
2-0	6	243.03	245.38	0.96	
2-50	6	250.03	247.48	1.02	
2-100	6	250.41*	251.02	0.24*	Average of 12 measure- ments = 0.63%
1-0	8	n. d.	362.96	--	
2-0	8	338.49	339.75	0.37	
2-50	8	351.12	346.07	1.44	
2-100	8	350.32*	350.76	0.13*	
1-0	10	n. d.	470.18	--	
2-0	10	n. d.	444.04	--	
2-50	10	n. d.	450.38	--	
2-100	10	453.53*	455.08	0.34*	

n. d. No data

* The 1953 data at 2-100 included 13 cm of fresh snow (average density = 0.21 g/cm³) which caused its top 13 cm to contain 1.28 cm less water than that of 1954 (see data sheets). The value 1.28 g/cm² was added to the first 13 cm of 1953 data to adjust for this.

The load at a depth of 5 m below snow surface is shown for each station in Figure 46. At some stations a range of load value is indicated; the lower value represents the load computed by omitting ice masses, and the upper value includes an estimate for the contribution of ice masses to the load. Where the difference is negligible, only one value is shown.

Facies boundaries are indicated in Figure 46. The saturation line was clearly crossed in the north near station 0-35. It was not crossed in the south although it lies very close to station 5-230. The firn line is separated from the saturation line on the Thule peninsula by nearly 40 miles because of the gradual increase in elevation. In the vicinity of Disko Island the firn line and saturation line are much closer to each other because of the steeper surface slope. They probably are within 5 miles of each other.

The dry-snow line shows more clearly in the north because the traverse crosses normal to it. In the south the traverse ran nearly parallel to the dry-snow line in the vicinity of 5-0. If a westward course had been taken at station 4-325, the transition between the dry-snow and percolation facies would have looked like it does between 2-100 and 2-200.

Facies in terms of density data

The density data form the most complete basis for subdivision of the ice sheet, and glaciers in general, into facies. Temperature and hardness data will also locate the saturation line but the dry-snow line is more subtle, and is best defined at present in terms of density. The relation between density and facies is summarized as follows:

(a) Firn density decreases from soaked to dry-snow facies (Fig. 44):

Facies	Avg density in the upper 5 m (g/cm ³)
Soaked facies	Greater than 0.500
Percolation facies	0.430 to 0.390
Dry-snow facies	Less than 0.375

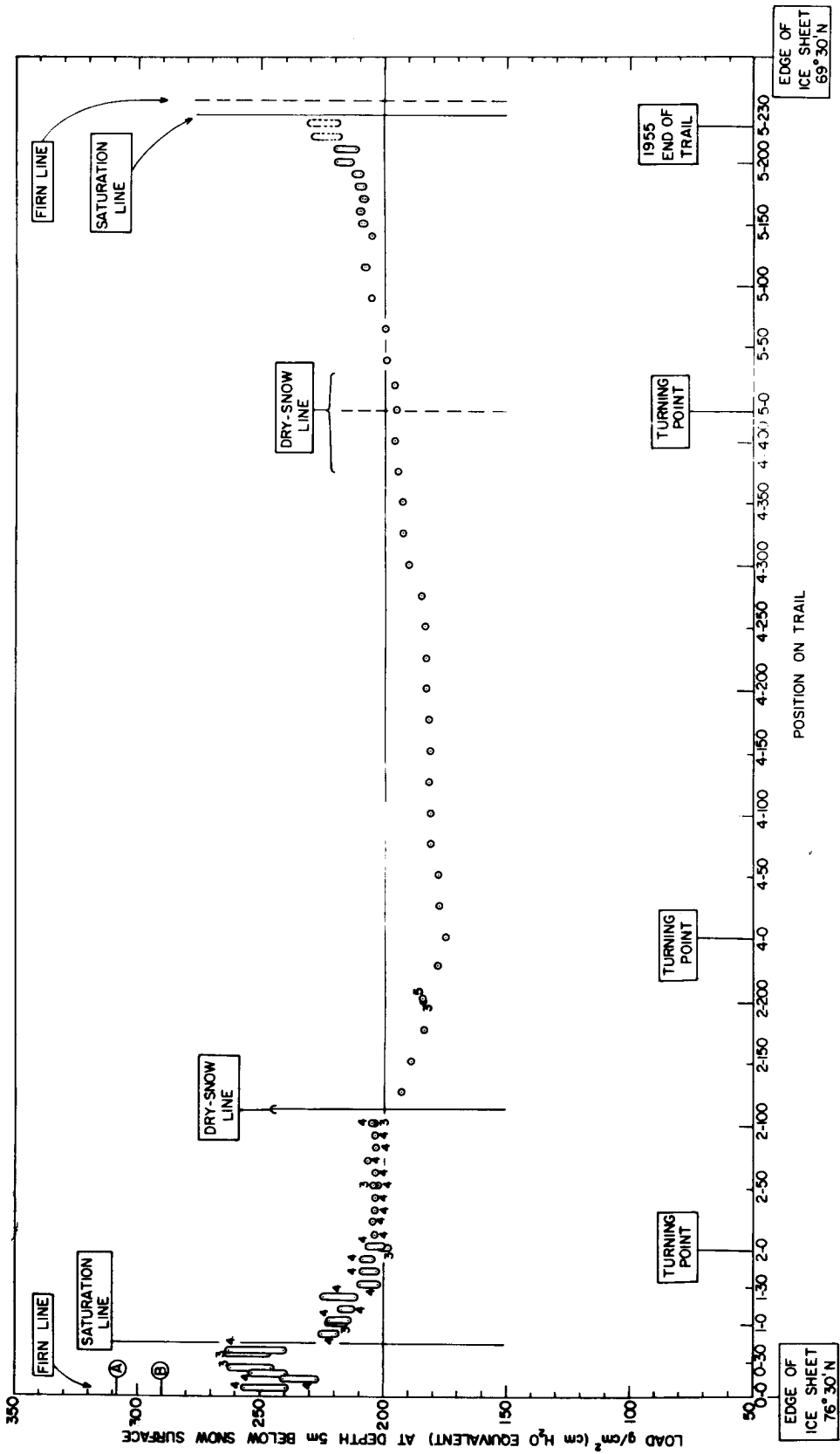


Figure 46. Load, in cm H₂O, at a depth of 5 m below the snow surface along the traverse in Figure 1. Points A and B indicate the upper extreme of the soaked facies. A - Snow Dome, Mt. Olympus, Washington, 47°48'N Lat, Elev 2070 m (measured by Benson in 1957). B - Upper Seward Glacier, Yukon Territory, 60°20'N Lat, Elev 1790 m (Sharp, 1951).

(b) The load at a given depth decreases from soaked to dry-snow facies (Fig. 45):

Facies	Load 5 m below snow surface (g/cm ²)
Soaked facies	240 - 300 and above
Percolation facies	200 - 225
Dry-snow facies	175 - 200

Glacier Facies — A Classification of Glaciers

The definition of boundaries between diagenetic facies, in terms of the measurements described above, provides the basis for a quantitative classification of glaciers. This "facies classification" does not require that Ahlmann's useful distinction between temperate and polar glaciers be abandoned. A temperate glacier exhibits only the two facies below the saturation line, whereas one or both of the facies above the saturation line are present on polar glaciers. However, the consideration of glacier facies goes beyond Ahlmann's classification in that it permits quantitative subdivision of large glaciers which span the entire range of environments from temperate to high-polar.

If the strata could be observed from top to bottom in a glacier with all facies present, we would find that: 1) Below the saturation line, all of the material has been soaked at one time or another; 2) Between the saturation line and the dry-snow line, soaked and non-soaked layers alternate; and 3) Above the dry-snow line, no soaked layers are observed (Fig. 15).

Some glaciers exhibit all facies; others have only those at one end of the spectrum. Data from ice shelves in the Ross Sea area (Wade, 1945) and from the Weddell Sea area at Maudheim (Schytt, 1954) indicate that the firn line and the saturation line lie below sea level; in these areas the glaciers exhibit only the percolation and dry-snow facies. At the opposite extreme, the saturation line lies above the highest point on temperate glaciers, which exhibit only the soaked and ablation facies.

The main advantages of this classification are: 1) it extends and refines Ahlmann's geophysical classification without abandoning its major point, 2) the facies concept is familiar to all geologists and glaciologists and emphasizes the fact that glaciers are rock units, and 3) the classification is quantitative and areal in extent, with the facies boundaries defined by simple physical measurements.

Characteristics of the glacier facies may be summarized as follows:

- 1) The ablation facies extends from the edge, or snout, of the glacier to the firn line. The firn line is the highest elevation to which the snow cover recedes during the melt season.
- 2) The soaked facies becomes wet throughout during the melting season and extends from the firn line to the uppermost limit of complete wetting, the saturation line. The saturation line is the highest altitude at which the 0C isotherm penetrates to the melt surface of the previous summer.
- 3) The percolation facies is subjected to localized percolation of melt water from the surface without becoming wet throughout. Percolation can occur in snow and firn of sub-freezing temperatures with only the pipe-like percolation channels being at the melting point. A network of ice glands, lenses, and layers forms when refreezing occurs. This facies extends from the saturation line to the dry-snow line. Negligible soaking and percolation occur above the dry-snow line.
- 4) The dry-snow facies includes all of the glacier lying above the dry-snow line.

The saturation line is marked by discontinuities in temperature, density, and Rammsonde data, and may also be located by examination of melt evidence in firn strata. It is as sharply defined as the firn line, but the dry-snow line, although determined by the same methods, is a 10- to 20-mile wide zone of transition in Greenland.

Location of the facies boundaries, i. e., the firn line, saturation line, and dry-snow line, will change with changes in climate; therefore, they may serve as long-term climatic indicators. The altitude of facies boundaries depends on latitude and on meteorological factors similar to those which govern the altitude of the snow line (Matthes, 1942, p. 157-161). On glaciers the snow line is the firn line, herein defined as a facies boundary.

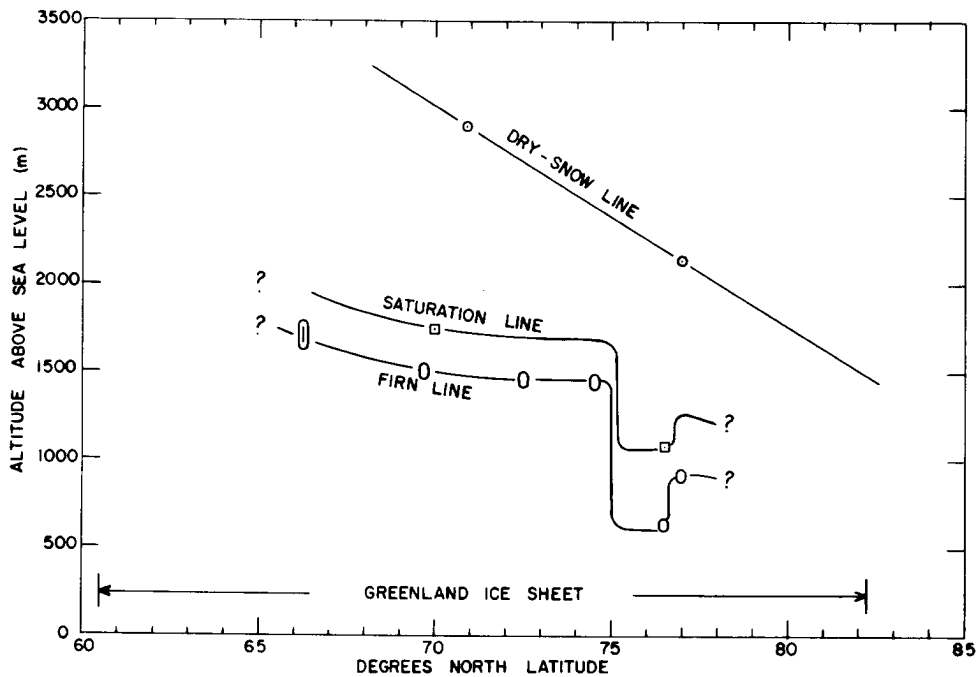


Figure 47. Variation of facies boundaries with altitude and latitude on the west slope of the Greenland ice sheet. The descent of the firn line and saturation line at 75°N is due to the increase in accumulation on the south slope of Thule peninsula (Fig. 30). On the north side of Thule peninsula these lines rise again. The dry-snow line is independent of accumulation. Data points were obtained during this study except for the firn line observations at:

- 66°16'N Mint Julep (Schuster, 1954)
- 69°42'N Heuberger (1954)
- 72°30'N Koch and Wegener (1930)
- 74°30'N Belknap (1934)

In particular, the altitude of the firn line and of the saturation line, but not of the dry-snow line, is dependent on the amount of annual accumulation. This follows directly from definition because the complete stripping away or the complete soaking of an annual layer depends on its thickness, among other things, whereas the presence or absence of detectable melt does not.

The variation of facies boundaries with altitude and latitude on the west slope of the Greenland ice sheet is shown in Figure 47. The descent of the firn line and the saturation line at 75°N is due to the increase in accumulation on the south slope of Thule peninsula. On the north slope of this peninsula these lines rise again. The dry-snow line has a constant slope of 1.15 m/km, and crosses the 3000 m elevation at 70°N latitude. The distribution of diagenetic facies on the Greenland ice sheet is shown in Figure 48.

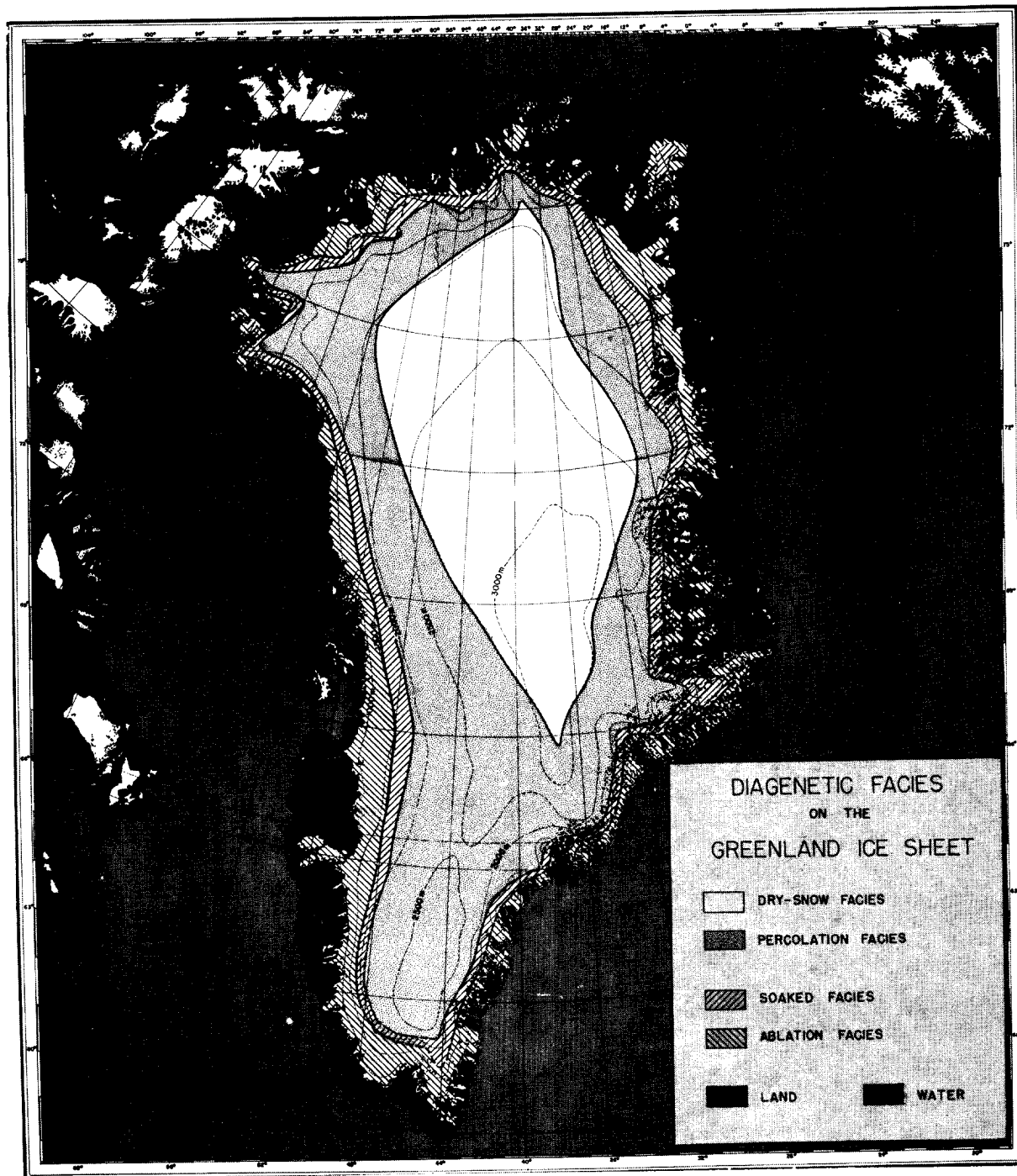


Figure 48. Distribution of facies on the Greenland ice sheet. The location of facies boundaries is most certain along the west side of the crest between 66 and 79°N. Away from this region, the dry-snow line may be extrapolated with the greatest confidence because it is independent of accumulation. The dry-snow line on this map was drawn along the intersection between a plane, sloping 1.15 m/km to the north, and the surface of the ice sheet. Location of the firn line and saturation line in south and east Greenland is highly speculative.

CHAPTER VI. DENSIFICATION OF SNOW AND FIRN

Load - Volume Relationship

The depth-density curve is linear over the depth range of 10 to 50 m, but non-linear above and below. This has made it difficult to derive a simple functional relationship between depth and density. As stated by Landauer (1959)* "...So far we have not been able to express this relationship in any simple yet accurate way." Actually, there is no a priori reason why depth should be a significant variable. Compressive stresses on the firn increase with depth, but because the firn density is not constant, we cannot replace the load at a given depth by the depth itself. In an attempt to get an analytic expression for the phenomenon of densification, load rather than depth is used as the independent variable. In place of firn density as the dependent variable, its reciprocal (specific volume) is used, with the assumption that it approaches the value for pure ice (1.09 cm³/g) as a limit. The use of volume rather than density enables us to think directly in terms of changes in volume produced by changes in applied stress.

To obtain a first approximation some simplifying assumptions are made. First, where melt is negligible it is assumed that the only cause of densification is the load of overlying snow and firn. It is further assumed that this load is applied at a constant rate of A g/cm² per year and that an equal amount of material is lost each year by flow at depth within the metamorphic part of the ice sheet. Thus, a steady-state system exists within the sedimentary veneer of the ice sheet with firn moving downward as it becomes densified, while the depth-density curve remains invariant with time as stated by Sorge's law (Bader, 1954) and as shown in Table VIII. Along with these assumptions the existence of a vertical pressure gradient is recognized in the ice sheet. Within the metamorphic part unbalanced horizontal components of stress result in flow; however, this aspect of the problem is neglected here. It is also assumed that the ice composing the firn grains remains at constant density, † and as a direct result of this the observed volume changes in firn are solely due to the elimination of pore space. The rate at which pore space may be eliminated with increase in load, under the assumed steady-state conditions, must be related in some manner to the amount of pore space present; the simplest possible relation between these quantities is a linear one. The implications of this simplest of assumptions, expressed in eq 8, are investigated below:

$$\frac{dv_p}{d\sigma} = -mv_p, \text{ or}$$

$$\frac{dv}{d\sigma} = -m(v - v_i) \quad (8)$$

where $v = \frac{1}{\rho} =$ specific volume of snow or firn ($\rho =$ density)

$v_i =$ specific volume of ice (1.09 cm³/g)

$v_p = (v - v_i) =$ volume of pore space,

$\sigma = \int_0^z \rho dz =$ load at depth z below snow surface, and

\underline{m} is a function of the mechanism of compaction, including time-dependent and stress-dependent terms. The functional nature of these mechanisms is unknown, but under the assumed conditions of a steady-state system with constant temperature and rate of accumulation, \underline{m} will be treated as a constant. This permits immediate examination of the first approximation outlined above and expressed in eq 8. In particular, the consequences of this approach will be compared with observation.

* See also the discussions in Bader, et al., (1955) and Benson (1959).

† This assumption is reasonable because the maximum pressure at the base of the ice sheet does not exceed 300 atm and this produces a total density increase of the order of 0.005 g/cm³.

Eq 8 may readily be solved for \underline{v} in terms of σ to obtain:

$$v = v_i + (v_0 - v_i) e^{-m\sigma} \quad (9)$$

where v_0 is the specific volume when $\sigma = 0$. Depth-density data for station 2-100, and several other stations* expressed in terms of specific volume and load are compared with eq 2 in Figure 49. The data of station 2-100 will be discussed in detail because they are the most complete.

At station 2-100, the change in rate of densification, apparent at a depth of 10 m below snow surface in Figure 44, is more pronounced in Figure 49. For convenience, the depth at which this discontinuity occurs is called the "critical depth" \underline{z}_c and the load, density, specific volume, porosity, void ratio, and temperature values measured at this depth will be referred to as the critical values σ_c , ρ_c , \underline{v}_c , \underline{n}_c , ϵ_c , and \underline{T}_c , respectively.

The slope of the load-volume curve is given by eq 8 both above and below \underline{z}_c but the parameter \underline{m} is nearly 4 times greater above \underline{z}_c than below. For eq 9 at station 2-100, the constants used in Figure 49 are:

Load values (g/cm ²)	\underline{m} (cm ² /g)	v_0 (cm ³ /g)
$0 < \sigma < 455$	16.0×10^{-4}	2.65
$455 < \sigma < \infty$	4.3×10^{-4}	2.00

The abrupt change in rate of densification seen in the 2-100 data is present in data from other stations shown in Figure 49. The beginning of the change shows at 1-0. It is clear also in the data from Upper Seward Glacier (Sharp, 1951), even though the original assumption that melt is negligible is not true here.

It is proposed that the main reason for the abrupt change in rate of densification is a change in the basic mechanism of densification. It is assumed that, in the complete absence of melt, densification above \underline{z}_c occurs primarily by packing of the ice grains comprising snow. The minimum porosity that can be attained experimentally by this mechanism alone is about 40% (i. e., snow density of about 0.55 g/cm³). This lies between the values for loosest (47.6%) and closest (26.0%) theoretical packing of spheres.

"... it is found experimentally that assemblages of spheres, or even sand particles, will have porosities averaging about 40 per cent in spite of careful efforts to induce closer packing, and even though the predominant array in the assemblage is rhombohedral with a porosity of only 26 per cent" [Muskat, M. (1937) The Flow of Homogeneous Fluids Through Porous Media, New York: McGraw-Hill, p. 13].

This agrees well with the critical values on load-volume curves measured where melting is slight or absent. The observed values of critical porosity at 2-100, 2-200, and 1-0 range between 36.7 and 43.3% (Table IX).

An extreme example of the packing process is commonly observed in the sudden collapse† of depth-hoar and other "soft layers" of relatively low density. Such layers are common in the upper 7 m (see data sheets, Fig. 6a, b, 8). They constitute flaws which are first to deform under the compressive stress of the overburden. The density profiles on Data sheet 5 clearly show the effect of this; the soft layers, common above 7 m, have been practically eliminated below 10 m.

* Points A (0.82 g/cm³ at 60 m depth) and B (0.88 g/cm³ at 100 m) from Maudheim (Schytt, 1954, p. 238) also appear to be compatible with eq 9, falling near the curves drawn for 1-0 and 2-100. The range of density values recorded at Maudheim suggests that they should fit the facies described here somewhere between 1-0 and 2-100, i. e., midway in the percolation facies.

† The actual collapse of soft layers is frequently observed when one walks in an undisturbed area, and when pit digging begins. Sometimes the effect is spectacular. During an airdrop at 2-120 on 29 Aug 1952, a barrel broke out of its parachute harness and penetrated more than 2 m below the snow surface. A sudden settling of weak layers spread from the point of impact and was accompanied by a startling sound. Similar examples, not started by man, were recorded by Sorge (cont'd p. 78).

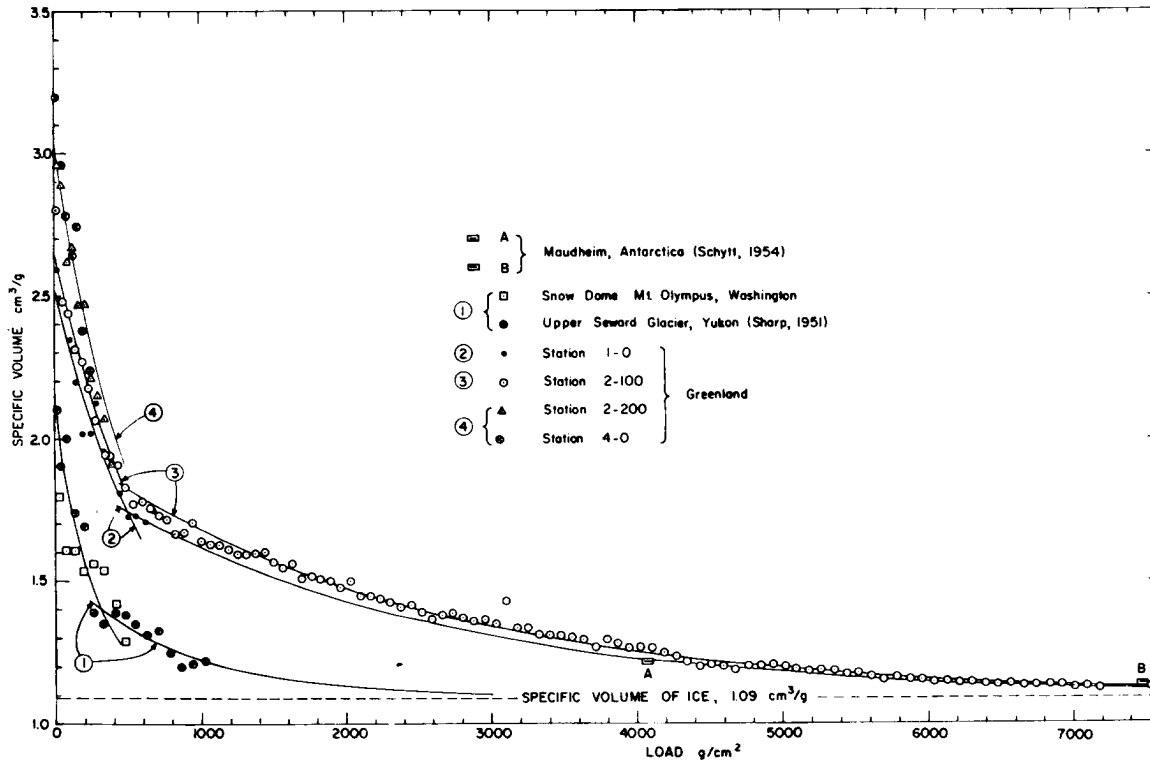


Figure 49. Specific volume plotted against load. Computed curves from eq 9; for values of constants, see Figure 44. Points A and B are from Maudheim, Antarctica (Schytt, 1954, p. 238).

Table IX. Critical values observed on Seward Glacier and in Greenland.

Station	z_c (m)	v_c cm ³ /g	ρ_c g/cm ³	n_c porosity %	T_c (C)
Seward Glacier*	4.5 ± .5	1.35 - 1.40	0.715 - 0.74	22.0 to 19.3	0 to -2
0-35	5 to 6	1.54 - 1.67	0.60 - 0.65	34.6 to 29.1	-9 ± 3
1-0	10	1.73 - 1.78	0.56 - 0.58	38.9 to 36.7	-16 ± 0.5
2-100	10	1.82 - 1.86	0.54 - 0.55	41.1 to 40.0	-24 ± 0.5
2-200	10	1.88 - 1.92	0.52 - 0.53	43.3 to 42.2	-30 ± 0.5

* From Sharp (1951).

(cont'd from p. 77) "Several times we heard and felt a kind of earthquake: on 2 October 1930, at 06.55 a.m. (Middle Greenland Time). We called it "Firnstoss" (Firnpush or Firncrash). It consisted of a noise approaching rapidly; then followed a large crash; and then the noise ran away. Our mercury barometer, which had been hung in a separate ice cave at a depth of 6 to 8 feet, was caught and got nearly broken. The layers were compressed by one inch" (Sorge, 1933, p. 340).

When the critical density is reached, compaction by grain packing is no longer possible, as signified by a marked reduction in the rate of densification (Fig. 49). Compaction beyond the critical density brings other mechanisms into predominance; grains change size and shape by growing together to relieve stress, and plastic deformation of the grains increases as load increases. Basically, densification is the elimination of pore space. As pore space is eliminated there is also a reduction in the amount of intercommunicating pore space, and therefore in permeability. When all pores are isolated, the measurable air permeability vanishes and snow or firn becomes glacier ice by definition.

The distinction between material above and below the critical point is based on a change in the primary mechanism of densification, which reflects a structural change, and produces the discontinuity in the load-volume curves. On the other hand, the transition from snow, or firn, to glacier ice is gradual and the distinction between the two materials is based solely on the loss of measurable air permeability. It appears that changes occur in most physical properties at the critical density. Because of this, Anderson and Benson (1959) use the critical density as a physical distinction between "old snow" and "firn" since there is no such distinction at present. The steady-state relationship between $dv/d\sigma$ and \underline{v} at station 2-100 is plotted in Figure 51.

The critical values vary from one location to the next as shown in Table IX and Figure 50. The data appear to satisfy the following equation:

$$\rho_c = \rho_{c1} + (\rho_{c0} - \rho_{c1}) e^{ST_c} \tag{10}$$

where $\rho_{c1} = 0.50 \text{ g/cm}^3$,

$\rho_{c0} = 0.73 \text{ g/cm}^3$,

$S = 0.07 \text{ C}^{-1}$, and

$T_c =$ critical temperature (a negative quantity).

This empirical equation provides a quantitative description of the relation between critical temperatures and densities defined here, and has some interesting implications. First, as \underline{T}_c approaches the melting point, ρ_c approaches its maximum value, ρ_{c0} . Secondly, as \underline{T}_c decreases without limit, the value of ρ_c also decreases, but approaches a lower limit, ρ_{c1} . Thus, it appears that the minimum critical density is about 0.50 g/cm^3 regardless of how low the temperature may be.

It must be noted that, although Figure 50 shows the observed relationship between critical density and temperature, the relation between these variables is not simple because temperature changes have many ramifications. A very important temperature-dependent factor is the amount of melt water, which is especially notable on Seward Glacier and at 0-35, of minor importance at 1-0, negligible at 2-100, and completely absent at 2-200. Average grain size decreases from left to right in Figure 50; this is primarily a temperature effect. Strength of ice increases with decreasing temperature and decreases the rate of densification. The rate of accumulation is roughly an inverse function of temperature. The latter two factors combine to make the age of the material at the critical density increase from left to right. These factors are all involved in the abscissa \underline{T}_c which is the most significant critical value to correlate with critical density.

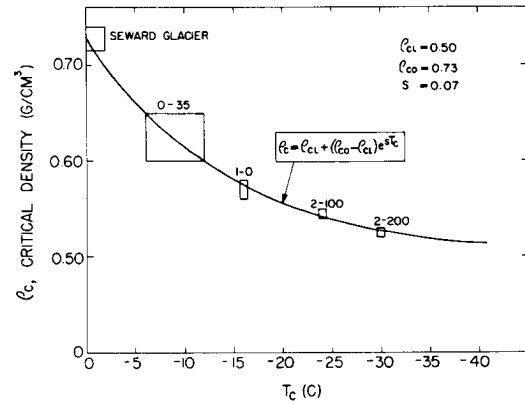


Figure 50. Critical density vs critical temperature.

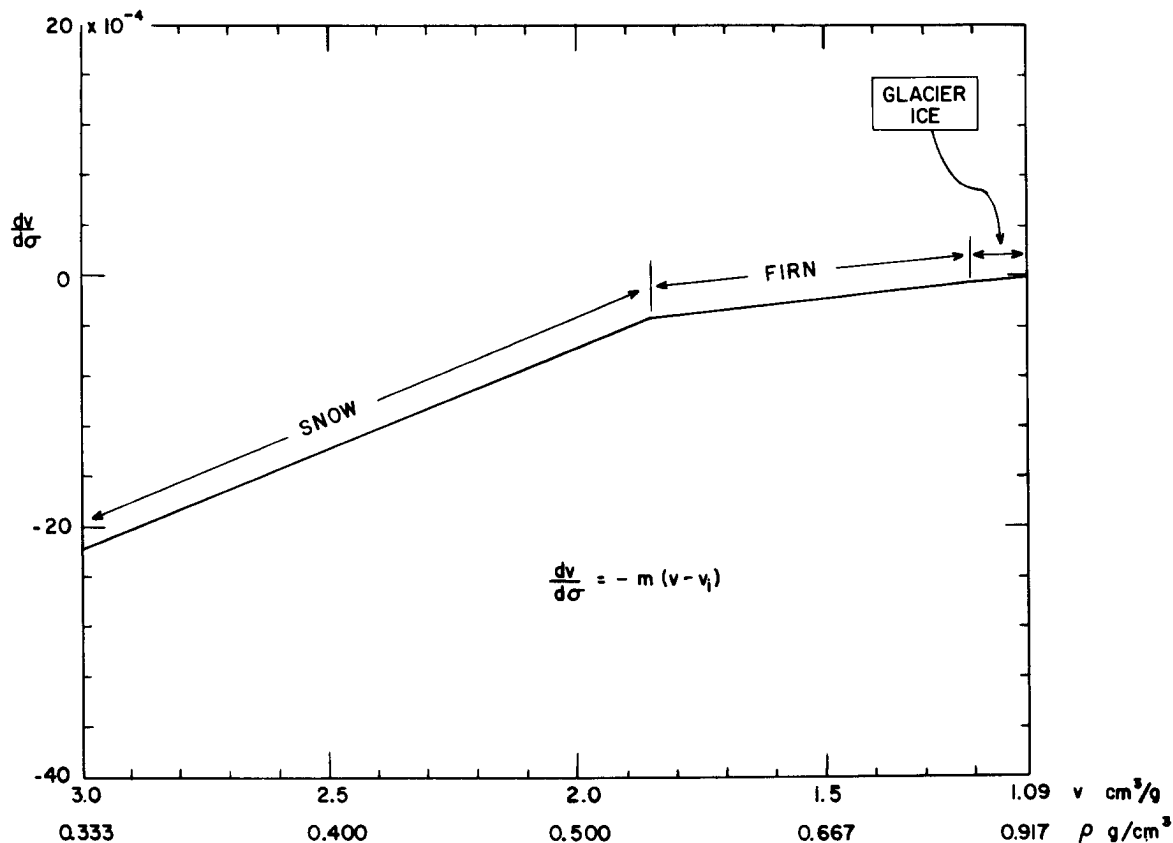


Figure 51. Relation between $dv/d\sigma$ and v at station 2-100.

Even though melting occurs the discontinuity at the critical point still reflects the same change in the densification process. The presence of "free water" in the snow permits closer packing than can be obtained by packing dry snow. For example, if dry snow can be compacted to a minimum porosity of 39% it would be expected that 39% free water added to the snow would lead to complete densification (i.e., the final product when frozen would be impermeable ice). Actually, in such a case, complete densification requires only about 29% free water (Anderson and Benson, 1959), because the presence of water in the snow has allowed tighter packing, partly by lubrication of the grains. As a result of this, values of critical porosity are lower where melt occurs than where no melt occurs. However, this effect caused by melt water is merely superimposed on the primary mechanism of densification by packing.

Assume that the minimum critical porosity obtained by packing dry snow is n_{c0} %. Then the reduction of pore space caused by melt action at any location will be given by

$$(n_{c0} - n_c)\%$$

where n_c is the critical porosity at the given location. If $n_{c0} = 41\%$ then an estimate of the reduction of pore space by melt water at critical depth is:

Seward Glacier	19 to 22%
0-35 Greenland	6 to 12%
1-0 "	2 to 4%
2-100 "	0 to 1%
2-200 "	0%

On this basis the following estimates are made:

Facies	Reduction of pore space by melt action at z_c
Ablation	approaches 100%
Soaked	6 to 25%
Percolation	1 to 4%
Dry-snow	less than 1%

Depth-Density Relationship

An explicit relationship between depth and density may be obtained from eq 8 after making the following substitutions:

$$v = \frac{1}{\rho}, \quad dv = -\frac{d\rho}{\rho^2}$$

$$\sigma = \int_0^z \rho \, dz, \quad \text{and } d\sigma = \rho \, dz.$$

Then eq 8 becomes

$$\frac{d\rho}{dz} = m\rho^3 \left(\frac{1}{\rho} - \frac{1}{\rho_i} \right) = m\rho^2 \left(\frac{\rho_i - \rho}{\rho_i} \right) = m\rho^2 n \quad (11)$$

where $n = \text{porosity} = \frac{\rho_i - \rho}{\rho_i}$.

Eq 11 may be integrated to obtain the depth-density relationship as follows:

$$\frac{d\rho}{dz} = m\rho^2 \left(\frac{\rho_i - \rho}{\rho_i} \right) \quad (11)$$

$$\int_0^z \frac{m}{\rho_i} dz = \frac{m}{\rho_i} z = \int_{\rho_0}^{\rho} \frac{d\rho}{\rho^2 (\rho_i - \rho)} \quad (12)$$

Integration of the right hand side of eq 12 may be carried out to obtain:

$$z = \frac{1}{m\rho_i} \left[\frac{\rho_i - \rho}{\rho} + \ln \frac{\rho_i - \rho}{\rho} \right]_{\rho_0}^{\rho} \quad (13)$$

When the limits of integration are substituted in eq 13, we obtain:

$$z = \frac{1}{m\rho_i} [K - (\epsilon + \ln \epsilon)], \quad (14)$$

$$\text{where } K = \frac{\rho_i - \rho_0}{\rho_0} + \ln \frac{\rho_i - \rho_0}{\rho_0} = \epsilon_0 + \ln \epsilon_0,$$

$$\epsilon = \frac{\rho_i - \rho}{\rho} = \text{void ratio for firn of density } \rho, \text{ and}$$

$$\epsilon_0 = \frac{\rho_i - \rho_0}{\rho_0} = \text{void ratio for firn of density } \rho_0.$$

Curves obtained by plotting eq 14 are shown in Figure 52.

It is of interest to examine the nature of the depth-density curve as revealed by the derivatives $\frac{d\rho}{dz}$ and $\frac{d^2\rho}{dz^2}$.

The first derivative is given by eq 11 which states that the change in density with depth is proportional to the product of porosity and the square of the density.

The second derivative is:

$$\begin{aligned} \frac{d^2\rho}{dz^2} &= m \frac{d}{dz} \left(\rho^2 - \frac{\rho^3}{\rho_i} \right) \\ &= m^2 \left(2\rho - \frac{3\rho^2}{\rho_i} \right) \left(\rho^2 - \frac{\rho^3}{\rho_i} \right) \\ &= \left(\frac{m}{\rho_i} \right)^2 \rho^3 (2\rho_i - 3\rho) (\rho_i - \rho). \end{aligned} \quad (15)$$

Several interesting points about the curvature of the depth-density curve revealed by eq 15 are summarized below:

- (a) $\frac{d^2\rho}{dz^2} = 0$ when $\rho = \frac{2}{3}\rho_i \cong 0.61 \text{ g/cm}^3$,
- (b) $\frac{d^2\rho}{dz^2} > 0$ when $\rho < \frac{2}{3}\rho_i$ and
- (c) $\frac{d^2\rho}{dz^2} < 0$ when $\rho > \frac{2}{3}\rho_i$.

The point of inflection at $\rho = \frac{2}{3}\rho_i$ is independent of the value of the parameter m , but is a direct consequence of the functional relationship assumed in eq 8.

The overall curvature of the depth-density curve is slight; therefore, the existence of a point of inflection demands that the curve be nearly linear for some distance on either side of it. The point of inflection, with the second derivative being positive for $\rho < \frac{2}{3}\rho_i$ and negative for $\rho > \frac{2}{3}\rho_i$, shows clearly in Figure 52.

A physical reason for the existence of a point of inflection is that the model does not allow negative densities. Thus, from a purely mathematical point of view, the depth-density curve obtained from the steady-state assumption expressed in eq 8 is asymptotic to zero density as z approaches $-\infty$, and asymptotic to the density of pure ice as z approaches $+\infty$; with $z = 0$ at the snow surface. This depth-density curve explicitly includes a nearly linear relation between depth and density in the depth range $10 < z < 50$ m, and this agrees well with observation.

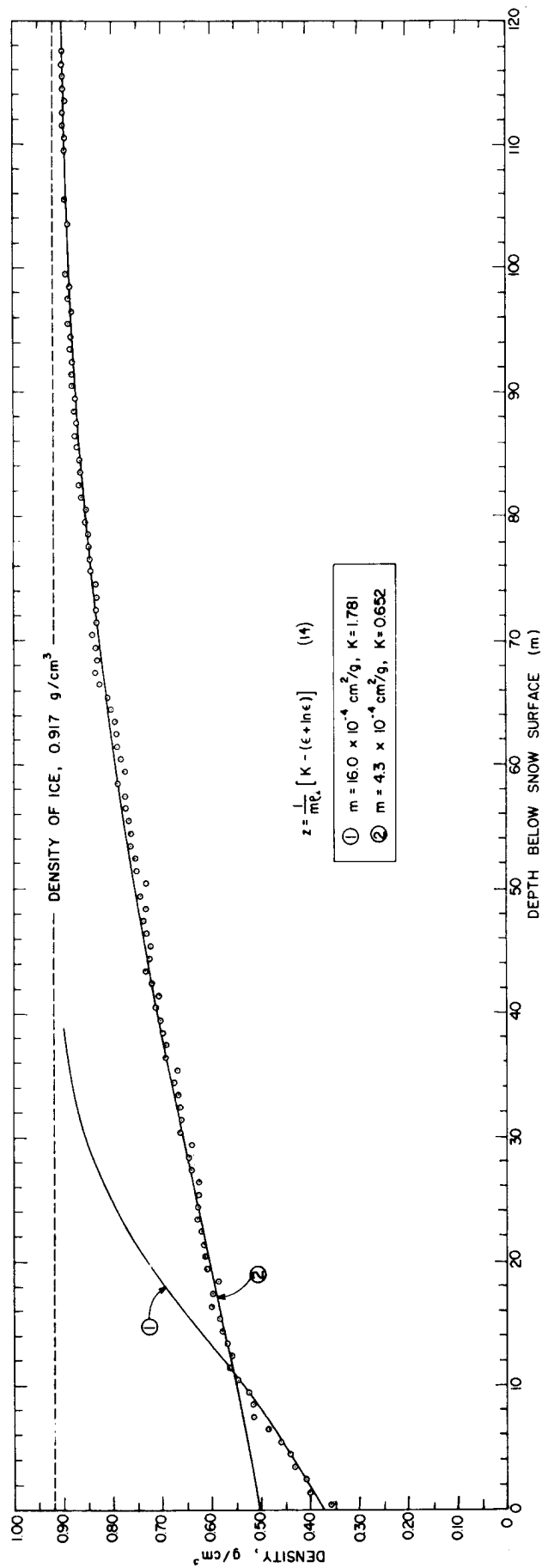


Figure 52. Depth-density relationship at station 2-100. Curves were computed from eq 14. Data points were obtained by averaging the writer's measurements made in 1953, 1954 and 1955 in the upper 14 m with measurements made by Langway (1958a) at the lower depths.

CHAPTER VII. CLIMATOLOGICAL IMPLICATIONS

Introduction

Knowledge of weather and climate in the polar regions is fragmentary. During the past 10 yr significant increases in arctic meteorological data for the western hemisphere have resulted chiefly through the efforts of the late Charles J. Hubbard; yet the overall picture is not complete. Many phenomena of arctic climatology are hemispherical in extent, but Greenland constitutes a special problem because of its extensive ice cover (see Hare, 1951, p. 961-963). Some climatological results of this study have been presented above, i. e., the distributions of gross annual accumulation (Fig. 30), mean annual temperature (Fig. 40), and diagenetic facies (Fig. 48). The purpose of this chapter is to discuss several implications which were not directly involved in the above discussion.

It is significant that as late as 1950 the erroneous "glacial anticyclone theory" was still prevalent (in the U. S.) to the extent that Matthes (1946) and Matthes and Belmont (1950) devoted papers to its refutation. After extensive review of recent meteorological data from Greenland, Matthes concluded:

"that there is no evidence of a virtually permanent 'glacial anticyclone' centered over the Greenland ice sheet. On the contrary, there is consistent evidence from all parts of Greenland that the weather over the ice sheet is controlled by alternating cyclonic and anticyclonic movements. Cyclonic activity is most intense in southern Greenland and weakest in northern Greenland. The entire ice sheet is supplied with snow brought by rising maritime air masses, not by air descending from the upper troposphere" (Matthes, 1946, p. 324).

The results of the present study are completely compatible with Matthes' conclusions; and they contribute quantitative information on the amount and distribution of precipitation for part of the ice sheet.

Katabatic Winds and Accumulation

If a staunch proponent of the glacial anticyclone were found today, he might argue that "the maximum accumulation shown at low elevations, near the margin of the ice sheet (Fig. 28), is due to katabatic winds which sweep the snow outward from the interior." This is not a valid argument because, although the katabatic winds prevail they are weaker and cause much less drifting of snow than do the storm winds. This is known by direct observation of the drifts which form around objects, such as huts or piles of barrels, in the course of a year. Such drifts are always lined up with the storm winds which come from the southwest and erosion-deposition features from the prevailing katabatic winds are merely superimposed on them. Thus, the distribution of accumulation shown in Figure 28 exists in spite of, not because of, the katabatic winds.

Rather than adding to the net accumulation at a given point, the katabatic winds may actually detract from it. The ability of the air to hold moisture increases markedly as it moves from the cool, dry interior toward the warmer coastal areas. As an example, saturated air at 0C contains 3.5 times more water by weight than saturated air at -15C. Thus katabatic winds, originating over the interior highlands of the ice sheet, absorb moisture as they descend, especially in summer months, and leave the shores of Greenland with a net increase in water vapor. This is similar to the process which acts over the United States as outlined by Holzman (1937, p. 38):

"The principal amount of moisture returned to the atmosphere by continental evaporation is absorbed by continental, or dry, air masses that are generally incapable of immediately releasing their moisture and that pass off continental areas with large gains in moisture."

Therefore, desert regions like Inglefield Land are dry not only because they lie in precipitation shadows, but also because much of what they do receive is "blotted up" and carried off by the katabatic winds.

Annual Heat Exchange

Consider a column of unit cross-section extending from the snow surface to a depth of 10 m. By definition, \underline{Q} is the amount of heat required to raise the temperature of this column of firn to the melting point. The maximum and minimum values of \underline{Q} , \underline{Q}_{\max} , and \underline{Q}_{\min} , occur during winter and summer respectively. \underline{Q} , sometimes called "cold content," is computed by summing increments ΔQ over depth increments Δz (taken to be 20 cm each for convenience). Then

$$\Delta Q = mcT$$

where m = the mass in grams of the 20 cm³ volume
 T = the average temperature, and
 c = 0.5 cal/mC.

A summary of data obtained in the top 5 m in late summer is shown in Figure 53. Except for the spacing between curves of the soaked and non-soaked facies, the cold content increases fairly smoothly with elevation. The environmental difference existing between points lying well above the firn line is shown by the fact that the curve for \underline{Q}_{\max} at 1-0 (not shown) is about the same as that shown for \underline{Q}_{\min} at 2-200. Thus, the amount of heat required to melt the upper layers of snow at 2-200 in summer is the same as that required at 1-0 in winter. Values of \underline{Q}_{\min} (to 10 m) for several positions are:

Station	\underline{Q}_{\min} (cal)
Seward Glacier	0.0 $\times 10^3$
0-35	1.0 to 2.0 $\times 10^3$
1-0	3.5 $\times 10^3$
2-100	4.7 $\times 10^3$
2-200	6.0 $\times 10^3$

\underline{Q}_{\min} may prove useful as a climatic index for glaciers, being zero for a truly temperate glacier.

The amount of heat exchanged annually between the top 10 m of firn and the atmosphere is denoted by ΔH . If heat exchanges associated with phase transformations are ignored,

$$\Delta H = \underline{Q}_{\max} - \underline{Q}_{\min}$$

At 77°N lat ΔH remains essentially constant, within 10%, even though measured in different temperature ranges at different altitudes as summarized below:

Station	Date	\underline{Q} (cal)	ΔH (cal)
1-0	3 March 1954	4856	1382
	17 August 1952	3474	
2-100	Feb - March 1954	6285	1543
	26 August 1953	4742	

The 10% difference between ΔH at 1-0 and 2-100 is in the right direction to indicate more melt at 1-0, and sufficient to completely melt a 5 cm layer of snow of density 0.40 g/cm³. This is not an unreasonable estimate for the difference in melting between 1-0 and 2-100.

The Balance of the Greenland Ice Sheet

Bauer (1955) came to the conclusion that the Greenland ice sheet is in negative balance, i. e., more material is being lost than gained. Bauer's estimate is based on the following:

1) The assumption that the firn line separates the regions of accumulation and ablation. He then estimated the firn line for each of the USAF World Aeronautical Charts.

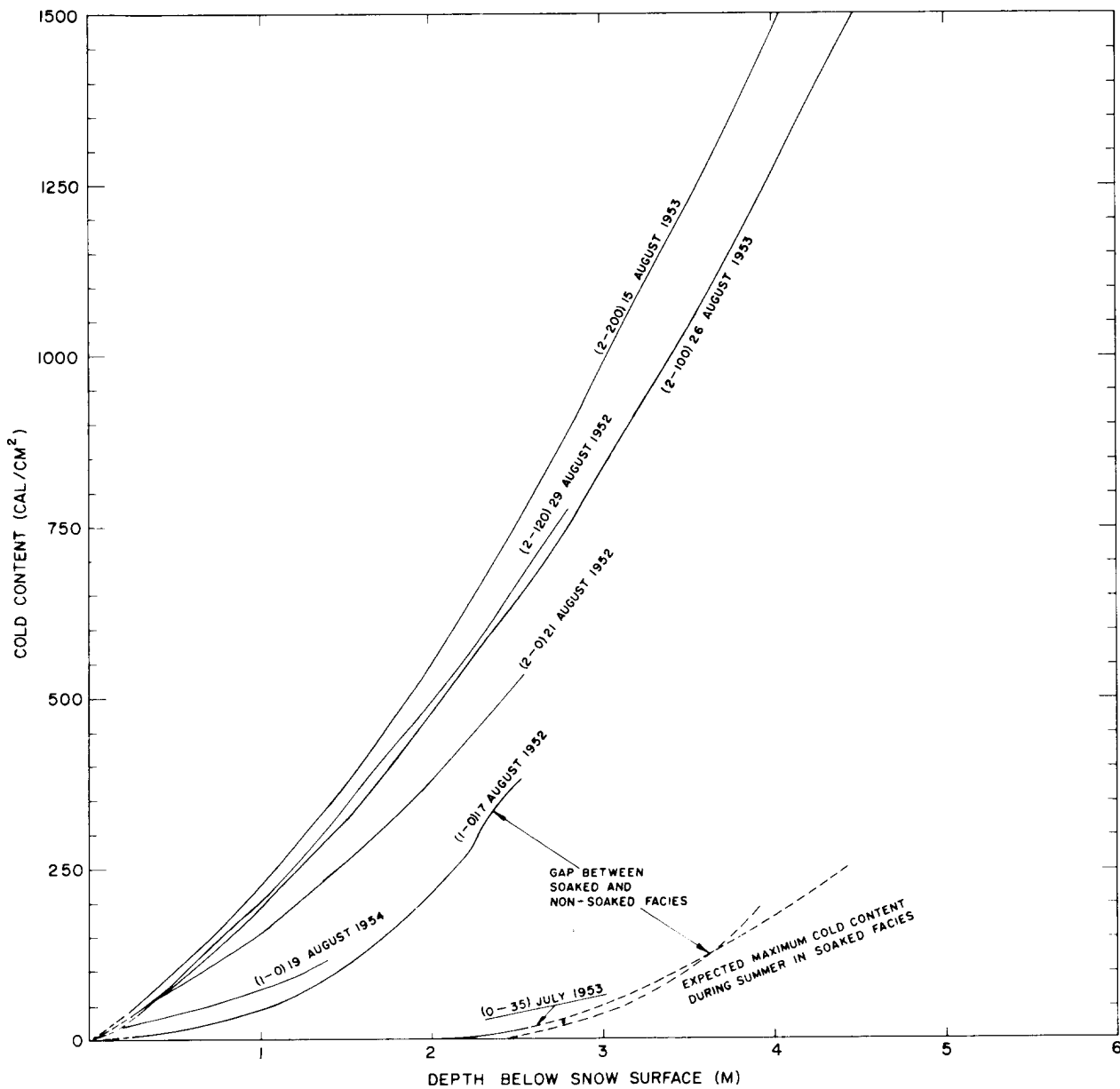


Figure 53. "Cold content" in the top 5 m during the peak of the melt season at 77°N. The cold content is defined as the amount of heat (in calories) required to raise a unit column of snow to the melting point.

2) Loewe's (1936) estimates for mean ablation (110 cm H₂O per yr) and for mean accumulation (31 cm H₂O per yr) for the entire ice sheet.

3) An estimate of the total discharge of icebergs from glaciers.

Bauer used a firn line at 4000 ft (1220 m) for the Smith Sound and Humbolt Glacier maps. This is definitely too high because pits at 4000 ft in this area are well above the firn line; indeed, they are above the saturation line. It is also known that the firn line does not separate the regions of ablation and accumulation in Greenland because of the formation of superimposed ice (Schuster, 1954; Schytt, 1955, p. 52-57). Thus the stated figure for total ablation area is too high.

Bauer's ablation area is reduced by 32,000 km² if the average altitude of the firn line is placed at 3000 ft (915 m) north of 76°N, except on the south slopes of Thule and Inglefield peninsulas where it is known to lie at about 2300 ft (700 m). The amount of area transferred from the ablation to the accumulation area on each of the maps involved is as follows:

World Aeronautical Chart	Area (km ²)	
#20 Smith Sound	13,000	
#19 Humbolt Glacier	6,000	19,000 west slope
# 8 Robeson Channel	0,000	
# 9 Independence Fjord	3,500	13,000 east slope
#18 Germania Land	9,500	
Total	32,000	

The average accumulation value of 31 cm H₂O for the entire ice sheet is too low. Planimetric measurements of the areas between accumulation contour lines on the 1:5,000,000 map of Figure 30 give an overall average accumulation value of 34 cm H₂O as summarized in Table X and Figure 54.

From the work reported herein, no comments can be made about Bauer's estimate for the amount of discharge of icebergs by glaciers. His value is accepted as being the best available estimate. Loewe's estimate of average gross ablation is also accepted here in the absence of sufficient data to apply a correction. His quoted value of 110 cm H₂O per year refers to net ablation; therefore, the addition of 3 cm H₂O per year to gross accumulation, as determined above, reduces his net ablation by the same amount to give 107 cm H₂O per year. The three* attempts to determine the balance of the Greenland ice sheet are summarized in Table XI.

I would estimate, as did Loewe (1936), that the Greenland ice sheet is in balance with present-day climate, or that it is so close to being in balance that our present methods of measuring the variables involved cannot show significant deviations one way or the other.

* Based on observations from his 1912 expedition, deQuervain concluded that the balance of the ice sheet was positive. He dealt with the west slope only so he did not estimate the magnitude of the positive balance but generalized that the ice sheet was maintaining itself at present and was not strictly a relic of the past.

Table X. Distribution of gross accumulation on the Greenland ice sheet.

A = Annual accumulation (cm H ₂ O) Range	Surface area (km ²)	Surface area (%)	Annual accumulation (cm H ₂ O)
5 - 10	138,000	7.8	0.58
10 - 20	397,000	22.4	3.36
20 - 30	314,000	17.7	4.42
30 - 40	267,000	15.0	5.25
40 - 50	259,000	14.6	6.57
50 - 60	197,000	11.1	6.10
60 - 70	91,000	5.1	3.32
70 - 80	51,000	2.9	2.18
80 - 90	40,000	2.3	1.96
greater than 90	20,000	1.1	1.04
	1,774,000	100.0	34.78

The total area of the ice sheet obtained from these measurements is 2.8% greater than that obtained by Bauer on the 1:1,000,000 map. Bauer's figure is more accurate than the one obtained here from the 1:5,000,000 map. Therefore, the average annual accumulation value of 34.78 cm H₂O should be reduced by 2.8% to give 33.86, or to the nearest centimeter, 34 cm H₂O.

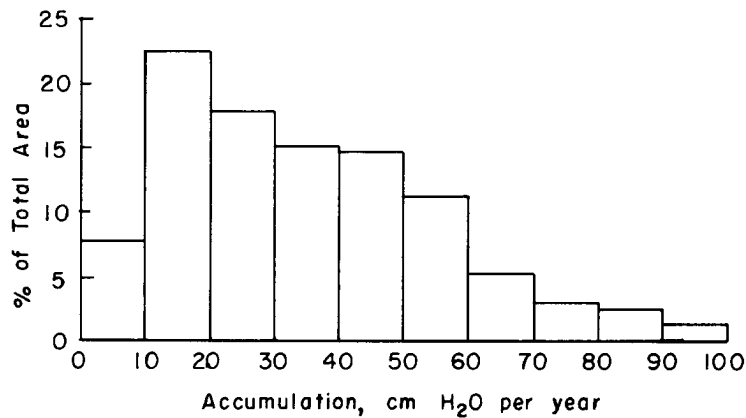


Figure 54. The areal distribution of gross accumulation on the Greenland ice sheet.

Table XI. Balance of the Greenland ice sheet.

	Loewe (1936)	Bauer (1955)	Present study
Area: (km ²)			
Accumulation zone	1,380,000	1,439,800	1,471,800
Ablation zone	270,000	286,600	254,600
Total ice sheet	1,650,000	1,726,400	1,726,400
Average Annual Rates: (cm H ₂ O/yr)			
Accumulation	31	31	34
Ablation	110	110	107
Net Values: (km ³ H ₂ O/yr)			
Accumulation	425	446	500
Ablation	295	315	272
Excess of accumulation over ablation	130	131	228
Discharge of icebergs from glaciers	150	215	215
Balance (km ³ H ₂ O/yr)	-20	-84	+13

REFERENCES

- Ahlmann, Hans W. (1935) Contribution to the physics of glaciers, Geogr. Jour., vol. 86, p. 97-113.
- _____ (1936) Scientific results of the Norwegian-Swedish Spitsbergen Expedition 1934. Part VII. The firn structure on Isachsen's Plateau, Geografiska Annaler, vol. 18, p. 48-73.
- _____ (1940) Scientific results of the Swedish Icelandic investigations 1936-37-38, Geografiska Annaler, vol. 22, p. 188-205.
- _____ (1948) Glaciological research on the North Atlantic coasts, Royal Geographical Society Research Series No. 1, 83p.
- _____ (1949) The contribution of polar expeditions to the science of glaciology, Polar Record, vol. 5, no. 37 & 38, p. 324-331.
- _____ (1953) Glacier variations and climatic fluctuations, Bowman Memorial Lecture Series 3. New York: American Geographical Society.
- Anderson, Don L., and Benson, Carl S. (1959) The densification of snow (in preparation).
- Bader, Henri (1954) Sorge's law of densification of snow on high polar glaciers, Journal of Glaciology, vol. 2, no. 15, p. 319-323. Also published as U. S. Army Snow Ice and Permafrost Research Establishment, Corps of Engineers, Research Paper No. 2, 1953.

- Bader, et al. (1939) Der Schnee und Seine Metamorphose (Snow and its metamorphism): Beitrage zur Geologie der Schweiz, Geotechnische Serie, Hydrologie, Lieferung 3, Bern. U. S. Army Snow Ice and Permafrost Research Establishment, Corps of Engineers, Translation 14, 1954.
- Bader, et al. (1955) Excavations and installations at SIPRE Test Site, Site 2, Greenland, USA SIPRE Technical Report 20, 32p.
- Bauer, A. (1955) The balance of the Greenland ice sheet, Journal of Glaciology, vol. 2, no. 17, p. 456-462.
- Belknap, R. L. (1934) The Michigan - Pan American Airways Greenland Expedition, Preliminary results, Geographic Review, vol. 24, p. 205-218.
- Benson, Carl S. (1955a) Scientific work of Party Crystal (Preliminary report), USA SIPRE Report 24.
- _____ (1955b) Operations and logistics of Ice-Cap Party Crystal, 1954, USA SIPRE Report 25, 21p.
- _____ (1955c) Resupply of ice-cap expeditions by air drop, USA SIPRE Special Report 17, 3p.
- _____ (1959) Physical investigations on the snow and firn of northwest Greenland during 1952, 1953, and 1954, USA SIPRE Research Report 26, 62p.
- Benson, Carl S. and Ragle, R. H. (1956) Report on special foods provided by the Quartermaster Food and Container Institute, USA SIPRE Special Report 18. Also published in Activities Report, Quartermaster Food and Container Institute, vol. 9, no. 1, p. 8-23, March 1957.
- Barnes, D. F., and Zavadil, R. J. (1954) "Gravity studies on the Greenland Ice Cap," in Final Report, Scientific Program (Program B) Operation Ice Cap, 1953, p. 377-393. Printed by Stanford Research Institute for Transportation Research and Development Command, Transportation Corps U. S. Army, (Department of the Army Project 9-98-07-002).
- Bey, Paul B. (1951) "The heat economy of the snow pack," in Review of the properties of snow and ice, SIPRE Report 4, Ch. VII.
- Black, Robert F. (1954) Precipitation at Barrow, Alaska, greater than recorded, Transactions American Geophysical Union, vol. 35, p. 203-207.
- Brooks, C. R. (1938) Need for universal standards for measuring precipitation, snow-fall, and snow cover, Bull. 23, International Association of Hydrology, I.G.G.U. Riga.
- Bull, Colin (1956) Seismic investigations on the northern part of the Greenland Ice Sheet, Geographical Journal, vol. 122, p. 219-225.
- _____ (1958) Snow accumulation in North Greenland, Journal of Glaciology, vol. 3, no. 24, p. 237-248.
- Butkovich, T. R. (1954) Ultimate strength of ice, USA SIPRE Research Paper 11.
- Church, J. E. (1933) Snow surveying - its principles and possibilities, Geographical Review, vol. 23, p. 529-563.
- _____ (1942) "Snow and snow surveying," in Hydrology, Physics of the Earth. New York: Dover Publications, Inc., vol. IX, Ch. IV.
- Conrad, Victor (1944) Methods in climatology. Cambridge, Massachusetts: Harvard University Press, 228p.
- DeQuervain, Alfred, and Mercanton, P. L. (1925) Resultats Scientificues de l'expedition Suisse au Groenland 1912-1913, Meddelelser om Grønland, Bind. 59.
- DeQuervain, M. (1945) Schnee als kristallines Aggregat (Snow as a crystalline aggregate), Experimentia, vol. 1, USA SIPRE Translation 21, 7p.

- Diamond, M. (1958) Air temperature and precipitation on the Greenland Ice Cap, USA SIPRE Research Report 43, 9p.
- Dorsey, H. G. (1945) Some meteorological aspects of the Greenland Ice Cap, Journal of Meteorology, vol. 2, p. 135-142.
- Epstein, S. and Benson, Carl (1961) Variation of the O¹⁸/O¹⁶ ratios in Greenland snow, (in preparation.
- Epstein, S. and Mayeda, T. (1953) Variation of O¹⁸ content of water from natural sources, Geochim. et Cosmochim. Acta, vol. 4, p. 213-224.
- Epstein, S. and Sharp, R. P. (1959) Oxygen-isotope variations in the Malaspina and Saskatchewan Glaciers, Journal of Geology, vol. 67, p. 88-102.
- Flint, R. F. (1947) Glacial geology and the Pleistocene Epoch. New York: John Wiley and Sons, 589p.
- Fristrup, B. (1952) Physical geography of Peary Land, Meddelelser om Grønland, Bind 127, no. 4.
- Grout, F. F. (1932) Petrography and petrology. New York: McGraw-Hill Book Co., 522p.
- Hare, F. K. (1951) "Some climatological problems of the arctic and subarctic," in Compendium of Meteorology, American Meteorological Society, p. 952-964.
- Henry, A. J. (1919) Increase of precipitation with altitude, Monthly Weather Review, vol. 47, p. 33-41.
- Heuberger, Jean-Charles (1954) Groenland, glaciologie, Vol. I, Forages sur L'inlandsis (Greenland, glaciology, vol. I, Borehole studies on the ice cap). Paris: Hermann & Cle, Editeurs.
- Holzman, Benjamin (1937) Sources of moisture for precipitation in the United States, U. S. Department of Agriculture, Tech. Bull. No. 589.
- Hubley, R. C. (1954) The problem of short period measurements of snow ablation, Journal of Glaciology, vol. 2, no. 16, p. 437-440.
- Koch, J. P. and Wegener, A. (1930) Wissenschaftliche Ergebnisse der Dänischen Expedition nach Dronning Louises-Land und quer über das Inlandsis von Nordgrønland 1912-1913 unter Leitung von Hauptmann J. P. Koch (Scientific results of the Danish expedition to Dronning Louises Land and the traverse across North Greenland's inland ice 1912-1913, under the leadership of J. P. Koch, Meddelelser om Grønland, Bind. 75.
- Krumbein, W. C. (1933) Textural and lithological variations in glacial till, Journal of Geology, vol. 41, p. 382-408.
- _____ (1936) The use of quartile measures in describing and comparing sediments, American Journal of Science, vol. 32, p. 98-111.
- _____ (1943) Size frequency distributions of sediments, Jour. Sed. Petrology, vol. 4, p. 65-77.
- Krumbein, W. C. and Sloss, L. L. (1951) Stratigraphy and sedimentation. San Francisco, California: W. H. Freeman & Company, 497p.
- Landauer, J. K. (1959) From Discussion, Symposium de Chamonix, Bull de l'assoc. Int. Hydrol. Sci., no. 13, p. 43.
- Langway, C. C., Jr. (1958a) Bubble pressures in the Greenland glacier, Symposium of Chamonix, 16-24 September 1958. International Association of Scientific Hydrology, Publication 47.
- _____ (1958b) A 400-m deep ice core in Greenland, Preliminary Report, Journal of Glaciology, vol. 3, p. 217.

- Lee, C. H. (1941) Total evaporation for Sierra Nevada watersheds by the method of precipitation and runoff differences, Part I, Trans. A.G.U., p. 50-71.
- Loewe, F. (1936) Höhenverhältnisse und Massenhaushalt des Grönlandischen Inlandeises (Height relations and mass content of the Greenland inland ice), Gerlands Beiträge zur Geophysik, Band 46, Ht. 3, p. 317-330.
- Matthes, F. E. (1942) "Glaciers," in Hydrology Physics of the Earth IX. New York: McGraw-Hill Book Company, Ch. V.
- _____ (1946) The glacial anticyclone theory examined in the light of recent meteorological data from Greenland, Part I, Trans. A.G.U., vol. 27, p. 324-341.
- Matthes, F. E. and Belmont, A. D. (1950) The glacial anticyclone theory examined in the light of recent meteorological data from Greenland, Part II, Trans. A.G.U., vol. 31, p. 174-182.
- Meyer, C. B. (1941) Discussion of paper by Lee, Part I, Trans. A.G.U., p. 67-71.
- Moore, R. C. (1949) Meaning of facies, Geological Society of America, Memoir 39, p. 1-34.
- Muskat, M. (1937) The flow of homogeneous fluids through porous media. New York: McGraw-Hill Book Company, 763p.
- Nakaya, V. and Matsumoto, A. (1953) Evidence of the existence of a liquidlike film on ice surfaces, USA SIPRE Research Paper No. 4.
- Nyberg, Alf (1938) Temperature measurements in an air layer very close to a snow surface, Geografiska Annaler, vol. 20, p. 234-275.
- Perutz, M. F. and Seligman, G. (1939) A crystallographic investigation of glacier structure and the mechanism of glacier flow, Proc. Roy. Soc. London, Series A, no. 950, vol. 172, p. 335-360.
- Schaefer, V. J.; Klein, G. J. and DeQuervain, M. (1951) Entwurf einer internationalen Schneeklassifikation (Draft of an international snow classification), Union geodesique et geophysique internationale, Assemblée Generale de Bruxelles.
- Schuster, Robert L. (1954) Project Mint Julep, Part III - Snow studies, USA SIPRE Report 19, 7p.
- Schytt, Valter, (1954) Report on glaciological investigations during the Norwegian-British-Swedish Antarctic Expedition, 1949-1952, Publication no. 39 de l'Association Internationale d'Hydrologie (Assemblée generale de Rome, Rome IV), Extrait.
- _____ (1955) Glaciological investigations in the Thule Ramp Area, USA SIPRE Report 28, 88p.
- Seligman, Gerald (1936) Snow structure and ski fields. London: MacMillan & Company, 555p.
- Sharp, Robert P. (1951) Features of the firn on Upper Seward Glacier, St. Elias Mountains, Canada, Journal of Geology, vol. 59, p. 599-621.
- Sorge, Ernst (1933) The scientific results of the Wegener expeditions to Greenland, Geographical Journal, vol. 81, p. 333-344.
- _____ (1935) "Glaziologische Untersuchungen in Eismitte (Glaciological investigations in Eismitte)," in Wissenschaftliche Ergebnisse der Deutschen Grönland Expedition Alfred Wegener 1929 and 1930-1931. Leipzig: F. A. Brockhaus, Band III.
- Thiel, G. A. (1935) Sedimentary and petrographic analysis of the St. Peter Sandstone, Bull. Geol. Soc. Amer., vol. 46, p. 559-614.

- Varney, Burton M. (1925) Seasonal precipitation in California and its variability, Monthly Weather Review, vol. 53, p. 148-163 and 208-218.
- Wade, F. Alton (1945) Physical aspects of the Ross Shelf Ice, Proc. Am. Phil. Soc., vol. 89, p. 160-173.
- Warniek, C. C. (1953) Experiments with windshields for precipitation gages, Trans. A.G.U., vol. 34, no. 3, p. 379-388.
- Wexler, H. (1936) Cooling in the lower atmosphere and the structure of polar continental air, Monthly Weather Review, vol. 64, p. 122-136.
- Weyl, W. A. (1951) Surface structure of water and some of its physical and chemical manifestations, Journ. Colloid. Sci., vol. 6, no. 5, p. 389-405.
- Wilson, Walter T. (1954) Discussion of paper by Black, Trans. A.G.U., vol. 35, p. 206-207.

APPENDIX A: STRATIGRAPHY, METEOROLOGY AND GLACIOLOGY

This appendix presents certain terms and concepts from stratigraphy, meteorology, and glaciology used in this paper. However, it also indicates specific applications of these fields to studies of the Greenland ice sheet.

Stratigraphy

Formation

"The formation is the fundamental unit in the local classification of rocks. Like other categories of rock units, the formation is a genetic unit, defined by objective criteria observable in the local stratigraphic column. Formations should be established with boundaries that may be readily traced in the field and represented on geologic maps to best express the geologic development and structure of the area.

"In most cases, formations should be distinguished as much as possible on the basis of lithologic unity – dominantly shale or dominantly sandstone, for instance – or repeated interlamination of two or more lithologies, as shale and limestone. Occasionally, however, a formation may contain a great variety of rock types, and such heterogeneity may itself distinguish the unit from more homogeneous units above and below.

"A formation is a genetic unit and represents a response to an environment, or a series of related environments, and such environments must be limited geographically as well as temporally. Therefore, there are limits to the geographic extent of formations, and the same name should be applied only over the area in which the lithology maintains a degree of unity.

"Formation names are binomial, usually consisting of a geographic name followed by a descriptive lithologic term (St. Louis limestone), the latter being uncapitalized" (Krumbein and Sloss, 1951, p. 27).

In view of the above statements the Greenland ice sheet (also the Antarctic ice sheet, the Vatnajökull ice cap, and most other glaciers) is unique as a formation in several respects. Its boundaries are unmistakably traced in the field. Lithologically, it is monomineralic; perhaps its closest competitor for purity is the St. Peter sandstone, which in size is only a fraction of the ice sheet. From the genetic standpoint it most certainly represents a response to an environment.

Diagenesis. The term "diagenesis" is used here in reference to the processes involved in transforming snow (the loose sediment) into firn (the sedimentary rock). The diagenetic environment is defined as follows:

"The diagenetic environment is the environment of post-depositional change. It extends an indefinite distance downward from the depositional interface. The nature of the diagenetic environment and the rapidity of the post-depositional changes depend upon the medium of deposition and the kind of sediment being deposited" (Krumbein and Sloss, 1951, p. 213).

On the ice sheet the depositional interface is the snow surface and the diagenetic environment extends downward from it for an unspecified distance, but includes most of the sedimentary member.

Facies

" 'Sedimentary facies' is defined as any areally restricted part of a definite stratigraphic unit which exhibits characters significantly different from those of other parts of the unit" (Moore, 1949, p. 32).

Facies in the Greenland ice sheet are based on differences in extent of melt action, and are produced by diagenetic processes.

Meteorology

Adiabatic processes. If a parcel of air is raised or lowered in the free atmosphere, it will expand or be compressed. No significant error is introduced by considering this process to be purely adiabatic. If the air is dry (not saturated with water vapor) its rate of temperature change will be approximately 1C/100 m (0.98C/100 m), regardless of whether the movement is upward or downward. This is called the 'adiabatic rate' or 'dry-adiabatic rate.' If the element of air is saturated with water vapor its cooling rate on ascent will be less than adiabatic because heat is added to the air by condensation of water vapor. It may be half of the dry-adiabatic rate of cooling. Descent of the air mass, on the other hand, will always produce the dry-adiabatic rate of warming regardless of the original moisture content.

Lapse rate. The term "lapse rate" is applied to the observed variation in air temperature with elevation. It pertains to vertical temperature gradients in the free atmosphere only. It is not generally applicable to air temperature measurements made at different elevations along the surface of the earth, because horizontal variations in air masses may be encountered. The normal lapse rate is about -0.65C/100 m, the negative sign indicating that temperature decreases with increasing elevation. If the lapse rate happens to coincide with the adiabatic rate of temperature change for dry air, the air is said to have a "dry adiabatic lapse rate." In continental Arctic regions and especially over snow surfaces, strong "inversions" (i.e., temperature increasing with height) are common (Wexler, 1936). Lapse rates less than adiabatic and especially those occurring in inversions are called "stable lapse rates." They result in the most stable stratification of air, vertical motions being strongly inhibited.

Inversions. At night, when short-wave solar radiation is absent, the snow surface radiates like a black body for all wave lengths. The atmosphere radiates with black body intensity only in certain bands of the spectrum, which are mainly due to water vapor. Also, the air loses energy both upward and downward but the snow surface radiates upward only. As a result of these conditions the snow surface will be in equilibrium with the air above when its temperature is lower than that of the air. This is the basic cause of inversions.

In the high latitudes of Greenland the process is effective even in summer because the sun never rises high above the horizon and much of its short wave energy is reflected by the snow surface. (Even though snow acts like a black body for terrestrial long wave radiation, it has a high albedo for solar radiation.) Polar maritime air shows normal lapse rates; however, Wexler (1936) has shown how it is transformed into polar continental air as it moves over a snow-covered continent. Therefore, an inversion will develop over the ice sheet regardless of the source of the air mass.

Glaciology

Firn line. The firn line is defined as "the highest level to which the fresh snow cover on a glacier's surface retreats during the melting season" (Matthes, 1942, p. 161).

Glacier classification. The classification of glaciers proposed by Ahlmann (1948) has been well received. It is a three-fold classification: a) morphological, b) dynamic, and c) geophysical. Of these, the "morphological classification" is the most quantitative. Greenland may be discussed according to these classifications as follows:

Morphological: In Ahlmann's morphological classification the Greenland and Antarctic ice sheets are included under the heading:

- "A. Glaciers extending in continuous sheets, the ice moving outwards in all directions:
 - (1) Continental glacier or inland ice, covering a very large area" (Ahlmann, 1948, p. 61).

Recently Bauer (1955) constructed the normal-area distribution curve, according to Ahlmann's convention, for the Greenland ice sheet. He found that it fits very well in the Ahlmann classification, and adds that this is the first classification which successfully includes the Greenland ice sheet.

Dynamic: An attempt to discuss Greenland's ice sheet according to an overall dynamic classification would be complex. The span of latitude is nearly 23°, 75% of which is above the Arctic Circle. This results in wide variation between local regimens and the rate of flow varies from fast in the south to slow in the north.

Geophysical: Ahlmann's geophysical classification divides glaciers into two broad groups, temperate and polar; the latter is further subdivided into high-polar and sub-polar. The most recent statement of this classification follows:

"I. Temperate glaciers consist of crystalline ice formed by fairly rapid recrystallization of the annual surplus of solid precipitation due to great quantities of fluid water. Throughout these glaciers the temperatures correspond to the melting-point of the ice, except in winter time, when the top layer is frozen to a depth of not more than a couple of meters. The glaciers of Scandinavia and the Alps are included in this group.

"II. Polar glaciers consist, at least in their higher and upper parts, of hard crystalline firn formed by slow recrystallization of the annual surplus of accumulated solid precipitation. The temperature of the glacier is negative even in summer down to a certain depth. These polar glaciers can be subdivided into: (a) High-polar glaciers, which consist, at least in their accumulation areas, of crystalline firn with temperatures below freezing-point to a considerable depth. Even in summer the temperature in the accumulation area is so low that as a rule there is no melting accompanied by formation of water. (b) Sub-polar glaciers, which in their accumulation areas consist of crystalline firn down to a depth of some 10 to 20 m. In the summer the temperature allows surface melting accompanied by the formation of fluid water" (Ahlmann, 1948, p. 66).

Ahlmann considers that most of the Antarctic together with the interior portions of the Greenland ice sheet are high-polar types. He recognizes more diversity in Greenland than in the Antarctic.

"At lower levels, where both the winter and the summer temperatures are higher than at 'Eismitte', the Greenland inland ice is of sub-polar nature, and its outlet glaciers are temperate, at least in the lower latitudes" (Ahlmann, 1948, p. 67).

If truly temperate outlet glaciers exist in Greenland they are most likely limited to the extreme south.

Snow and ice as rock units. The concept of snow and ice as rock units certainly is not new (Grout, 1932; Seligman, 1936; Bader et al., 1939; Flint, 1947). Grout mentions ice as one of the few examples of monomineralic deposits which attain the necessary dimensions to be properly classed as rocks. According to rock-type the following classification may be used.

1. Snow--sediment
 2. Firn--sedimentary rock
 3. Glacier ice--sedimentary and/or metamorphic rock
 4. Lake ice--crystallization from melt
 5. Sea ice--crystallization from solution
- } "igneous" rocks

The difference between firn (also called névé) and glacier ice is best expressed in terms of permeability. Firn has intercommunicating pore spaces, while glacier ice is impermeable, i. e., the pore spaces are sealed from each other. The transformation from firn to glacier ice occurs at density values of 0.82 to 0.84 g/cm³. (Perutz and Seligman, 1939; Schytt, 1954).

Temperate glaciers have received considerable treatment in the sense of being bona fide metamorphic rocks. However, firn as a stratified sedimentary rock has received little formal treatment. Ahlmann (1935, 1936, 1940, 1949) emphasized the importance of such studies and pioneered in the field.

APPENDIX B: MEAN ANNUAL TEMPERATURE.

Observed temperature data are corrected to mean annual values in this appendix by use of eq 3. These computations do not take convection into account. However, the effects of convection were minimized by excluding all measurements made in the upper 3 m of snow.

At some stations a range of temperature values is listed for a given depth and date. The actual temperature should lie within the indicated range.

In some cases, two values of the temperature correction are listed. This is done mostly where temperature data were obtained during August when differences between computed temperature corrections are greatest (Fig. 36).

The error in mean annual temperature values is between ± 0.5 and ± 1.0 .

Depth (cm)	Date	Observed temp	Correction	Mean annual temp	Avg
Station 1-0					
300	18-8-52	-14.5	-3.75	-18.2	-18.2
300	18-7-53	-16.0	-2.0	-18	
300	3-6-54	-20.5	+2.25	-18.2	
400	22-7-53	-17.0	0	-17	-17.6
400	4-6-54	-20.5	+2.35	-18.2	
500	22-7-53	-18.0	+0.8	-17.2	-17.6
500	4-6-54	-20.0	+1.9	-18.1	
600	22-7-53	-18.3	+1.0	-17.3	-17.7
600	4-6-54	-19.5	+1.3	-18.2	
700	7-6-54	-18.5	+0.8	-17.3	-17.3
800	7-6-54	-18.0	+0.35	-17.6	
900	7-6-54	-17.5	+0.15	-17.3	
1000	7-6-54	-17.0	+0.03	-17.0	
1100	7-6-54	-16.5	-0.06	-16.6	
1200	7-6-54	-16.5	-0.08	-16.6	-16.6
Station 1-10					
300	15-6-54	-21.0	+1.3	-19.7	
Station 1-20					
300	16-6-54	-21.5	+1.2	-20.3	
Station 1-30					
300	17-6-54	-22.0	+1.1	-20.9	
Station 1-40					
300	18-6-54	-22.5	+1.0	-21.5	
Station 1-50					
300	19-6-54	-23.0	+0.85	-22.2	
(300)	19-5-55	-27.0	+3.0	-24.0*	
	19-5-55	(-26)	+3.0	(-23.0)	
Station 1a-10					
300	19-5-55	-27.0	+3.0	-24.0	

Depth (cm)	Date	Observed temp	Correction	Mean annual temp	Avg
Station 1a-20					
300	20-5-55	-25.5	+3.0	-22.5	
Station 2-0					
300	21-8-52	-18.0	-3.9	-21.9	-22.5
300	27-7-53	-20.0	-2.5	-22.5	
300	20-6-54	-24.0	+0.75	-23.2	
400	27-7-53	-22.0	0	-22.0	-22.6
400	20-6-54	-25.0	+1.75	-23.2	
500	27-7-53	-23.0	+0.6	-22.4	-22.8
500	20-6-54	-25.0	+1.7	-23.3	
600	27-7-53	-24.0	+0.95	-23.0	-23.3
600	20-6-54	-25.0	+1.35	-23.6	
1132	24-6-54	-22.6	-0.2	-22.8	-22.8
1675	24-6-54	-23.0	-0.3	-23.0	
Station 2-10					
300	25-6-54	-24.0	+0.25	-23.8	-23.6
400	25-6-54	-25.0	+1.50	-23.5	
650	25-6-54	-23.0	+1.1	-21.9†	
Station 2-20					
300	26-6-54	-24.0	+0.2	-23.8	-23.9
400	26-6-54	-25.5	+1.4	-24.1	
500	26-6-54	-25.5	+1.55	-24.0	
900	26-6-54	-24.0	+0.25	-23.8	
Station 2-30					
300	28-6-54	-24.5	-0.05	-24.6	-24.2
400	28-6-54	-25.5	+1.35	-24.2	
500	28-6-54	-26.0	+1.50	-24.5	
600	28-6-54	-25.75	+1.30	-24.4	
1100	1-7-54	-23.75	+0.02	-23.8	
1500	1-7-54	-23.5	-0.03	-23.5	
Station 2-40					
300	4-7-54	-24.5	-0.70	-23.8	-23.7
400	4-7-54	-25.0	+1.0	-24.0	
800	5-7-54	-24.0	+0.55	-23.4	
Station 2-50					
300	6-8-53	-20.5	-3.1	-23.6	-24.1
300	21-8-53	-19.5	-3.9	-24.4	
300	18-9-53	-19.0	-4.7	-23.7	
300	9-7-54	-23.5	-1.15	-24.6	
(300)	24-5-55	-27.5	+2.75	(-24.8)*	
400	6-8-53	-22.5	-0.8	-23.3	
400	9-7-54	-25.0	+0.8	-24.2	-23.7
900	7-8-53	-23.2	+0.45	-22.8	
1000	10-7-54	-23	+0.2	-22.8	-22.8

APPENDIX B: (cont'd)

B3

Depth (cm)	Date	Observed temp	Correction	Mean annual temp	Avg
Station 2-60					
300	11-7-54	-23.5	-1.3	-24.8	-24.0
400	11-7-54	-25.0	+0.5	-24.5	
500	11-7-54	-25.0	+1.2	-23.8	
800	12-7-54	-24.0	+1.1	-23.9	
1000	12-7-54	-23.25	+0.2	-23.05	
Station 2-70					
300	24-8-52	-19	-4.0	-23	-23.6
300	24-8-52	-18.5	-4.0	-22.5	
300	16-7-54	-23.5	-1.8	-25.3	
400	16-7-54	-25.0	+0.4	-24.6	-24.4
500	16-7-54	-25.5	+1.0	-24.5	
600	16-7-54	-25.0	+1.0	-24.0	
800	16-7-54	-24.5	+0.6	-23.9	-23.5
1400	16-7-54	-23.25	-0.05	-23.3	
Station 2-80					
300	19-7-54	-23.0	-2.0	-25.0	-24
800	19-7-54	-23.75	+0.65	-23.1	
Station 2-90					
300	20-7-54	-22.5	-2.1	-24.6	-24.6
700	21-7-54	-25.5	+0.9	-24.6	
Station 2-100					
300	26-8-53	-19.2	-4.2	-23.4	-24
300	7-7-54	-24.0	-0.95	-24.9	
300	23-7-54	-21.5	-2.3	-23.8	
400	26-8-53	-21.2	-1.85	-23.0	-23.7
400	23-7-54	-24.2	-0.1	-24.3	
500	26-8-53	-22.5	-0.4	-22.9	-23
10 m	all year	-24.3 ±0.2			-24
35.45					-24.4
37.55		-24.4			
47.5					
Station A					
300	6-8-54	-21.75	-3.1	-24.8	-24.9
(400)	6-8-54	(-24.0)	-0.85	-24.8*	
Station B					
300	9-8-54	-21.5	-3.25	-24.8	-24.9
(400)	9-8-54	(-24.0)	-1.0	-25.0	
Station 2-120					
300	11-8-53	(-21.5)	-3.5	(-25.0)	-24.7
300	30-8-52	-20.0	-4.25	-24.2	
300	30-8-52	-20.5	-4.25	-24.8	
300	1-7-52	-25	-0.25	-25.2**	

APPENDIX B: (cont'd)

Depth (cm)	Date	Observed temp	Correction	Mean annual temp	Avg
Station 2-125					
300	30-5-55	-29	+2.4	-26.6	-26.6
(400)	30-5-55	-29	+2.4	-26.6*	
Station 2-150					
300	1-6-55	-29.75	+2.4	-27.4	-27.4
Station 2-175					
300	2-6-55	-30.75	+2.3	-28.4	-28.4
Station 2-200					
300	15-8-53	-25.0	-3.6	-28.6	(-28.7)
400	16-8-53	-27.0	-1.8	-28.8	
300	4-6-55	-32.0	+2.1	-29.9	-29.6
400	4-6-55	-31.5	+2.3	-29.2	
Station 2-225					
300	7-6-55	-32.0	+1.9	-30.1	-31.1
400	7-6-55	-32.0	+2.2	-29.8	
800	7-6-55	-31.0	+0.4	-30.6	
Station 4-0					
300	10-6-55	-32.5	+1.7	-30.8	-30.7
400	10-6-55	-33.0	+2.1	-30.9	
Station 4-25					
300	12-6-55	-32.5	+1.5	-31.0	-31.0
400	12-6-55	-33.0	+2.0	-31.0	
Station 4-50					
300	15-6-55	-31.75	+1.25	-30.5	-30.7
400	15-6-55	-32.5	+2.00	-30.5	
800	16-6-55	-31.5	+0.5	-31.0	
Station 4-75					
300	17-6-55	-32.0	+1.05	-31.0	-31
400	17-6-55	-32.5	+1.90	-30.6	
800	18-6-55	-31.75	+0.5	-31.2	
Station 4-100					
300	19-6-55	-31.25	+0.85	-30.4	-30.6
400	19-6-55	-32.0	+1.80	-30.2	
800	20-6-55	-31.75	+0.5	-31.2	
Station 4-125					
300	21-6-55	-31.5	+0.65	-30.8	-30.9
400	21-6-55	-32.5	+1.7	-30.8	
800	22-6-55	-31.5	+0.5	-31.0	
Station 4-150					
300	23-6-55	-31.0	+0.45	-30.6	-30.6
400	23-6-55	-32.0	+1.6	-30.4	
800	24-6-55	-31.25	+0.55	-30.7	

APPENDIX B: (cont'd)

B5

Depth (cm)	Date	Observed temp	Correction	Mean annual temp	Avg
Station 4-175					
300	25-6-55	-30.25	+0.25	-30.0	} -30.2
400	25-6-55	-31.00	+1.50	-30.5	
800	26-6-55	-30.75	+0.55	-30.2	
Station 4-200					
300	27-6-55	-30.25	+0.1	-30.2	} -30.3
400	27-6-55	-31.5	+1.4	-30.1	
800	28-6-55	-31.2	+0.55	-30.6	
Station 4-225					
300	30-6-55	-29.5	-0.25	-29.8	} -29.8
400	30-6-55	-31.0	+1.25	-29.8	
Station 4-250					
300	2-7-55	-29.5	-0.5	-30.0	} -30.0
400	2-7-55	-30.5	+1.1	-29.4	
800	3-7-55	-31.0	+0.55	-30.4	
Station 4-275					
300	5-7-55	-28.5	-0.75	-29.2	} -29.4
400	5-7-55	-30.5	+1.0	-29.5	
800	7-7-55	-30.0	+0.58	-29.4	
Station 4-300					
300	8-7-55	-28.75	-1.0	-29.8	} -29.7
400	8-7-55	-30.5	+0.8	-29.7	
Station 4-325					
300	10-7-55	-28.5	-1.2	-29.7	} -29.5
400	10-7-55	-30.0	+0.7	-29.3	
800	11-7-55	-30.0	+0.6	-29.4*	
Station 4-350					
300	12-7-55	-28.5	-1.5	-30.0	} -29.5
400	12-7-55	-30.0	+0.6	-29.4	
700	13-7-55	-30.0	+0.9	-29.1	
Station 4-375					
300	14-7-55	-27.75	-1.65	-29.4	} -29.0
400	14-7-55	-29.75	+0.5	-29.2	
(500)	14-7-55	-30.0	+1.1	-28.9*	
700	15-7-55	-29.5	+0.9	-28.6	
Station 4-400					
300	16-7-55	-28.0	-1.75	-29.8	} -29.2
400	16-7-55	-29.5	+0.4	-29.1	
700	17-7-55	-29.5	+0.9	-28.6	
Station 5-0					
300	18-7-55	-27.0	-1.95	-29.0	} -29.8
400	18-7-55	-29.0	+0.25	-28.8	
700	19-7-55	-29.75	+0.9	-28.8	

Depth (cm)	Date	Observed temp	Correction	Mean annual temp	Avg
Station 5-20					
300	20-7-55	-26.0	-2.1	-28	-27.7
400	20-7-55	-27.5	+0.1	-27.4	
Station 5-40					
300	23-7-55	-25.0	-2.25	-27.2	-27.2
400	23-7-55	-27.0	-0.1	-27.1	
1000	15-6-31	-28.4	+0.06	-28.3††	(27.8)
1000	Aug 1950	-27.35	+0.3	-27.0††	
		-27.20	+0.3		
		-27.50	+0.3		
2000	Aug 1950	-27.01	+0.01	-27	-27.8
10000	" "	-27.78		-27.8	
Station 5-65					
300	2-8-55	-23.5	-3.0	-26.5	-25.8
400	2-8-55	-25.0	-0.7	-25.7	
700	5-8-55	-26.0	+0.75	-25.2	
Station 5-90					
300	6-8-55	-22.0	3.1	-25.1	-24.35
300	6-8-55	-22.0	-3.3	-25.3	
400	6-8-55	-23.5	-1.0	-24.5	
700	7-8-55	-24.0	+0.75	-23.2	
Station 5-115					
300	8-8-55	-21.0	3.4	-24.4	-24.3
300			3.2	-24.2	
Station 5-140					
300	10-8-55	-19.5	-3.1	-21.6	-21.6
300	10-8-55	-19.5	-3.6	-22.1	
(700)	10-8-55	-22.0	+0.7	-21.3*	
Station 5-150					
300	12-8-55	-18.5	-3.7	-22.2	-21.8
"	"	"	-3.0	-21.5	
Station 5-160					
300	13-8-55	-18.0	-3.75	-21.75	-21.5
"	"	"	-3.25	-21.25	
(400)	13-8-55	-19.0	-1.4	-20.4	-20.7* } -21.1
"	"	-19.0	-1.0	-20.0	
"	"	-20.0	-1.4	-21.4	
"	"	-20.0	-1.0	-21.0	

APPENDIX B: (cont'd)

B7

Depth (cm)	Date	Observed temp	Correction	Mean annual temp	Avg
Station 5-170					
300	14-8-55	-18.0	-3.8	-21.8	-21.5
"	"	"	-3.3	-21.3	
(400)	14-8-55	-20.0	-1.95	-22.0	-21.2*
"	"	-20.0	-1.1	-21.1	
"	"	-19.5	-1.95	-21.4	
"	"	-19.5	-1.1	-20.6	
Station 5-180					
300	15-8-55	-17.0	-3.9	-20.9	-20.6
"	"	-17.0	-3.3	-20.3	
(700)	15-8-55	-19.8	-1.5	-21.3	-21.1*
"	"	-19.8	-1.1	-20.9	
Station 5-190					
300	16-8-55	-16.5	-3.9	-20.4	-20.1
"	"	"	-3.3	-19.8	
(400)	16-8-55	-18.5	-1.5	-20.0	-19.8*
"	"	"	-1.1	-19.6	
Station 5-200					
300	17-8-55	-16.0	-4.0	-20.0	-19.7
"	"	"	-3.4	-19.4	
(400)	"	(-18)	-1.6	-19.6	-19.4*
"	"	"	-1.2	-19.2	
Station 5-210					
300	18-8-55	-15	-4.0	-19.0	-18.75
"	"	"	-3.5	-18.5	
(400)	"	(-17)	-1.65	-18.65	-18.5*
"	"	"	-1.3	-18.3	
Station 5-220					
300	19-8-55	-13.75	-4.1	-17.85	-17.55
"	"	"	-3.5	-17.25	
(400)	"	(-16)	-1.7	-17.7	-17.52*
"	"	"	-1.35	-17.35	
Station 5-230					
300	20-8-55	-11.5	-4.15	-15.65	-15.10
"	"	"	-3.55	-14.55	
French Camp VI***					
1000	July '50	-12.28			-12.4
1000	30-8-50	-11.7			
1500	July '50	-12.45			
1500	30-8-50	-12.95			

APPENDIX B: (cont'd)

Depth (cm)	Date	Observed temp	Correction	Mean annual temp	Avg
Station 0-35†††					
(300)	31-5-54	(-11.5)	+2.5	-9.0	} best value -10
"	"	(-12.0)	+2.5	-9.5	
"	"	(-12.5)	+2.5	-10.0	
"	"	(-13.0)	+2.5	-10.5	
(400)	31-5-54	(-11.5)	+2.5	-9.0	} best value -10
"	"	(-12.0)	+2.5	-9.5	
"	"	(-12.5)	+2.5	-10.0	
"	"	(-13.0)	+2.5	-10.5	
(200)	16-5-55	(-14.5)	+2.7	-11.8	} best value -12
(300)	"	(-15.0)	+3.25	-11.75	
(400)	"	(-14.5)	+2.7	-11.8	

* Temperature values enclosed in parentheses were extrapolated beyond the measured temperature profiles as follows:

Station 1-50, 19-5-55, 300 cm value extrapolated from 260 cm
 Station 2-50, 24-5-55, 300 cm value extrapolated from 220 cm
 1954 Survey area pit A, 6-8-54, 400 cm extrapolated from 360 cm
 1954 Survey area pit B, 9-8-54, 400 cm extrapolated from 380 cm
 Station 2-125, 30-5-55, 400 cm value extrapolated from 360 cm
 Station 4-325, 11-7-55, 800 cm value extrapolated from 755 cm
 Station 4-375, 14-7-55, 500 cm value extrapolated between the
 values of 420 and 720 cm
 Station 5-140, 10-8-55, 700 cm value extrapolated from 675 cm
 Station 5-160, 13-8-55, 400 cm value extrapolated from 345 cm
 Station 5-170, 14-8-55, 400 cm value extrapolated from 358 cm
 Station 5-180, 15-8-55, 700 cm value extrapolated from 670 cm
 Station 5-190, 16-8-55, 400 cm value extrapolated from 350 cm
 Station 5-200, 17-8-55, 400 cm value extrapolated from 370 cm
 Station 5-210, 18-8-55, 400 cm value extrapolated from 370 cm
 Station 5-220, 19-8-55, 400 cm value extrapolated from 355 cm

† This value is about 1.5C higher than it should be, according to the measurements from stations 2-0 and 2-20.

** Measured by Bader one mile from the 1954 survey area "pit B."

†† The climatic warm up as seen in coastal stations (Fig. 39) shows up as a 1C rise in mean annual temperature at Eismitte between 1930 and 1950. The 1930 data are from Sorge (1935) and the 1950 data are from Heuberger (1954).

*** Data from French Camp VI are from Heuberger (1954).

††† The temperature profiles at 0-35 in May of 1954 and 1955 do not quite reach 200 cm depth. But from 15 May to 30 May the temperature profiles are very nearly vertical, i. e., isothermal, between 200 and 400 cm, so that the profiles can be extrapolated below 180 cm. The resulting range of mean annual temperature is -10 to -12C.

APPENDIX C: THE DATA SHEETS.

The locations of the data sheets are indicated in Figure C1. Four other data sheets summarizing the 1952 and 1953 results have been published (Benson, 1959) and are not reproduced here. A table showing the location of each test station, its altitude, the date or dates of occupation, and a summary of the work done at the station is available. It is not of sufficient general interest to be reproduced here, but may be obtained from the writer upon request.

Format

Data from each station are plotted around a stratigraphic columnar section which summarizes the appearance of the pit wall with main emphasis on features caused by melt and/or wind action.

Grain size is indicated only where it is extremely coarse or fine, or where it undergoes several significant variations over a short depth interval. Symbols used are described in Figure C2. The symbol depicting grain size of a given layer represents the most abundant size range; typical ranges of grain size in single layers are seen in Figures 17 and 18. In most layers where grain size is not indicated, it lies in the range 1.0 ± 0.5 mm. Grain size is always indicated where it exceeds 2 mm.

The temperature profile (points connected by a line) and the ram hardness profile (bar graph) are plotted to the left of the stratigraphic column. The ram hardness profile is crosshatched where it exceeds 50 kg force; snow is very soft below this value.

The density profile is plotted to the right of the stratigraphic column. It begins at 0.25 g/cm^3 , and is crosshatched where it exceeds 0.40 g/cm^3 . The crosshatching is useful in correlation between stations, and in comparing gross variations in density between facies (see Data sheets 1 and 7 for example). The zero point on the density scale coincides with the -15C point on the temperature scale. The depth and density scales were selected in such a way that each square centimeter under the depth density curve represents 1 cm of water equivalent. This made it an easy matter to integrate the depth-density profiles to obtain depth-load curves. The data sheets reproduced here are reduced (each ruled square represents 1 cm water equivalent).

Stratigraphic correlation

Stratigraphic interpretations have been correlated between stations. The year labels mark the fall layers of each year, i. e., 20 August to 10 September (see p. 30-33, Fig. 22-25). Specifically dated levels are indicated where they are known on Data sheets 3 and 5. Correlation lines are dashed where interpretations were not unequivocal.

Several general comments are in order.

- 1) The 1954 summer was the warmest one encountered as evidenced by the melt record in the snow and firn and by the meteorological record from Thule (see Fig. 31). Percolation from the mid-July 1954 snow surface penetrated into the snow layers of 1953 and 1952 at elevations of nearly 2000 m in northwest Greenland (see Fig. 24, 25, and station 2-70 on Data sheet 5). However, the extreme nature of the July 1954 melt was restricted to north Greenland. It apparently accompanied the occlusion of a storm over the region of 2-0 (personal communication, G. R. Toney, U. S. Weather Bureau).
- 2) The summers of 1941 and 1950 produced the most widespread melt evidence in Greenland, being observed at nearly all points along the traverse of this study. These years, especially 1941, were the only significant producers of melt evidence in the dry-snow facies (see Data sheets 6, 7, and 8; also 5 and 9).
- 3) In northwest Greenland the 1941 summer produced melt evidence comparable to that of the 1954 summer. It caused percolation through the 1940 and 1939 snow layers (see Data sheet 5).
- 4) Greater than average melt also occurred in northwest Greenland during the summers of 1945 and 1949. Localized percolation through the 1948 snow layers, of the percolation facies, apparently occurred during both 1949 and 1950.
- 5) The heaviest accumulation recorded between 1937 and 1955 occurred during the year 1945-46. The lightest accumulation during the same 18-yr period was during the year 1951-52.

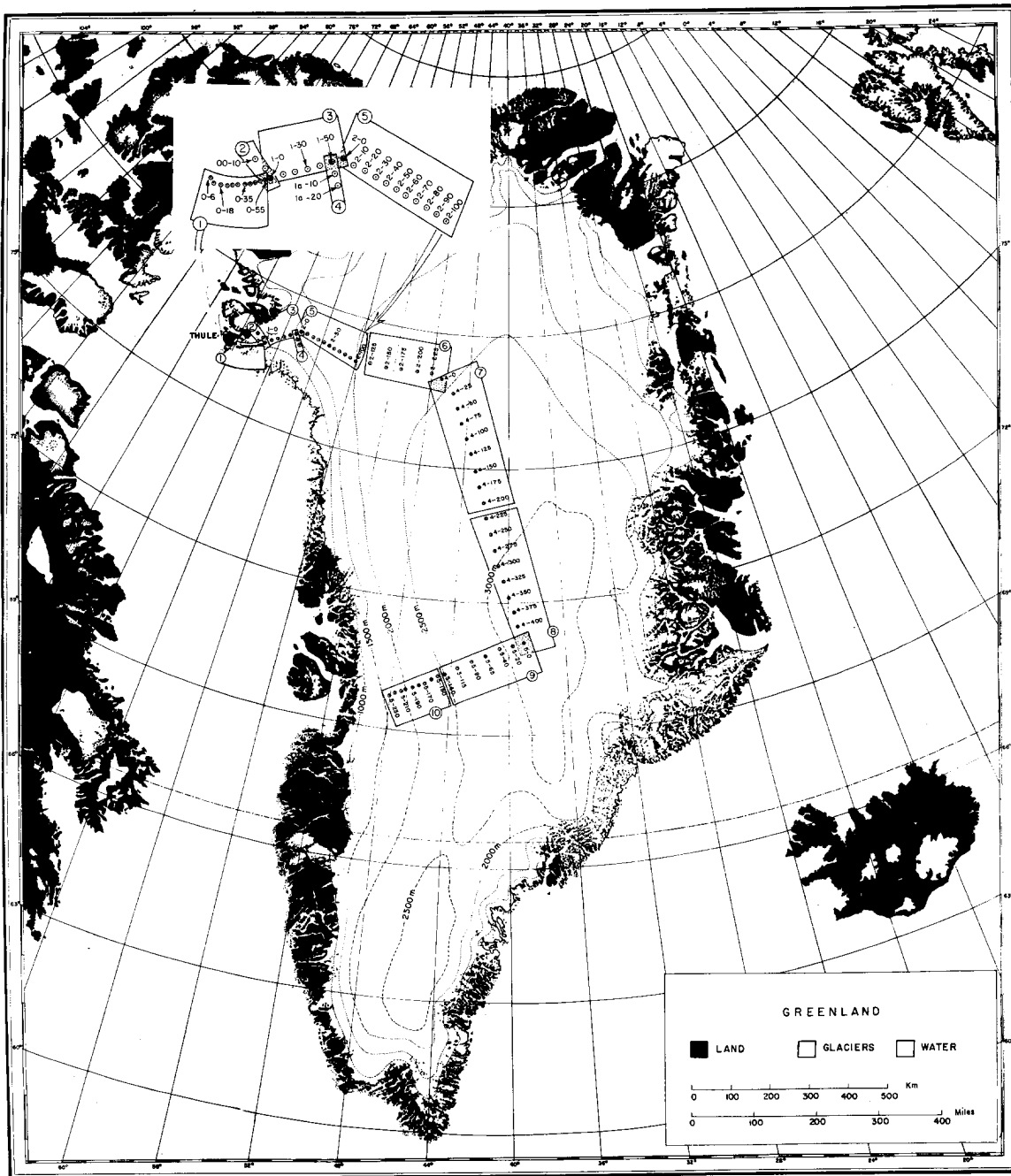
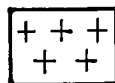
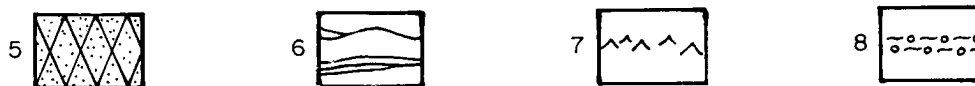


Figure C1. Location of data sheets. Data sheet 6a (not shown) contains the six stations made in 1953 between station 2-100 and 2-200 (see Fig. 2 facing p. 2).

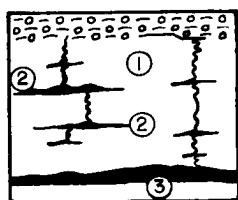
 New snow, original crystal forms still recognizable.



1. Fine- or very fine-grained snow, 1 mm.
2. Medium-grained snow, 1 to 2 mm.
3. Coarse-grained snow, 2 to 4 mm.
4. Very coarse-grained snow, 4 mm.



5. Wind slab, consisting of firmly bonded fine or very fine grains; from a little distance it has a dull, lusterless chalky appearance.*
6. Wind crusts, paper thin layers of firmly bonded very fine grains.† A thin line is also used to indicate discontinuities between adjacent layers.
7. Depth hoar, or coarse loosely bonded grains with vugs.
8. Melt crust or iced firn, consisting of coarse grains with small lenses and irregularly shaped chunks of ice scattered throughout.



Ice masses in snow, formed by downward percolation from surface melt

1. ice gland
2. ice lens
3. ice layer

Figure 2.

* Descriptive material on wind slabs is found in Seligman (1936, p. 159-205).

† The term wind crust is used here in a slightly different sense from that of Seligman (1936, p. 167).

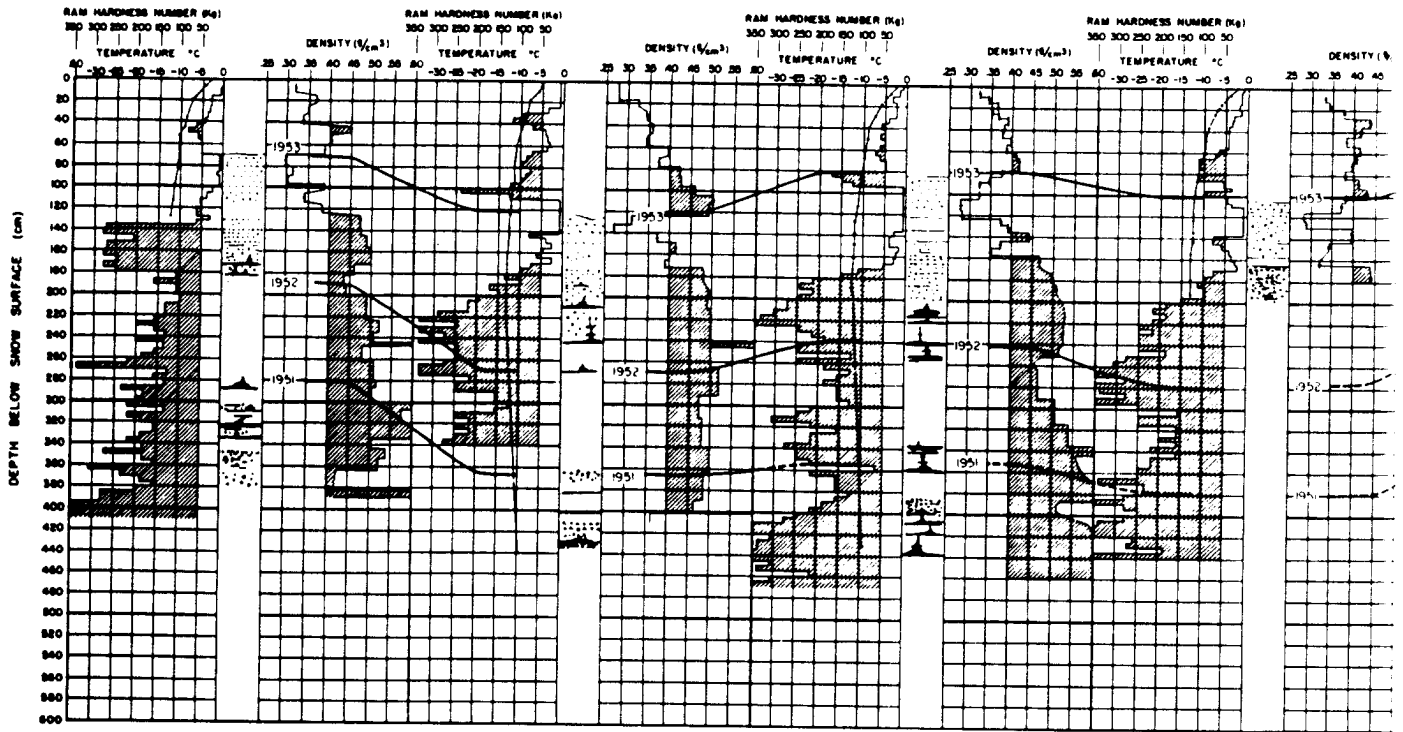
DATA SHEET I

STATION O-8
28 MAY 1954
ELEVATION 780 m (2560 ft)

STATION O-13
29 MAY 1954
ELEVATION 800 m (2625 ft)

STATION O-18
29 MAY 1954
ELEVATION 800 m (2625 ft)

STATION O-24
30 MAY 1954
ELEVATION 830 m (2725 ft)



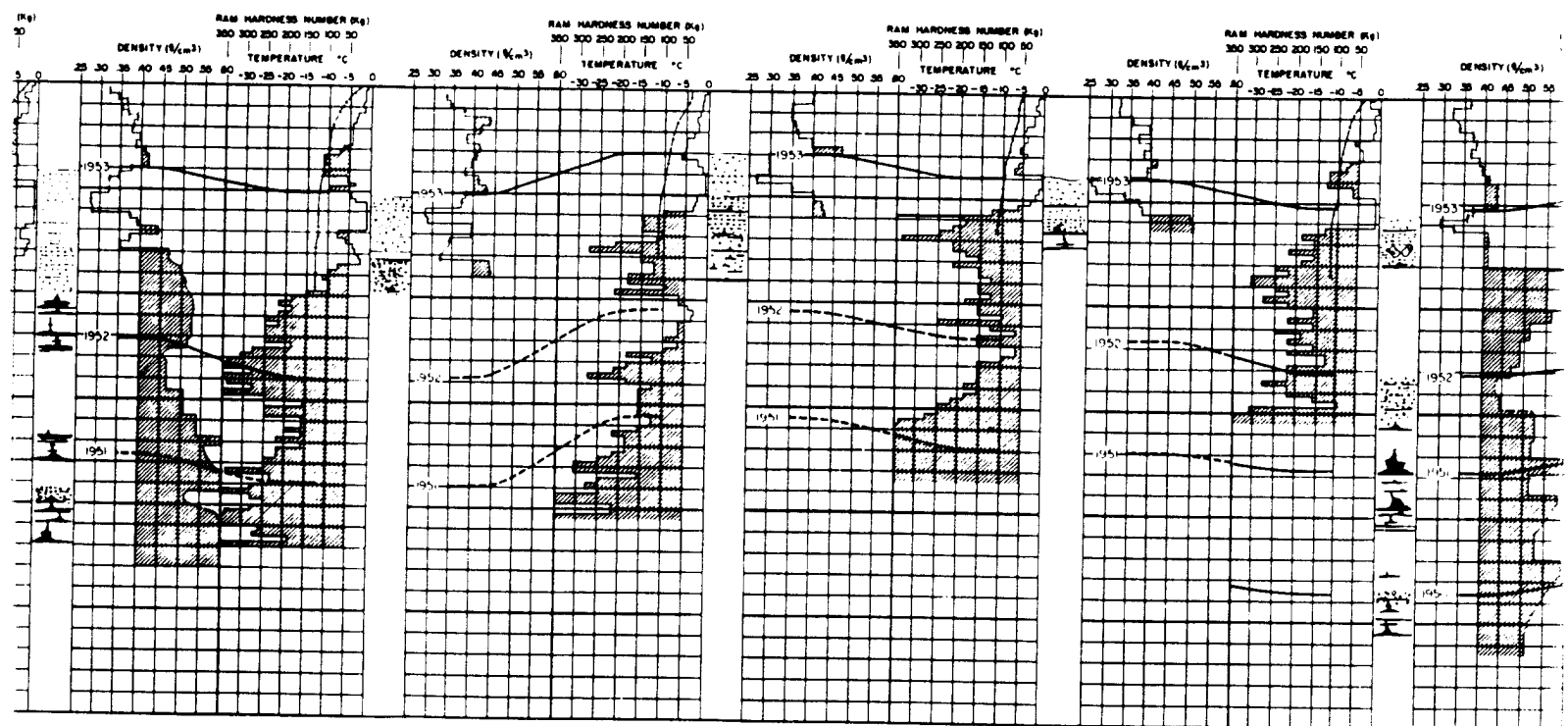
STATION O-18
29 MAY 1954
ELEVATION 900 m (2925 ft)

STATION O-24
30 MAY 1954
ELEVATION 830 m (2725 ft)

STATION O-27
30 MAY 1954
ELEVATION 785 m (2575 ft)

STATION O-31
31 MAY 1954
ELEVATION 700 m (2295 ft)

STATION O-36
31 MAY 1954
ELEVATION 674 m (2210 ft)

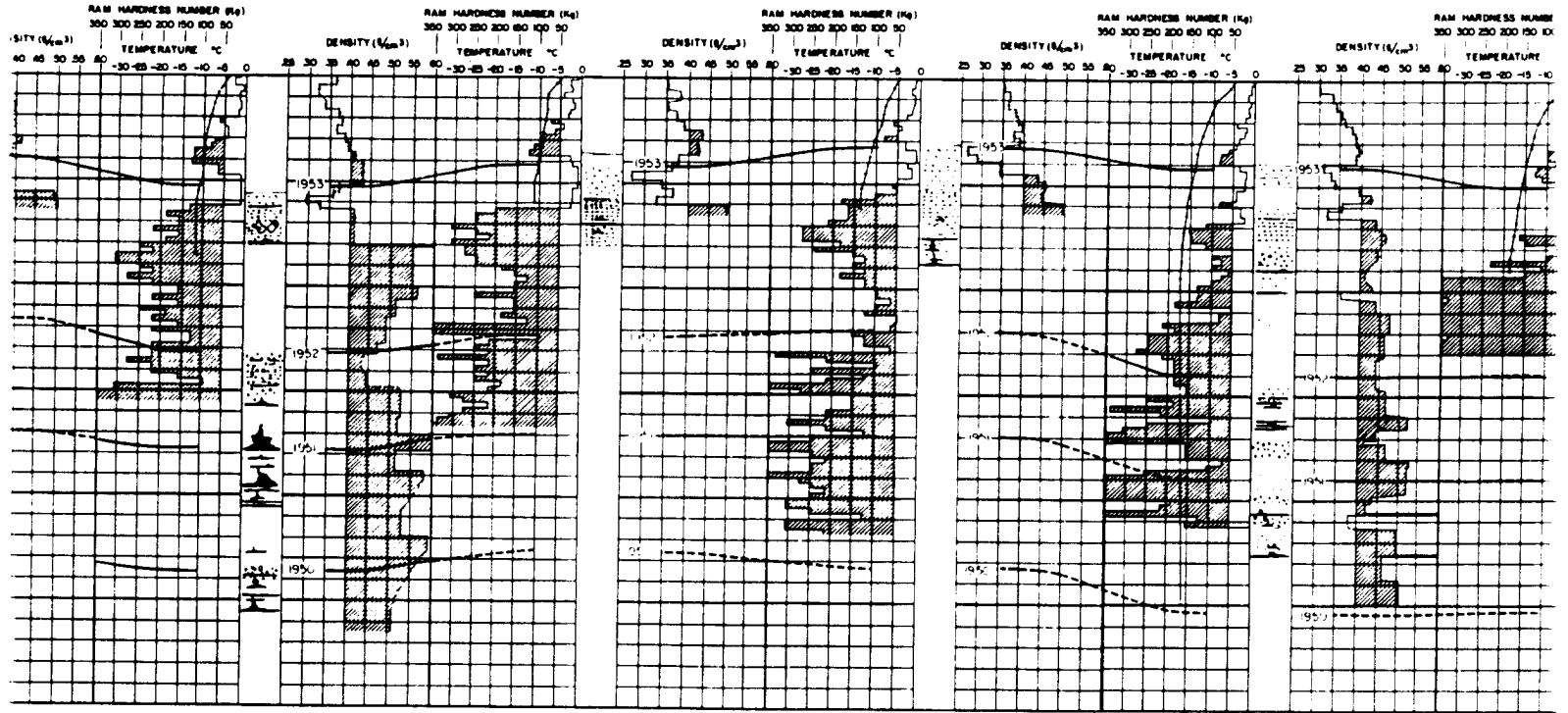


STATION O-38
31 MAY 1964
ELEVATION 874 m (2868 ft)

STATION O-40
1 JUNE 1954
ELEVATION 890 m (2920 ft)

STATION O-45
1 JUNE 1954
ELEVATION 1035 m (3461 ft)

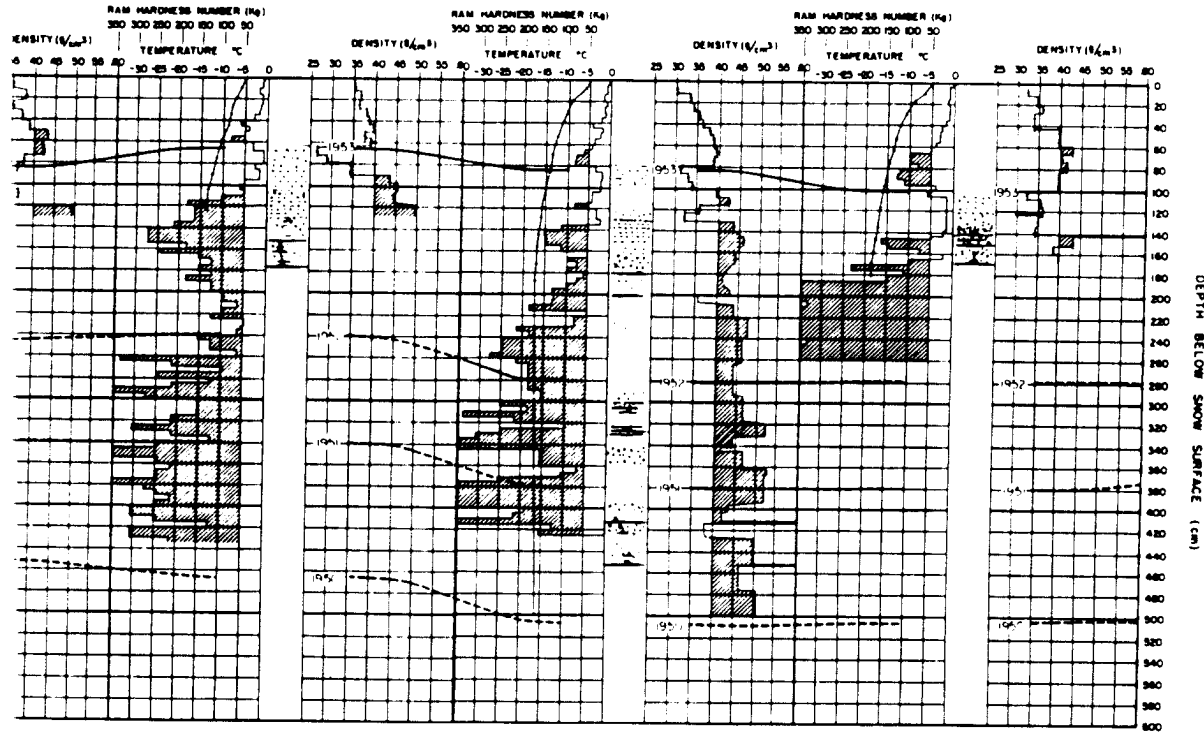
STATION O-50
1 JUNE 1954
ELEVATION 1212 m (3978 ft)



STATION O-45
1 JUNE 1954
ELEVATION 1055 m (3461 ft)

STATION O-50
1 JUNE 1954
ELEVATION 212 m (697 ft)

STATION O-55
2 JUNE 1954
ELEVATION 1254 m (4145 ft)

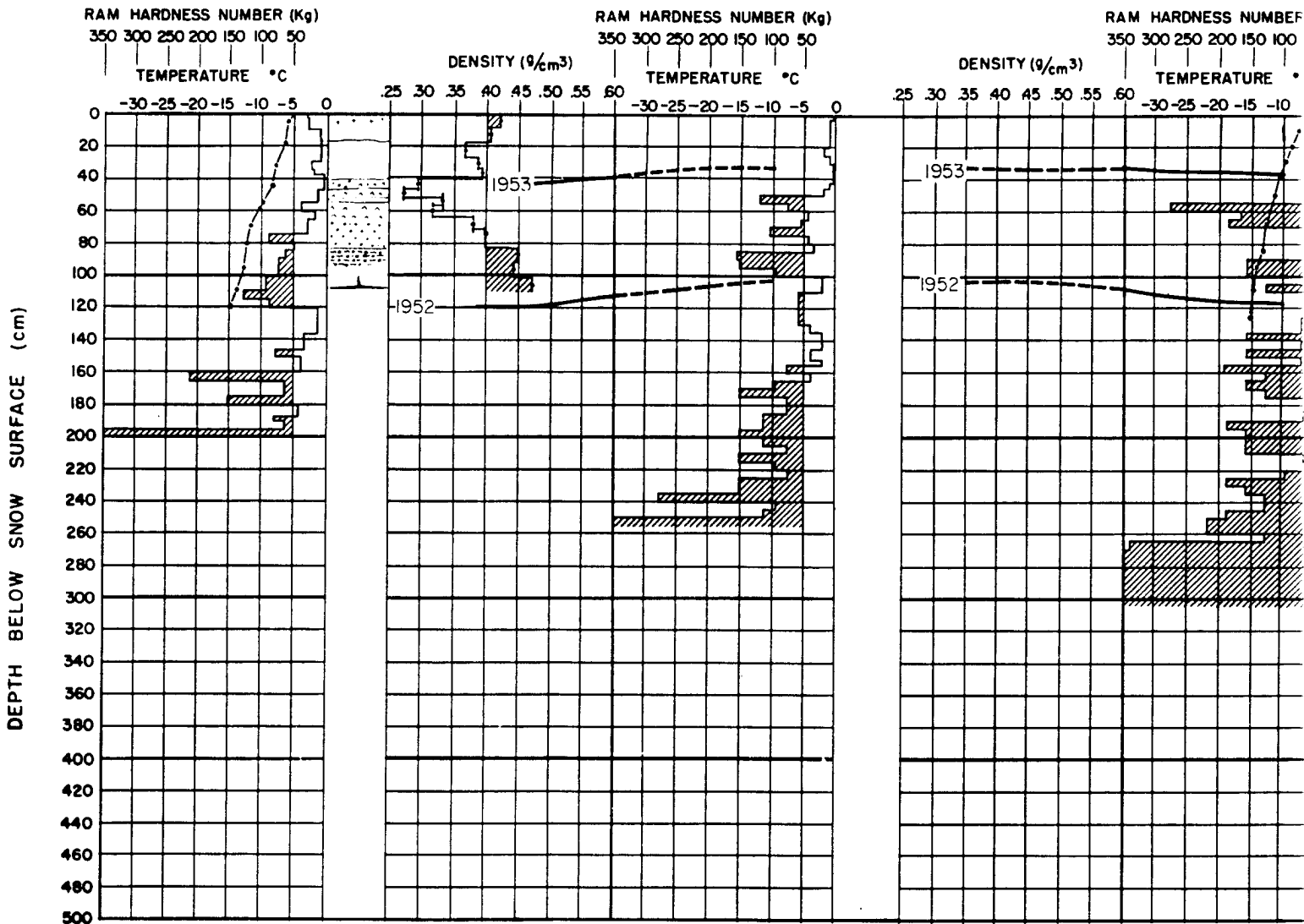


4

DATA SHEET 2

STATION 00-10
10 JUNE 1954
ELEVATION 1146 m (3760 ft)

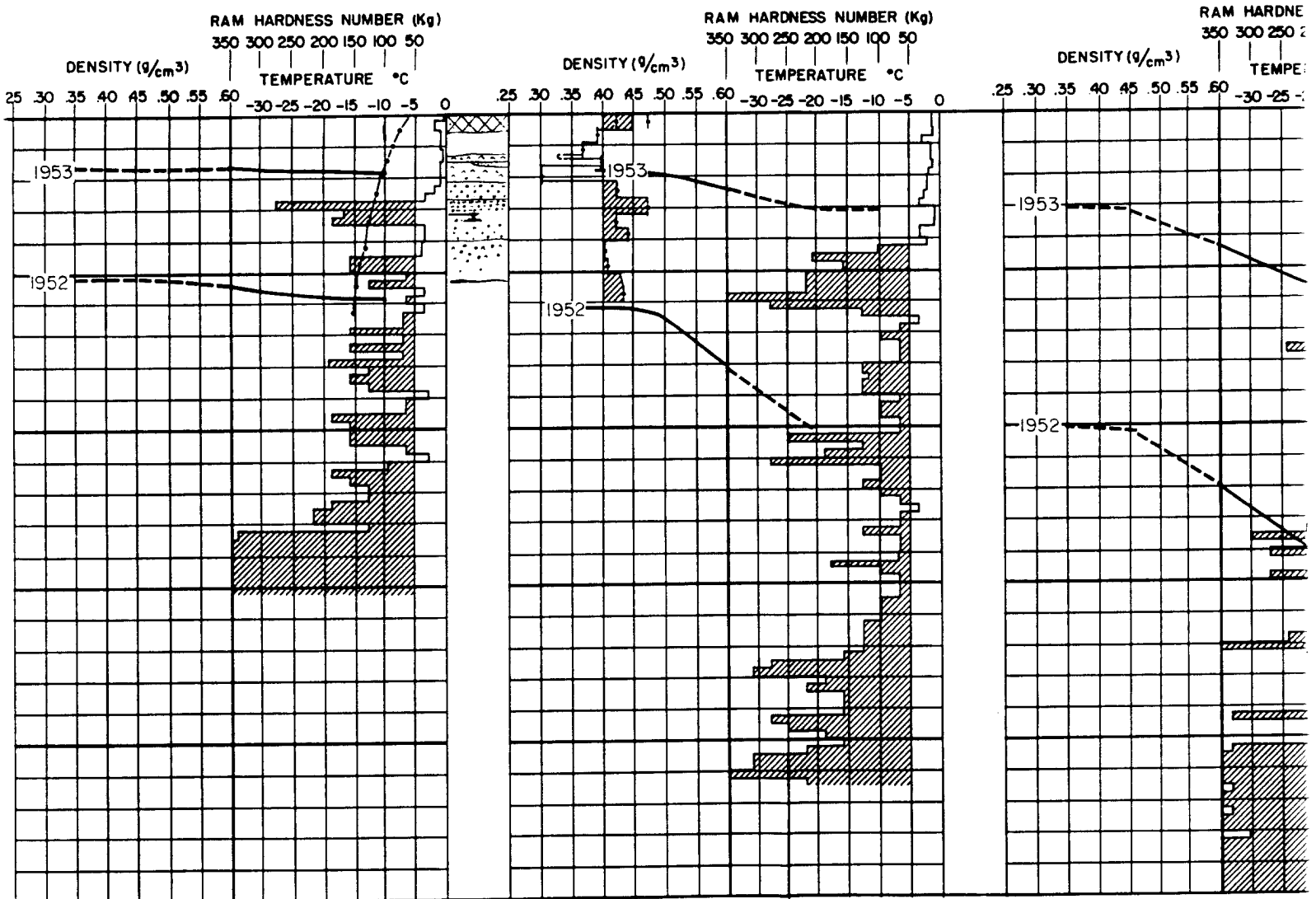
STATION 00-15
10 JUNE 1954
ELEVATION 1195 m (3920 ft)
(RAM ONLY)



-15
4
1195 m (3920 ft)

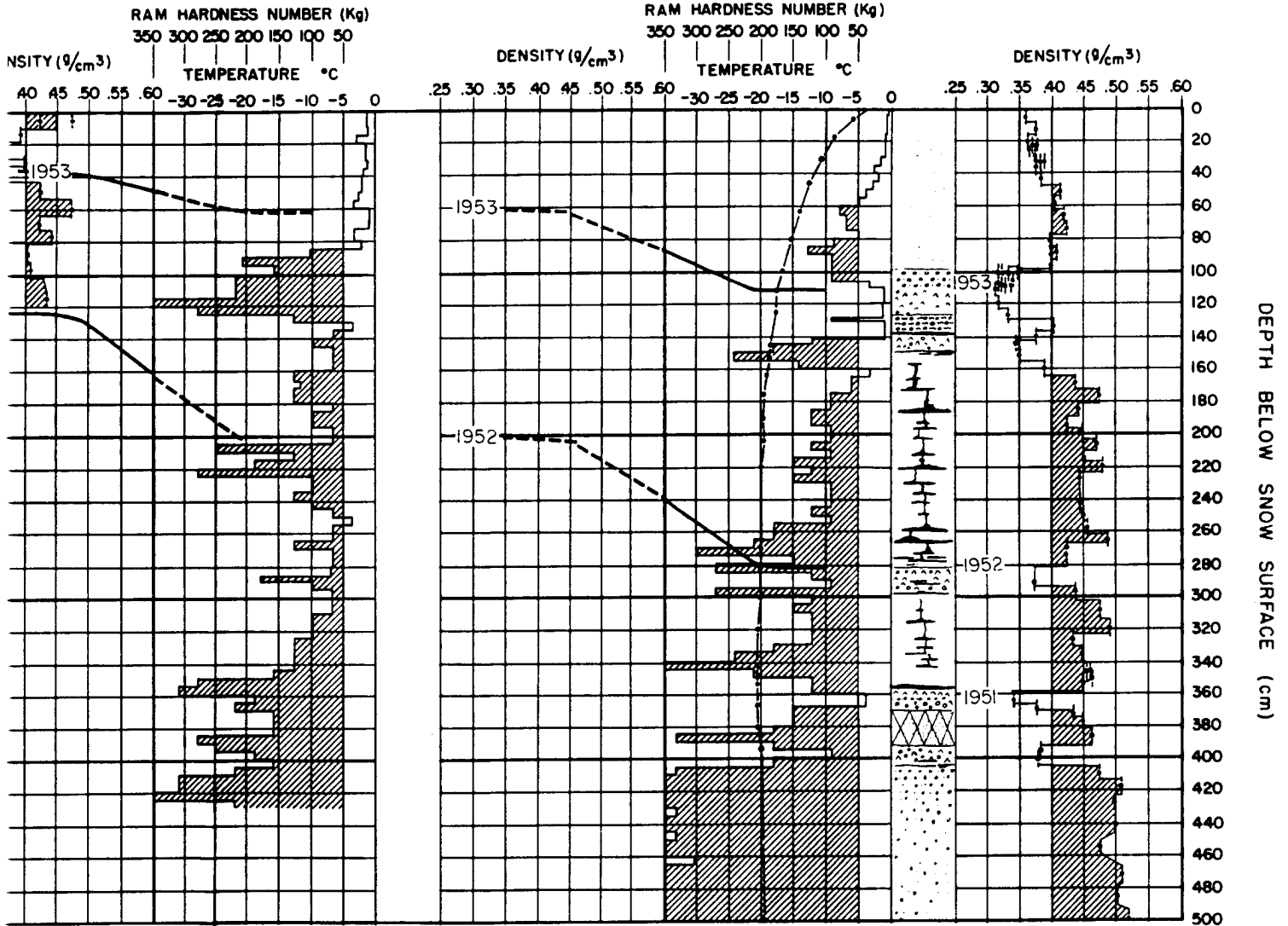
STATION 00-20
10 JUNE 1954
ELEVATION 1295 m (4250 ft)

STATION 00-25
10 JUNE 1954
ELEVATION 1300 m (4265 ft)
(RAM ONLY)



STATION 00-25
 10 JUNE 1954
 ELEVATION 1300 m (4265 ft)
 (RAM ONLY)

STATION 1-0
 3 JUNE 1954
 ELEVATION 1310 m (4300 ft)



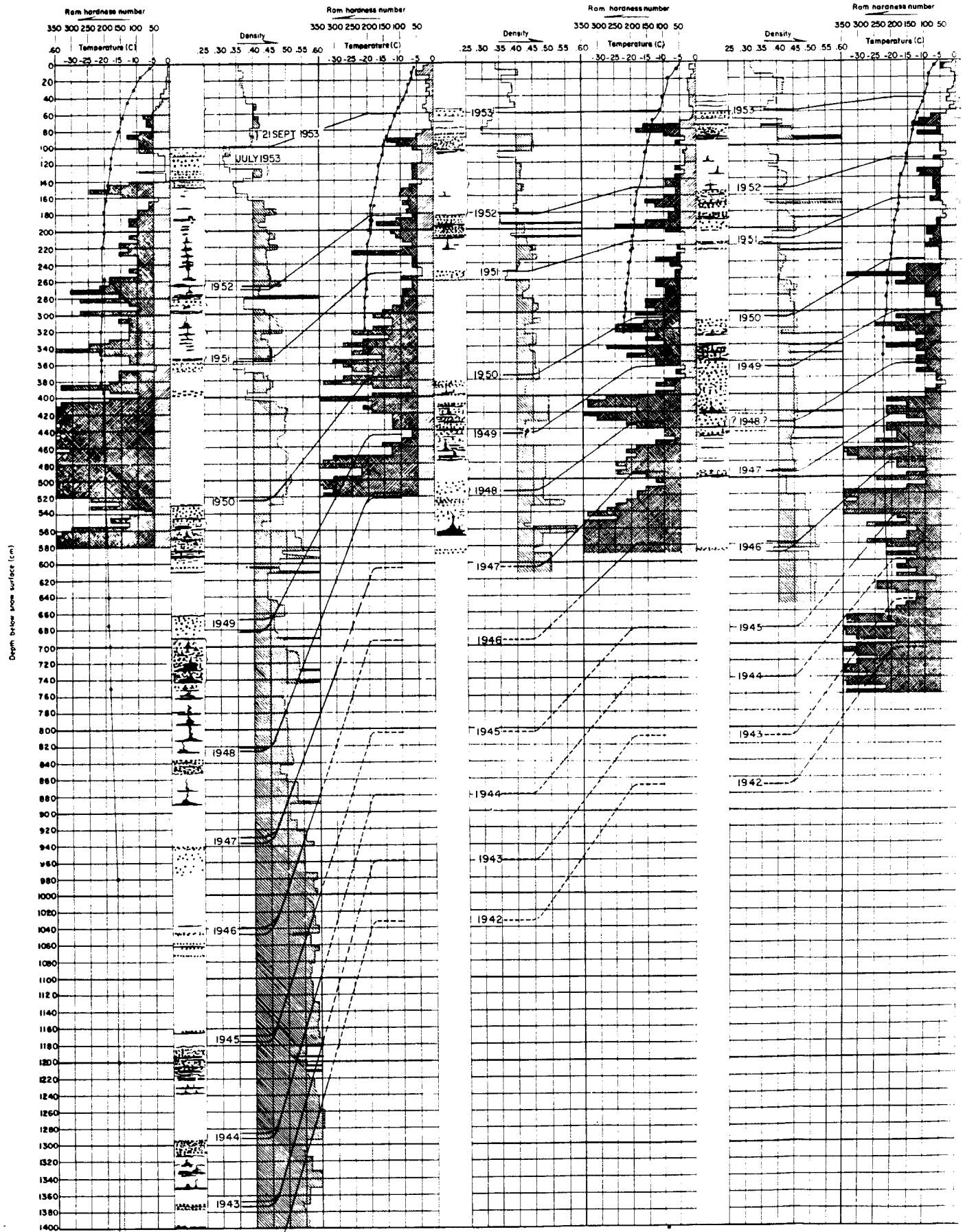
DATA SHEET

Station I-0
3 June 1954
Elev 1310 m (4300 ft)

Station I-10
15 June 1954
Elev 1418 m (4654 ft)

Station I-20
16 June 1954
Elev 1486 m (4875 ft)

Sta
17 J
Elev 15



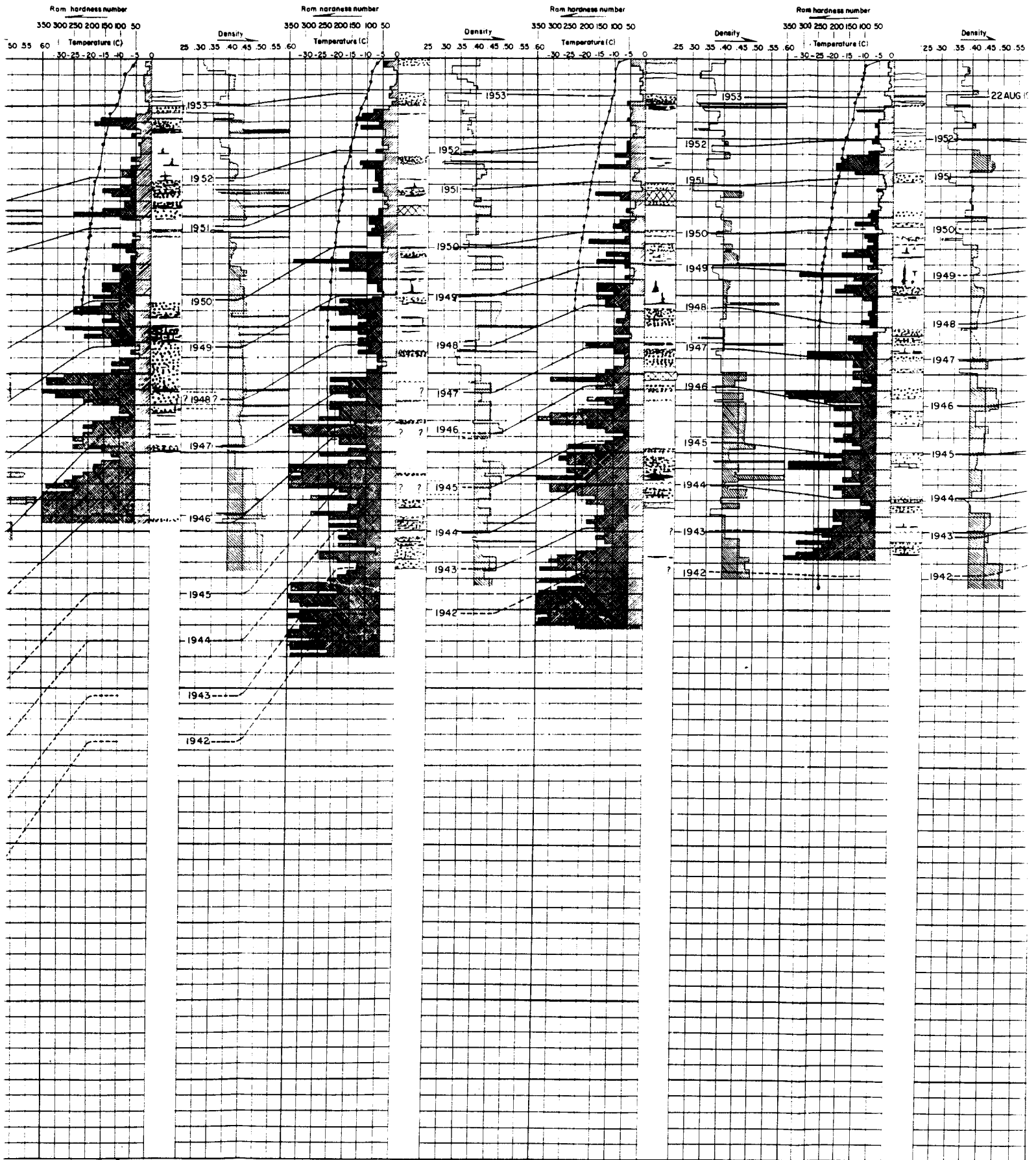
①

Station I-20
16 June 1954
Elev 1486m (4875 ft)

Station I-30
17 June 1954
Elev 1519m (4984 ft)

Station I-40
18 June 1954
Elev 1570m (5153 ft)

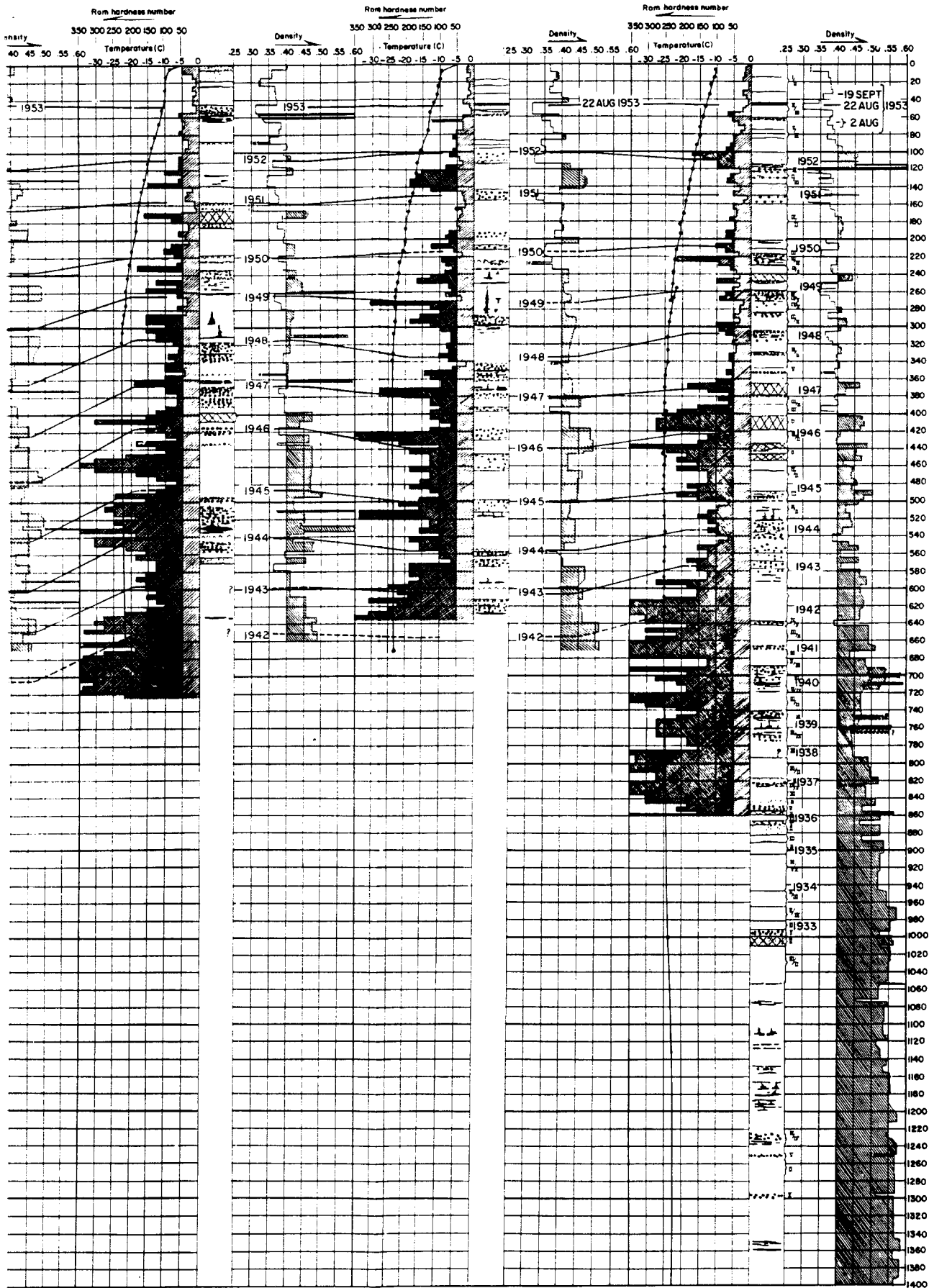
Station I-50
19 June 1954
Elev 1630m (5347 ft)



Station 1-40
18 June 1954
Elev 1570 m (5153 ft)

Station 1-50
19 June 1954
Elev 1630 m (5347 ft)

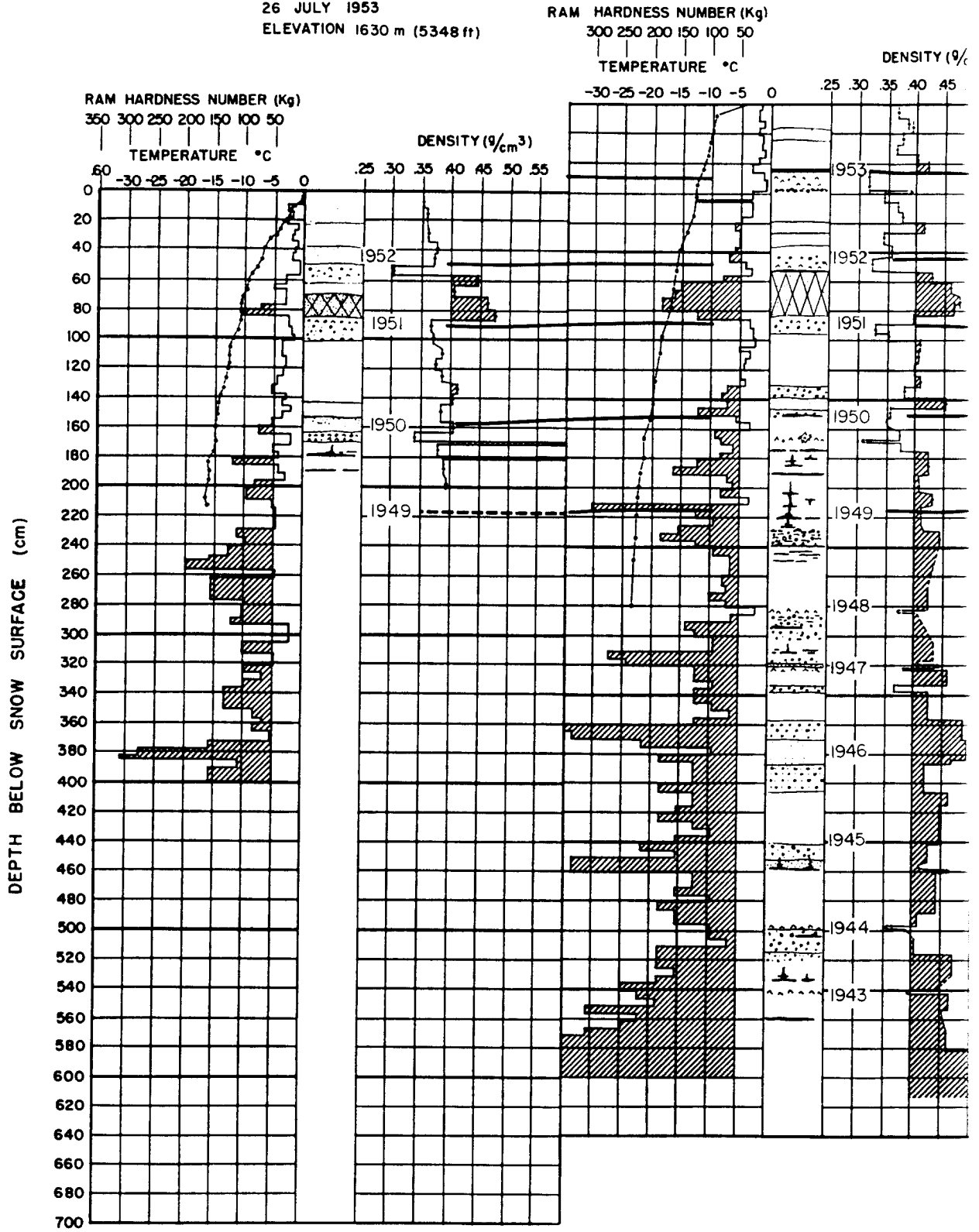
Station 2-0
21 June 1954
Elev 1704 m (5590 ft)



DATA SHEET 4

STATION I-50
19 MAY 1954
ELEVATION 1630 m (5348 ft)

STATION I-50
26 JULY 1953
ELEVATION 1630 m (5348 ft)



①

4

STATION 1-50
19 MAY 1955
ELEVATION 1630 m (5348 ft)

STA
19
ELE

STATION 1-50
19 MAY 1954
ELEVATION 1630 m (5348 ft)

RAM HARDNESS NUMBER (Kg)
300 250 200 150 100 50

RAM HARDNESS NUMBER (Kg)
350 300 250 200 150 100 50

RAM HARDNESS NUMBER (Kg)
300 250 200 150 100 50

TEMPERATURE °C
-30 -25 -20 -15 -10 -5 0

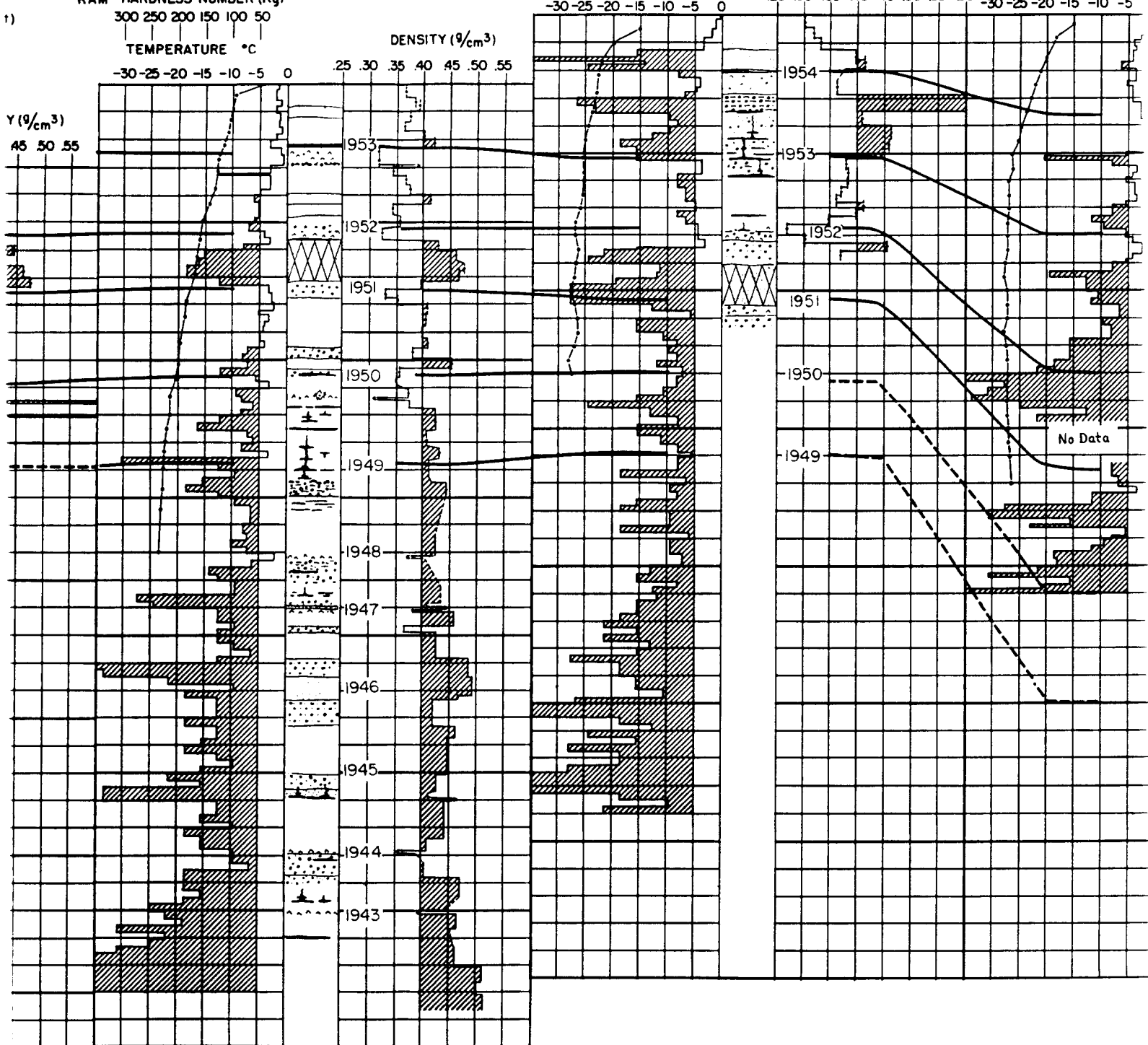
DENSITY (g/cm³)
25 30 35 40 45 50 55 60

TEMPERATURE °C
-30 -25 -20 -15 -10 -5

TEMPERATURE °C
-30 -25 -20 -15 -10 -5 0

DENSITY (g/cm³)
25 30 35 40 45 50 55

Y (g/cm³)
45 50 55



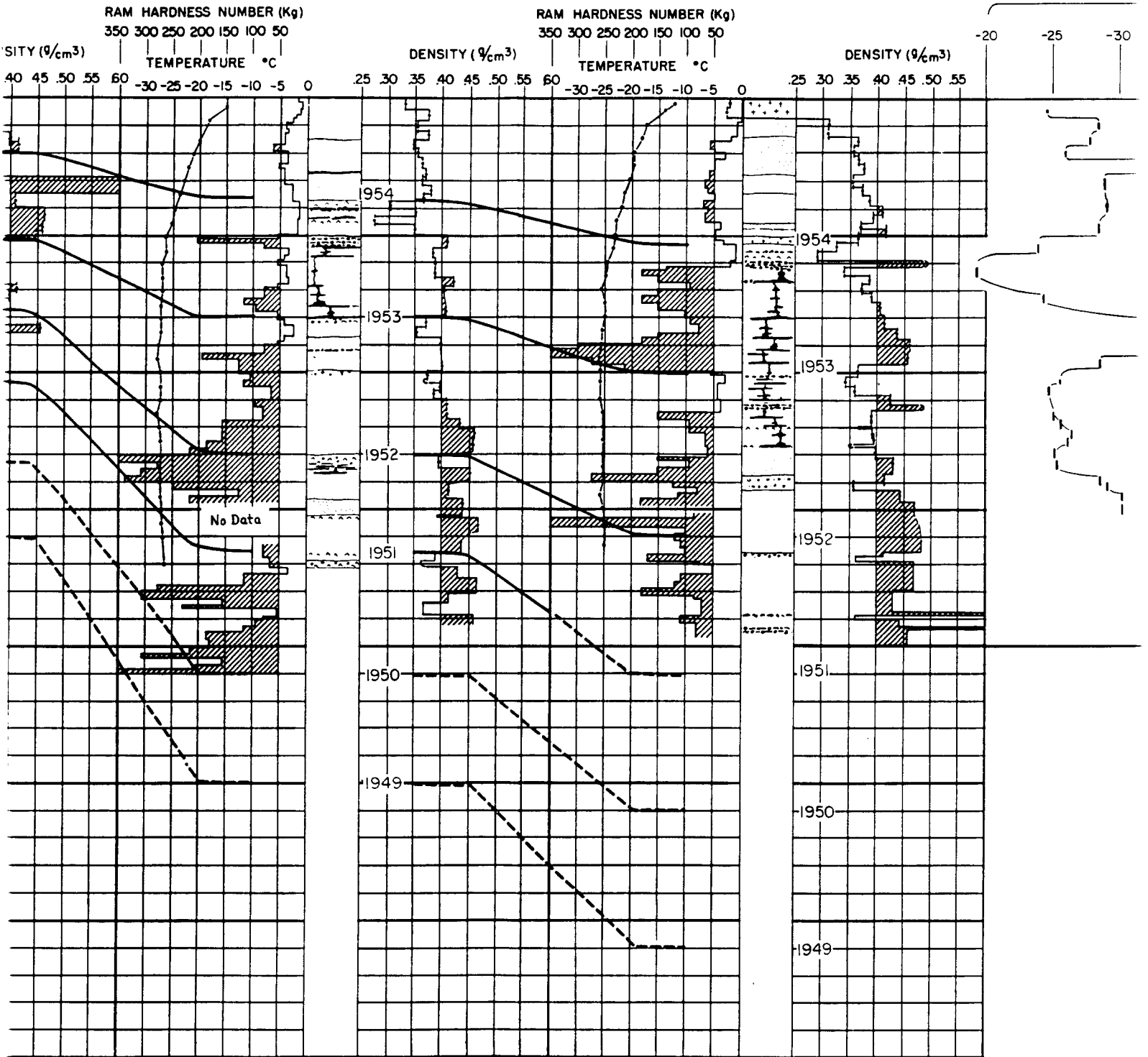
2

STATION 1a-10
19 MAY 1955
ELEVATION 1720 m (5643 ft)

STATION 1a-20
20 MAY 1955
ELEVATION 1660 m (5446 ft)

$\delta = \frac{O^{18}}{O^{16}}$ RATIO RE

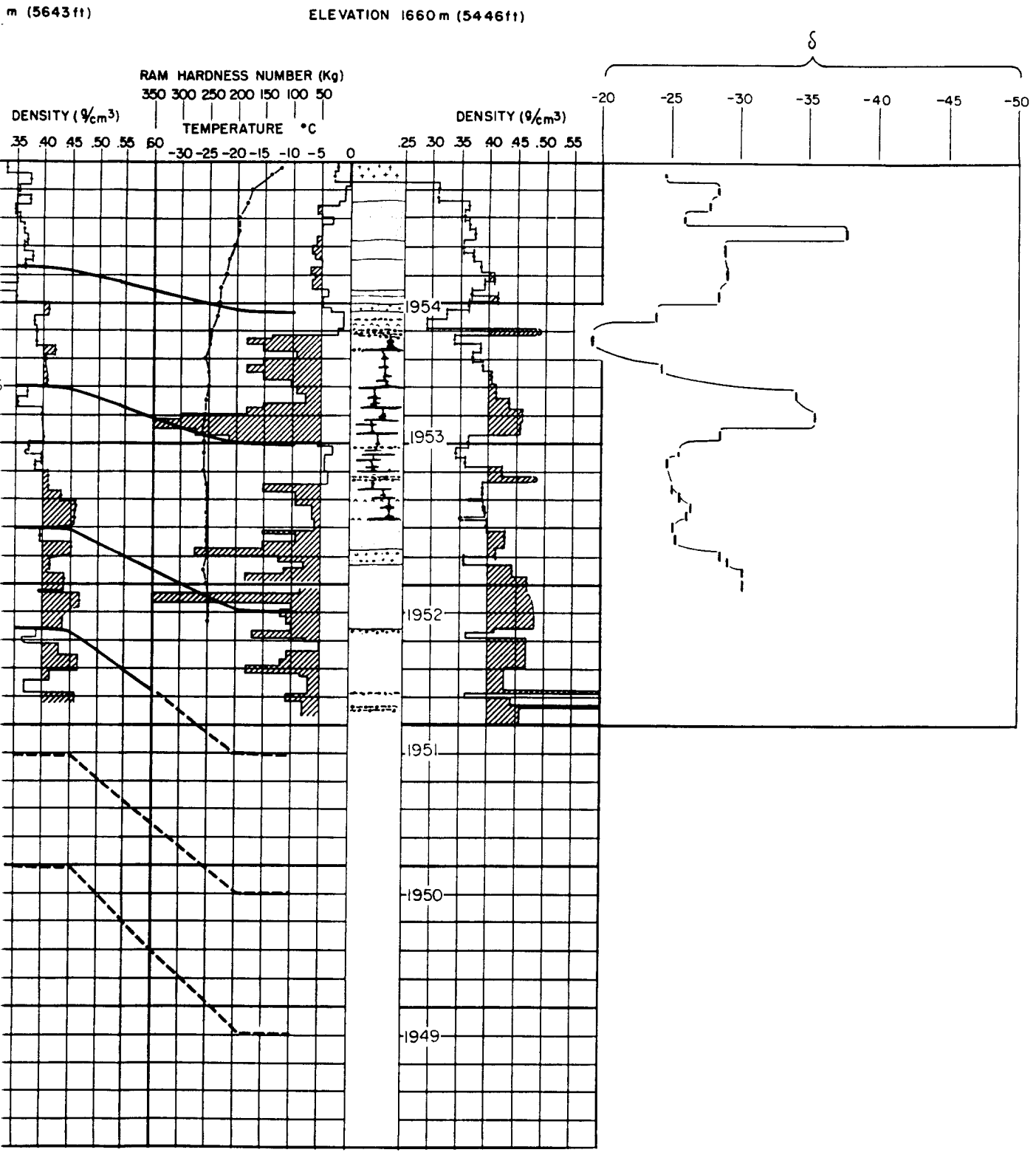
348 ft)



3

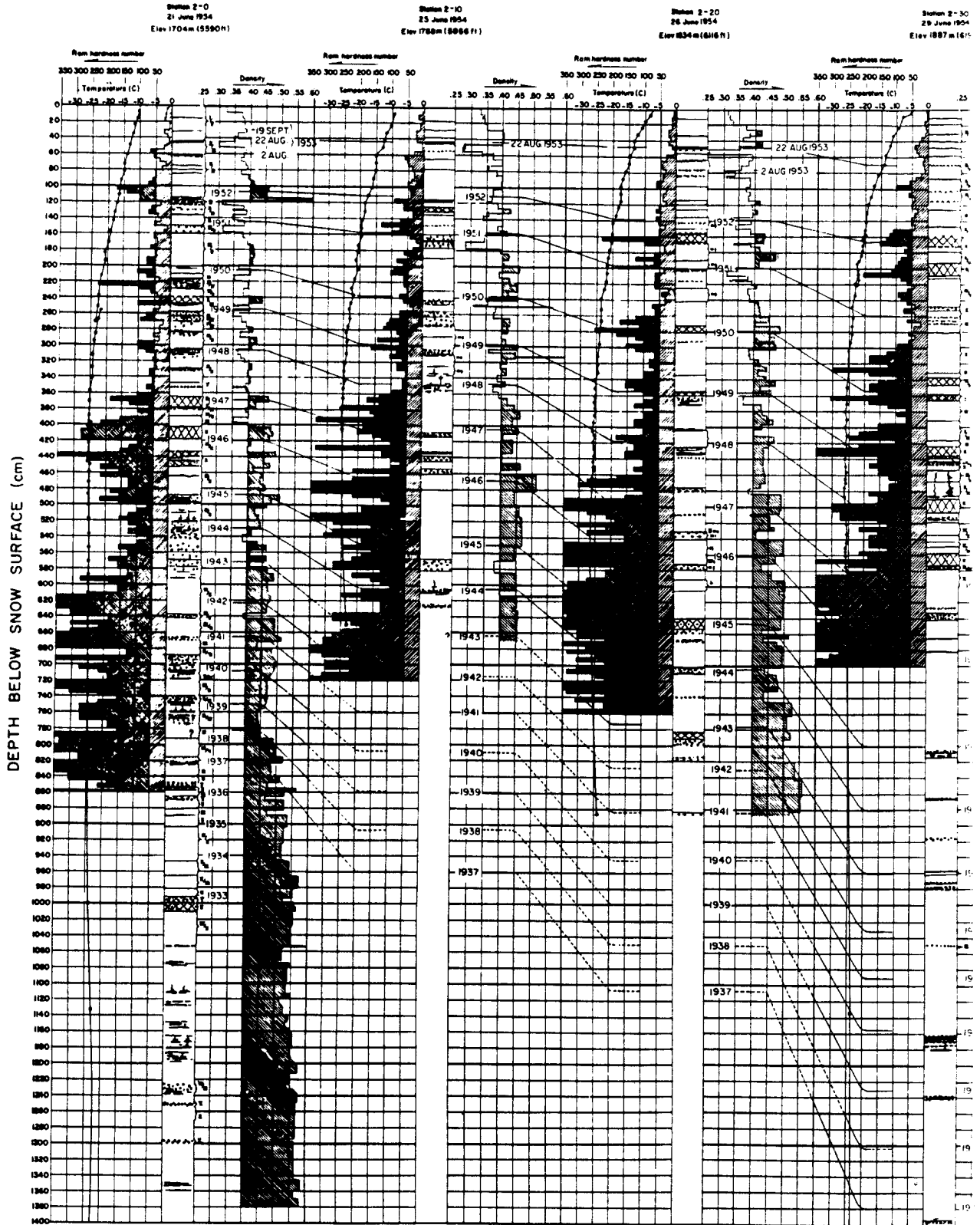
STATION 1a-20
20 MAY 1955
ELEVATION 1660 m (5446 ft)

$\delta = \frac{O^{18}}{O^{16}}$ RATIO RELATIVE TO MEAN OCEAN WATER



(4)

DATA SHEET 5



①

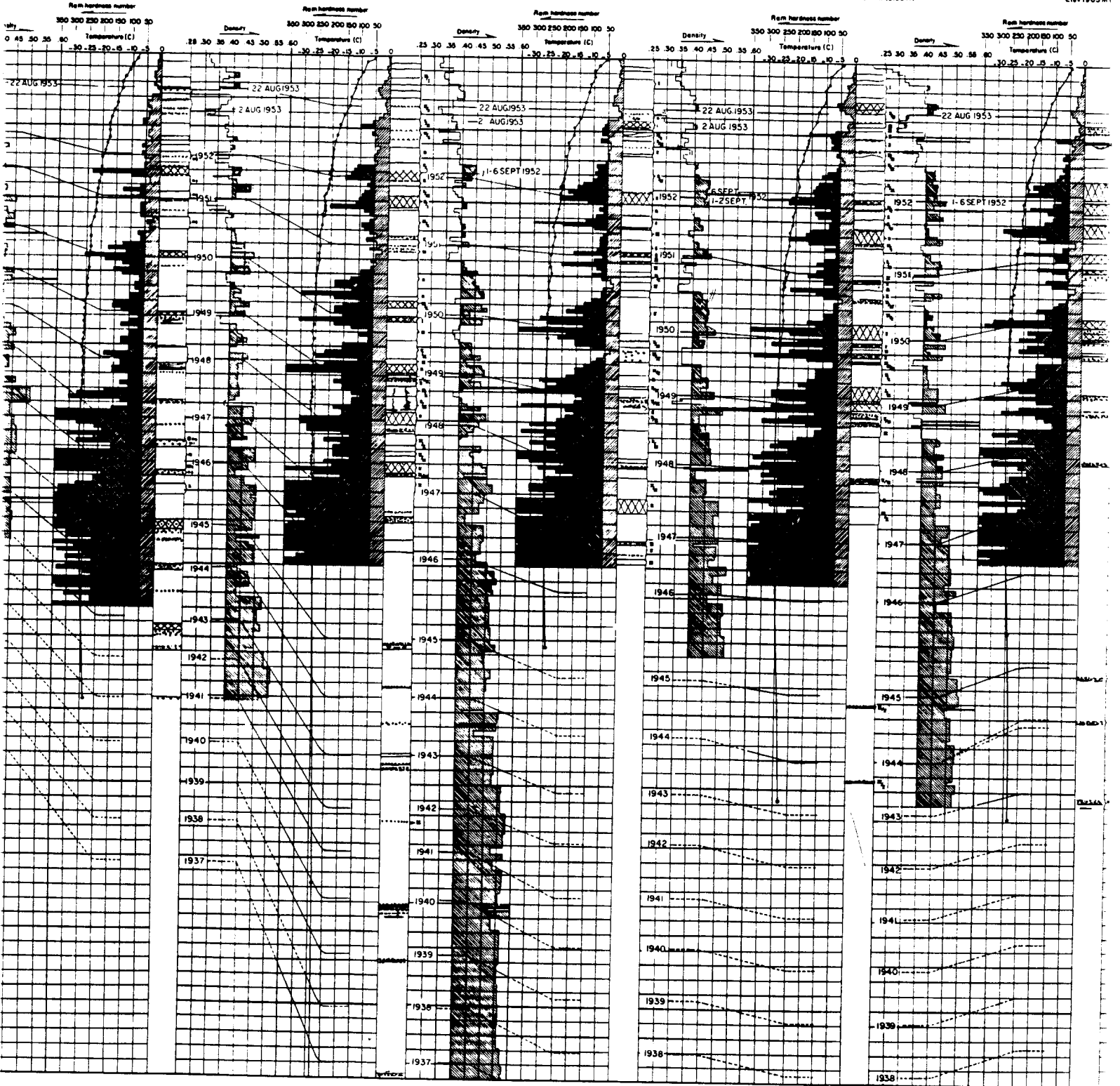
Station Z-20
28 June 1954
Elev 1834 m (6016 ft)

Station Z-30
29 June 1954
Elev 1867 m (6124 ft)

Station Z-40
4 July 1954
Elev 1885 m (6184 ft)

Station Z-50
9 July 1954
Elev 1877 m (6158 ft)

Station Z-60
8 July 1954
Elev 1905 m



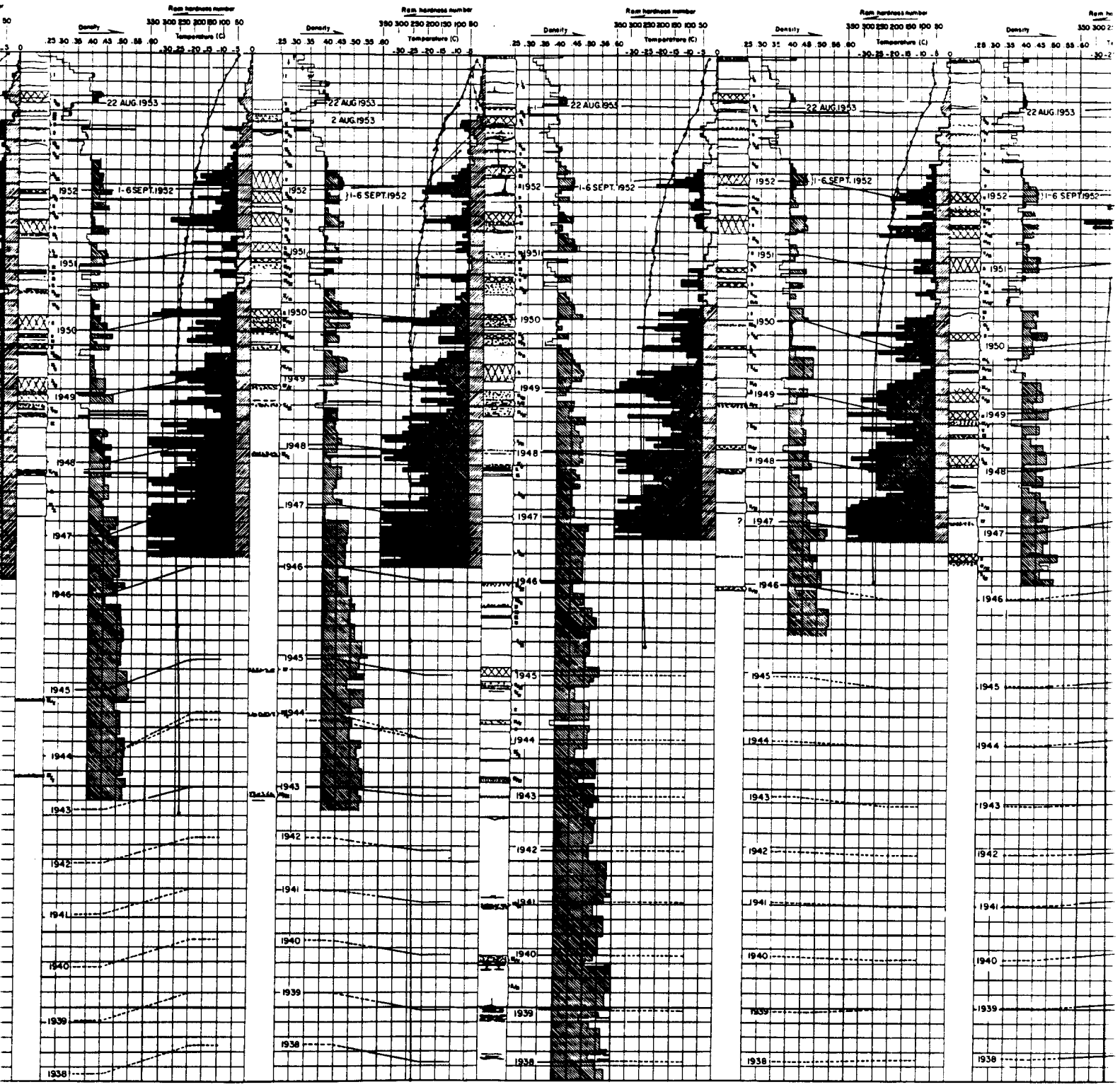
Station 2-50
9 July 1954
Elev 1877 m (6158 ft)

Station 2-60
1 July 1954
Elev 1905 m (6251 ft)

Station 2-70
16 July 1954
Elev 1919 m (6297 ft)

Station 2-80
19 July 1954
Elev 1944 m (6379 ft)

Station 2-90
20 July 1954
Elev 1959 m (6428 ft)

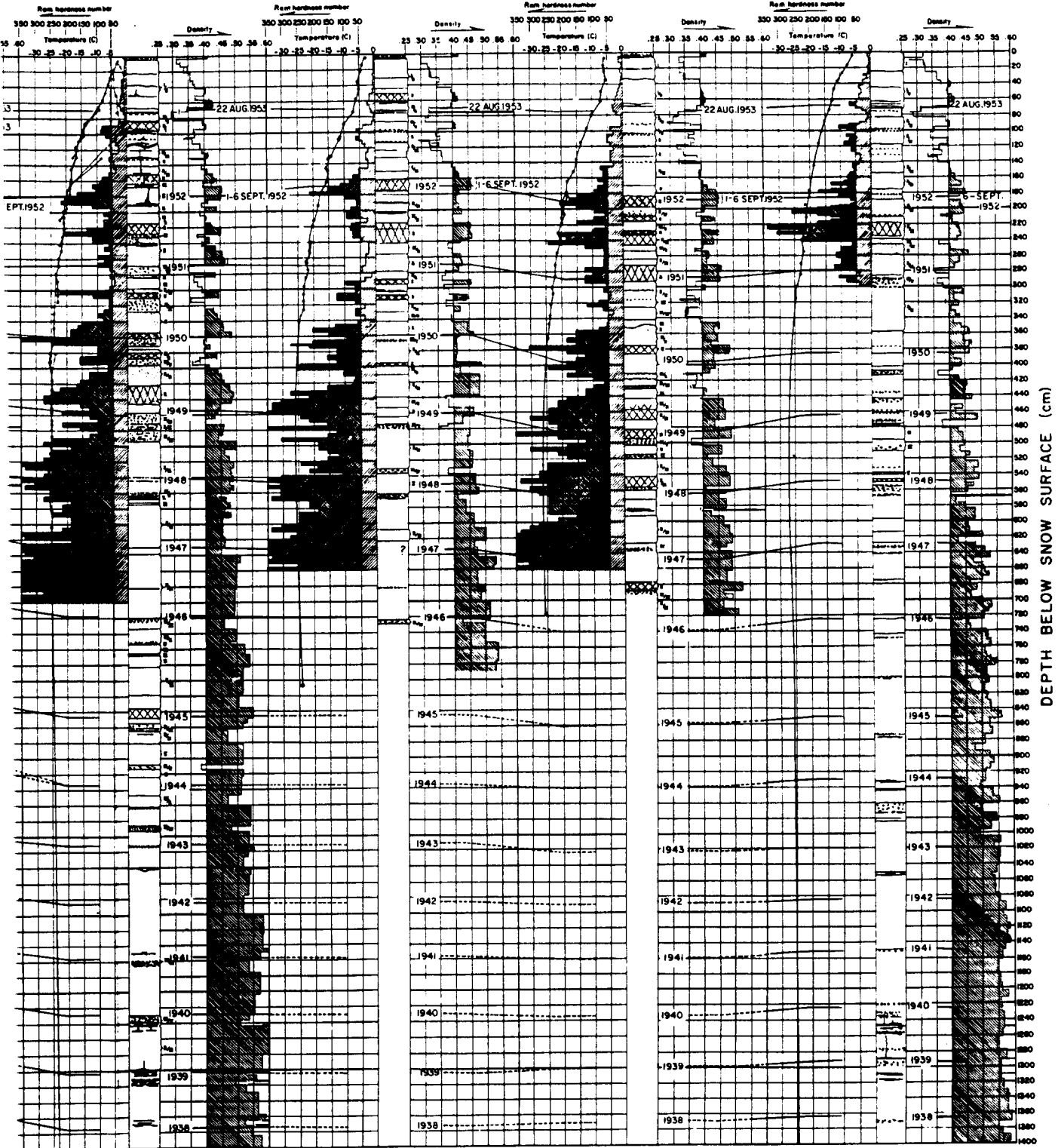


Station Z-70
16 July 1954
Elev 1919 m (6297 ft)

Station Z-80
19 July 1954
Elev 1944 m (6379 ft)

Station Z-90
20 July 1954
Elev 1959 m (6428 ft)

Station Z-100
7 July 1954
Elev 1992 m (6534 ft)

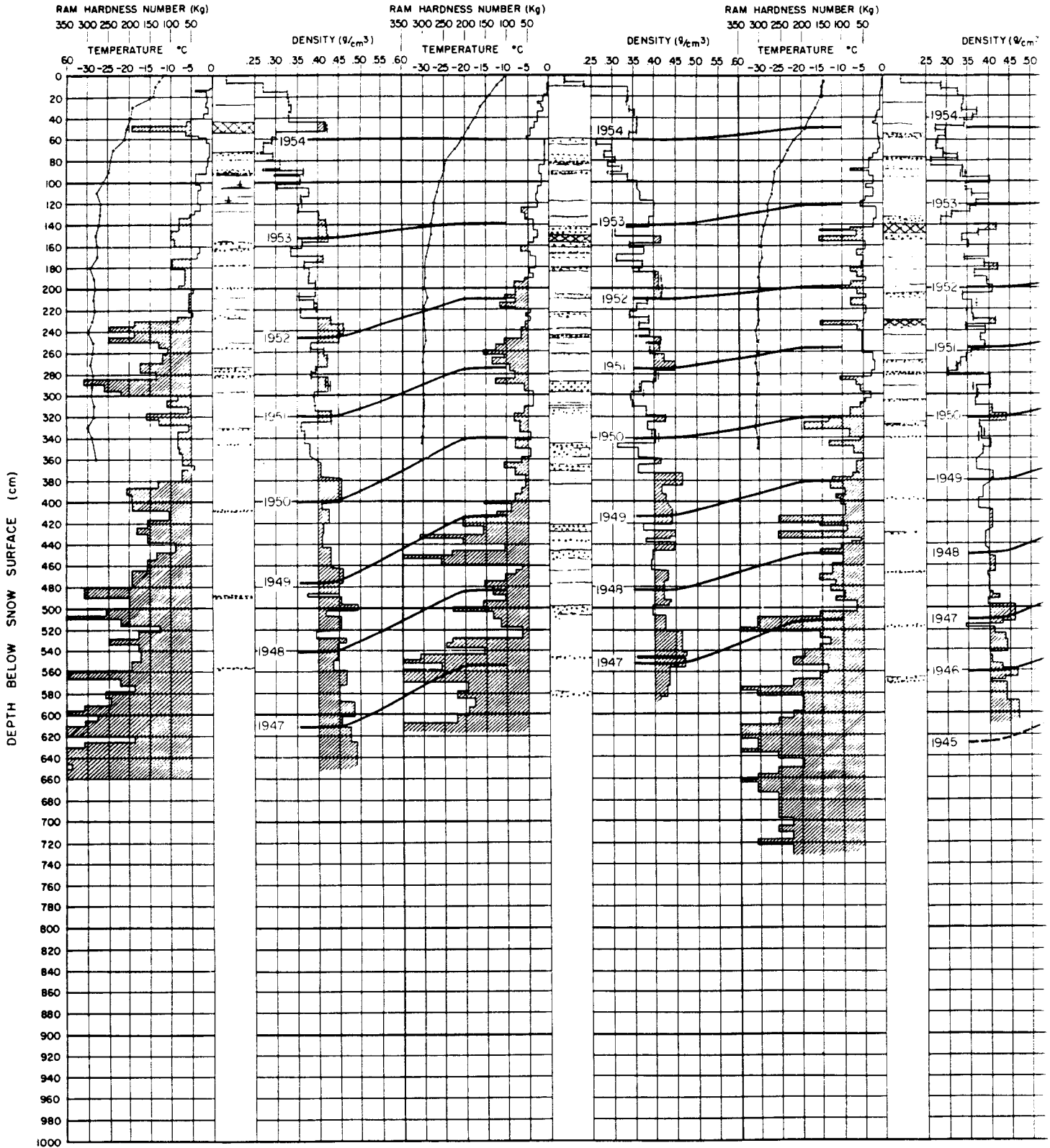


DATA SHEET 6

STATION 2-125
29 MAY 1955
ELEVATION 2152 m (7060 ft)

STATION 2-150
31 MAY 1955
ELEVATION 2273 m (7456 ft)

STATION 2-175
2 JUNE 1955
ELEVATION 2392 m (7848 ft)

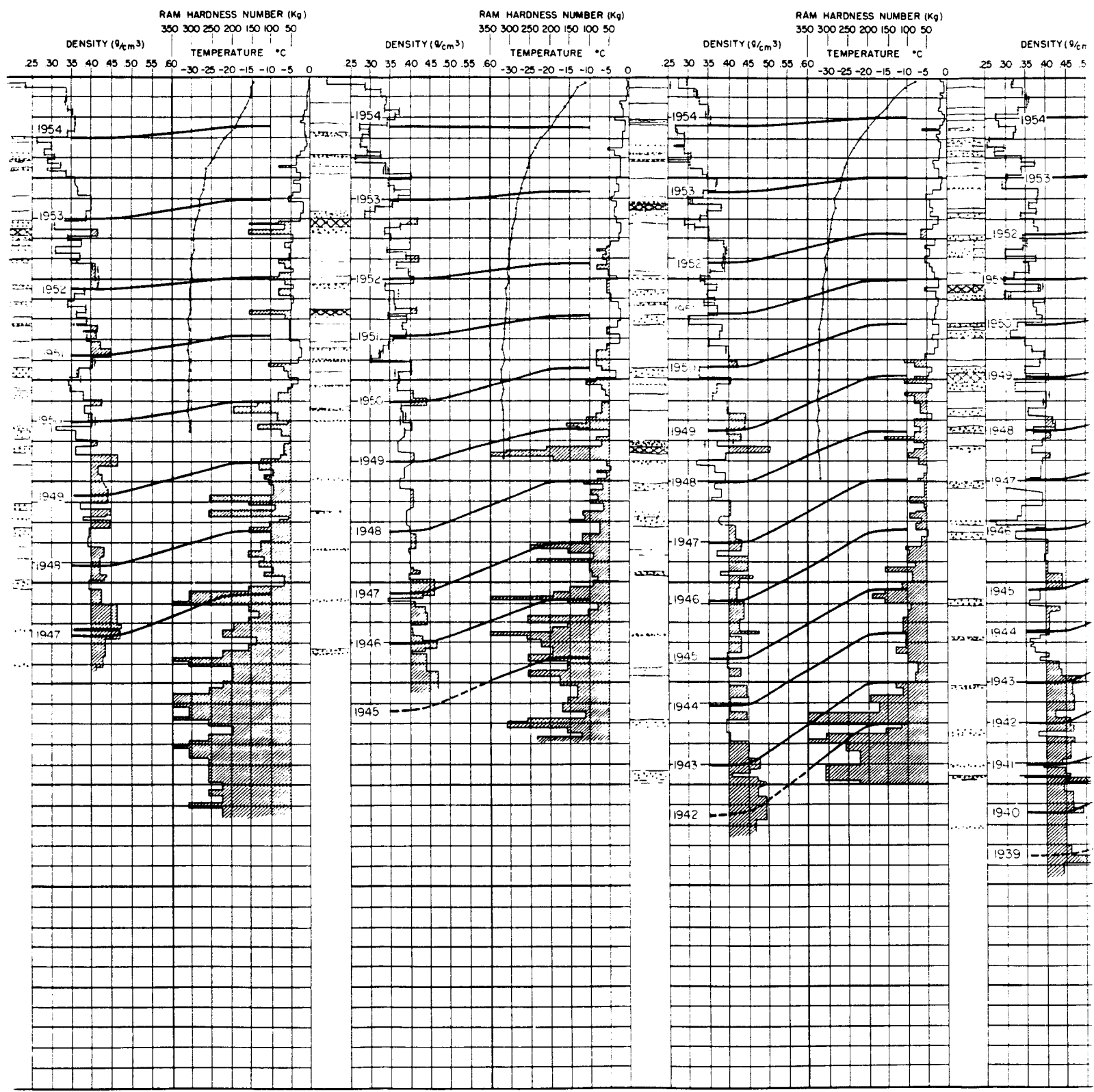


2-150
1955
DN 2273 m (7456 ft)

STATION 2-175
2 JUNE 1955
ELEVATION 2392 m (7848 ft)

STATION 2-200
4 JUNE 1955
ELEVATION 2475 m (8120 ft)

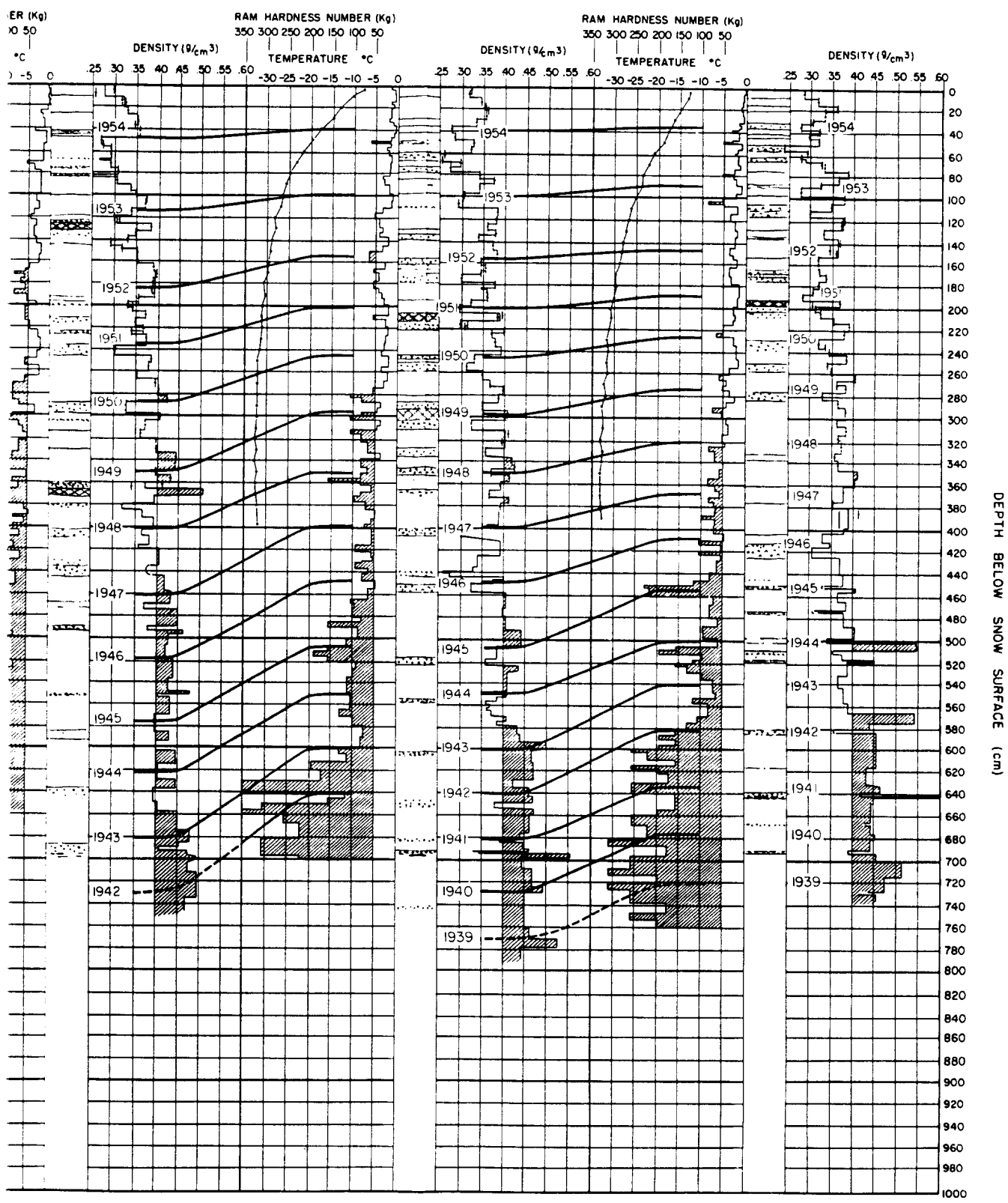
STATION 2-225
6 JUNE 1955
ELEVATION 2536 m (8320 ft)



STATION 2-200
4 JUNE 1955
ELEVATION 2475 m (8120 ft)

STATION 2-225
6 JUNE 1955
ELEVATION 2536 m (8320 ft)

STATION 4-0
10 JUNE 1955
ELEVATION 2616 m (8582 ft)

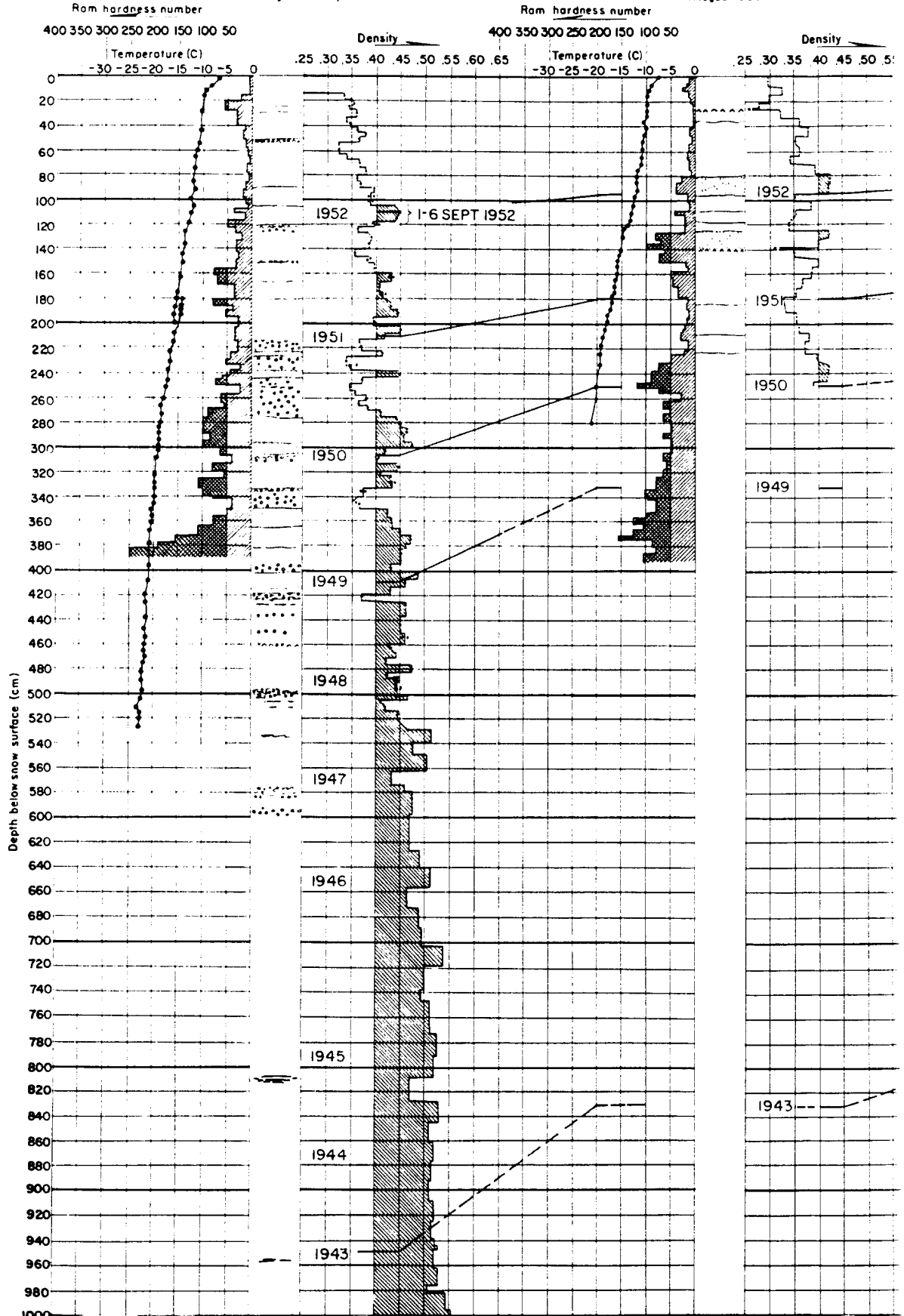


③

DATA SHEET 6A

Station 2-100
Elev. 6700ft.
26 August-17 Sept. 1953

Station 2-120
Elev. 7020ft.
11 August 1953



Station 2-120
Elev. 7020ft.
11 August 1953

Station 2-140
Elev. 7310ft.
14 August 1953

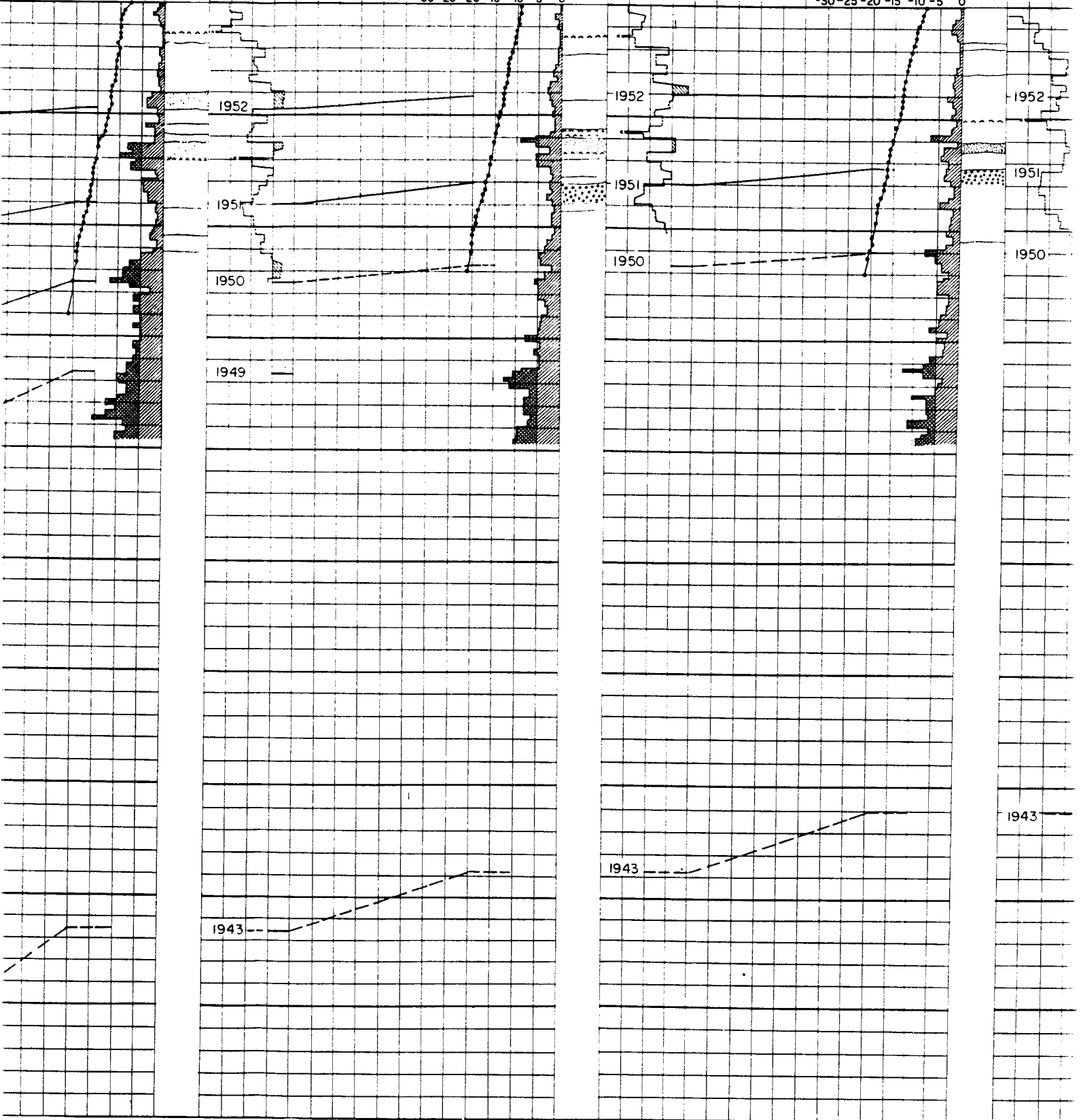
Station 2-160
Elev. 7590ft.
14 August 1953

Ram hardness number
350 300 250 200 150 100 50
Temperature (C)
-30 -25 -20 -15 -10 -5 0

Ram hardness number
400 350 300 250 200 150 100 50
Temperature (C)
-30 -25 -20 -15 -10 -5 0

Ram hardness number
400 350 300 250 200 150 100 50
Temperature (C)
-30 -25 -20 -15 -10 -5 0

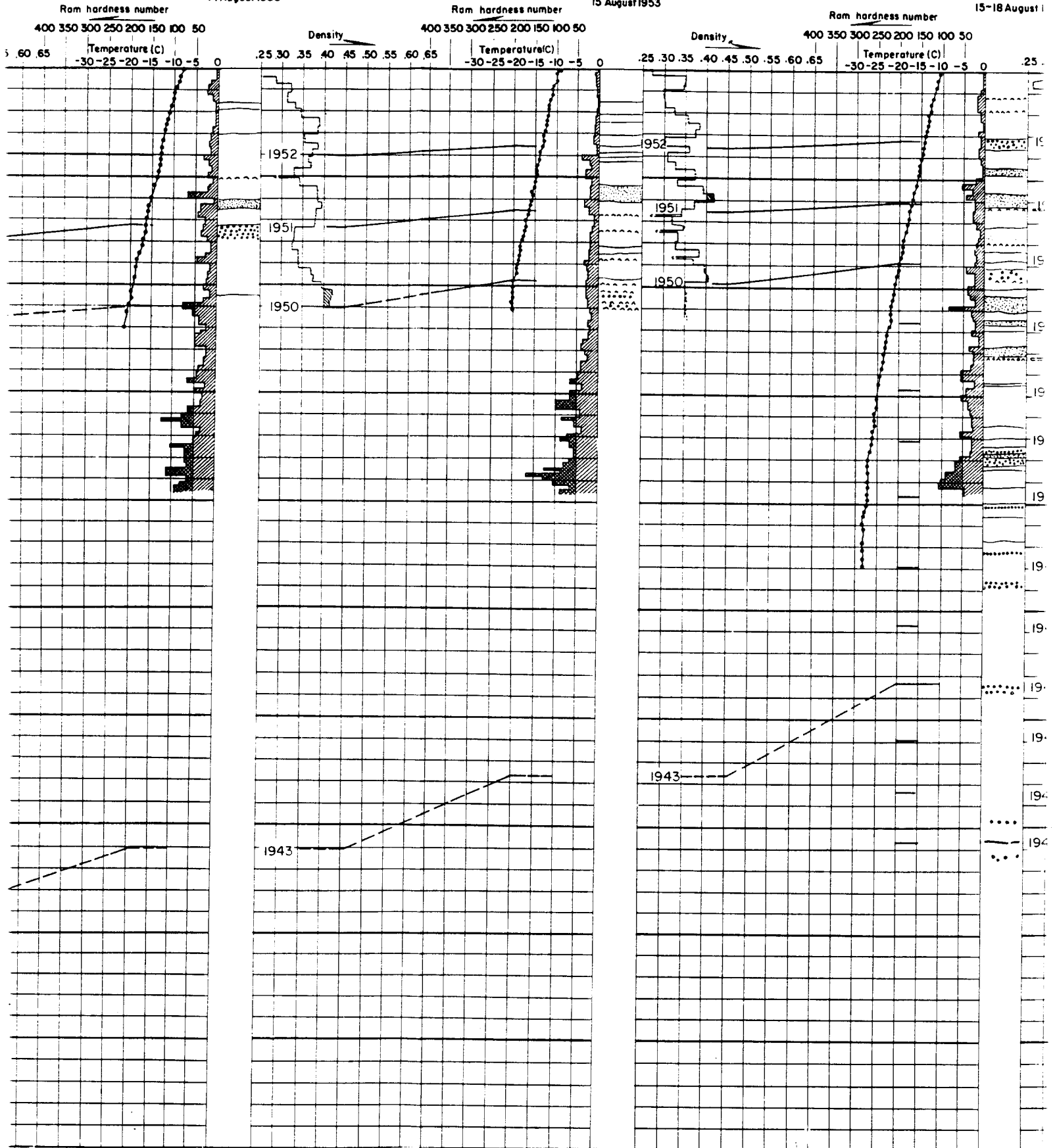
Density
25 30 35 40 45 .50 .55 .60 65



Station 2-160
Elev. 7590ft.
14 August 1953

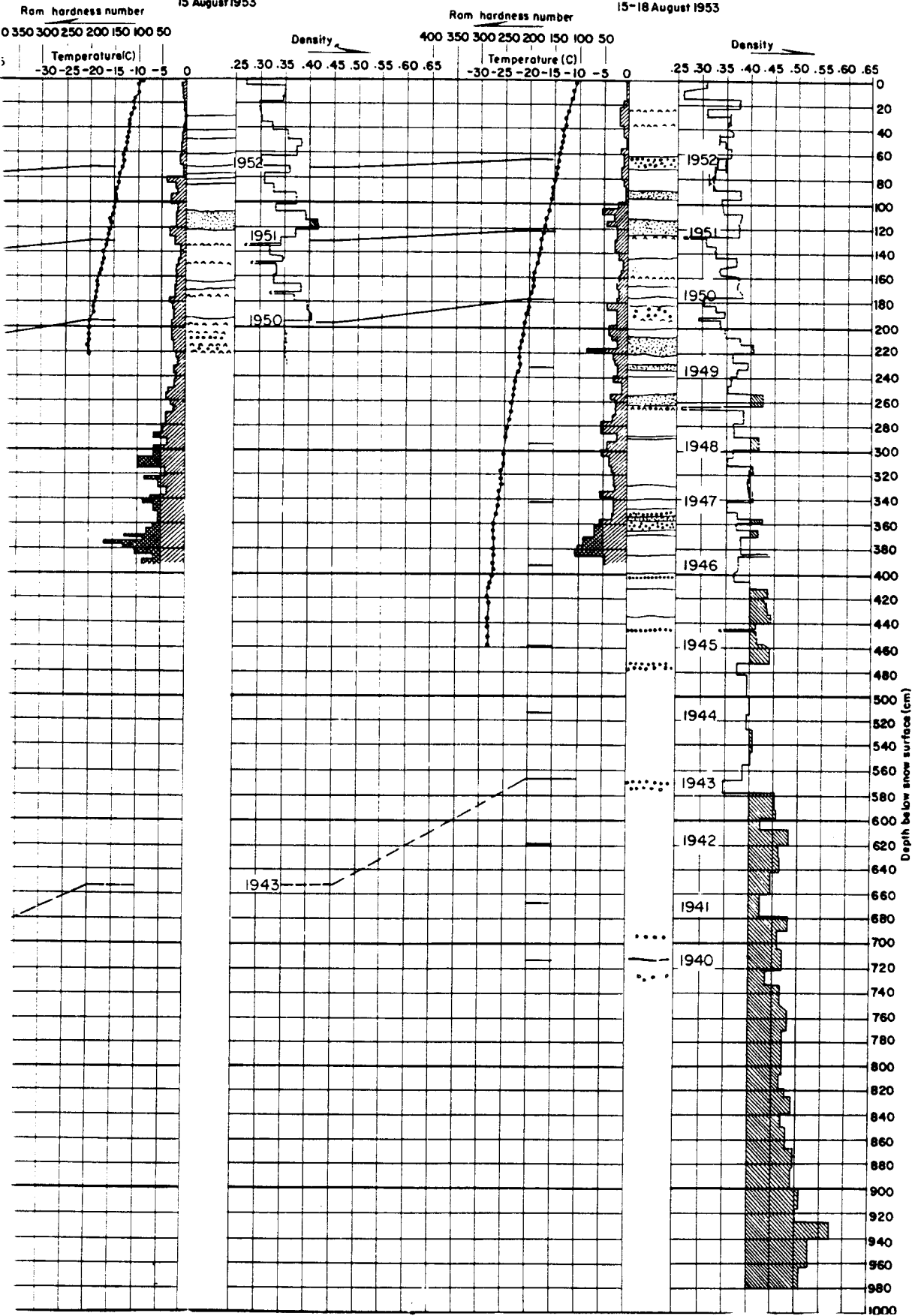
Station 2-180
Elev. 7830ft.
15 August 1953

Station 2-200
Elev. 8010ft.
15-18 August 1953



Station 2-180
Elev. 7830 ft.
15 August 1953

Station 2-200
Elev. 8010 ft.
15-18 August 1953

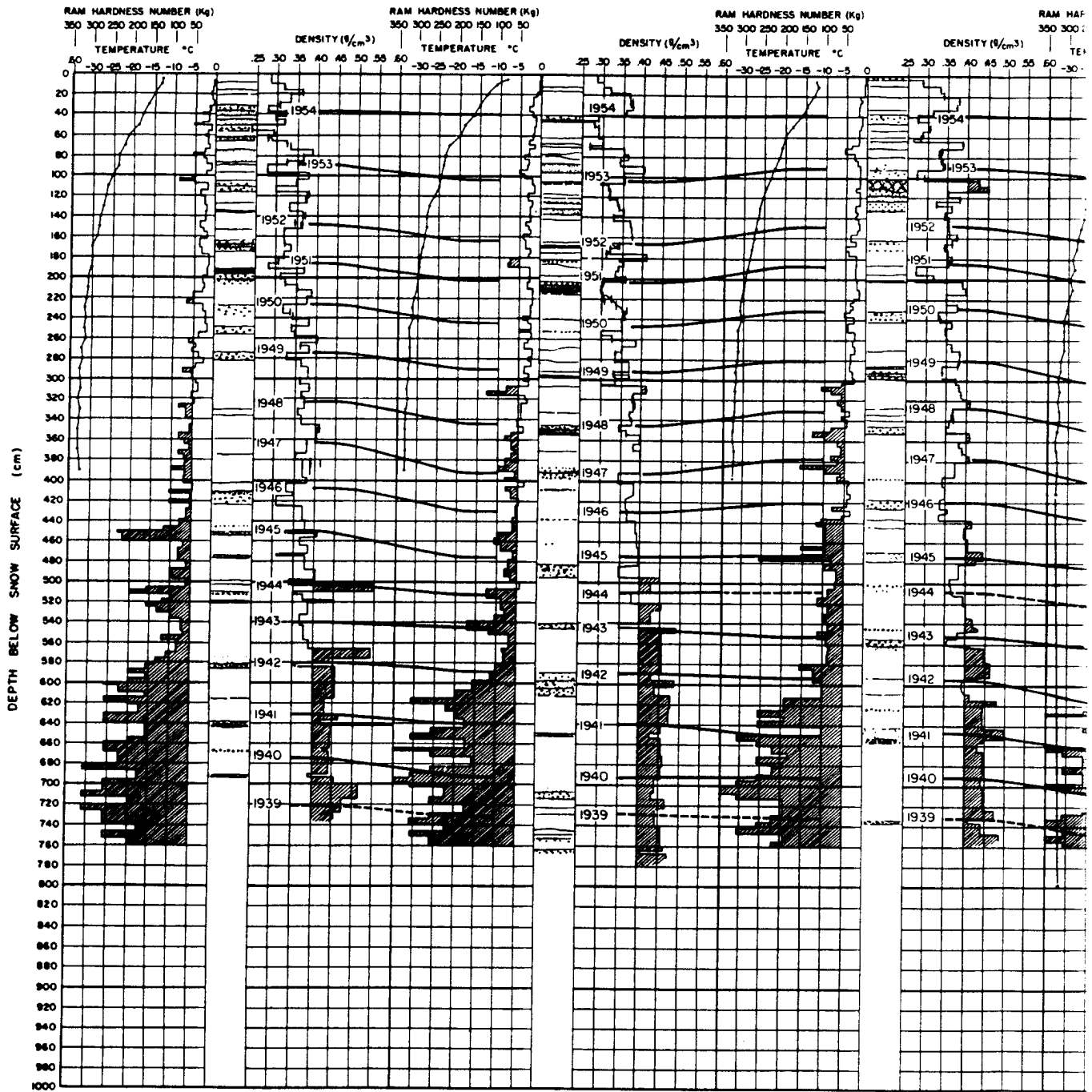


DATA SHEET 7

STATION 4-0
10 JUNE 1955
ELEVATION 2616 m (8582 ft)

STATION 4-25
12 JUNE 1955
ELEVATION 2674 m (8772 ft)

STATION 4-50(AD)
14 JUNE 1955
ELEVATION 2720 m (8925 ft)



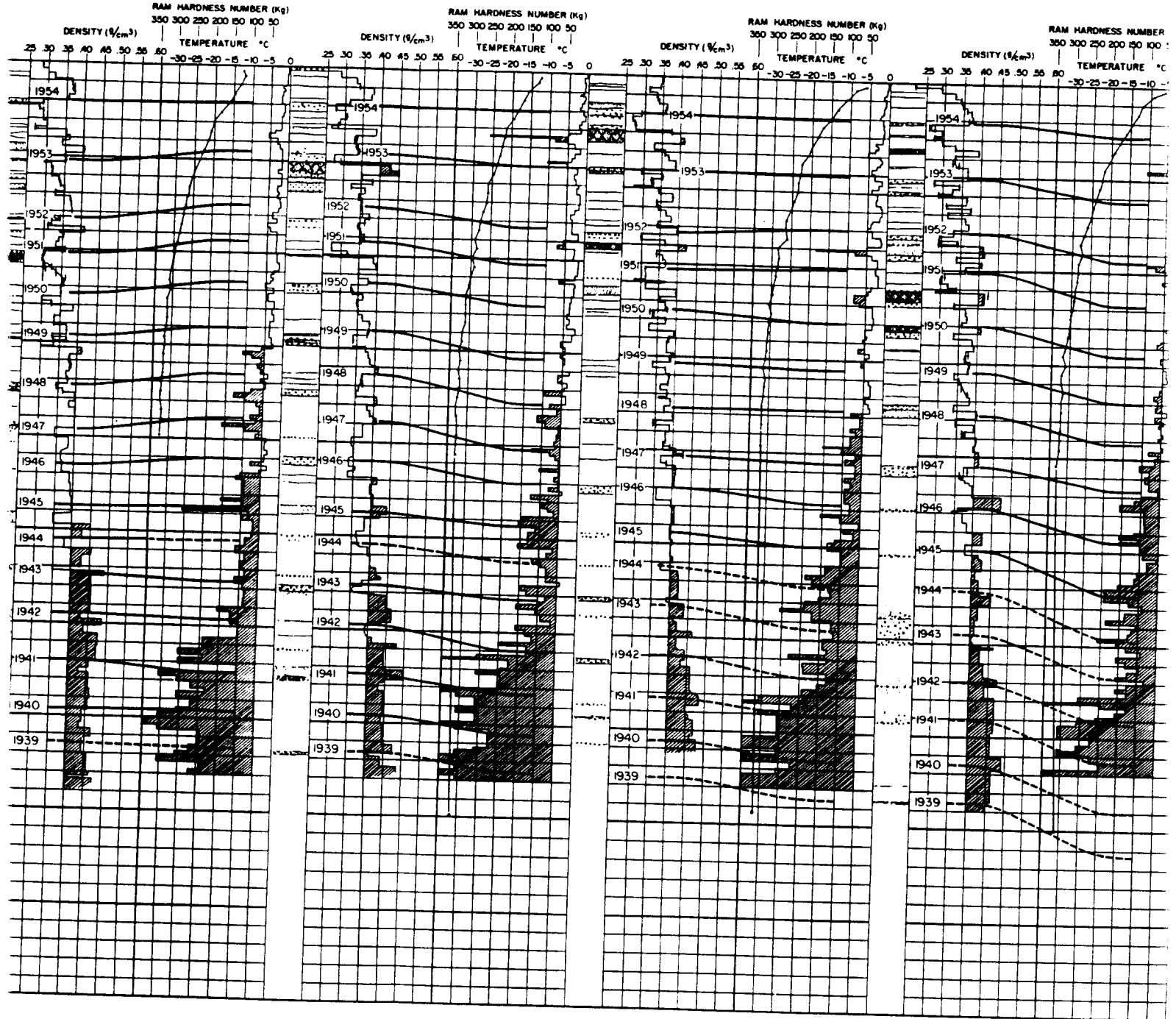
4-25
1955
ON 2874 m (8772 ft)

STATION 4-50 (AD)
14 JUNE 1955
ELEVATION 2720 m (8925 ft)

STATION 4-75
17 JUNE 1955
ELEVATION 2748 m (9019 ft)

STATION 4-100
19 JUNE 1955
ELEVATION 2778 m (9114 ft)

5
2
E

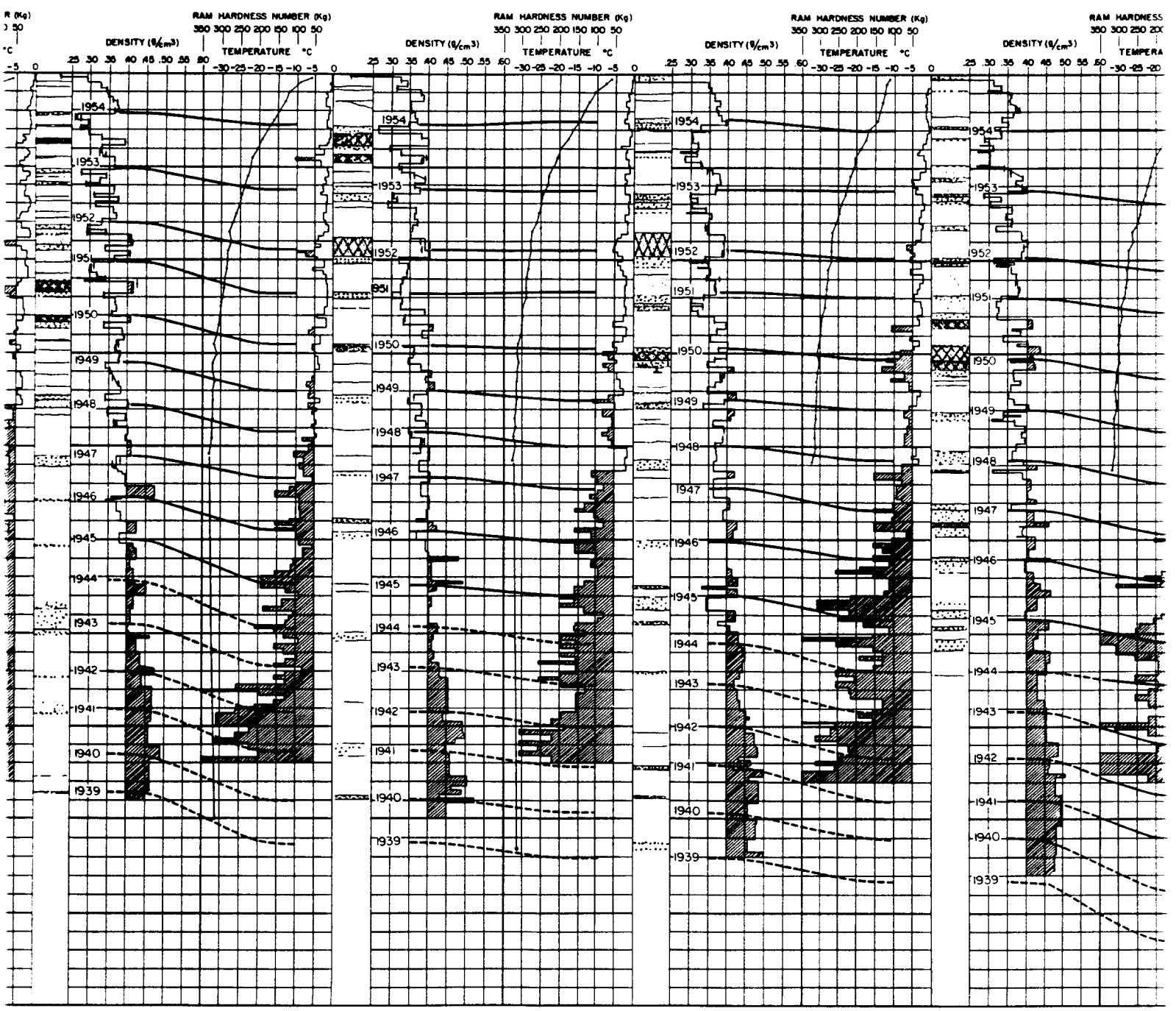


STATION 4-100
19 JUNE 1955
ELEVATION 2778 m (9114 ft)

STATION 4-125
21 JUNE 1955
ELEVATION 2821 m (9256 ft)

STATION 4-150
23 JUNE 1955
ELEVATION 2851 m (9354 ft)

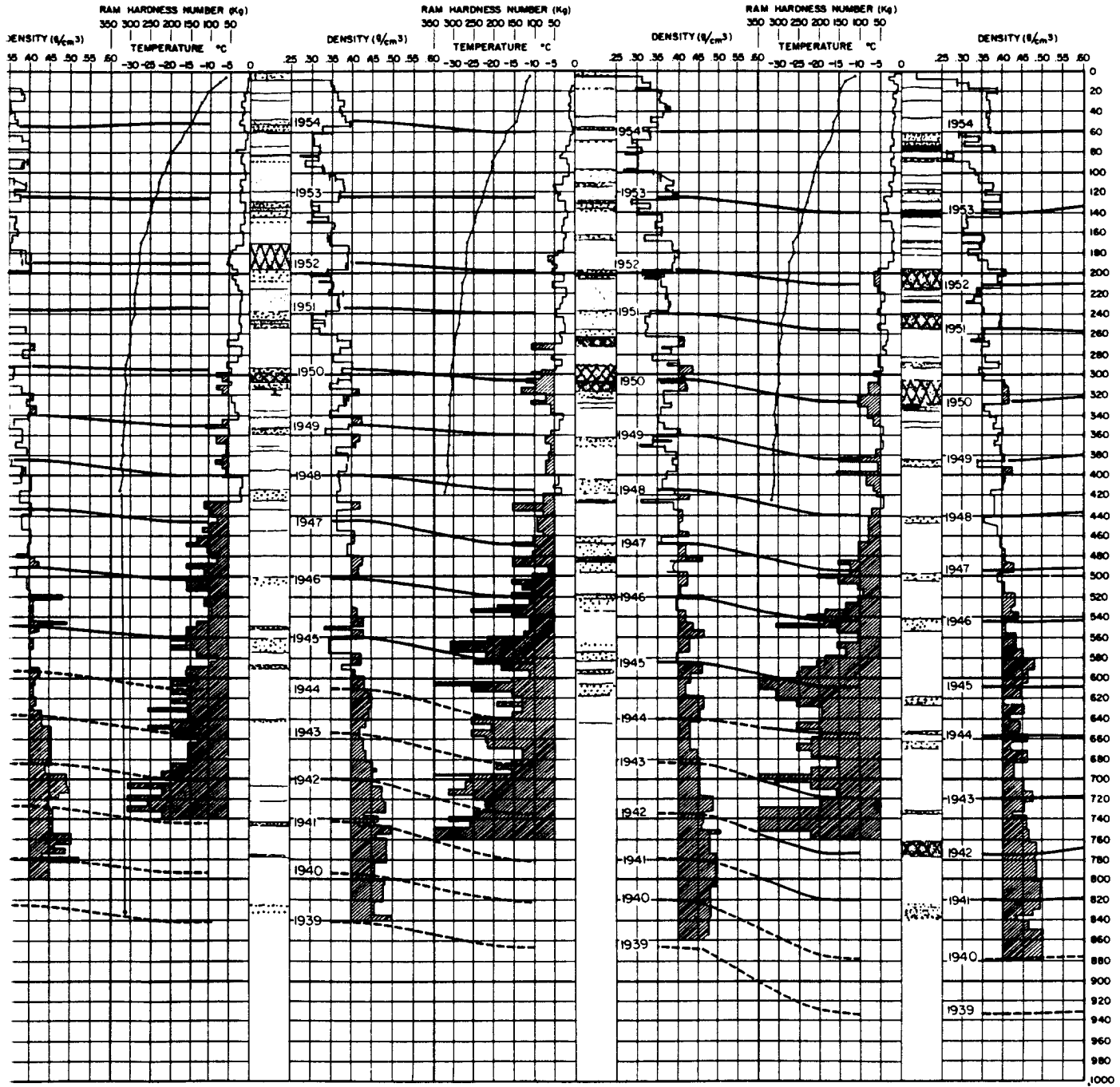
STATION 4-175
25 JUNE 1955
ELEVATION 2873 m (9426 ft)



STATION 4-150
23 JUNE 1955
ELEVATION 2851 m (9354 ft)

STATION 4-175
25 JUNE 1955
ELEVATION 2873 m (9428 ft)

STATION 4-200
27 JUNE 1955
ELEVATION 2918 m (9574 ft)

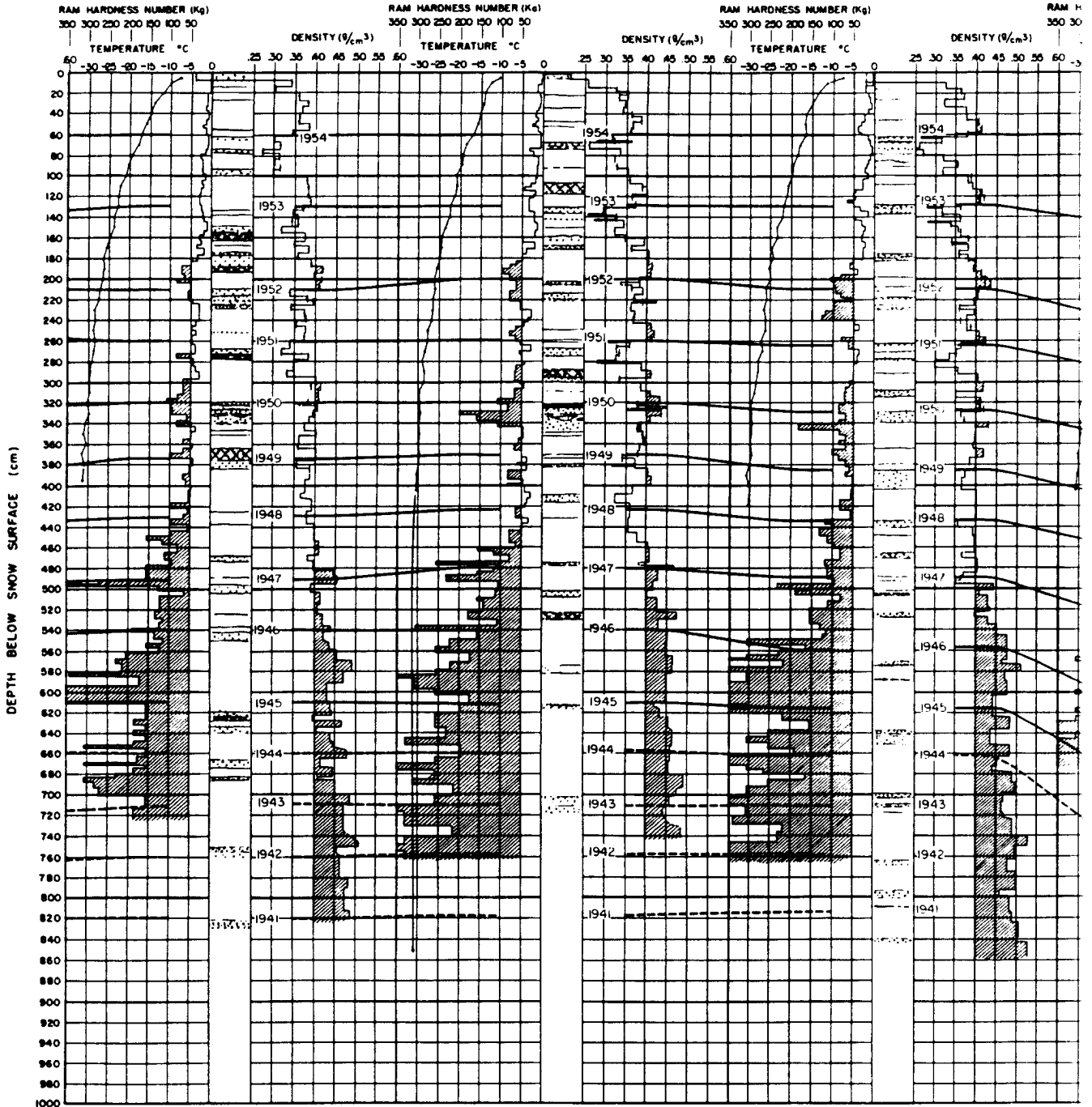


DATA SHEET 8

STATION 4-225
30 JUNE 1955
ELEVATION 2940 m (9649 ft)

STATION 4-250
2 JULY 1955
ELEVATION 2972 m (9752 ft)

STATION 4-275 (AD)
4 JULY 1955
ELEVATION 3003 m (9853 ft)



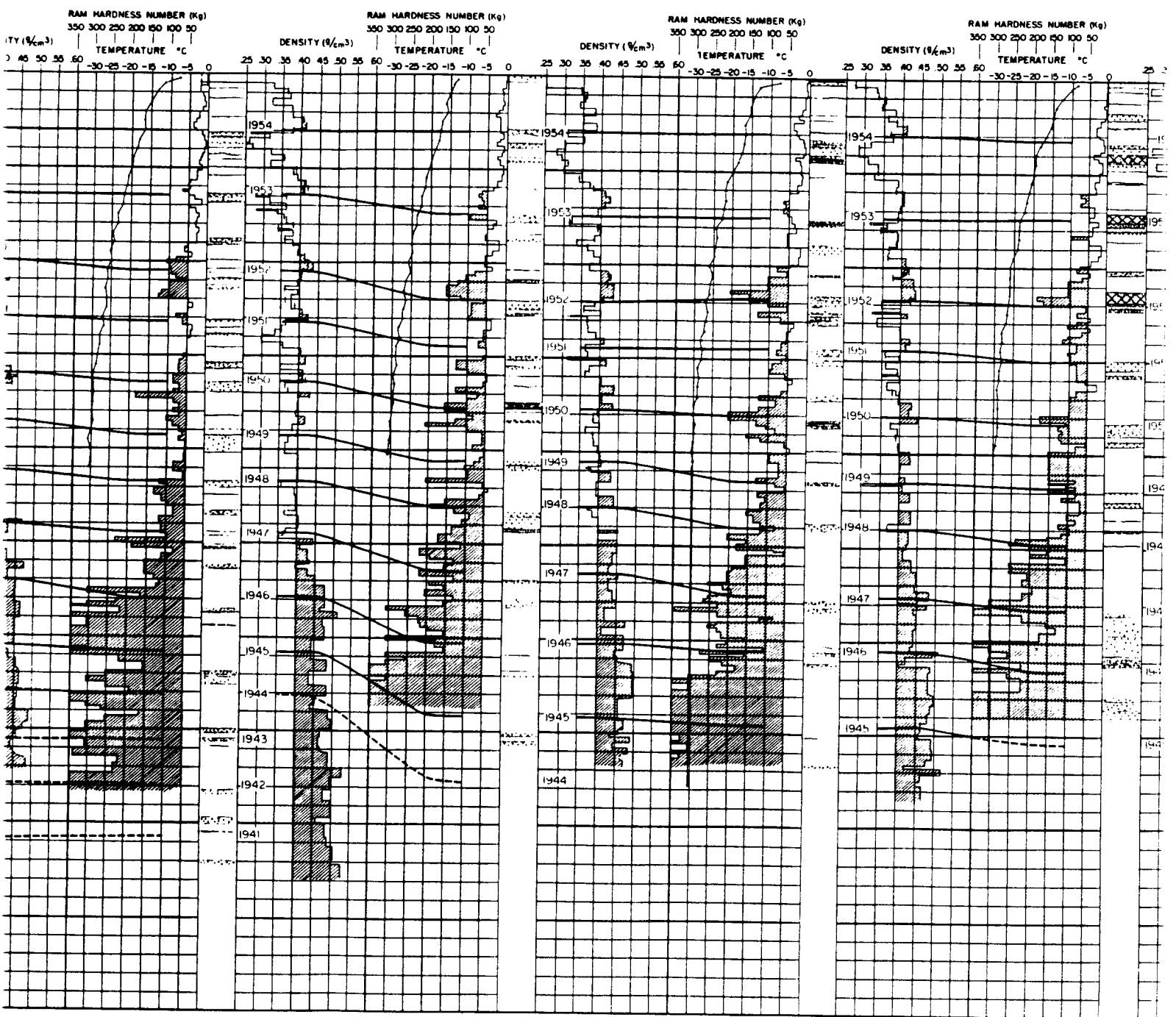
①

STATION 4-275 (AD)
4 JULY 1955
ELEVATION 3003 m (9853 ft)

STATION 4-300
8 JULY 1955
ELEVATION 3046 m (9993 ft)

STATION 4-325
10 JULY 1955
ELEVATION 3104 m (10,185 ft)

STATION 4-350
12 JULY 1955
ELEVATION 3126

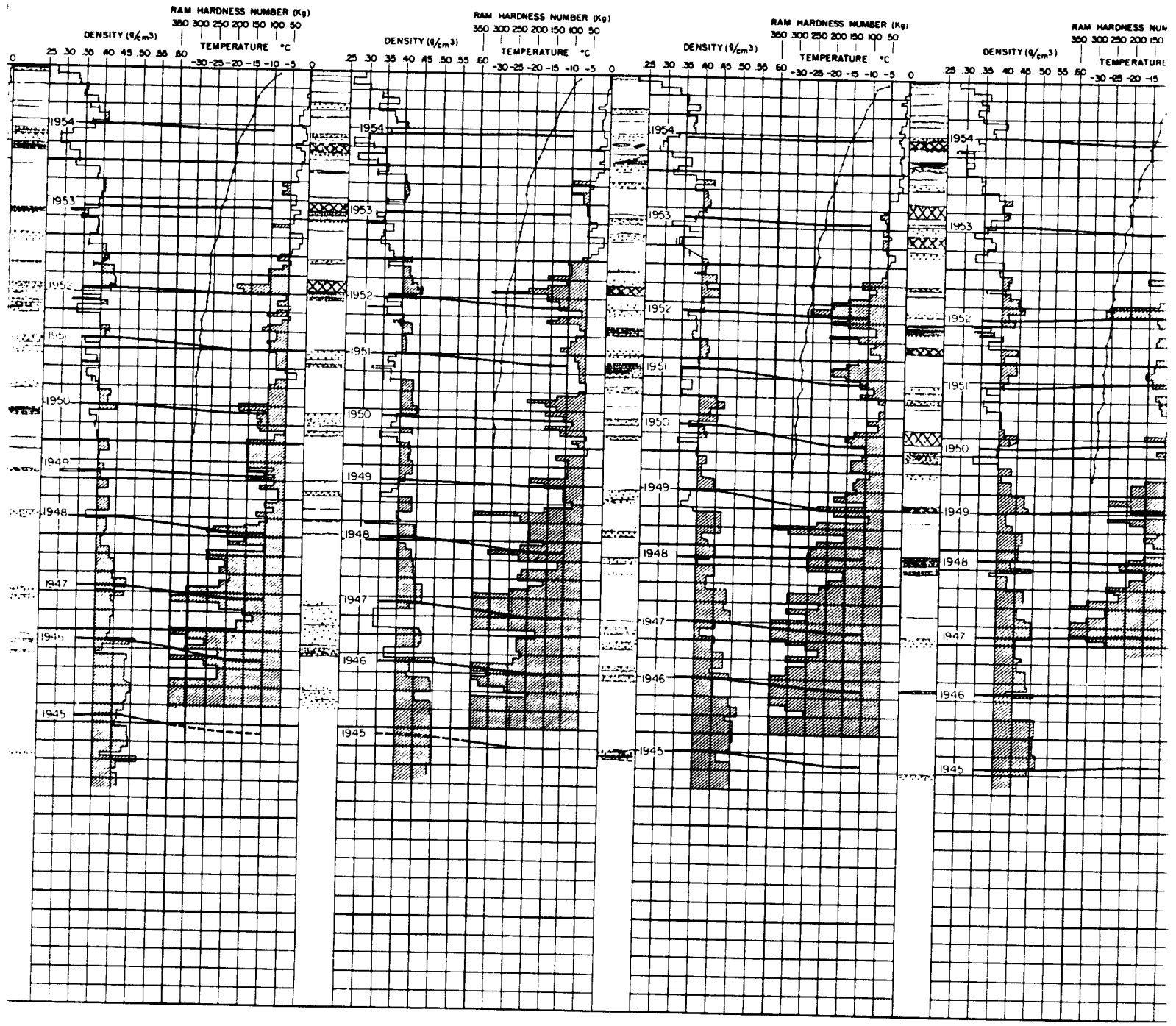


STATION 4-325
12 JULY 1955
ELEVATION 3104 m (10,185 ft)

STATION 4-350
12 JULY 1955
ELEVATION 3128 m (10,262 ft)

STATION 4-375
14 JULY 1955
ELEVATION 3131 m (10,271 ft)

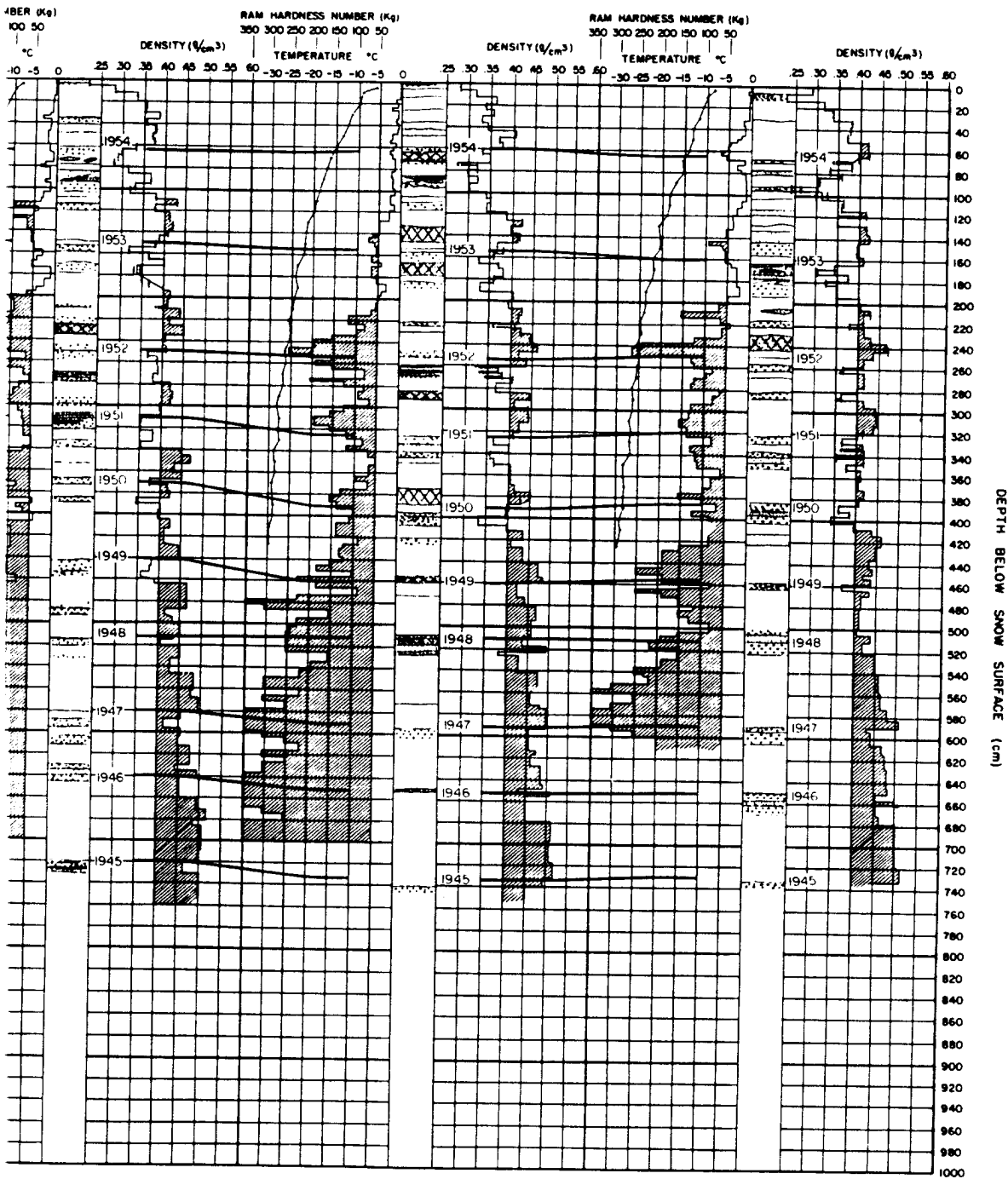
STATION 4-400
16 JULY 1955
ELEVATION 3126 m (10,256 ft)



STATION 4-375
14 JULY 1955
ELEVATION 3131 m (10,271 ft)

STATION 4-400
16 JULY 1955
ELEVATION 3126 m (10,256 ft)

STATION 5-0
18 JULY 1955
ELEVATION 3123 m (10,247 ft)

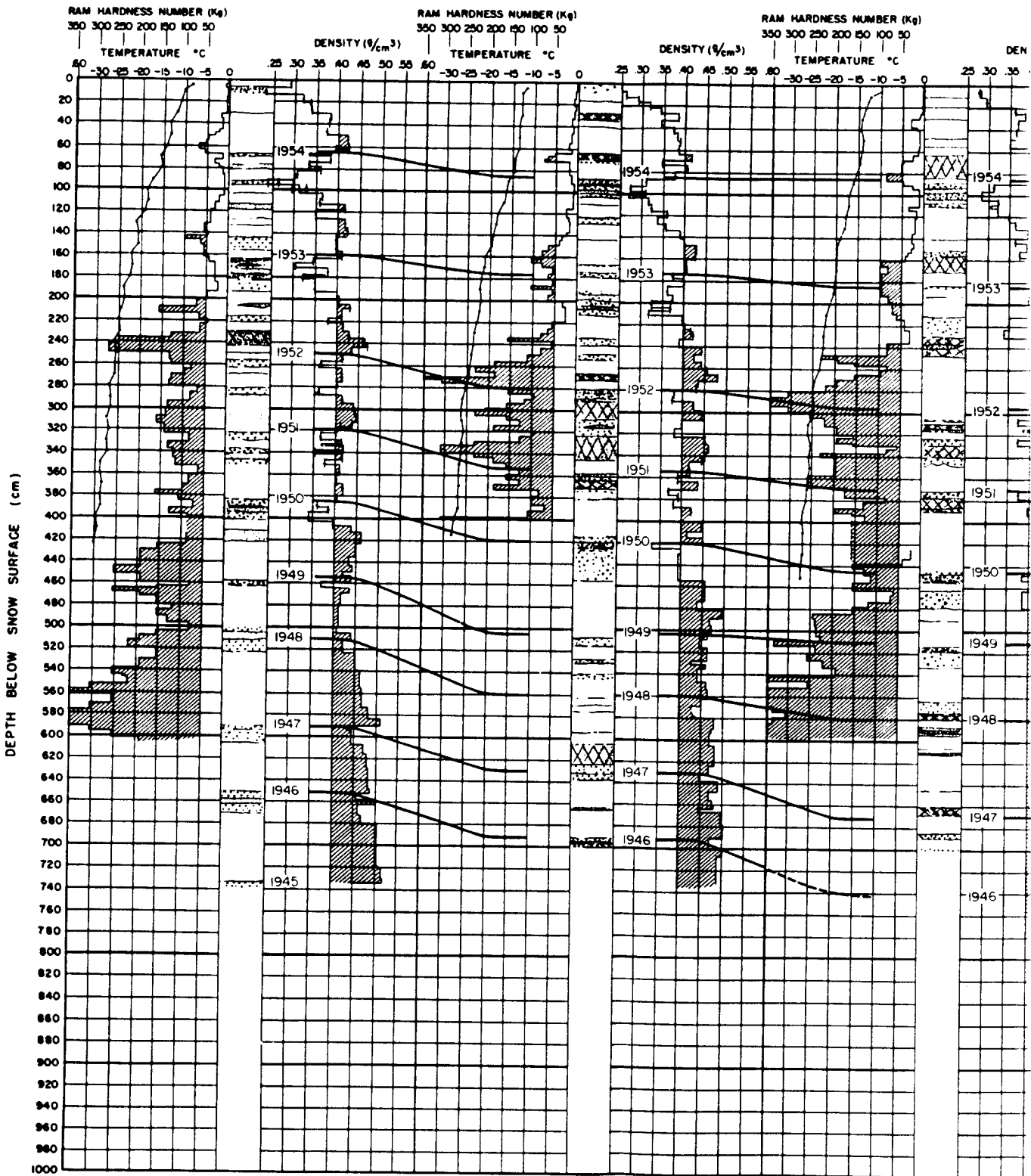


DATA SHEET 9

STATION 5-0
18 JULY 1955
ELEVATION 3123 m (10,247 ft)

STATION 5-20
20 JULY 1955
ELEVATION 3072 m (10,077 ft)

STATION 5-40, PIT II,
23 JULY 1955
(FRENCH CENTRAL STA
ELEVATION 3005 m (9



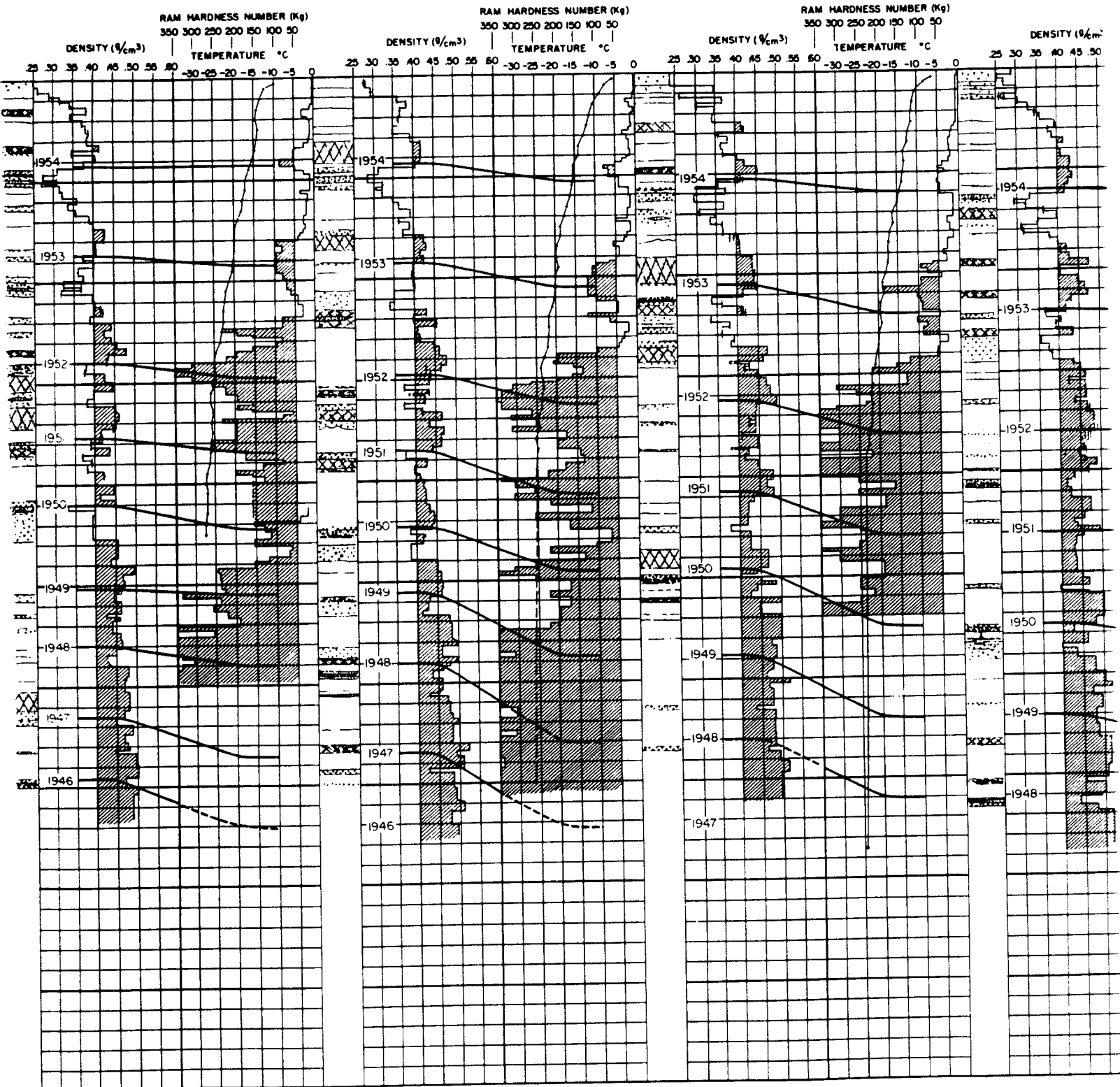
①

STATION 5-20
23 JULY 1955
ELEVATION 3072 m (10,077 ft)

STATION 5-40, PIT II. (1/4 ADJ)
23 JULY 1955
(FRENCH CENTRAL STATION)
ELEVATION 3005 m (9858 ft)

STATION 5-65. (1/4 ADJ)
2 AUGUST 1955
ELEVATION 2882 m (9454 ft)

STATION 5-90
6 AUGUST 1955
ELEVATION 2763 m (9064 ft)

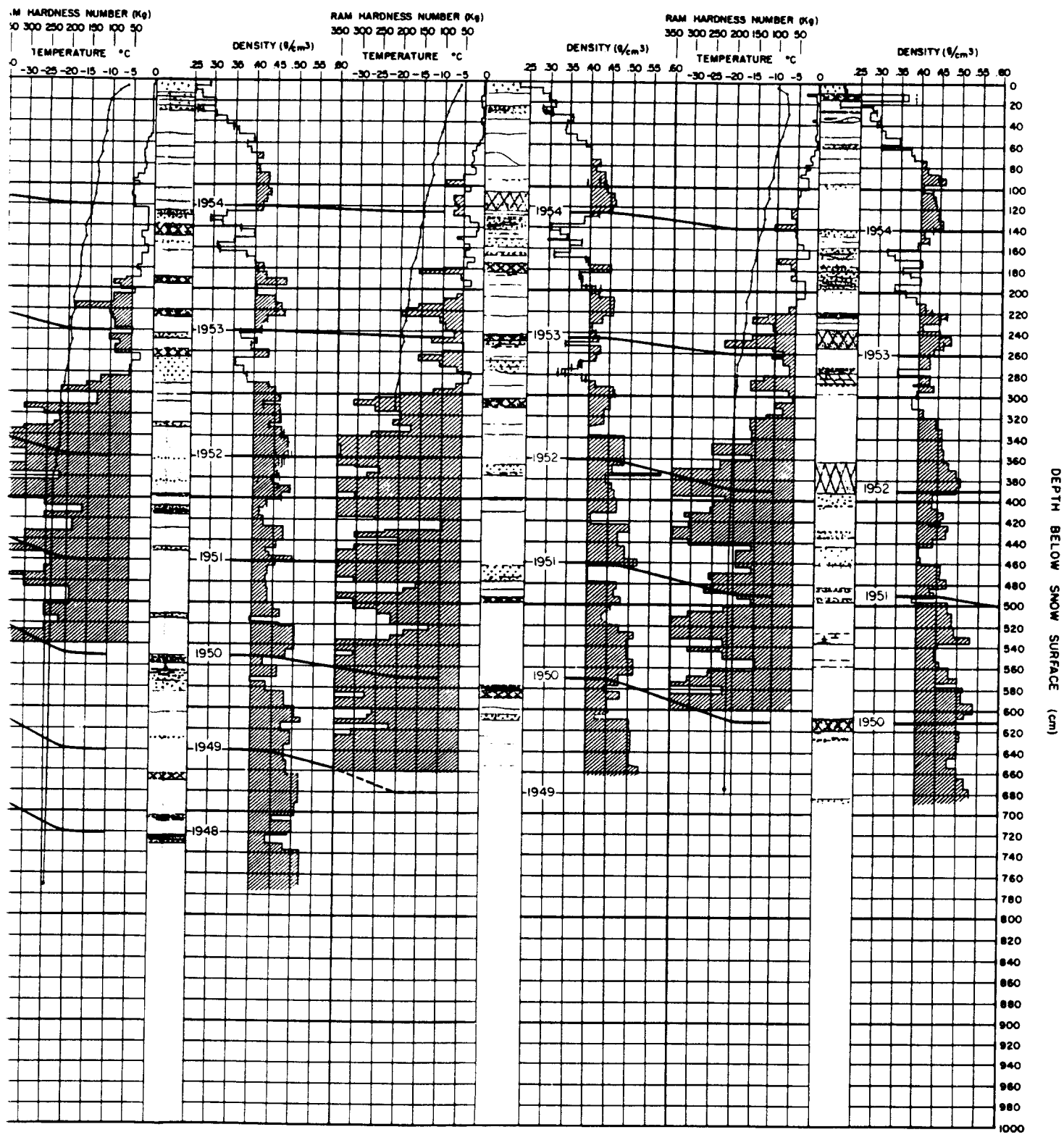


(2)

STATION 5-90
6 AUGUST 1955
ELEVATION 2763 m (9064 ft)

STATION 5-115
8 AUGUST 1955
ELEVATION 2646 m (8680 ft)

STATION 5-140
10 AUGUST 1955
ELEVATION 2466 m (8090 ft)



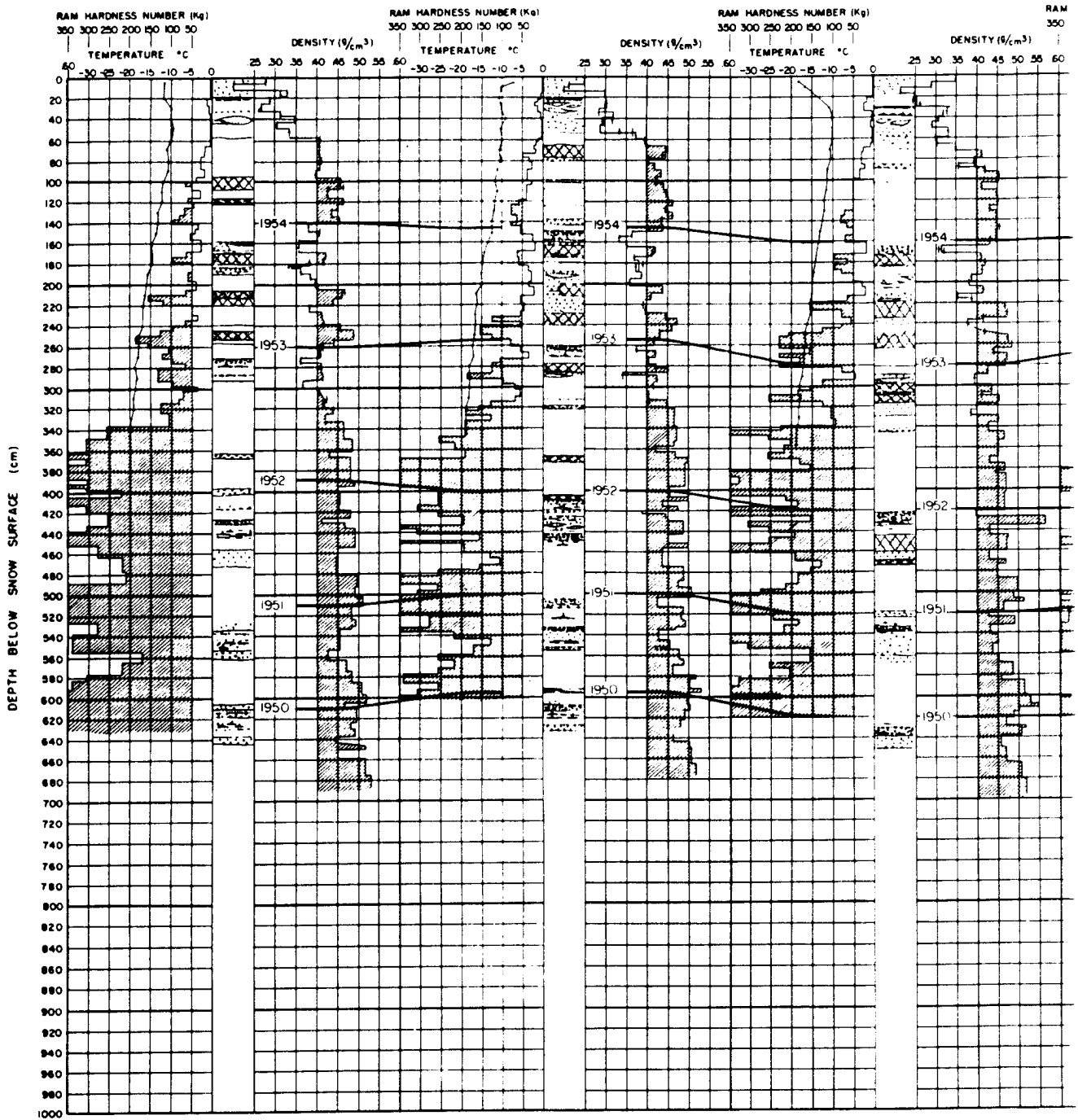
③

DATA SHEET 10

STATION 5-150
12 AUGUST 1955
ELEVATION 2407 m (7896 ft)

STATION 5-160
13 AUGUST 1955
ELEVATION 2342 m (7683 ft)

STATION 5-170
14 AUGUST 1955
ELEVATION 2283 m (7489 ft)



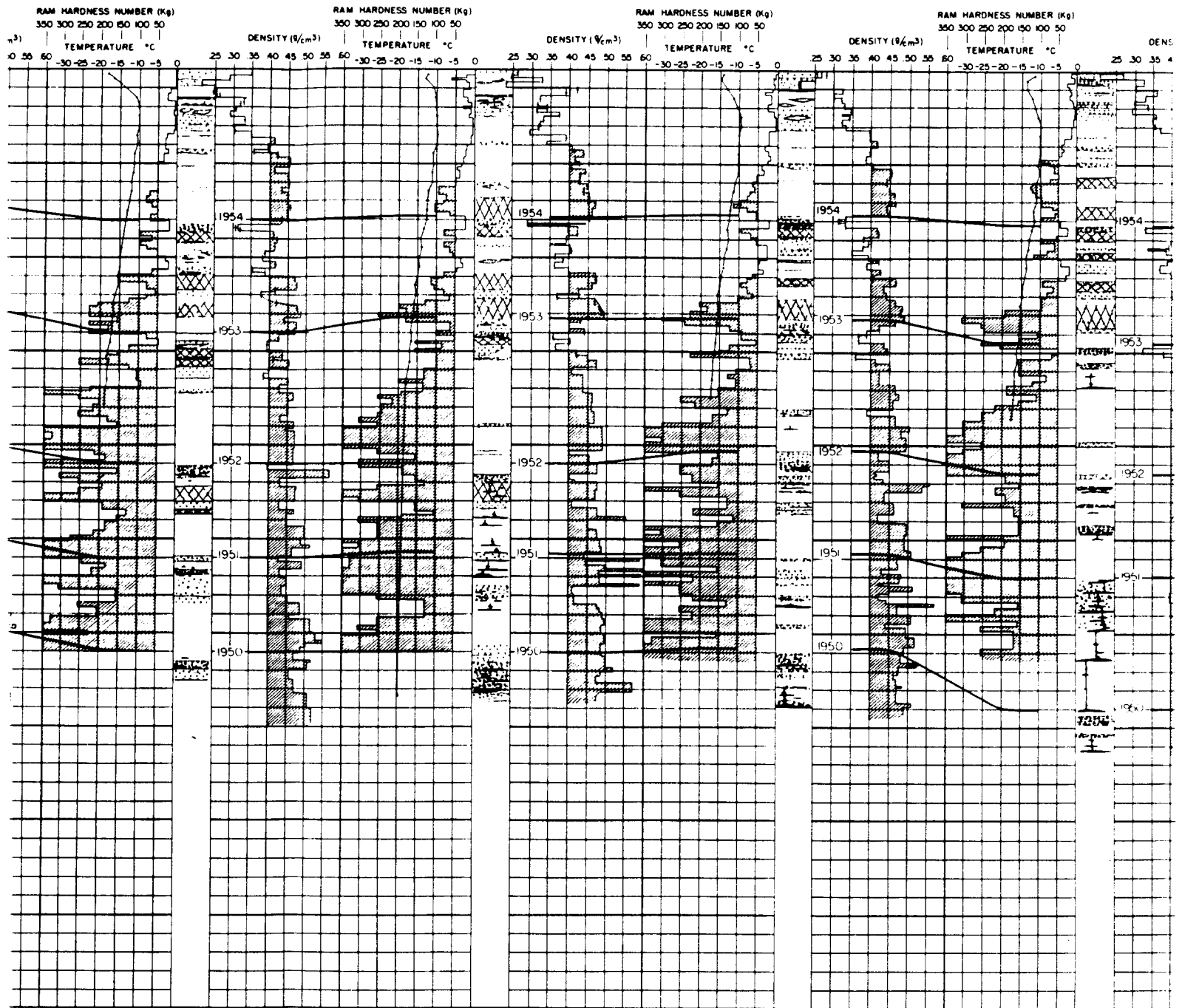
①

STATION 5-170
14 AUGUST 1955
ELEVATION 2283 m (7489 ft)

STATION 5-180
15 AUGUST 1955
ELEVATION 2206 m (7239 ft)

STATION 5-190
16 AUGUST 1955
ELEVATION 2146 m (7040 ft)

STATION 5-200
17 AUGUST 1955
ELEVATION 2012 m (6601 ft)



2

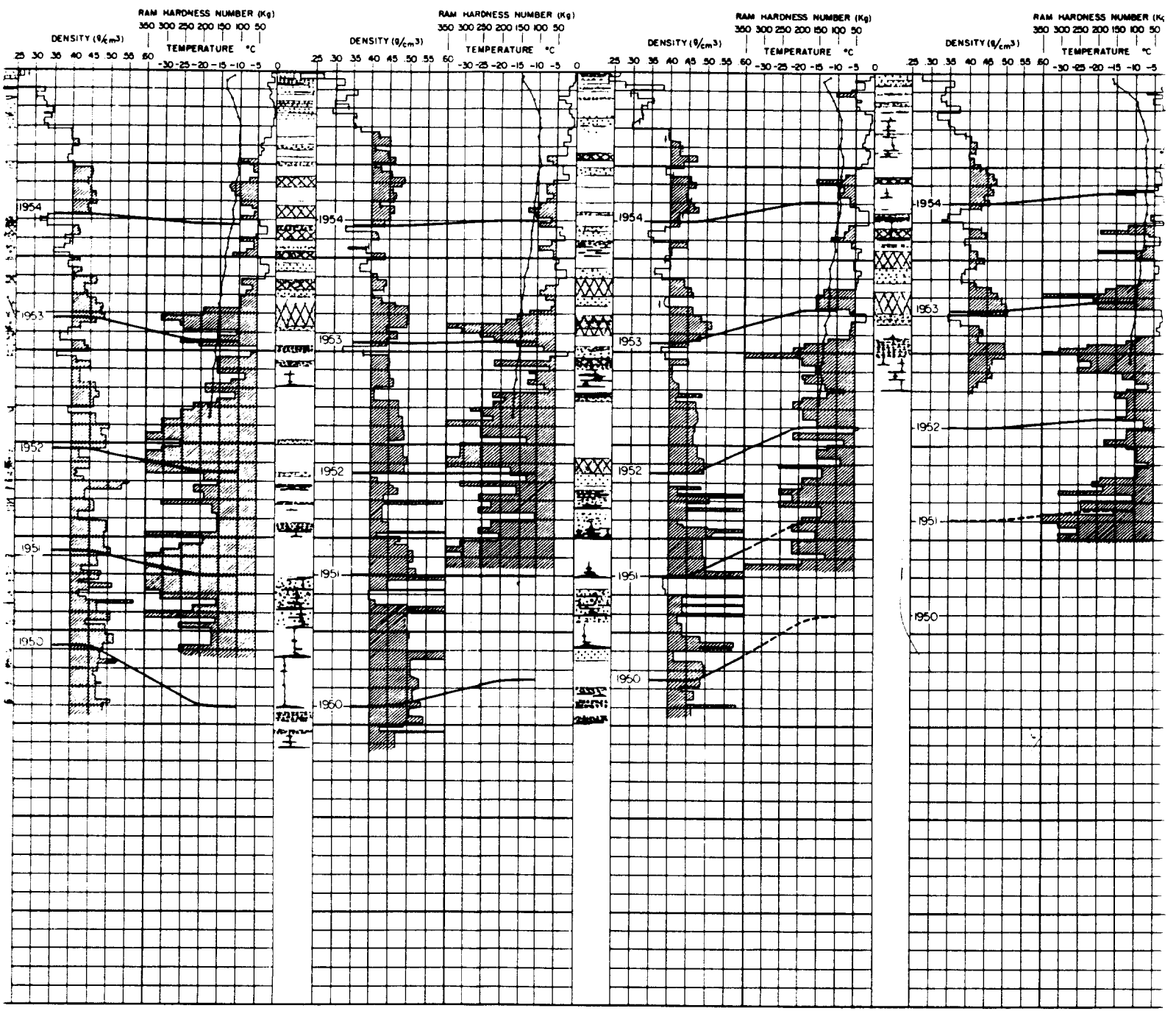
5-190
1955
2146 m (7040 ft)

STATION 5-200
17 AUGUST 1955
ELEVATION 2012 m (6602 ft)

STATION 5-210
18 AUGUST 1955
ELEVATION 1963 m (6440 ft)

STATION 5-220
19 AUGUST 1955
ELEVATION 1861 m (6107 ft)

STA
20
ELE



3

ON 5-210
AUGUST 1955
ELEVATION 1863 m (6110 ft)

STATION 5-220
19 AUGUST 1955
ELEVATION 1881 m (6171 ft)

STATION 5-230
20 AUGUST 1955
ELEVATION 1746 m (5729 ft)

